Synthesis and Elucidation of Biochemical Mode of Action of Organoselenium Compounds Against Cancer

Dissertation

zur Erlangung des Grades
des Doktors der Naturwissenschaften
der Naturwissenschaftlich-Technischen Fakultät III
(Chemie, Pharmazie, Bio- und Werkstoffwissenschaften)
der Universität des Saarlandes

von

Aman K.K. Bhasin
aus Chandigarh (India)

Saarbrücken 2014

Tag des Kolloquiums: 31 October, 2014

Dekan: Prof. Dr. Volkhard Helms

Berichterstatter:
1. Prof. Dr. Claus Jacob (Doktorvater)

2. Prof. I. Bernhardt

Vorsitz: Prof. Dr. Gregor Jung

Akad. Mitarbeiter: Dr. Harish Bokassam

Dedicated to my loving Parents

Table of Contents

Acknowledgements

Abstract

Amongst the plethora of organic compounds of selenium studied till date, bivalent organodiselenides have been of topical interest as validated from their potential anti-infective and anti-carcinogenic properties. In due consideration, the present research work is primarily focused on the design and synthesis of versatile diselenides, in addition to other related chalcogen derivatives, with an aim to delineate their potential molecular and cellular modes of action.The most active organodiselenides were confirmed to induce caspase-mediated apoptosis in KB-3-1 cancer cells. A highly active quinoline-functionalized organo-diselenide targeted the translational machinery in addition to a dual inhibition of the Raf/MEK/ERK and the PI3K/Akt/mTOR pathways of KB-3-1 cells. ERK2 was identified as its potential cellular targetin a DARTS experiment.Unlike the chalcophenes, the most active organodiselenides exhibited a poor radical scavenging and reducing ability. In contrast, the phenolic hydroxyl group was hypothesized as a probable antioxidant pharmacophore in the very active chalcophenes. This study also identified thioredoxin reductase as a potential cellular target of certain chalcogen-containing naphthoquinones which could possibly explain their ability to induce tumour cell death via ROS generation. Considering the unprecedented potential of organoselenium compounds to target important cellular proteins in tumour cells, future interdisciplinary studies are required for a more comprehensive elucidation of their chemical and biochemical modes of action against cancer and other life-threatening diseases.

Zusammenfassung

Von den zahlreichen Organoselenium-Verbindungen, die bis heute untersucht wurden, sind die Organodiselenide wegen ihrer potentiellen Wirkung als Anti-Infektiva und Anti-Krebsmittelvon besonderem Interesse. Aus diesem Grund fokussierte sich diese Doktorarbeit in erster Linie auf die Synthese und Skizzierung der molekularen und zellulären Wirkmechanismen der Organodiselenide und verwandter Organochalkogen-Verbindungen. Für die erste Gruppe konnte bestätigt werden, dass sie in KB-3-1-Krebszellen eine Caspase-vermittelte Apoptose induziert. Ein hochaktives Chinolin-funktionalisiertes Organodiselenidhemmte den Raf/MEK/ERK und den PI3K/Akt/mTOR-Signalweg und wirkte auf das Translations system der KB-3-1-Zellen. ERK2 wurde in DARTS-Experimenten als das mögliche zelluläre Zielprotein identifiziert. Anders als die Chalkophene zeigten die aktivsten Organodiselenide eine geringe Aktivität als Radikalfänger und geringes Reduktions potential. In den in dieser Hinsicht sehr aktiven Chalkogenen wurde die phenolische Hydroxylgruppe als mögliches Pharmakophorangesehen. Diese Studie identifizierte die Thioredoxin-Reduktase als ein mögliches zelluläres Zielprotein einiger Chalgogen-enthaltender Naphtochinone, was möglicherweise ihre Fähigkeit erklärt, durch ROS-Generierung den Tod von Tumorzellen zu induzieren. Im Hinblick auf das beispiellose Potential der Organoselenium-Verbindungen, zelluläre Proteine von zentraler Bedeutung in Tumorzentralen zu adressieren, sind in Zukunft interdisziplinäre Untersuchungen nötig, um ihre chemischen und biochemischen Wirkmechanismenbei Krebszellen und anderen lebensbedrohenden Krankheiten aufzuklären.

Abbreviations

AIF	Apoptosis inducing factor
ABTS	2,2'-azino-di-(3-ethylbenzathiazoline-6-sulfonic acid)
Akt/PKB	Protein kinase B
ALS	Amyotrophic lateral sclerosis
AMP	Adenosine monophosphate
ATP	Adenosine triphosphate
BBSKE	1,2-[Bis(1,2-benzisoselenazolone-3-(2H)-ketone)]ethane
Bcl-2	B-cell lymphoma 2
BH3	Bcl-2 homology 3
BIM	Bcl-2interacting mediator of cell death
BIM-EL	BIM-extra long
BSA	Bovine serum albumin
CBP	CREB-binding protein
CNS	Central neural system
CREB	Cyclic AMP-responsive element binding protein
DARTS	Drug-affinity responsive target stability
DMEM	Dulbecco´s Modified Eagle Medium
DMF	Dimethyl formamide
DMSO	Dimethyl sulfoxide
DNA	De-oxy ribonucleic acid
DPPH	2,2-Diphenyl-1-picrylhydrazyl
DTNB	5,5'-Dithiobis(2-nitrobenzoic acid)
4E-BP1	Eukaryotic translation initiation factor 4E-binding protein 1
EBSS	Earle's balanced salt solution
ECCG	Epigallocatechin gallate
E Coli	Escherichia coli
EDTA	Ethylenediaminetetraacetic acid
EGF	Epidermal growth factor
eIF	Eukaryotic translation initiation factor

ELISA	Enzyme linked immuno-sorbent assay
E_{pa}	Electrode potential (anodic)
E_{pc}	Electrode potential (cathodic)
ER	Endoplasmic reticulum
ERK	Extracellular signal-regulated kinase
FDA	Food and drug administration
FRAP	Ferric reducing ability of plasma
GABA-A	Gamma-aminobutyric acid type A
GAP	GTPase-activating protein
GPx	Glutathione peroxidase
GSeSeG	Oxidized seleno-glutathione
GSH	Glutathione (reduced)
GSSG	Oxidized glutathione
HCC	Hepatocellular carcinoma
HeLa/KB-3-1	Henrietta Lacks (name of patient from whom the cervix cancer cell line was named)
HIF	Hypoxia inducible factor
HPLC	High Pressure Liquid Chromatography
HPV	Human Papilloma Virus
HRP	Horseradish peoxidase
IRES	Internal ribosome-entry site
JNK	c-Jun N-terminal kinase
K562	Myelogenous leukaemia cell line
MAPK	Mitogen-activated protein kinase
Mcl-1	Myeloid cell leukemia-1
MCT-1	Multiple copies of T-cell lymphoma-1
MEK	Mitogen-activated protein kinase
MEM	Minimum essential medium eagle
IRES	Internal ribosome-entry site
MRSA	Methicillin-resistant staphylococcus aureus
MSK-1	Mitogen/stress-activated kinase

mTOR	Mammalian target of rapamycin
MTT	3-(4,5-dimethylthiazol-2-yl)-2,5-diphenyltetrazolium bromide
MudPIT	Multidimensional protein identification technology
NADPH	Nicotinamide adenine dinucleotide phosphate
NIH	National Institutes of Health
NPCT	Nutritional prevention of cancer trial
MRSA	Methicillin-resistant staphylococcus auras
MTT	3-(4,5-dimethylthiazol-2-yl)-2,5-diphenyltetrazolium bromide
MudPIT	Multidimensional protein identification technology
OD	Optical density
OS	Oxidative stress
OTC	Oxytetracycline
PARP	Poly-(ADP-ribose)- polymerase
p38	P38- mitogen activated protein kinase
p90RSK	p90 ribosomal S6 kinase
PBS	Phosphate buffered saline
PEI	Polyethylenimine
PI3K	Phosphoinositide 3-kinase
PKC	Protein Kinase C
Rheb	Ras-homolog enriched in brain
RKIP	Raf-1 kinase inhibitor protein
Se	Selenium
SELECT	Selenium and Vitamin E Cancer Prevention Trial
rpS6K	Ribosomal protein S6 kinase
SD	Standard deviation
SDS	Sodium dodecyl sulphate
SeC	Selenocysteine
SEM	Selenomethionine
SeMC	Se-Methyl-selenocysteine
Ser	Serine
STAT 3	Signal transducer and activator of transcription 3

TBAP	Tetrabutylammonium perchlorate
Tca8113	Tongue cancer cell line
TEPG	Triethyl phosphine gold chloride
THF	Tetrahydrofuran
Thr	Threonine
TLC	Thin layer chromatography
TNB	2-nitro-5-thiobenzoic acid
TPA	12-O-tetradecanoylphorbol-13- acetate
TR	Thioredoxin
Tris	Tris(hydroxymethyl)aminomethane
Tr_{ox}	Oxidoreductase thioredoxin
TrxGR	Thioredoxin glutathione reductase
TrxR	Thioredoxin reductase

Chapter 1

1.1   Selenium- a valuable micronutrient

Selenium is an indispensable micro-nutrient that occurs in a low percentage in nature. In contrast to its availability in trace amounts in its elemental state, it is found more often as selenides of iron, lead, silver or copper. Most of the physiological content of selenium is derived from the diet, in addition to a fraction that constitutes important cellular proteins, in the form of selenocysteine, SeC. The selenium content in food varies with nature and location of cultivation of the forage. Broadly, seafood, nuts, poultry and grains are well-recognized sources of selenium.

Before delving into the chemotherapeutic effects of selenium, it is pertinent to have a brief overview of selenium and the diverse chemical forms, in which this element exists in nature. In nature, selenium exists primarily intwo forms- seleno-proteins and non-selenoproteins. The naturally occurring seleno-proteins like GPx and TrxR are cellular enzymes that exist, in varying amounts, in all forms of life and are characterized with a common selenocysteine (SeC) containing amino acid residue. To date, 25 different SeC-containing selenoproteins have been identified in mammalian cells. However, SeC that serves as an important structural unit of selenoproteins also finds its non-physiological source in a variety of foods of either animal or plant origin. In food, however, in addition to its primary availability in the form of selenomethionine (SEM), selenium is also found in the form of selenates and selenites [1]. Amongst the various food sources, Brazil nuts and sea-food have been widely considered as the richest source of selenium [2].

Apart from seleno-proteins, several types of selenium-containing compounds are also available in nature and may also be prepared through synthetic methodologies. These can be broadly classified furtherinto two chemical forms-inorganic selenium and organic selenium which are available in four different oxidation states [1].

Table 1.1 Representation of different chemical forms of selenium

Group	Members
Diselenides/ monoselenides	Ar_2Se_x or R_2Se_x; x=1/2; Ar = Aryl group, R = alkyl or alkynyl group (also includes metal diselenides/monoselenides like tungsten diselenide and iron(II) selenide)
Compounds with Se^{6+}	Selenates (M_2SeO_4) ; M = alkali metal
Compounds with Se^{4+}	Sodium selenite (Na_2SeO_3); Alkyl/Aryl seleninic acid; Selenous acid (H_2SeO_3); Selenium dioxide (SeO_2)
Se-heterocyclic compounds	1,3-Selenazolin-4-one derivatives; 2,5-Bis(5-hydroxymethyl-2-selenienyl)-3-hydroxymethyl-N-methylpyrrole;2-Phenyl-1,2-benzisoselenazol-3(2H)-one(ebselen);1,2-[Bis(1,2-benz-isoselenazolone-3-(2H)-ketone)]ethane (BBSKE); 2-Butyl-selenazolidine-4-(R)-carboxylic acid (BSCA); 2-Cyclo-hexylselenazolidine-4-(R)-carboxylic acid (ChSCA),Se_4N_4
Selenocyanates	Ar/R-SeCN (Ar=aryl group; R= alkyl/alkynyl group); Ar-Se_2CN[7]
Halogenated seleno-compounds/ (electrophilic selenium-containing molecules)	RSeX (R= aryl/metal; X= halogen); selenonium ion (H_3Se^+ or $(CH_3)_3Se^+$)

In addition, the availability of elemental selenium in minerals and as nanoparticles in soils has also been observed. The soils in the state of Punjab in Northern India, for instance, have been reported to be enriched with selenium nanoparticles by the reducing action of certain bacteria on water-soluble selenites [3]. In its elemental form, selenium exists in six natural isotopic forms and 24 unstable isotopic forms [4].

As can be seen in **Table 1.1**, representative examples of various inorganic and organic forms of selenium have been demonstrated. Briefly, the inorganic forms of selenium include selenites, selenates, halogenated selenium compounds, selenoacids and even potential explosives like Se_4N_4. Organic forms of selenium include selenides, diselenides, aryl/akyl functionalized seleno acids, selenocyanates and several selenium-

containing heterocyclic compounds. Recently, a novel selenium compound called selenoniene has been identified a predominant form of organic selenium in the blood of tuna fish [5].This compound has been further characterised as a potential antioxidant with an ability of attenuating methyl-mercury induced toxicity [5, 6].

1.2   Etiology of Cancer

In view of its significant anti-oxidant and anti-inflammatory properties, selenium is more popularly recognised to harbor potential efficacy in reducing the development and progression of cancer. Therefore, prior to a discussion regarding the role of selenium in combating cancer, an insight into this disease and its etiology become important [8].

1.2.1   What is cancer?

Popularly referred to as the "King of maladies", cancer is generally characterized by an uncontrolled growth of cells in a specific region (benign tumour) or throughout the living body (metastasized tumour). Since all forms of cancer originate from cells, so the cells that are often termed as building blocks of life may also serve as building blocks of death. More than 100 different types of cancer have been reported so far, depending on the region or organ of the body being affected by it. The onset of this disease is often characterized by several physical symptoms that may or may not be specific to a certain type of cancer. An early diagnosis of cancer-related symptoms can therefore, be highly instrumental in curbing the disease before it metastasizes to other parts of the body.

1.2.2   Why do people get cancer?

"It's all in the genes!"- A saying that is befitting to one of the plausible causes of cancer. Cancer can be the outcome of a genetic predisposition that is inherited from family members. This means anyone born with mutations in one copy of a damage-controlling gene which normally protects against cancer has a genetic predisposition for one or more types of cancer. For instance, approximately 5% of all cases of colon cancer are due to genetic inheritance of corresponding mutated and cancer-causing syndromes [9]. Environmental factors in the form of carcinogens also play a prominent

role in enhancing the risk of cancer. This group of substances is widely responsible for inducing mutations in the cellular DNA that activates an unprecedented number of intracellular biochemical events, eventually leading to cancer. For instance, a big section of the population is under the influence of smoking-a major cause of cancer. Though harmless in physical appearance and regarded as a stress buster, the tobacco of a cigarette releases a lethal cocktail of approximately 70 carcinogens with hundreds of cumulative poisons including nitrosamines and polycyclic aromatic hydrocarbons that serve as neurotoxins and found to induce DNA-methylated lesions [10].Apart from smoking, sporadic exposure to high-energy radiations such as gamma and X-rays also promote melanoma via oxidative cellular damage and production of immune suppressive cytokines[11].Moreover, the increasing role of pathogenic agents in the etiology of cancer can be partially comprehended by recent reports recognizing HPV infection as a prominent cause of cervical cancer [12]. These and several other forms of viruses like hepatitis B and C suppress the immune resistance of the body, thereby making it vulnerable to carcinogens.

1.3 Biochemistry of cancer

In an attempt to circumvent as well as combat cancer, an unprecedented number of natural and synthetic selenium-incorporated compounds have been exhaustively investigated for their chemotherapeutic efficacy. Although numerous *in-vitro* and *in-vivo* studies have reported the positive role of selenium in the fight against cancer, results obtained from various case studies and random clinical trials have given a rather mixed response regarding the futuristic fate of selenium as a chemotherapeutic agent. This response has been found to vary both on the basis of gender of the patients and source of selenium supplements given to them. Results from the NPCT and SELECT trials have also introduced questions regarding the probable toxicity from long-term exposure to selenium supplements [13].Therefore, in order to exploit the maximal chemotherapeutic advantage of selenium under a safe pharmacological profile, it is essential to strengthen and broaden the existing knowledge of the anti-carcinogenic mode of action of selenium-containing compounds under varying modes of dosage and chemical source. Prior to doing so, it is indispensable to understand the basics of the etiology of cancer and the biochemical role played by selenium in its combat against cancer.

1.3.1 Cancer cells *versus* normal cells

Under physiological conditions, normal cells and tumorigenic cells monitor their biological activities including development, tissue repair, immunity as well as normal tissue homeostasis on the basis of their complex system of inter and intra-cellular pathways of communication[14]. An important and striking difference in the functioning of normal cells and tumorigenic cells lies, therefore, in the extent of activity of their cellular signalling pathways. Mutation(s) in any of these pathways often lead to their abnormal and dys-regulated functioning, resulting in uncontrolled cellular growth and enhanced cell survival, accompanied by a disruption of intra-cellular redox homeostasis [15]. Such events individually or synergistically lead to cellular disparities that can be characterized in the form of ectopic hypertrophy,enhanced cellular motility and deformity of cellular tissues. An in-depth comprehension of the intricacies of these biochemical pathways and their relevance with respect to cellular insults like cancer has played an important role in opening new therapeutic windows in fighting cancer and several other degenerative diseases. Within the library of chemotherapeutic agents, a plethora of selenium-incorporated molecules, via a cascade of active metabolites, have been reported to exhibit anti-proliferative activity against tumour cells by targeting some of these crucial intra-cellular biochemical pathways [16]. However, the biochemical mode of interaction of selenium with these signalling modules has been observed to fluctuate with dose and chemical form. Due to the biological scope of the work done in this thesis, the content of discussion of selenium´s biochemical effects will be limited to the modulatory effects of organodiselenides towards twoparticular signalling pathways that have been frequently observed to be constitutively over-activated in tumorigenic cells,*in-vitro* and *in-vivo*, and share a cross-talk with its intra-cellular protein translational machinery.

1.3.2 Hyper-activated protein translation in cancer cells

In eukaryotes, in particular, protein translation is a tightly regulated and a highly energy-demanding process required for cellular survival and proliferation[17]. Playing a pivotal role in regulation of gene expression, mRNA translation is highly dysregulated and over-activated in tumour-struck cellular tissues as characterized by subsequent genetic alterations leading to abnormal cellular mass and irregular

morphology [18].Proceeding in three distinct, yet highly orchestrated steps, protein biogenesis basically involves the translation of mRNA into proteins in the cytoplasmic region of a cell by utilizing ribosomes as a template. In eukaryotic cells, the process of translation has been widely studied to operate mainly via a "cap-dependent process". However, another form of translation that is independent of the presence of intact 5' cap is called cap-independent translation or IRES-mediated translation. In approximately 10% of eukaryotic mRNA, translation is initiated via this cap- independent mechanism and is the preferred method of protein synthesis when cap-mediated translation is partially or completely attenuated under conditions of patho-physiological cellular stress including hypoxia, genotoxic stress and apoptosis [19].

1.3.2.1   eIF4E-driven protein translation

In context to this thesis, the discussion will be directed towards the more commonly observed cap-dependent process. Briefly, this involves the binding of eIF4E complex to the 5' end of all nuclear-encoded eukaryotic mRNAs, commonly referred to as the "cap structure". This complex consists of the cap-binding protein, eIF4E, the RNA helicase (eIF4A) and the scaffolding protein eIF4G [20, 21]. The process of cap-dependent mRNA translation occurs in three stages: initiation, elongation and termination, all of which are highly regulated although the initiation phase is proposed to be the limiting step [18].

Amongst the various translation-promoting factors mentioned above, the oncogenic role of eIF4E is perhaps the most well established [22]. Being a relatively lesser abundant translation factor, eIF4E which is highly expressed and widely recognised as an oncogene in various types of tumour is hypothesized to be a rate-determining component of the translational machinery [20, 23]. Hyper-activation of eIF4E is a consequence of its over-expression and/or alterations in its regulatory cell signalling pathways [20]. Over-activation of eIF4E in tumorigenic cells has been reported to proceed mainly through two levels. One method involves the direct phosphorylation of eIF4Edirectly by MAPK kinase interacting Ser/Thr kinase 1 and 2 (MNK1 and MNK2). This is evident from the observation that non-phosphorylated mutant of eIF4E have been reported to drastically impair oncogenic potential as compared to the wild-type eIF4E [24]. To further establish the role of the phosphorylation of eIF4E in tumorigenesis, knock-in mice expressing a non-phosphorylable

form of eIF4E were observed not to display any conspicous phenotypecontrary to that depicted by phosphorylated (activated) eIF4E [25].

An alternate mechanism of eIF4E regulation involves its availability to form the eIF4F complex. When eIF4E is bound to translation suppressor 4E-BP1, it is unavailable for binding with translation-promoting factor eIF4G. 4E-BP1 can only bind to eIF4E when it is hypo-phosphorylated. Therefore, when eIF4E is not bound to 4E-BP1 due to hyper-phosphorylation, it is free to interact with eIF4G and promote translation [20].

1.3.3 Hyper-activated signalling pathways in cancer cells

1.3.3.1 mTOR-mediated signalling: Promoting cancer via eIF4E-driven protein translation

It has been proposed that the mTOR gene is apivotal signalling module that can influence the rate of cellular translation by inactivating the translation suppressor gene4E-BP1 via phosphorylation at residues Thr70 and Ser65 [26]. As a consequence, an enhanced disassociation of 4E-BP1 from eIF4E results in an increased availability of functional eIF4E for the formation of the eIF4F complex subsequently leading to enhanced protein translation [27]. Inactivation of such translation-initiation repressor proteins like 4E-BP1 by dephosphorylation has been thereby implicated in aberrant cellular protein biogenesis and consequently carcinogenesis. As can be seen in **Figure 1.1**, mTOR, which forms an important node of the PI3K-mediated signallingpathway, forms two complex esmTORC1 and mTORC2 out of which mTORC1, plays the most influential role in regulating translation.
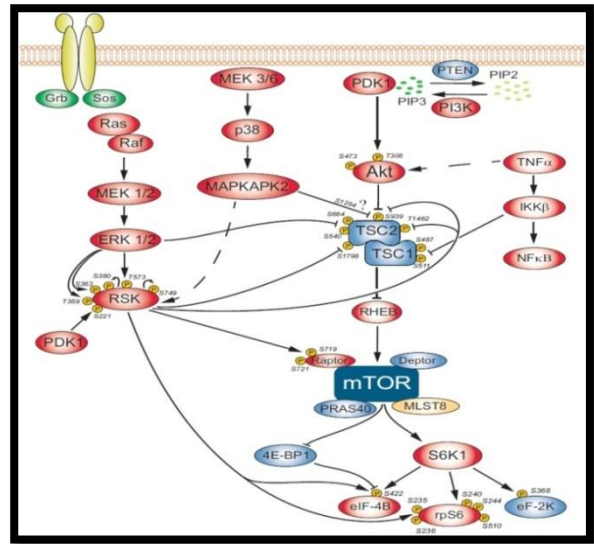
Figure 1.1 Regulation of translation by synergistic effect of the Raf-MEK-ERK and PI3K Akt-mTOR signalling pathway. Figure has been adopted from [29].

7

mTORC1 complex includes mTOR that is in association with a scaffold protein, Raptor. The primary role of Raptor is to recognize and phosphorylate substrates carrying TOR signalling motifs including the translation repressor 4E-BP1 and rpS6K.

Upon phosphorylation by TORC1 complex, activated S6K disassociates from eIF3 and phosphorylates its downstream substrates- rpS6 and eIF4B. Phosphorylation of eIF4B stimulates an association between eIF4B and eIF3 which boosts translation probably by activating eIF4A [28]. Therefore, an aberrant mTOR signalling as commonly observed in malignant cells promotes ectopic stimulation of oncogenic eIF4B, 4E-BP1 and ribosomal S6K1. This, in turn, facilitates uncontrolled cap-mediated protein translation that serves as a hallmark of cancer. The prominent oncogenic role of the mTOR-mediated pathway has also been observed in this study. In accordance with the obtained findings, **12** has been observed to antagonize the proliferation of KB-3-1 cells via inhibition of mTOR-mediated phosphorylation of 4E-BP1. This effect has been further reflected in the observation of a down-regulation of the translational efficiency in **12**-treated KB-3-1 cells.

1.3.3.1.1 Significance of mTOR in oncology: Evidence of success of mTOR inhibitors against cancer

The predominant role of mTOR as a tumour-agonist has made way for the development of several mTOR-inhibiting small molecules.

a) First-generation mTOR inhibitors

The development of Sirolimus (also called rapamycin),for instance, as an anticancer agent, began after its isolation and identification as a macrocyclic triene antibiotic from the soil bacterium,*Streptomyces hygroscopicus,*in the mid-1970s.However, rapamycin has met with substantial pharmacokinetic challenges due to its poor lipophilic chemistry. Due to this, rapamycin has been used in combination with other chemotherapeutic drugs, to avoid side-effects [30]. In addition, various formulations of rapamycin have been analysed to improve its poor water solubility and bioavailability for clinical applications. Amongst these improvised rapamycin analogues, Temsirolimus and Everolimus have demonstrated a promising potential in the treatment of different lineages of cancer (**Table 1.2**). In view of its drug-like features, Temsirolimus has been recently approved by the FDA for treating renal-cell carcinoma [31]. Developed by Novartis,

Everolimus is another analogue of rapamycin that has been approved for the treatment of renal cell carcinoma in USA, in addition to breast cancer and tuberous schelorisis in the European Union [32]. A third and the latest analogue of rapamycin, Ridaforolimus (earlier called Deforolimus and developed by Merck) is currently being assessed for treatment of sarcoma and has yet to be approved by the FDA [30]. However, the success of rapamycin derivatives in clinical trials has been limited to a few types of cancer. This is because despite their partial mTOR inhibition, rapalogs (analogues of rapamycin) have been unsuccessful inrepressing a negative feedback loop that exists between mTORC1 and its upstream factor Akt in certain tumour cells thereby resulting in phosphorylation and activation of oncogenic Akt.

b) Second-generation mTOR inhibitors

In order to counter this problem, a second-generation small-molecule mTOR inhibitors (TORKinibs) have been generated that simultaneously inhibit the ATP-binding domain of mTOR and the catalytic activity of both mTORC1 and mTORC2. Therefore, the dual inhibition of both mTOR complexes with a higher degree of selectivity has led these agents to have stronger anti-proliferative potential than the naturally available mTORC1 inhibitor-sirolimus [33]. A representation of several important mTOR inhibitors, assessed to date, can be seen in **Table 1.2**.

Table1.2 Examples of rapamycin analogues and second generation mTOR inhibitors

Compound	Class	Disease
Temisirolimus (FDA approved)	Rapamycin	Renal cell carcinoma
Ridafirolimus	Rapamycin	Breast cancer, Head and neck cancer, Soft tissue sarcoma, Colorectal cancer, Non-small cell lung cancer (NSCLC)
Everolimus (FDA approved)	Rapamycin	Hormone receptor positive, HER2 Negative breast cancer
Agent OSI-027	2nd generation mTOR-inhibitor	Lymphoma; solid tumour
XL765	2nd generation mTOR-inhibitor	Combinatorial therapy
PP242	2nd generation mTOR-inhibitor	Multiple myeloma

1.3.3.2 Signalling via MAPK pathway: Another lead promoter of carcinogenesis

In addition to mTOR -mediated signalling, the ERK-mediated MAPK pathway has also been reported to serve as an important contributor to cancer. The activity of the Ras-Raf-MEK-ERK cascade-mediate signalling which constitutes one of the streams of the overall mitogen-activated protein kinase (MAPK) cascade has been reported to be over-activated in about 30% of all human cancers. This is evident from several reports that have highlighted the contribution of active ERK as the other important promoter of carcinogenesis via uncontrolled intra-cellular protein translation and enhanced cellular survival [35]. This is partially evident from the report by Monick *et al.* that demonstrated the oncogenic role of activated ERK in promoting protein biogenesis in human alveolar macrophages through activation of eIF2α [36].

1.3.3.2.1 Protein kinase: general class of MAP kinases

Owing to the importance of protein kinases, in general, and the ERK-mediated signalling cascade in particular, protein kinases represent bonafide drug targets that are receiving considerable attention from a large cadre of biomedical scientists for the treatment of several life-threatening diseases [37]. In order to comprehend the biochemistry of the Raf-MEK-ERK mediated MAPK signalling and its oncogenic role upon dys-regulation, an overview of the protein kinase family to which it belongs, therefore, becomes indispensable.

Protein kinases are one of the largest and most influential amongst the gene families and constitute almost 2% of the entire proteome. Protein kinases, in general, play a predominant regulatory role in transmission of extracellular signals into their intracellular targets by a network of interacting proteins that regulate a large number of cellular processes. Comprising of a set of cytoplasmic serine/threonine kinases, protein kinases participate in the phosphorylation of substrate proteins and modify the activity, location and affinities of approximately 30% of all cellular proteins. These signalling modules which are highly conserved from yeasts to vertebrates, have been demonstrated to participate in the regulation of numerous cellular processes including cell adhesion, cell cycle progression, cell migration, cell survival, differentiation, metabolism, proliferation and transcription [38].

Collective efforts from many research groups, over the past decade, have facilitated the elucidation of one such signalling mechanism that involves the stimulation of several signalling molecules followed by a sequential stimulation of several cytoplasmic protein kinases collectively known as mitogen-activated protein kinase (MAPK) signaling cascade. The MAPK signalling pathway contributes to the amplification and specificity of the transmitted signals that eventually activate several regulatory molecules in the cytoplasm and in the nucleus to initiate cellular processes such as proliferation, differentiation and development. Moreover, since many oncogenes have been demonstrated to encode proteins that transmit mitogenic signals upstream of this cascade, the MAPK pathway provides a common platform for the mode of action of most, if not all, non-nuclear oncogenes [39].

Due to the scope of the work done in relation to organoselenium compounds, emphasis will be directed primarily towards the first MAPK cascade that mediates its signalling via MEK and ERK, its cross talk with the Akt-mTOR pathway (that has been discussed above) and the modulatory effects exerted by compound **12** on the synergistic regulation of the ERK and mTOR-mediatedsignalling pathways in cervix carcinoma (KB-3-1) cells.

1.3.3.2.2   General overview of functioning within the MAPK family

All eukaryotic cells possess multiple MAPK pathways which coordinately regulate gene expression, mitosis, metabolism, motility, survival, apoptosis and differentiation. In mammals, MAPK can be activated by a plethora of stimuli but in general, activation of JNK and p38-kinasesis primarily due to stress-stimuli including ionizing radiation and inflammatory cytokines. Whereas JNK plays a role in the induction of apoptosis through extrinsic and intrinsic pathways, p38 MAPK is predominantly involved in inflammation by regulating cytokine production [40]. Conversely, activation of ERK-mediated MAPK is largely dependent on mitogenic stimuli like growth factors and phorbol esters that drive cellular proliferation via cell cycle regulation, in addition to various cell- survival mechanisms (**Figure 1.2**).Although each member of the MAPK family has distinct functions, they share some common characteristics as well. All pathways that collectively constitute the MAPK signalling have a sequence of events consisting of at least three components, a MAPK kinase kinase (MAP3K/MKKK), a MAPK kinase (MAP2K/MKK), and the MAPK. At the top,

MAP3Ks are often activated through phosphorylation and/or as a consequence of their interaction with a small GTP-binding protein of the Ras/Rho family, in response to extracellular stimuli. These serine/threonine kinases phosphorylate and activate the downstream MAP2Ks which in turn phosphorylate and activate MAPKs through dual phosphorylation on threonine and tyrosine residues. These activated MAPKs subsequently phosphorylate a plethora of substrate proteins that are involved in the regulation of cellular transcription and translation.
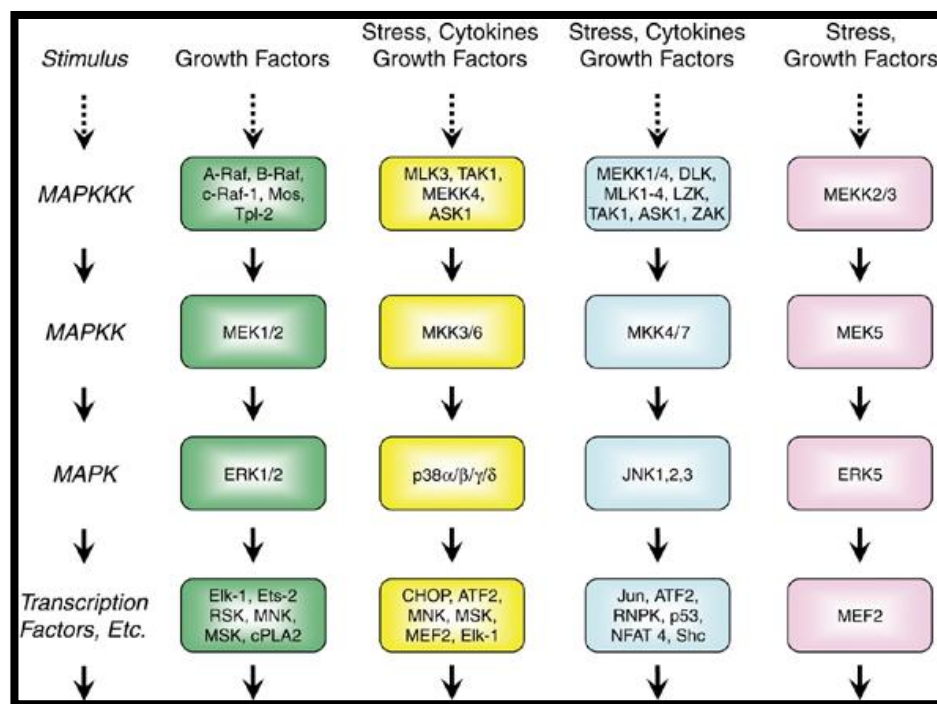
Figure 1.2 Representation of different tiers of the MAPK family in the eukaryotic system. Figure adopted from [28].

Therefore, phosphorylation serves as a basic mechanism by which the activity of MAPK proteins is turned "on" or "off" across a wide array of biological processes from cell growth and differentiation through apoptosis to disease.

The over-activation of the MAPK pathways has been frequently implicated in the etiology of several diseases like Alzheimer's, Parkinson's, ALS and cancer, thus making them potential targets for therapeutic intervention. For instance, over-activated JNK and p38 MAPKs have been proposed to mediate neuronal cell death in Alzheimer's, Parkinson's and ALS. On the other hand, constitutive activation of the ERK pathway is believed to play a pivotal role in tumorigenesis through cell

proliferation and cell survival mechanisms. Therefore, the Raf-MEK-ERK signalling cascade shall be discussed in more detail, with due relevance to its modulation by anti-carcinogenic selenium-containing compounds.

1.3.3.2.3   Raf-MEK-ERK- mediated signalling pathway

In an attempt to outline the pivotal nodes of the Raf-MEK-ERK cascade, at the level of MAP3Ks, the Raf genes are categorized into A-Raf, B-Raf and Raf-1 (or c-Raf). These three different isoforms constitute the first tier in the MAPK cascade. These three isoforms differ in their ability to activate their immediate downstream substrate, MEK1/2. Amongst them, A-Raf is a relatively less-characterized isoform amongst the Raf members and is apparently a poor activator of MEK1/2 [41]. Ser432, Thr452 and Thr455 sites in A-raf are the important phosphorylation sites, responsible for its catalyticactivity. In addition to these sites, Zhu and colleagues have reported that phosphorylation of c-Raf at Ser471 is required for its interaction with its protein substrates, namely MEK1/2 [42].

B-Raf,on the other hand, has also been found to be widely expressed but more predominantly in neuronal tissues [43]. Amongst these Raf members, B-raf has been observed to play a more prominent role in activating the downstream substrate, MEK. To summarize, within the Raf family, B-Raf is considered to be the most potent and A-raf has been found to be the weakest activator of its MAPK pathway. However, in context with the content of thesis, the relation and implications of c-Raf with respect to its oncogenic role will be considered in more detail in this study.

a)   c-Raf: Role in promoting oncogenesis

c-Raf (Raf-1) is a well-studied and pivotal member of the growth factor signalling molecules at the MAP3K level of the cascade. It is a 70-75 kDa serine/threonine kinase which upon stimulation by various mutagens undergoes a rapid and transient activation via phosphorylation. Extensive research has provided sufficient evidence that Raf-1 is located downstream of RAS, which seems to interact directly with the NH_2- terminal portion of Raf-1 on stimulation [44]. In addition to Ras, several other kinases like PKC and tyrosine kinases have also been proposed to activate Raf by distinct mechanisms [45].Although several proteins and peptides have been reported to

serve as substrates for Raf-1, current studies suggest that it has very selective substrate specificity, highly preferring the native form of MEK over a list of other proteins and peptides. Constitutive activation of Raf-1 due to oncogenic mutations in upstream Ras genes has been implicated in the onset and progression of solid tumours [46]. This has been observed in Ras-mutated NIH-3T3 fibroblasts that activate its downstream substrate, Raf-1, during metastasis in mice [47]. In addition, RKIP, a member of the phosphatidylethanolamine-binding protein family, has also been proposed as a suppressor of metastasis in prostate cancer, thereby indicating the potential oncogenic role of c-Raf. The high incidence of activating c-Raf mutations in melanoma cells has made it an ideal target for cancer therapy. Of the various chemotherapeutic agents targeting Raf, sorafenib is apparently the most promising as it is at the most advanced stage of clinical development.

b) MEK1/2: Downstream of Raf-1

Downstream of Raf, there exists MAP2Ks in the form of MEKs. Bearing an approximate molecular weight of 45kDa, MEK1 and MEK2 constitute the two isoforms of the MEK family. They are commonly referred to as MEK1/2. MEK1 and MEK 2 are expressed ubiquitously in mammalian cells, although in mice MEK2 appears to be more expressed during development with MEK1 being more highly expressed in adult animals[48]. MEK1 and MEK2 share approximately 85% similarity in their amino acid sequence. Although it is commonly assumed that the two isoforms are functionally equivalent, several lines of evidence indicate that they are regulated differently and may exert non-redundant functions [49]. This feature has been highlighted by the translocation of its downstream substrate, ERK2, to different regions of the cell upon stimulation by activated MEK1 and MEK2 [50]. In addition, MEK1 has been reported to down regulate MEK2-dependent ERK1/2 signalling, suggesting that MEK1 and MEK2 may not be completely interchangeable [51].This suggests that MEK1and 2 provide a specificity towards the activation of its downstream substratesERK1 and ERK2, in addition to an amplification of the MAPK.

This, thereby, justifiesMEK1/2 as an important regulatory component of the mitogenic signaling cascade. The role of both MEKs in angiogenesis is indicated by their over-expression in a significant percentage of tumours. Stimulated by various stimuli, dephosphorylation of MEK1/2 proteins at two serine residues at positions 217

and 222 in the activation loop has been reported to inhibit *in-vitro* and *in-vivo* proliferation of a variety of tumour cell models, including HCC [52, 53].

c)   ERK1/2: Critical promoters of carcinogenesis

As mentioned earlier, MEK1/2 has been found to catalyze the activation of human ERK1/2, via phosphorylation, in a sequential reaction at Tyr204/187 and then Thr202/185. A subsequent activation of the ERK isoforms results in a further activation of a plethora of transcriptional factors promoting cellular protein synthesis and survival.

Until hitherto, ERK has been characterised by a bag of mixed roles as far as stimulation of apoptotic cell death is concerned. Although there are many reports that highlight the pro-apoptotic role of ERK [54,55], a good number of reports have also demonstrated the opposite as well [56]. However, here again, in context to the work done, the anti-apoptotic role of ERK shall be primarily discussed, as has been observed in regard to the mode of action of **12** against cancer.

1.4   ERK and cancer

The ERK proteins have been widely reported to regulate the proliferation and survival of cancer cells in several ways. Although ERK has been demonstrated to behave either as a promoter and suppressor of apoptosis in tumour cells, the role of ERK in suppressing apoptosis shall be primarily discussed in view of the scope of this thesis. Before discussing the distinct mechanisms of ERK-mediated suppression of apoptosis in cancer cells, a brief outline of the biochemical events leading to cellular apoptosis is necessary.

1.4.1   What is apoptosis?

Apoptosis is a systematic cell-death pathway which is important not only in normal cellular development, but also in cellular maintenance and monitoring the extent of cellular damage induced by external sources. Apoptosis, often termed as a "programmed cell-death process", is elicited by several unique cellular processes including the activation of caspases, release of mitochondrial cytochrome C, cleavage of PARP, the appearance of a distinctive DNA ladder, and a distinct and characteristic cellular morphology (**Figure 1.3**) [57].
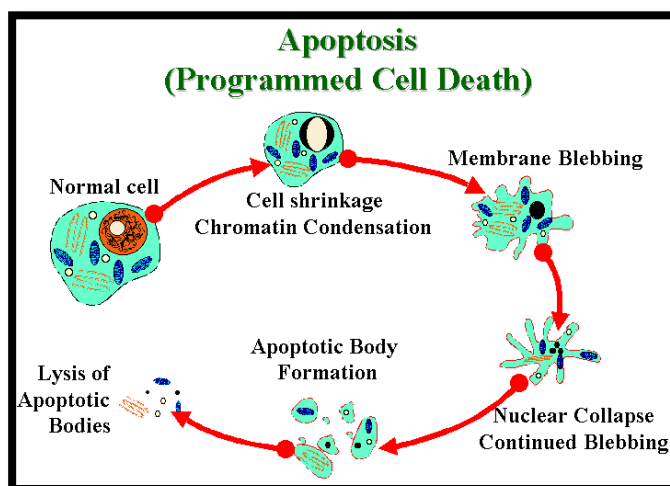
Figure 1.3 Mechanistic mode of apoptotic cell death. Figure has been adopted from [16].

In addition to apoptosis, necrosis is also a form of cell death which is, however, characteristically distinct from apoptosis. Necrotic cell death is initiated by mitochondrial inhibition and is associated with the breakdown of the cytoskeleton, cellular swelling and progressive increases in plasma membrane permeability [58]. Apart from morphological differences as mentioned earlier, whereas apoptosis is a synchronized and frequently energy-driven process, involving the stimulation or suppression of multiple genes and kinases, necrosis does not involve gene expression and is a passive externally-driven process that results in cell death in the absence of any metabolic activity [59]. In short, apoptosis mechanism removes the specific cell with a minimum of risk or damage to nearby cells.

Amongst the various factors that suppress apoptotic cell death, the ERK-mediated MAPK pathway plays a significant role via different mechanistic pathways. In tumorigenic cells, in particular, over-activation of the ERK-mediated pathway is responsible for suppressing apoptosis, thereby resulting in uncontrolled proliferation and enhanced cell survival. Many ways that ERK-mediated MAPK signalling adopts in suppressing apoptosis has been elucidated in the following section.

1.4.2   Role of ERK in disablingapoptosis

The mechanisms by which ERK1/2 activation inhibits apoptosis are intricate and vary, depending on the cell and tissue type involved and the cellular regulatory influences that the cell receives. In mammalian cells, ERK 1/2 activation can suppress

apoptosis at levels which are either upstreamor downstream or unrelated to the process of change in mitochondrial trans-membrane potential and cytochrome-c release [60].

1.4.2.1 ERK-mediated inhibition of apoptosis via BAD phosphorylation

Several signalling pathways have been demonstrated to regulate protein tyrosine phosphorylation of the pro-apoptotic protein BAD at specific serine residues [61]. In addition to phosphorylation at Ser136 by phosphoinositol 3-kinase/AKT signalling, ERK2-activated p90 ribosomal S6 kinase p90RSK has also been reported to induce BAD phosphorylation at Ser112and its subsequent sequestration by 14-3-3 chaperon proteins from the mitochondria. In contrast, dephosphorylation of BAD by ERK1/2 inhibitors, as depicted in **Figure 1.4**, is characterized by its translocation into mitochondria and its heterodimerization with pro-apoptotic proteins lke Bcl-2, thereby inducing apoptosis [62]. This highlights a pivotal role played by ERK-mediated signalling pathway in preventing BAD-mediated apoptosis.
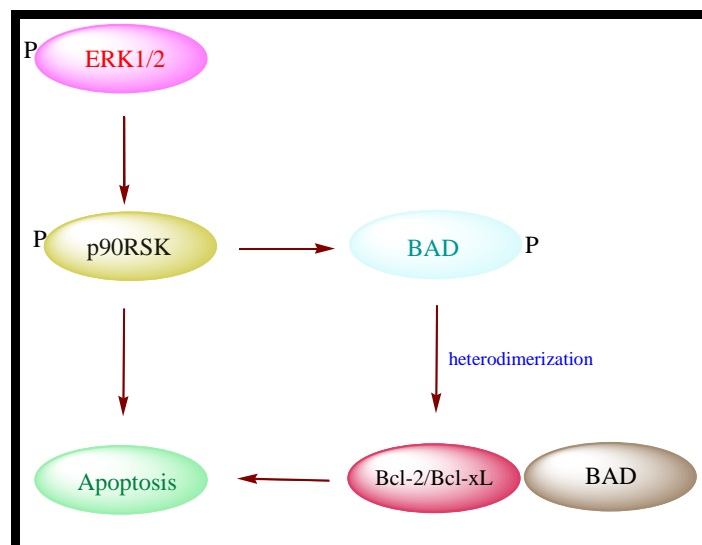
Figure 1.4 ERK-mediated inhibitions of apoptosis via BAD phosphorylation

1.4.2.2 ERK-mediated upregulation of anti-apoptotic Mcl-1

Apart from suppressing the activity or expression of pro-apoptotic proteins, ERK1/2 can also promote cellular survival by enhancing the activity of anti-apototic molecules like myeloid cell leukemia-1 (Mcl-1). Mcl-1 protein, homologous to the Bcl-2 family, is another of the most over-expressed genes in cancer cells [63]. Mcl-1 promotes cell survival by disrupting the release of cytochrome-c from mitochondria

thereby, suppressing apoptosis.It has been reported that phosphorylation and activation of Mcl-1 by ERK1/2 proceeds at two residues Thr92 and Thr163 resulting instabilization of Mcl-1. This is evident from the report that paclitaxel, a chemotherapeutic drug, has been reported to induce apoptosis by down regulation of Mcl-1 by ERK1/2inhibition in breast cancer cells [64].

1.4.2.3 ERK-mediated cellular survival via proteosomal degradation of pro-apoptotic BIM protein

The Bcl-2 homology 3(BH3) domain only protein, BIM, is a potent pro-apoptotic protein belonging to the Bcl-2 protein family.BIM acts like a tumour repressive gene and is positively and negatively regulated by transcription, phosphorylation and degradation [65]. Multiple BIM phosphorylation sites have been identified which are linked to both suppression and induction of apoptosis. In recent years, advances in basic biology have provided a clearer picture of the mechanism by which BIM kills tumour cells and how BIM expression and activity are repressed by growth factor signalling pathways. In the presence of ERK1/2 for instance, BIM undergoes polyubiquitination and subsequent proteosomal degradation, upon phosphorylation at multiple sites (**Figure 1.5**).
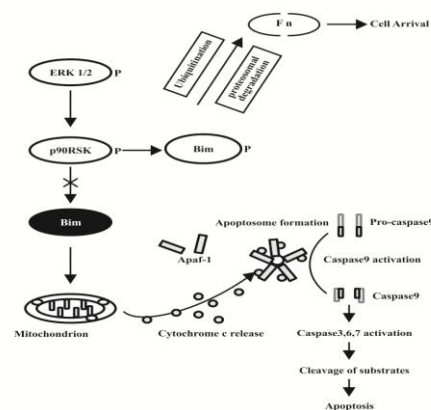
Figure 1.5 ERK-mediated cellular survivals via proteosomal degradation of proapoptotic BIM protein

This is evident from blockage of BIM phosphorylation sites by MEK inhibitors, thereby confirming that ERK1/2 is a probable BIM-regulatory kinase. Another report has demonstrated the role of ERK-mediated p90RSK in mediating the phosphorylation and degradation of BIM-EL at Ser69hence blocking caspase-mediated apoptosis in K562 cells [66].Therefore, a decreased availability of pro-apoptotic BIMvia ERK-mediated proteosomal degradation results in attenuated levels of apoptosis and thereby, enhanced cellular survival [67].

1.4.2.4 ERK-mediated stimulation of anti-apoptotic transcription factors-CREB and STAT3

CREB is a post-translationally activated transcription factor that has been implicated in numerous brain functions including cell survival. This is evident by the observation that inhibition of CREB phosphorylation at Ser133 triggers neuronal apoptosis [68].In addition, the anti-apoptotic role of CREB has been demonstrated by its loss resulting in triggering a Bax-mediated apoptosis [69].

In response to both mitogenic and stress-related signals, ERK-activated p90RSK phosphorylates and stimulates the transcription factor CREB, by allowing the recruitment of its co-activators- CBP and p300 [70].In particular, MSK-1, a p90rsk family member with 45% sequence similarity torsk-2, phosphorylates CREB with high stoichiometry [71].Relative to other risk family members, MSK-1 seems to have a higher affinity for CREB, indicating that MSK-1 might have a primary function in regulating CREB activity in response to mitogen/stress stimuli [72]. In addition, ERK1 has also been reported to single-handedly direct phosphorylate CBP *in-vitro* and increase its transcriptional activity, thereby resulting in attenuated apoptosis [73].

In addition to CREB, STAT3 is a latent cytoplasmic transcription factors that is uniquely activated at the plasma membrane by tyrosine and serine phosphorylation and translocate into the nucleus to activate anti-apoptotic factors. Another evidence of the anti-apoptotic role ofERK comes from the upregulation of STAT3 via phosphorylation at Ser727in both *in-vitro* and *in-vivo* experiments [74].

1.4.2.5 ERK-mediated stimulation of oncogenic MCT-1

Additionally, multiple copies of oncogenic T-cell lymphoma-1 (MCT-1) have been demonstrated to require ERK-mediated phosphorylation at Thr81 for stability [75]. MCT-1 promotes malignant transformation of normal cells and inhibits apoptosis, potentially through Akt activation and dysregulation of the cell cycle. SinceERK is required for MCT-1 stability, inhibition of ERK activity could potentially render transformed cells susceptible to therapeutic agents. Accordingly, the use of ERK1/2

inhibitors in MCT-1-expressing cells could potentially attenuate cellular proliferation and lead to apoptosis.

1.4.2.6   ERK-mediated stimulation of AIFs

Interestingly, it has been suggested that ERK can regulate apoptosis induction via apoptosis inducing factor (AIF) in breast cancer cells.AIFs are flavoproteins that are that are involved in triggering cellular apoptosis via a caspase-independent pathway [76].Originally localized in the mitochondrial membrane, AIFsare translocated to the nucleus upon activation of death stimuli. This results in pro-apoptotic effects like chromatin condensation, fragmentation as well as PARP cleavage that serve as typical hallmarks of apoptosis [77]. The role of ERK inhibition in inducing apoptosis inducing factor (AIF)-mediated apoptosis in epithelial breast cancer cells is evident from the nuclear translocation of AIF induced by ERK- inhibitors likePD98059, thereby resulting in apoptosis in MCF-7 cells. Thus, the effect of PD98059 provides evidence that suppression of ERK-mediated MAPK can result in apoptosis via disruption of mitochondrial membrane with the release of AIFs.

1.4.2.7   ERK-mediated regulation of pro-apoptotic caspases

Belonging to a family of cysteine proteases, caspases are observed to play a distinct role in the initiation and execution of apoptotic cell death, failure of which leads to tumorigenesis and various other auto-immune diseases [78]. Of the 12 caspases that have so far been identified in humans, more than half of them serve as proapoptotic cell death inducers.Amongst the commonly studied pro-apoptotic caspases, caspase-2, 8, 9 and 10 serve as apoptotic initiators whereas caspase-3 and 7 serve as executioner caspases.There is direct evidence of the inhibition of caspase-mediated apoptosis upon ERK1/2 stimulation (**Figure 1.6**). There have been reports highlighting the regulation of pro-apoptotic caspase 9 by ERK2. Caspase 9 is inhibited by phosphorylation at Thr125 in a MEK1/2-dependent manner in cells stimulated with EGF or TPA. Phosphorylation at Thr125, a conserved MAP kinase consensus site targeted by ERK2, *in- vitro*, is sufficient to block caspase-9 processing and subsequent caspase-3 activation thereby preventing apoptosis.
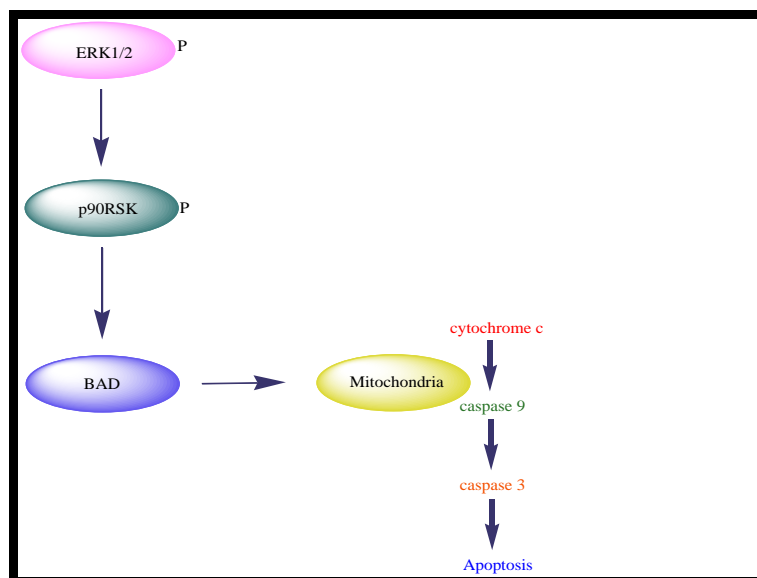
Figure 1.6 Anti-apoptotic mode of action of ERK1/2 via caspase inhibition

In summary, ERK1/2 has been demonstrated to suppress apoptosis by down regulation of pro-apoptotic molecules via a decrease in their activity or their protein expression by transcriptional repression. Conversely, ERK1/2 can also promote cell survival by upregulating anti-apoptotic molecules via enhancement of their activity or their transcription. Evidence to support the role of ERK in antagonizing the extent of apoptosis in KB-3-1 cells has also been observed in this study. In accordance with the findings, compound **12** that has been demonstrated to induce apoptosis in KB-3-1 cellshas also been observed to inhibit the activation of ERK1/2 in KB-3-1 cells. This further corroborates the notion of the anti-apoptotic effects of ERK1/2 in mammalian cells.

1.4.3 ERK asstimulator of protein translation in cancer cells

The higher eukaryotic ribosomes are composed of two subunits that are designated as 40S (small) and 60S (large) subunits. The mammalian 40S subunit is composed of a single RNA molecule, 18S ribosomal (r) RNA and 33 proteins whereas the 60S subunit consists of three RNA molecules: 5S, 5.8S and 28S rRNAs and 46 proteins [82]. Ofallribosomal proteins, it is ribosomal protein S6 (rpS6) that has attracted much attention since it was the first protein that was shown to undergo inducible phosphorylation. Ribosomal protein S6 (rpS6) is a key component of the translational machinery in eukaryotic cells and is essential for ribosome biogenesis.This

is evident from a study that demonstrated that a 33kDa protein, later identified as rpS6 protein and residing in the small ribosomal subunit undergoes phosphorylation in rabbit reticulocytes.This has led to a number of reports validating the susceptibility to its phosphorylation by a range of stimuli rps6 is phosphorylated on five evolutionarily conserved serine residues with Ser236 being the primary site of phosphorylation.

The S6Ks were initially reported to phosphorylate several proteins that are associated with mRNA translation, including rpS6 by an Akt-mediated pathway (**Figure 1.7**). According to this mechanistic pathway, activatedAkt phosphorylates TSC2within theTSC1–TSC2 tumour suppressor dimerat multiple sites [83]. This phosphorylation blocks the ability of TSC2 to act as a GTPase-activating protein (GAP) for Rheb thereby allowing Rheb–GTP to accumulate and to operate as an activator of the rapamycin-sensitive TOR complex 1 (TORC1) [84].It is TORC1 that finally activates S6Ks that phosphorylate rps6.However, the Akt-mTOR mediated signalling is not the only mechanistic pathway involved in protein translation via rps6 phosphorylation. Initial hints to the role of the ERK-mediated signalling in promoting protein biogenesis came from a report highlighting that RSK-mediated rpS6 phosphorylation contributes to cellular mRNA translation (**Figure 1.7**).
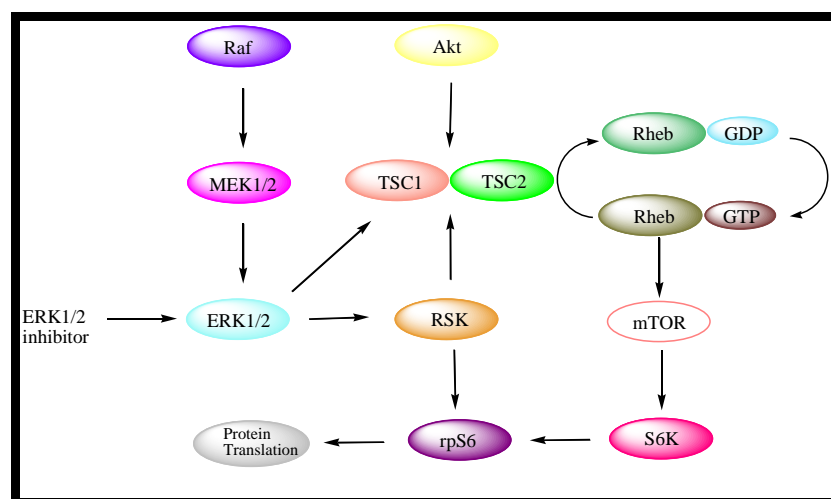
Figure 1.7 ERK promotes protein translation via an Akt-mTOR-independent pathway

This is evident fromRSK-mediated rpS6 phosphorylation that was reported to facilitate assembly of translation pre-initiation complex and to correlate with cap-dependent translation [85].In addition, RSK mediated phosphorylation of GSK3β at Ser9 causes a subsequent stimulation of translation factor eIF2B that

contributes to cap-dependent translation [86].Several reports have detected low levels of phosphorylation ofrpS6 at Ser235 and Ser236 in cells lacking both S6K1 and S6K2.This phosphorylation is abolished by treatment by either U0126 (ERK/MEK inhibitor) or PD184352 (ERK inhibitor), indicating the involvement of a MEK/ERK-dependent kinase [87]. Likewise,arecentstudywithHEK293Ecells has shown that Ser235 and Ser236 remained partially phosphorylated in cells treated with rapamycinwhich completely inhibits mammalian target ofrapamycin (mTOR) and thereby its downstream target S6K indicating the presence of an mTOR-independent pathway leading to rps6 phosphorylation.In addition, in $TSC2^{+/-}$ tumour cells, activated ERK has also been reported to directly repress post-translational activation of TSC2 at sites that are distinct from those that are phosphorylated by Akt thereby resulting in suppression of TSC1-TSC2 complex formation and a subsequent attenuation of protein translation [88].In contrast, wild-type TSC2 appeared to be ineffective in suppressing tumorigenecity in the presence of activated ERK. Therefore, ERK1/2, in addition to its direct substrates-RSKs servesto mediate the phosphorylation of ribosomal protein rpS6 by an mTOR-independent pathway, thereby contributing to intra-cellular protein translation. An evidence of a cross-talk between the ERK-mediated MAPK pathway and protein translation has also been observed in this study. In experiments carried out to delineate the cellular mode of action of **12** against mammalian cells, the synergistic down-regulation of the ERK-mediated signalling pathway and rate of intra-cellular protein translation in **12**-treated KB-3-1 cells has been observed.

1.4.4   **S**mall-**molecule inhibitors of MEK/ERK as chemotherapeutic agents**

As mentioned earlier, MEK1/2 are the only known proteins to phosphorylate ERK 1/2 [89]. As a consequence, targeting MEK also facilitates a subsequent inhibition of its downstream substrates, particularly ERK. During the past decade, the design and analysis of MEK inhibitors like PD98059 and U0126 have become instrumental in widening the therapeutic window for treatment of cancer and related disorders [90]. However, since ERK is recognised to affect a
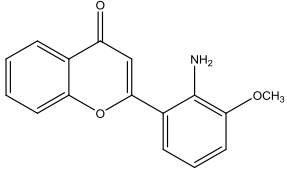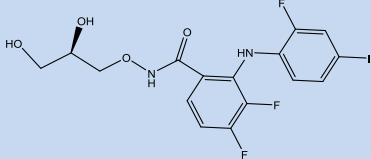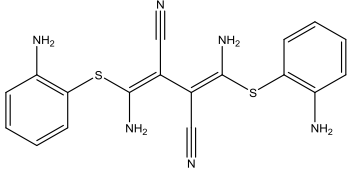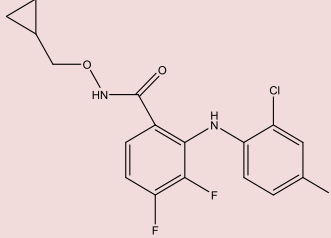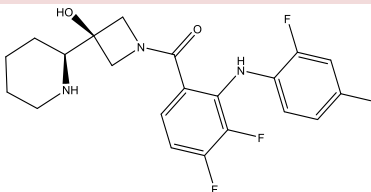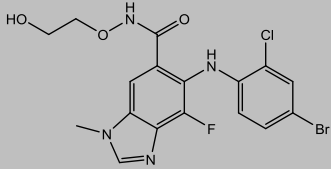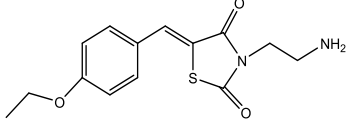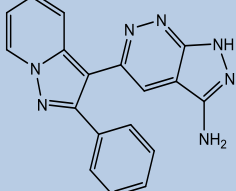
plethora of vital cellular proteins necessary for cellular survival, an indiscriminate modulation of the MEK-ERK mediated pathway has resulted in unwarranted cellular toxicity in both normal and tumorigenic cells. As a consequence, such inhibitors have been characterised with a poor pharmacological profile that raised questions about their clinical efficacy. Until hitherto, some representative examples of MEK/ERK inhibitors analysed for their clinical efficacy against tumorigenesis have been listed in **Table 1.3.**

1.4.5   Structural and biochemical differences between ERK 1 and ERK 2

In a majority of research papers, ERK1 and ERK2 isoforms are generally grouped together as ERK1/2. This implies that the structure and functions of both these isoformsare apparently interchangeable.

However, during the past couple of years, several animal studies have reported critical differences in ERK1 and ERK2 isoforms on the basis of their relative cellular abundance, structure and vitality. For instance, Saba-El-Leil *et al*. reported a not-so similar effect of the vitality of ERK1 and ERK2 in a mouse model. According to them, ERK1 gene was indispensable for the development of mice but a depletion of the ERK2 gene served lethal to the mouse embryo due to impairment in development of the mouse embryonic trophoblasts [79].These findings clearly highlight a difference in the vitality and functions of ERK1 and ERK2, irrespective of their similar homology. Results from such experiments indicate that deficiency or inhibition in ERK2 activity apparently exerts more severe consequences on biological mortality relative to ERK1. This hypothesis is further evident from the invalidation of ERK2 in the central neural system (CNS) leads to anomalies in multiple aspects of social behaviors, decreased anxiety-related attitude, and impaired long-term memory [80].

Table 1.3 Representative small molecules serving as MEK/ ERK inhibitors

Compound	Molecular Target	Tumour Type	Trial Phase	FDA Approval	Structure
PD98059	MEK 1/2		N/A	Disapproved	
PD0325901	MEK 1/2	Breast; Colon; Melanoma; NSCLC	I/II	Disapproved	
U0126	MEK 1/2		N/A	Disapproved	
CI-1040	MEK 1/2	Breast; Colon; Pancreatic; NSCLC	I/II	Disapproved	
XL518	MEK 1/2	Advanced solid tumours		Disapproved	
AZD6244/ ARRY-142886 I	MEK 1/2	Advanced solid tumours	I/I	Disapproved	
76	ERK2		N/A	Disapproved	
FR180204	ERK 1/2	N/A		Disapproved	

Inhibition of ERK1 and ERK2 is a frequently observed feature of several chemotherapeutic agents. However, the degree to which some of these compounds inhibit the activation of these ERK isoforms either by repression of its catalytic activity or direct binding to these kinases has been found to vary. For instance, FR-148083 has been earlier reported to be a potent and selective ERK2 inhibitor. The compound has been revealed to bind to the ATP-binding site of ERK2 by making a hydrogen bond with Met108 in the hinge region [81]. However, a similar extent and nature of binding has not been observed in case of ERK1. Such examples of selective binding preference, of certain small molecules, towards a specific isoform of ERK underscores a certain degree of distinct structural and biochemical activity of the different ERK isoforms. In regard to this upcoming topical aspect, the varying roles of ERK isoforms demand further investigation and confirmation in terms of their potential, individualistic interactions with chemotherapeutic selenium-containing compounds. An attempt to identify and distinguish between the individualistic interactions of **12** with ERK1 and ERK2 isoforms has been made in a DARTS experiment using a HeLa cell line that shall be discussed in its corresponding section. Nevertheless, future studies in underscoring the distinct biochemical roles of the ERK isoforms could be helpful in filtering out the characteristic roles of selenium-compounds on the basis of their varying interactions, if any, with the ERK isoforms.

1.5   Identification of protein targets of anti-cancer molecules

In our age of ever-rising diseases of known and unknown origin, the need for more efficacious drugs is on the rise. In order to develop any potent drug of either natural or synthetic origin, a very important parameter has always been to assess the ability and nature of interactions of the drugs with specific cellular targets of interest, inside the biological system.Basic research focused on comprehending the molecular mechanism of action of small molecules has proved to be a goldmine for comprehending the role of importance of pivotal cellular proteins in the etiology of biological disorders. A large fraction of potent compounds have been, till date, filtered out successfully from primary screening methodologies involving *in-vitro* and *in-vivo* experiments, in addition to phenotypic and molecular read-outs. While the opportunity of hunting novel compounds from such assays is great, the utility in further pushing

these compounds to the clinic still remains largely limited. This is primarily due to the paucity of information regarding the compounds´ actual physiological behaviour with potential cellular targets. An identification and validation of the same is apparently the most challenging and time-consuming job, in addition to its utmost importance for labelling potential molecules as "drugs". Moreover, the small molecules, screened for analysing their ability to specifically modulate activity of a given protein of interest, often have been observed to bind with non-specific proteins also, many of which may not be predicted conveniently by sequence or structural homology [91]. Although mechanistic studies towards analysing the mode of drug action has a long history, identification of direct drug-targets has its origin in state-of-the-art techniques like affinity chromatography, biochemical fractionation and radioactive ligand binding assays. Purification of enzymes, on the basis of their relative binding affinities with small molecule inhibitors, was first initiated in the mid-1900s by Leonard Lerman and subsequently employed for novel identifications by the McCormick and Anfinson laboratories in the 1960s[92]. During the same period, several other research teams had begun the use of radioisotope-labelled compounds and biochemical fractionation to enrich drug-binding proteins from crude tissue extracts and cell lysates. A nicotinic acetylcholine receptor was the first neurotransmitter receptor to be purified, using a radioactive snake toxin in a binding assay [93].

Amongst the many prominent target-identification techniques deployed so far including radioaffinity and photoaffinity approaches, affinity chromatography is still apparently the most sought-after technique [94]. However, due to its several limitations, an alternative approach called DARTS has been recently adopted for a convenient identification of cellular targets of potential drugs and drug-like molecules.

1.5.1   DARTS - an alternative target-identification approach

Given the limitations of current target identification methodologies, a target identification strategy referred to as "DARTS "relies only identifying a possible interaction of the compound with a target protein without any chemical modifications of the former. Therefore, such an approach could potentially identify any protein target of a small molecule, with no limitations posed by chemical-modifying strategies or mechanism of action. In addition, the concept that a small molecule would stabilize its

target protein's structure and result in a protease resistance has offered a possible solution to the problem of target identification. Stabilization of a protein upon substrate-binding is a well-known phenomenon that offers enhanced resistance to cellular proteins against structural disruption and subsequent denaturation by heat and chaotropic agents. This enhanced stability has been proposed to result from a shift in the protein's thermodynamic stability in order to favor its ligand-bound state which restricts the drug-bound protein's original flexibility and movement. One recent example that lends support to this concept comes from the finding that Tacrolimus has been observed to protect the immunoenzyme FKBP1A from proteolytic degradation in a DARTS experiment. It actually leads to stabilization of a high-energy backbone conformation of the enzyme that is otherwise not commonly observed in the native conformation of unbound FKBP12 [95].In accordance with a similar DARTS experiment carried out in this study, **12** has been observed to exhibit a concentration-dependent and selective protection of ERK2 from pronase-mediated proteolytic degradation in a KB-3-1 cell model. This finding could,therefore, open a new window towards a more comprehensive understanding of the cellular mode of interaction of chemotherapeutic organodiselenides like **12** with potential oncogenes like ERK2.

1.5.1.1 Advantages of DARTS over chromatography techniques

With respect to the relatively few reports regarding small molecule-induced protease resistance, there has been, however, an insufficient realization regarding the generalisation of this scheme as a discovery approach for identifying unknown drug-targets. DARTS offers an unprecedented ability to identify new proteins targeted by small molecules by exploiting this approach. It is similar to affinity chromatography in terms of its affinity-based methods that employ complex protein samples and selectively enrich the target protein(s) while removing all non-target proteins. However, whereas affinity chromatography utilizes a positive enrichment approach by selectively pulling out the target proteins and leaving behind non-targets, DARTS uses a negative enrichment methodology by digesting non-target proteins while retaining the target proteins on account of their resistance to proteolysis (**Figure 1.8**). In case of the affinity chromatography approach, a primary limitation is the extensive binding of non-specific proteins to the matrix that restricts the isolation of true targets. Although extensive washing of the matrix can help decrease the number of non-specific binders, weaker

specific binding agents will often be lost during the process. In contrast, DARTS does not require washing and can, therefore, be used to analyse lower affinity interactions too. DARTS is also novel since it can screen and identify putative protein-binding small molecules without the need for their chemical derivatization or chemical identification. This is a tremendous advantage over affinity chromatography and other prior methods.
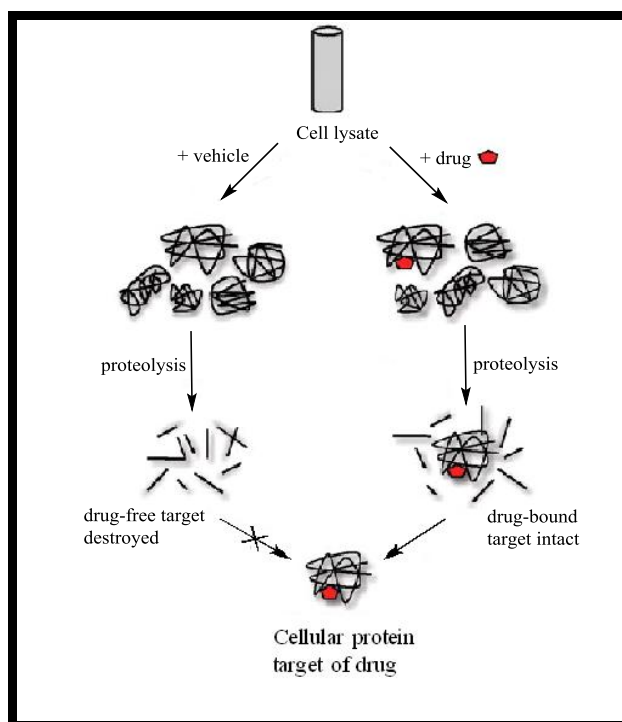
Figure 1.8 Schematic representation of drug-target identification approach (DARTS)

1.5.1.2 Improvisation of DARTS: introduction of gel-free approach

The success and reliability of DARTS primarily depends on the abundance of the target-proteins to be identified, in addition to their sensitivity (or resistance) towards proteolytic degradation. In certain cases, the level of target proteins within the cell is not sufficient enough to be stained for visualization. Even in case it is, its enrichment in the biological sample is susceptible to masking due to its co-migration with many other low or moderately abundant proteins of the same molecular weight on the gel.To counter such limitations, Lomenick *etal*. have attempted to improvise the DARTS approach by the introduction of a more sensitive gel-free proteomics approach. Briefly, this approach involves the enrichment of protein samples upon dialysis after protease treatment, by elimination of unwanted non-tryptic peptides from the sample (generated during the protease treatment [95]. This has been proposed to attenuate sample complexity, thereby

facilitating the convenient gel-free proteomic analysis of complex protein mixtures. This involves the subjection of digested protein samples to a MudPIT analysis that is based on separation of tryptic peptides by strong cation exchange and reversed-phase HPLC for analysing complex protein mixtures by mass spectrometry. This gel-free proteomics approach has been proposed to be more sensitive than a gel-based approach, in addition to its compatibility with all the mentioned label and label-free quantitative techniques.

In conclusion, DARTS offers a novel proteomic approach to circumvent the restrictions in the way of target-identification of drugs and drug-like molecules by invalidating the need for chemical modification of the screened molecules. This approach shall not only strengthen the basic concepts of chemical genetics but also facilitate a wider impact of the same on cellular biology and medicine.

1.6 Effects of chemical speciation on chemotherapeutic efficacy of selenium-containing compounds by modulation of biochemical pathways

1.6.1 Metabolism of selenium

The physiological pathways contributing to the metabolism of selenium are intricate and involve the formation of a plethora of many intermediate metabolites. A schematic diagram showing basic selenium metabolism is presented in **Figure 1.9**.Selenium is incorporated into its combined form either as an inorganic form (selenite, selenate) or as an organic form (SEM or SeC). Further, these are rapidly metabolized into broadly two groups of metabolites- the hydrogen selenide pool and the methyl selenol pool. In animals, hydrogen selenide is a critical selenium metabolite which can be formed from inorganic selenite via selenodiglutathione or from selenium-containing amino acids via enzymatic activity (**Figure 1.9**). However, hydrogenselenide is relatively toxic but excess of it is susceptible to varying degrees of methylation and excretion. Monomethylated forms are the primary excreted products at normal selenium levels but in cases where large quantities are ingested, trimethyl selenonium ions have also been reported to be excreted in the urine [96].
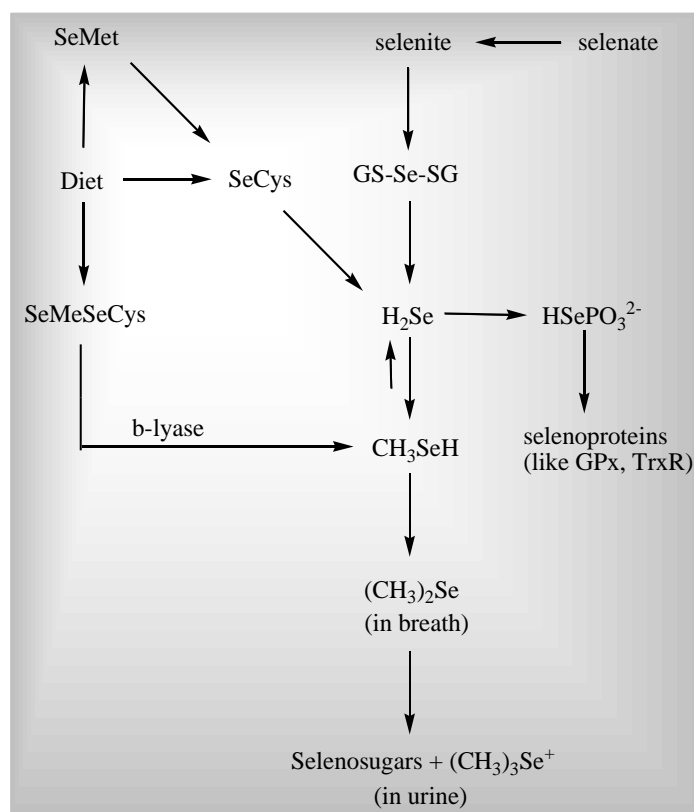
Figure 1.9 The metabolic cycle of selenium in the eukaryotic system

1.6.2   Biochemical effects of different chemical pools of selenium

Numerous *in-vitro* studies have shown that the monomethylated selenium pool induced numerous cellular, biochemical and gene expression responses that were distinct from those induced by the forms of selenium that enter the hydrogen selenide pool. Together, these findings support the presence of these two different pools of Se metabolites that induce distinct types of biochemical and cellular responses and exert differential impacts on angiogenic processes. It has been proposed that the active chemotherapeutic metabolite of selenium is apparently a monomethylated species (presumably methylselenol) and that the chemopreventive efficacy of a given selenium-containing compound might depend on the degree of its metabolic conversion into that form [97]. Supporting evidence to strengthen this hypothesis was obtained by comparing the *in-vivo* cancer-preventing efficacy of these different forms of active selenium metabolites. Methyl selenol displayed greater preventing efficacy than hydrogen sulfide or dimethyl selenide in the chemically induced rodent mammary carcinogenesis model [98]. Moreover, it was found that sodium arsenite which retards the conversion of hydrogen sulfide to methyl selenolled to an attenuation of the overall

anticancer activity whereas an inhibition of further methylation of methyl selenol increased the efficacy [99].

Both inorganic and organic forms of selenium can be utilized as nutritional and supplemental sources of selenium. Amongst the inorganic forms, sodium selenite was the first compound to be assessed for its chemopreventing studies. Found in low concentrations in nature, this compound is reduced into hydrogen selenide in the presence of GSH, by a number of intermediate steps (**Figure 1.9**). On the other hand, organic selenium is represented by selenoamino acids likeSeC and SEM. The main nutritional form SEM is not an oxidizing agent, however its metabolites like hydrogen selenide have strong oxidant potential [100, 101]. SEM is transformed into its active metabolite hydrogen selenide either through the trans-selenation pathway into SeC followed by β-lyase reaction into methylselenol, followed by demethylation reaction (**Figure 1.9**.)

1.6.2.1 Chemotherapeutic effects of selenium incorporated compounds: Role in apoptosis

The molecular basis of chemotherapeutic efficacy of selenium-incorporated compounds has been extensively studied to depend on their contribution in predisposing tumour cells toapoptosis. As mentioned earlier, the first studies linking selenium to apoptosis came out in the early 1990s when Pence *et al.* demonstrated the cytotoxic effects induced by selenite and selenocystamine in mouse keratinocytes, via apoptotic induction [102]. Since then there have been several studies investigating the relationship between selenium and apoptosis [103, 104 and 105].

In contrast to sodium selenite (an inorganic representative of selenium), the effects of organoselenium compounds on apoptosis are far more consistent (**Figure 1.10)**

For instance, there is substantial evidence that MSA can induce apoptosis in multiple cell types including breast cancer cell lines, hepatoma cell lines, prostate cancer cell lines, and in the same type of vascular endothelial cells we use as controls.
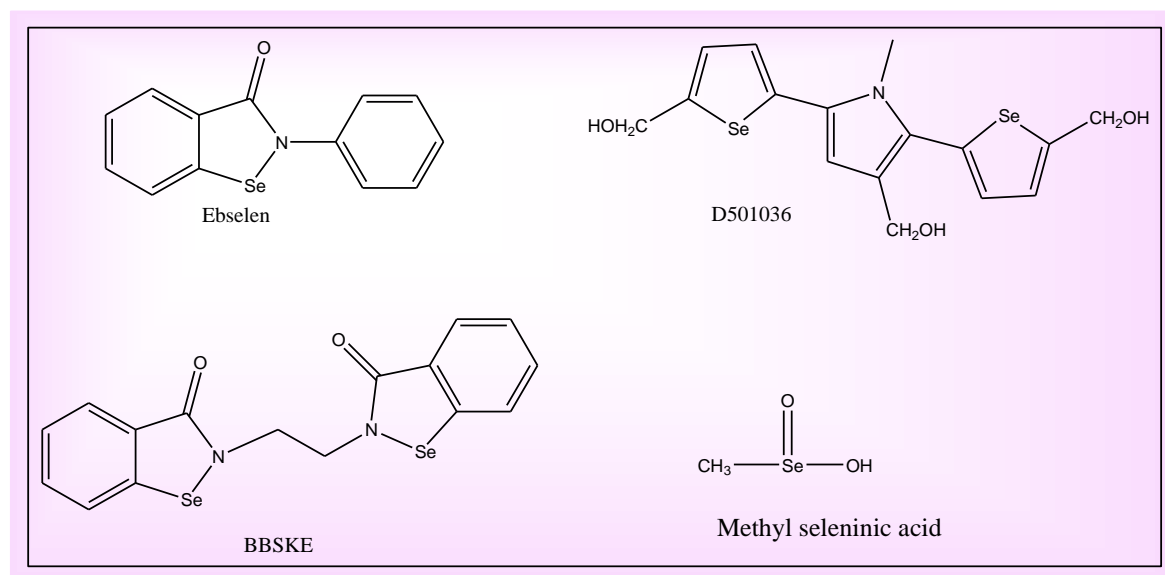
Figure 1.10 Representative examples of organoselenium compounds inducing caspase-mediated apoptotic inducers in tumor cells.

Among the recently identified organoselenium compounds, D-501036 induces apoptosis through an increase in the activities of caspase-9 and -3 in a dose and time dependent manner. An analogue of ebselen, BBSKE is a TrxR inhibitor that has demonstrated inhibition in the growth on the tongue cancer Tca8113 by induction of apoptosis via caspase-3 [106].Since the main compound of study in this study (**12**) is amethylenated diselenide and bears a close resemblance with recognised precursors of methy selenol, it is assumed that the potency of **12** could be attributed to its methyl selenol-like metabolites. As a result, the biochemical effects of methyl selenol shall be taken into account in more detail. As has been reported in numerous articles, methyl selenol is widely considered to be a critical metabolite and a potent apoptotic inducer in carrying out the chemotherapeutic effects of selenium [107, 108].

This is evident from its precursors like SeMCandMSA that have been demonstrated to be more effective in their chemopreventing efficacy compared to several other selenium-containing compounds [109]. In *in-vitro* systems, precursors of methyl selenol,likeMSA have beenshown to block progression of cell cycle, induce apoptosis and inhibit angiogenesis of cancer cells. The mechanisms by which these effects are obtained may involve redox cycling linked to oxidative stress-induced apoptosis and include changes in the expression of genes that control the cell-cyclecheckpoint and regulate signalling pathways and caspase-mediated apoptosis. For instance, Wang *et al.* have demonstrated that methyl selenol induces apoptosis and cell-

cycle arrest via caspase stimulation in prostate and leukemia cells [110].SeMC, a naturally occurring organoselenium compound, has been shown to cause caspase-dependent apoptosis of HL-60 human leukemia cellsand mouse mammmary epithelial tumour cells [111].Specifically, apoptosis has been observed to involve cell detachment, the activation of multiple caspases, mitochondrial release of cytochrome *c*, cleavage of PARP and DNA nucleosomal fragmentation [112]. This is evident from the apoptotic action of MSA in DU-145 and PC-3 human prostate cancer cells that is reported to be mediated by caspase-8 activation and cell detachment [103].

Caspase-12, an ER-resident caspase which is essential for ER-stress-induced apoptosis is also stimulated during MSA-induced apoptosis in PC-3 cells suggesting a probable role for ER stress in apoptosis induced by methyl selenol [113].Several groupshave also demonstrated the relation between the activation of intracellular signalling pathways like the ERK and AKT-mediated pathways as a consequence of caspase stimulation [104].

1.6.2.2 Modulator effects of selenium-incorporated compounds on intracellular biochemical pathways

As described earlier, mutations in genes that encode components of the PI3K/AKT/mTOR and RAS/RAF/MEK/ERK pathways occur at high frequency in a majority of cancers. In fact, a concurrent activation of the AKT and ERK-mediated pathways by separate mutations has been extensively observed in a significant portion of human tumours [114]. Abnormal activation of these pathways has, therefore, led to aberrant levels of protein translation and enhanced tumour cell survival as a result of decreased apoptosis.Inthis regard, attempts to delineate the mode of action of organoselenium compounds against cancer led to several reports that highlighted the inhibitory effects of a series of methyl seleno-imidocarbamates synthesized by Plano *et al.* against mTORC1 which is a critical protein within the PI3K-mediated pathway [16]. In addition, a concomitant downregulation of the ERK pathway was also observed by the same set of compounds. A little later in 2012, Plano *etal.* again observed this effect by inhibition of the PI3K and MAPK pathways by quinolinimidoselenocarbamates (another methyl selenium precursor) [115]. MSA,a prominent organoselenium compound and a potent source of methyl selenol has also been reported to effectively

inhibit the angiogenic factor-stimulated DNA translation (G1 to S progression) in tumour cells in the lower micromolar range [116].Methyl selenol which has been implicated on numerous accounts to be a critical selenium (Se) metabolite for its anticancer activity has demonstrated a significant inhibition of migration and invasive potential of HT1080 tumour cells at sub-micromolar doses and a potent inhibition of the ERK-mediated MAPK pathway in breast cancer cells [110, 117]. In 2009, Zeng *et al.* reported the direct inhibition of the anti-apoptotic ERK signalling by methyl selenol thereby inducing caspase-stimulated apoptosis. The same group also reported the down-regulation of several other oncogenic and anti-apoptotic genes in cells treated with methyl selenol [108]. These findings clearly highlight the anti-oncogenic and pro-apoptotic behaviour of methyl selenol against tumour cells.

1.7 Selenium: A janus-faced entity

A body of evidence indicates that selenium harbors a split personality in terms of its role in monitoring cellular proliferation and cell survival. This feature is further evident with variation in its chemical speciation and dosage at physiological levels [118]. Supra-nutritional levels of selenium have been apparently the main contributors in the prevention of several types of cancer, including lung, colon- rectum and prostate cancers by its regulatory effects on cell cycle and apoptosis [119].This also reflects that the observation of inhibitory effects of organo-selenium compounds, as described above, upon the corresponding intracellularsignalling pathways in tumour cellshave been observed mostly at higher doses.At relatively lower doses, these compounds behave in quite an opposite manner. Low doses of selenium from SEM, for instance, have been reported to stimulate ERK-mediated protein translation and, therefore, enhance cellular survival [120].In addition, only supra-nutritional doses of selenium have been proven to be effective in preventing tumour in animal models. Such doses are at least ten times greater than those required to prevent clinical signs of deficiency and are considerably higher than most human selenium intakes [99]. This observation also reflects a plausible cause of the negative findings observed in the SELECT and NPCT clinical trials in assessing the chemotherapeutic efficacy of selenium- supplementation in humans [23].However, an unregulated intake of dietary or pharmacological selenium supplements mainly in the form of SEM has a potential to expose the body tissues to

toxic levels of selenium with subsequent negative consequences on DNA integrity. Therefore, in order to cater to the broad interests to exploit the beneficial effects of selenium for better health and against chemotherapy, studies investigating the appropriate dose and suitable chemical form of selenium uptake are highly warranted to minimise the selenium-induced negative effects like toxicity and DNA damage.

1.8 Role of thioredoxin reductase in cancer

It has been widely observed that in addition to hypoxia, tumour cells thrive on enhanced levels of oxidative stress, compared to normal cells. These conditions can partly be attributed to a growing tumour mass that quickly outgrows its vascular networks and therefore lacks sufficient oxygen and essential nutrients [121]. In response to hypoxia, specific proteins like HIF-1 protein are stabilized in tumour cells that induce the expression of specific oncogenes that function to improve oxygenation through angiogenesis and erythropoiesis. Paradoxically, the HIF-1 protein in particular is regulated by oxidative stress-inducing factors like free radicals such as the superoxide anion, H_2O_2 and NO, in addition to many other factors including ontogenesis, growth factors and hypoxia [122]. As a consequence, the tumour-cell environment is characterised by levels of oxidative stress that are relatively higher when compared to those in normal cells. However, when oxidative-stress levels exceed their critical threshold, these tumour cells are also susceptible to oxidative damage. In order to maintain these levels to an extent that are sufficient for their proliferation without posing any risk of cellular suicide, tumour cells have adopted certain biochemical pathways including the over-expression of the natural cellular antioxidant enzymes like thioredoxin reductase (TrxR). This is quite evident from the abnormally enhanced levels of TrxR found in highly invasive and metastatic tumours [123]. Furthermore, high levels of TrxR have been implicated with increased resistivity of tumour cells towards chemotherapeutic agents including doxorubicin, cisplatin, docetaxel and tamoxifen. For example, in one study, breast cancer cells with high TrxR expression showed a significantly lower response rate to docetaxel than those with low TrxR expression.In addition to TrxR, over-expression of thioredoxin (TR), a direct substrate of TrxR, has also been observed in several primary cancers [124].

To date, TrxR is the only selenoprotein that can reduce the TR_{ox} in a NADPH-dependent manner. Three isoforms of TrxR have been identified in mammalian cells with all these isoforms containing the conserved active site. They are TrxR1, a cytoplasmic protein; TrxR2, a mitochondrial protein and the testis-specific TrxGR [125, 126 and 127].

1.8.1   Thioredoxin reductase: A potential chemo-therapeutic target

While TR itself has been regarded as a potential target, TrxR has been the focus of most TR system inhibitors [128]. An inhibition of TrxR leads to oxidation of TR and, therefore, an altered functionality of the entire TR system (**Figure 1.11**). A number of TrxR inhibitors have been tested in clinical trials with some approved by the FDA for use as cancer therapeutic reagents [129]. Curcumin is an example of a naturally occurring compound commonly found in turmeric that, in part, exhibits anticancer effects and irreversibly inhibits TrxR function [130]. Recently, both green and black teas have been found to contain antioxidant components that can inhibit TrxR and are capable of inhibiting HeLa cell growth *in-vitro* [131].
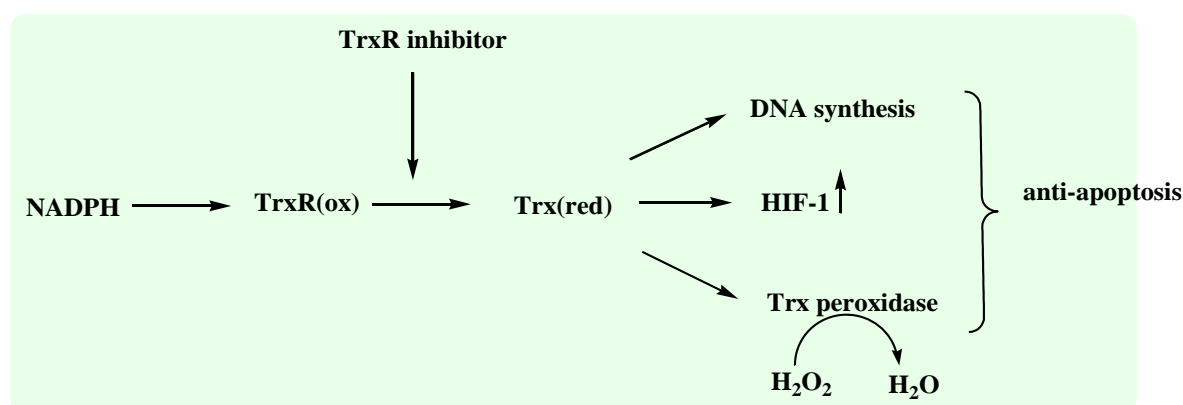
Figure 1.11 ROS-scavenging and anti-apoptotic role of the mammalian thioredoxin system

1.8.2   Role of selenium-containing compounds towardsthioredoxin reductase: substrate or inhibitor?

Mammalian TrxR can reduce a number of small molecule substrates in addition to their role in maintaining TR in their reduced form. These substrates include small molecules like ascorbic acid, lipid hydroperoxides, α-lipoic acid, and hydrogen peroxide. In addition to these molecules, mammalian TrxR also bear specificity towards reducing inorganic and organic forms of selenium. Most of the selenium-containing compounds investigated so far have extensively served as excellent substrates of TrxR. There have been plenty of reports citing the potential effects of selenium-containing compounds on the thioredoxin system. Poerschke *et al.* studied the behavior of several selenocompounds derivativesin lung cancer cells and observed that TrxR-1 modulated the cytotoxic effects of these compounds by modulation of mitochondrial dysfunction [132]. Similar effects were also observed in colon cancer cells with SeM and MSA [133]. Gundimeda *et al.*have also suggested that the employment of selenium-incorporated compounds, for example MSA, with agents that target TrxR-1 could influence their efficacy against malignant cells [134, 135].

Amongst the recently identified non-selenoproteins serving as TrxR inhibitors, ethaselen (also called BBSKE) has been reported to serve as a potent selenium-containing inhibitor of mammalian TrxR, subsequently inducing apoptosis in lung cancer cells (**Figure 1.12**) [136]. It must be specified that BBSKE is one of the derivatives of ethaselen with a relatively better pharmacological profile compared to ethaselen. Ethaselen, on the other hand, is marred by poor solubilityfeatures in water and commonly available organic solvents. In addition, bioavailability of ethaselen after oral administration has also been reported to be considerably less. Therefore, the formulation and successful chemotherapy with ethaselen as a TrxR inhibitor still remains a challenge. Moreover, the addition of selenites has been proposed to enhance cell- sensitivity towards some chemotherapeutic agents, such as acylfulvenes or illudin S by inhibition of TrxR-1 [137]. Recently, supranutritional doses of selenite have been demonstrated by Huang *et al.* to inhibit the TR system by directly modifying the thiol groups of TrxR, thereby predisposing SW480 cells to selenite-induced apoptosis [138]. Pathogenic parasites like *Trypanosoma brucei* that cause *African Trypanosomiasis,*possess a cellular enzyme calledtrypanothione reductase that serves as an analogue of mammalian TrxR.
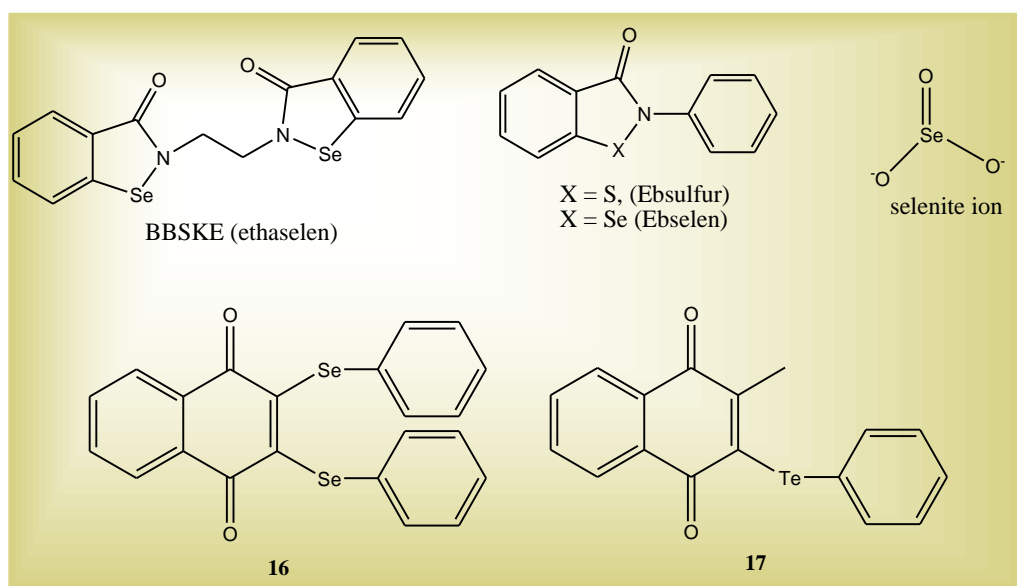
Figure 1.12 Representative examples of selenium-containing compounds serving as TrxR inhibitors

The sulfur analogue of ebselen, ebsulfur, has been recently demonstrated to potently inhibit this TryR in these tropical parasites, thereby resulting in their eradication by ROS-mediated apoptosis. Ebselen, itself, which serves as an excellent substrate of mammalian TrxR is a competitive inhibitor of TrxR of *E.Coli* in the sub-micromolar range. This can also partially explain its bacteriocidal effects against *E.Coli* and other bacterial agents like *MRSA* [139]. Taking the aforementioned discussion into account, TrxR is considered to be an important anticancer drug target due to its pivotal role in promoting both carcinogenesis and cancer progression.

In addition to the existing small library of selenium-incorporated TrxR-inhibiting molecules, the present study presents a first-hand evidence of two additional chalcogen-incorporated molecules (**16** and **17**) serving as potent inhibitors of mammalian TrxR.

Overall, the chemistry and biology of organic selenium compounds has been a topical area of research, particularly in due recognition of its potentialanti-proliferative effects against cancer,as observed in both *in-vitro* and *in-vivo* experimental models. This has been observed to be a consequence of an unprecedented number of biochemical interactions of organo-selenium species with indispensable intra-cellular bio-enzymes of known and unknown origin. However, the mystery surrounding the frequently observed split-personality of organic selenium, in terms of its diverse

therapeutic effects in general and anti-cancer mode of action in particular, still remain to be solved. This could partially be achieved by analysing the individualistic interactions of selenium-containing compounds with pivotal switches in the cellular biochemical pathways that may aid in framing a clearer picture in comprehending the true potential of organo-selenium species against cancer.

Aim and Strategy

Despite its trace levels in humans, selenium plays an essential and distinct role in the physiological system. From being an important constituent in mammalian cellular enzymes like glutathione peroxidase (which contains a selenocysteine) to being isolated from several organisms in a diverse chemical and biochemical format, selenium has emerged as an issue of topical interest both in terms of basic and applied research. Amongst the divergent biological roles discharged by this element, its promising anti-cancer properties have been an area of prime focus in this study and elsewhere. With regard to the extensive information that exists regarding the potential chemotherapeutic properties of several prominent selenium-containing compounds and their metabolites, there still exists a wide scope for a deeper investigation into the precise biochemical mode of action in a particular selenium-selenium bridge containing molecules. Considering the relatively poor natural access to such selenium-containing compounds, their chemical synthesis is yet another challenge in this area.

In view of these considerations, the first objective of this project was focussed towards the chemical synthesis of a diverse set of selenium-containing organic compounds as a tool for a subsequent biological evaluation at the comparative and individual scale. This part involved the chemical synthesis and physical characterisation of several monoselenides (**1**-**9**) and organodiselenides (**10**-**15**) followed by a biological analysis of the differences in their chemotherapeutic efficacy. With regard to the synthesis of the organodiselenides, apart from multiple benzene-substituted organodiselenides which have been extensively synthesized previously by several research groups, this study focussed towards the chemical synthesis of a rather less commonly investigated group of heteroarene-substituted diselenides.In view of *N*-containing heterocyclic systems like pyridines or quinolines in several synthetic and naturally-occurring biologically active molecules, the conjugation of *N*-containing heterocyclic rings with the redox-active diselenide moiety was carried out in an attempt to synergize the biological efficacy of these heterocyclic pharmacophores with those of the diselenide moiety [140-142]. With regard to aryl monoselenides, although such compounds have been reported previously and display a rather average anti-cancer activity, synthetic attempts were carried out to impart a certain degree of lipophilicity into these molecules for a probable enhancement in their biological activity [153]. This

has been based on the assumption of a probable enhancement in their cytotoxicity via a probable increase in their bioavailability and also uptake into tumour cells. In addition, on a relatively small scale, few previously studied chalcogen-containing naphthoquinones (**16** and **17**) were re-synthesized with a primary motive to elucidate the hidden biochemical reasons responsible for their chemotherapeutic mode of action using an array of sophisticated techniques for "intra-cellular diagnostics" now available at the HZI and its partner institutes in Braunschweig.

The second and main objective of this project involved the biochemical and biological analysis of several organodiselenides, some of which were used as benchmarks or controls. The monoselenides and diselenides synthesized were also compared for their anti-cancer activity relative to a lesser investigated set of organoselenium compounds called selenophenes. More importantly, an identification of potential cellular targets of organodiselenides and chalcogen-containing naphthoquinones was made to elucidate their mode of action against cancer.

Therefore, in a nutshell, the ultimate aim of the project has been the identification of novel organo-selenium compounds as promising chemotherapeutic candidates followed by a delineation of their mechanistic mode of action against tumour cells, both at the molecular as well as at the cellular level. A combination of chemical, biochemical and analytical techniques have been employed to synthesize and evaluate the anti-tumour efficacy of these organoselenium compounds. The studies have been multi-disciplinary in nature and involved the use of electrochemical methods, *in-vitro* bioassays, cell culture techniques and cutting-edge biological techniques like DARTS in attempts to identify potential intra-cellular targets of the most active compounds in tumour cells.

As part of the synthetic strategy, some previously established synthetic methodologies were employed to synthesize a range of heteroarene-containing organodiselenides (**10**-**15**) in substantial yields and in high purity [140-142]. Furthermore, attempts to enhance the cytotoxicity of organo monoselenides (**1**-**9**) against tumour cells were made to lend a higher degree of amphiphlicity to their chemical structure via a functionalization of heteroarene-substituted monoselenides with hydrophobic alkyl chains of varying carbon chain-length. Such synthetic endeavours were carried out with the assumption of a possible improvisation in the uptake of

monoselenides in tumour cells via an enhanced lipophilicity.The purity of the organoseleniums, prior to biological analysis was checked. Prior to an in-depth biological evaluation of the most active organodiselenides (**10-12**), their detailed physico-chemical studies namely ^{1}H, ^{13}C, ^{77}Se NMR and mass analysis werecarried out to re-confirm their synthetic purity.

To the best of my information, there is still a paucity of basic research focussed towards the identification of potential cellular targets of chemotherapeutic organodiselenides. In basic cancer research, it is imperative to obtain a comprehensive understanding of the precise mode of action of drug-like molecules at the molecular and cellular level. Therefore, as a preliminary step to underscore the vitality of organodiselenides in the futuristic design of anti-cancer molecules, a primary cytotoxicity screening of the synthesized organoselenium compounds was carried out using a standard MTT assay. Following an identification of the most active organoselenium compounds, several biochemical assays like the ATP assay, ELISA assay and the caspase 3/7 assay were performed to highlight the basic bio-molecular mode of action of such compounds against a particular KB-3-1 cancer cell line. Amongst the screened organoselenium compounds, a representative example (**12**) amongst the most active group of organodiselenides was subjected to a deeper analysis for a more comprehensive investigation into its molecular and cellular mode of action against KB-3-1 cells. In due recognition of a well-documented link between apoptosis-mediated tumour cell death and intracellular protein translation, *in-vitro* and *in-cell* translation assays were carried out to assess the modulatory effects exerted by **12**, if any, in the translational machinery of KB-3-1 cells. Furthermore, due to sufficient evidence which has highlighted the individualistic and/or synergistic role of several cellular signalling pathways in regulating the protein translation and hence proliferation of tumour cells, the modulatory effects of **12** on the oncogenic ERK-mediated and mTOR-mediated signalling pathways were also assessed via Western Blot analysis. Finally, in attempts to identify potential cellular targets of **12** in KB-3-1 cells, a relatively new yet highly advantageous drug-target identification approach called DARTS was carried out. Based on the principle of an altered susceptibility of specific cellular proteins towards proteolysis when bound to drug-like molecules, this approach can provide valuable insight into the selective affinity of compounds towards oncogenic proteins like ERK2, as in this study. In addition to anti-cancer effects, the cytotoxicity

of the most active organoselenium compounds were also analysed at a primary level against several pathogenic strains.Further, in attempts to identify the biochemical reasons responsible for the ROS-mediated induction of tumour cell death by representative examples of chalcogen-containing naphthoquinones (**16** and **17**), a thioredoxin reductase (TrxR) inhibition assay was carried out to assess the modulatory effects of **16** and **17** on mammalian TrxR. The TrxR enzyme was selectively analysed since the very same enzyme has been identified as a prime target of various ROS-inducing chemotherapeutic molecules in several previous reports [151]. In addition, several non-cell based redox assays like electrochemistry in addition to the DPPH and FRAP assays were performed in order to investigate into a possible cross-talk between the anti-cancer activity and anti-oxidant features of the organoselenium compounds which have displayed the highest anti-cancer effects*in-vitro*.

In summary, the objective and strategy of this thesis has involved a comparativeanalysis of the anti-cancer activity of a chemically and structurally distinct range of organoselenium compounds followed by a partial elucidation of the biochemical mode of action of a representative example (**12**) amongst the group of organodiselenides, and representative examples (**16** and **17**) of chalcogen-containing naphthoquinones for their futuristic applications against cancer.

Chapter 2

Materials and Methods

As a part of this project, a range of organoselenium compounds were synthesized to investigate their anti-carcinogenic and anti-microbial efficacy. The synthetic protocols employed for this purpose were based on two biological objectives.

The first objective involved an investigation into the biological efficacy of heteroarylselenoalkanes that have not received as much attention as the more popular selenium-containing compounds like methyl selenol and ebselen. Within this approach, variations in the alkyl side chain were introduced to investigate any probable modification in their corresponding biological efficacy. The second strategy was based on the synthesis of heteroaryldiselenides as a mean of comparative analysis of their biological activity with mono-selenoalkanesthat were synthesized in accordance with the first approach.

On the basis of these objectives,in addition to the re-synthesis of certain previously published compounds, several new heteroaryl group-conjugated monoselenides and diselenideswere synthesized using previously established synthetic procedures, for a broad and comparative biological analysis [140-142]. A part of the this work was carried out in the research group of Prof. K.K. Bhasin (Department of Chemistry, Panjab University, Chandigarh, India).

Upon primary cytotoxic screening of various heterocyclic organo-monoselenides, diselenides and chalcophenes against tumour cell lines, **12**was identified as the most active compound in terms of its anti-proliferative potential against selected tumorigeniccell lines. The isomeric diselenides **10** and **11** also demonstrated considerable anti-tumour efficacy in comparison to the otherdiselenides (**13**-**15**). As a result, the focus of this study was eventually diverted towards a detailed investigation of the biological efficacy of the most potential (di)aryldiselenides (**10**-**12**).It is important to mention that during thiswork; only aryl-functionalized diselenides were included in the

panel of the synthesized organodiselenides due to their higher chemical stability and lower toxicity profile, in comparison to the dialkyldiselenides.

In accordance with the results obtained from a preliminary cytotoxicity analysis, a deeper investigation into the cellular mode of action of a significantly active compound **12** was carried out. The cyclic framework of the diselenide moiety endows this compound **12** with unique properties of both an aryl and alkyl diselenide. As a result, an in-depth biological analysis of **12** was performed together with an evaluation of the more general anti-carcinogenic and anti-microbial potential of the other two significantly potent compounds **10** and **11**.

2.1   Chemicals for synthesis

Sodium borohydride, hydrazine hydrate (monohydrate), elemental selenium, diphenyldiselenide, diphenylditelluride, 6-bromohexane, 2-bromopropene, bromo-methane, 2-chloro-quinoline-3-carbaldehyde, pyridine-3-carbaldehyde, pyridine-4-carbaldehyde, anhydrous magnesium sulfate, ammonium chloride, 2,3-dibromo-naphthalene-1,4-dione, 2-bromo-3-methylnaphthalene-1,4-dione, uracil, 2-bromo-pyridine, urea, piperidine hydrochloride, barbituric acid and organic solvents (technical grade)were purchased from Sigma-Aldrich Chemie (Steinheim, Germany). Barbituric acid was stored in a dessicator prior to use. Deionised water (Millipore, Darmstadt, Germany, 18.2 MΩ.cm^{-1}) was used in all experiments, unless stated otherwise. Melting points have been uncorrected. TLC analysis was performed on aluminium TLC plates (silica gel 60G F$_{254}$, Merck, Darmstadt, Germany). All experiments were carried out under nitrogen or an argon atmosphere.

2.2   Chemical Synthesis

2.2.1   Synthesis of 4-methyl-2-(methylselanyl)pyridine(1), 2-(allylselanyl)-4-methylpyridine (2) and 2-(hexylselanyl)-4-methylpyridine (3)

To a vigorously stirred solution of 1,2-bis(4-methylpyridin-2-yl)diselane (3.1 g, 8.8 mmol) in THF under a N$_2$ atmosphere, sodium borohydride (0.7 g,

18.6 mmol) was added. The mixture was stirred at room temperature for 15 min until the solution turned colourless. Afterwards, 1-bromomethane (2.1 g, 22.1 mmol) or 3-bromoprop-1-ene (2.6 g, 21.7 mmol) or 1-bromohexane (3.6 g, 21.8 mmol) respectively were added dropwise via a septum to the colourless solution. The final mixture was stirred for approximately 1 h without exposing the reaction mixture to atmospheric oxygen. The formation of the product was assessed periodically using TLC. Upon disappearance of the reactant spot on the TLC plate, the reaction was quenched by addition of a saturated aqueous solution of ammonium chloride.

The crude product (containing **1**, **2** or **3**) present in the organic phase was washed repeatedly with distilled water. Ethyl acetate was used for extracting the crude product from the aqueous phase. Subsequently, the combined organic layers were dried over anhydrous magnesium sulfate and the solvents were removed under reduced pressure.

Silica gel chromatography was used for the separation and isolation of the desired compounds obtained from the organic phase. For this, the crude mixture was dissolved in a minimum amount of dichloromethaneand silica to form homogenous slurry of silica and the sample. This was then loaded onto a silica gel column, followed by elution with a mixture of ethyl acetate and hexane (5 : 95) to obtain the products as yellow oily liquid in moderate yield (around 61 %, 53 % and 43 % for compounds **1**, **2** and **3** respectively).

2.2.2 Synthesis of 3-methyl-2-(methylselanyl)pyridine(4), 2-(allylselanyl)-3-methylpyridine (5) and 2-(hexylselanyl)-3-methylpyridine (6)

To a vigorously stirred solution of 1,2-*bis*(3-methylpyridin-2-yl)diselane (3.2 g, 8.9 mmol) in THF under a N_2 atmosphere, sodium borohydride (0.7 g, 18.6mmol) was added. The mixture was stirred at room temperature for 15 - 20 min until the solution became colourless. Afterwards, 1-bromomethane (2.2 g, 22.5mmol) or 3-bromoprop-1-ene (2.7 g, 22.1mmol) or 1-bromohexane (3.7 g, 22.5mmol), respectively was added via a septum dropwise to the colourless solution. The final

mixture was stirred for approximately 1 h without exposing the reaction mixture to atmospheric oxygen. The formation of the product was assessed periodically using TLC. Upon disappearance of the reactant spot on the TLC plate, the reaction was quenched by addition of a saturated aqueous solution of ammonium chloride.

The crude product (containing **4**, **5** or **6**) present in the organic phase was washed repeatedly with distilled water. Ethyl acetate was used for extracting the crude product from the aqueous phase. Subsequently, the combined organic layers were dried over anhydrous magnesiumsulfate and the solvents (THF/ethyl acetate) were removed under reduced pressure.

Methyl-substituted
2,2'-dipyridyl diselenide

1, R = methyl	**4,** R = methyl
2, R = allyl	**5,** R = allyl
3, R = hexyl	**6,** R = hexyl
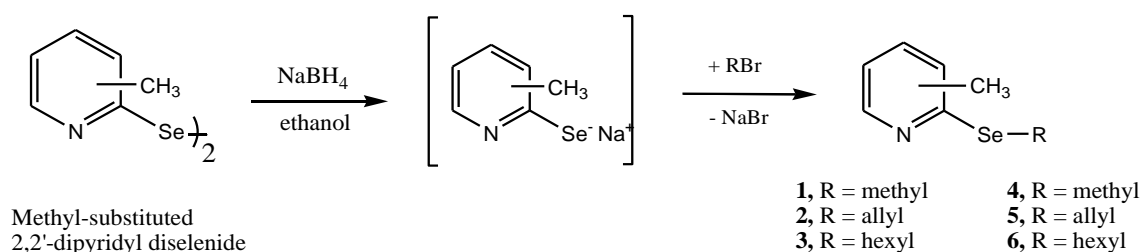
Figure 2.1 Scheme for the synthesis of methyl-functionalized (alkylselanyl)pyridines

Silica gel chromatography was used for the separation and isolation of the desired compounds from the organic phase. For this, the crude mixture was dissolved in a minimum amount of CH_2Cl_2 and silica to form homogenous slurry of silica and the sample. This was then loaded onto a silica gel column followed by elution with a mixture of ethyl acetate and hexane (5 : 95) to obtain the products as yellow oily liquids in moderate yield (around 49 %, 58 % and 51 % for compounds **4, 5** and **6**, respectively).

2.2.3 Synthesis of 2-fluoro-3-(methylselanyl)pyridine (7), 3-(allylselanyl)-2-fluoropyridine (8) and 2-fluoro-3-(hexylselanyl)pyridine (9)

To a vigorously stirred solution of 1,2-bis(2-fluoropyridin-3-yl)diselane (3.0 g, 8.5 mmol) in THF under a N_2 atmosphere, sodium borohydride (0.7 g, 18.6 mmol) was added. The mixture was stirred at room temperature for 15 min until the solution

became colourless. Afterwards, 1-bromomethane (2.2 g, 22.5 mmol) or 3-bromoprop-1-ene (2.7 g, 22.1 mmol) or 1-bromohexane (3.7 g, 22.5 mmol), respectively was added via septum dropwise to the colourless solution. The final mixture was stirred for approximately 1.5 h without exposing the reaction mixture to atmospheric oxygen. The formation of the product was assessed periodically via TLC analysis. Upon disappearance of the reactant spot on the TLC plate, the reaction was quenched by addition of a saturated aqueous solution of ammonium chloride.

The crude product (containing **7**, **8** or **9**) present in the organic phase was washed repeatedly with distilled water. Ethyl acetate was used for extracting the crude product from the aqueous phase. Subsequently, the combined organic layers were dried over anhydrous magnesium sulfate and the solvents (THF/ethyl acetate) were removed under reduced pressure.
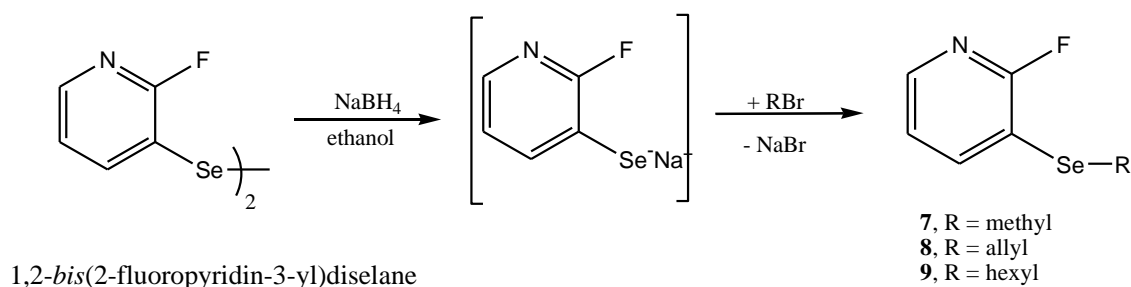
Figure 2.2 Scheme for the synthesis of 2-fluoro-3-(alkylselanyl) pyridines

Silica gel chromatography was used for the separation and isolation of the desired compounds from the organic phase. For this, the crude mixture was dissolved in a minimum amount of CH_2Cl_2 and silica to form homogenous slurry of silica and the sample. This was then loaded onto a silica gel column followed by elution with a mixture of ethyl acetate and hexane (3 : 97) to obtain the products as yellow oily liquids in moderate yields (around 36 %, 43 % and 37 % for compounds **7**, **8** and **9**, respectively).

2.2.4 Synthesis of 1,2-*bis*{(pyridin-3-yl)methyl}diselane (10) and1,2-*bis*{(pyridin-4-yl)methyl}diselane (11)

Compounds **10** and**11** were synthesized according to a previously established protocol as described by Bhasin *et al.* withminor modifications [142]. As displayed in **Figure 2.3**, the key step of this synthetic methodology involved the reduction of pyridine-3-carbaldehyde or pyridine-4-carbaldehyde by sodium hydrogen selenide which was prepared *in- situ* from elemental selenium. This reaction was carried out in the presenceof piperidine hydrogen chloride. The corresponding pyridine-3-selenoaldehyde or pyridine-4-selenoaldehyde thus formed was subsequently oxidized to yield the desired products (**10** or **11**).
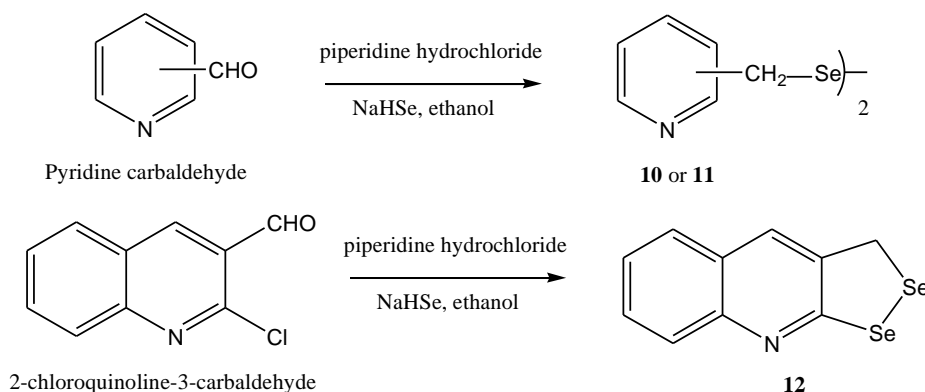
Figure 2.3 Scheme for the synthesis of heteroarene-conjugated diselanes

Absolute ethanol (100 ml) was added slowly to mixture of sodium borohydride (2.7 g, 73.2 mmol) and elemental selenium (2.4 g, 30.4 mmol) in a round-bottom flask followed by magnetic stirring at room temperature under N_2 atmosphere. To this ethanolic solution of sodium hydrogen selenide (around 30 mmol) prepared *in-situ,* piperidine hydrochloride (2.5 g, 20.7 mmol) was added followed by an addition of pyridine-3-carbaldehyde or pyridine-4-carbaldehyde (1.9 g, 17.8 mmol) respectively. The reaction mixture was refluxed for 1 h under N_2 atmosphere followed by cooling to room temperature to yield a brown-coloured solution. The progress of the reaction was assessed periodically by TLC until the disappearance of the starting reagents. After completion of the reaction, the reaction mixture was diluted with distilled water and extracted with chloroform (3 × 100 ml). The organic layer was filtered and dried over

anhydrous magnesium sulfate. Subsequently, the solvents (ethanol/chloroform) were removed under reduced pressure to obtain the crude product (**10** or **11**) in solid phase. The product was subjected to purification using silica gel chromatography using a mixture of chloroform and methanol (1**:**1) as eluent. Compounds **10** and **11** were obtained as lemon to orange coloured solids in a moderate yield of around 43 % and 39 % respectively.

2.2.5   Synthesis of 3H-[1,2] diselenolo [3,4 -b] quinoline, (12)

The methodology as employed previously for the synthesis of **10** or **11** was utilised for the preparation of **12** from 2-chloroquinoline-3-carbaldehyde. Such a compound has been selected due to its unique diselenide bond that constitutes a part of a closed ring system. In addition, the electronic environment of the two selenium moieties constituting this diselenide bridge apparently has been asymmetric and may, therefore, provide an interesting biological reactivity. It may also be hypothesized that due to a probable ring strain, the diselenide bridge could react rather rapidly and hence may cause a significant biological activity, in part due to an apparently facile cleavage under physiological conditions. Compound **12** was synthesized according to a previously established protocol as described by Bhasin *et al.* with some minor modifications [142]. Absolute ethanol (100 ml) was added slowly to mixture of sodium borohydride (2.7 g, 73.1 mmol) and elemental selenium (4.7 g, 59.5 mmol) and the resulting solution was stirred at room temperature under a N_2 atmosphere. After 2 h of stirring, piperidine hydrochloride (6.1 g, 50.1 mmol) and 2-chloroquinoline-3-carbaldehyde (9.4 g, 49.4 mmol) were added in succession. The reaction mixture was refluxed for 1 h and cooled to room temperature to yield a red coloured solution. An addition of sodium borohydride (0.5 g, 13.3 mmol) in small amounts resulted in a vigorous reaction. After the completion of the reaction, the reaction mixture was diluted with 250 ml of distilled water and the product was extracted with dichloromethane (3 × 50 ml). The organic layerwas separated and the solvent was removed under reduced pressure to obtain the crude solid product. The product was subsequently subjected to purification using silica gel chromatography eluting with a mixture of hexane and ethyl acetate (2:1). The isolated pure product was obtained as a reddish-orange coloured solid in a moderate yield of around 37 %.

2.2.6 Synthesis of 1,2-bis(4-chloropyrimidin-2-yl)diselane (13), 1,2-bis(4,6-dimethylpyrimidin-2-yl)diselane (14) and 1,2-di(pyridin-2-yl)diselane (15)

Compounds **13, 14** and **15** were synthesized according to a previously established protocolwith minor modifications [140, 141]. To a vigorously stirred solution of sodium hydroxide (3.1 g, 77.4 mmol), elemental selenium (3.9 g, 50.1 mmol) and *N*,*N*-dimethylformamide (20 ml), 100% hydrazine hydrate (0.6 g, 11.8 mmol) was added drop wise under an inert N_2 atmosphere. After 4 h of stirring, elemental selenium appeared to be completely dissolved, a solution containing approximately 80 mmol of 2,4-dichloropyrimidine (11.8 g) or 2-chloro-4,6-dimethylpyrimidine (11.4 g)or 2-bromopyridine (12.6 g) in DMF, respectively was added dropwise to the reaction mixture. The reaction mixture was allowed to reflux accompanied by a periodic monitoring of the progress of the reaction via TLC analysis. Upon maximal disappearance of the reactant spot on the TLC plate, the reaction was quenched by addition of distilled water. This was followed by extraction of the crude product from the aqueous phase with dichloromethane.
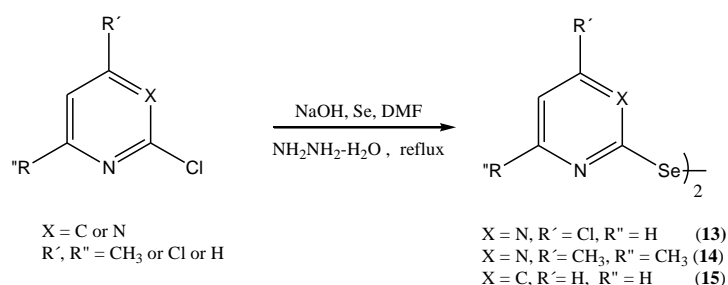
Figure 2.4 Scheme for the synthesis of heteroarene-conjugated diselanes

Subsequently, the combined organic fractions were dried over anhydrous magnesium sulfate and the solvents (dichloromethane/DMF) were removed under reduced pressure to yield a crude solid (**13** or **14 or 15** respectively). Silica gel chromatography was used for the separation and isolation of the desired compound using hexane as the eluent. The pure compound (**13** or **14)** was obtained as a red crystalline solid in a yield of around 44 % and 67 % respectively. Compound **15** was obtained as a green-coloured solid in a yield of around 73 %.

2.2.7 Synthesis of 2,3-*bis*(phenylselanyl)naphthalene-1,4-dione (16)and 2-methyl-3-(phenyltellanyl)naphthalene-1,4-dione (17)

Compounds **16** and **17** were synthesized according to a previously established protocol and described by Jacob *et al.* with some minor modifications [143]. Briefly, an aqueous solution of sodium borohydride (0.6 g, 16.1 mmol) was added dropwise to a solution of diphenyldiselenide (2.1 g, 6.7 mmol) or diphenyl ditelluride (2.6 g, 6.3 mmol) in THF, respectively, and stirred vigorously in a round-bottom flask, under a constant inert atmosphere of argon. This was followed by continuous stirring for another 30 min to allow the formation of phenyl selenolate/tellurolate *in-situ* as evident by the discolouration of the solution mixture. Subsequently, a solution of 2,3-dibromonaphthalene-1,4-dione (2.1 g, 6.6 mmol) or 2-bromo-3-methylnaphthalene-1,4-dione (3.2 g, 12.9 mmol) in THF were added via a septum (*i.e.,*without exposing the reaction mixture to atmospheric oxygen) with continuous stirring for approximately 3 h.The conversion of reactant was assessed periodically through TLC. Upon disappearance of the reactant spot on the TLC plate, the reaction mixture was left to stir in the open for another 1 h.

A = 2,3-dibromonaphthalene-1,4-dione
B = 2-bromo-3-methylnaphthalene-1,4-dione
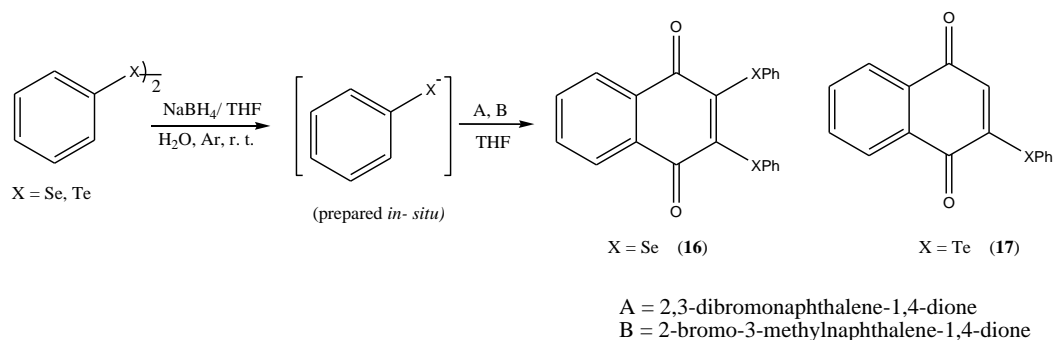
Figure 2.5 Scheme for the synthesis of chalcogen-containing naphthalene-1,4-diones

The reaction was quenched by addition of a saturated aqueous solution of ammonium chloride. The crude product (**16** or **17**) present in the organic phase was repeatedly washed with distilled water. Ethyl acetate was used for extracting the crude product from the aqueous phase. The combined organic layers were dried over

anhydrous magnesium sulfate and the solvents (THF/ethyl acetate) were removed under reduced pressure.

Silica gel chromatography was used for the separation and isolation of the desired compounds from the organic phase. For this, the crude mixture was dissolved in minimum amount of dichloromethane and silica to form homogenous slurry of silica and the sample. This was then loaded onto a silica gel column followed by elution with a mixture of ethyl acetate and petroleum ether (3 : 97) to obtain the products as black-coloured solids (**16** and **17**) in moderate yield (around 53 % and 47 %, respectively).

2.3 Physico-chemical characterization of chalcogen containing compounds

2.3.1 Spectroscopic analysis

The chalcogen containing compounds which have been synthesized as part of the current study were soluble in common organic solvents like methanol, chlorinated hydrocarbons, DMSO and ether. The purity of the compounds was confirmed via ^{1}H and ^{13}C NMR spectroscopic analysis and was judged to be greater than 95%. ^{1}H and ^{13}C NMR spectra were recorded either on Bruker Avance DRX-500 (500.0 MHz, ^{1}H; 125.8 MHz, ^{13}C) or Bruker Avance III-HD (700.0 MHz, ^{1}H; 176.1 MHz, ^{13}C) spectrometer. Deuterated dimethyl sulfoxide (d_6-DMSO) or deuterated chloroform (CDCl$_3$) were used as solvents to obtain the ^{1}H and ^{13}C NMR spectra which were calibrated against their residual solvent peaks for ^{1}H NMR (2.5 ppm, d_6 -DMSO; 7.2 ppm, CDCl$_3$) and ^{13}C NMR (39.5 ppm, d_6 -DMSO; 77.2 ppm, CDCl$_3$ ppm). The NMR spectra corresponding to the re-synthesized compounds were in accordance with published literature values.

Due to a prime focus on organodiselenides, in general, and compounds **10**-**12**, in particular, ^{77}Se NMR analysis of these compounds was carried out in CDCl$_3$ solution using dimethylselenide as the external reference on a Jeol 300.0 MHz spectrometer at 57.0 MHz. In addition, an elemental analysis of compounds **10**-**12** was also carried out on a Perkin-Elmer 2400 CHN Elemental analyser. The electron impact (EI) mass

spectra of the main compounds of study (**10-12**) were obtained using a Q-TOF micro mass spectrometer by direct injection.

2.3.2   X-ray structure analysis of compound, 11

Orange coloured crystals of diffraction quality were grown by the slow evaporation of the compound **11** after dissolution in dichloromethane: hexane (1: 4). The data collected from the single crystal x-ray crystallographic studies of **11** has been illustrated in **Table 2.1**.

Table 2.1 X-ray crystallographic structural information of compound**, 11**

Parameters	
Empirical formula	$C_{12}H_{12}N_2Se_2$
Formula weight	342.16
Temperature	273(2)
Radiation used, Wavelength	0.71073 Å
Crystal system, Space group	Monoclinic, P2(1)/c
Unit cell dimensions	a = 13.569(3) b = 7.8407(15) c = 11.984(2) α = 90.00 β = 109.101(4) γ = 90.00
Volume	1204.8(4)
Z	2
Absorption coefficient	6.144 mm^{-1}
F(000)	864
Crystal size	0.18 x 0.16 x 0.14 mm^3
Theta range for data collection	3.05 to 28.39º
Index ranges	-17≤ h ≤18 -10≤ k ≤10 -15≤ l ≤ 15
Reflections collected	10284
Independent reflections	3004
Refinement method	Full-matrix least-squares on F^2
Data / restraints / parameters	3004 / 0 / 227
Goodness-of-fit on F2	1.900
Final R indices, 1708 reflections [I>2 σ (I)]	R$_1$ = 0.1480,wR$_2$ = 0.5680
R indices (all data)	R$_1$ = 0.2510, wR$_2$ = 0.6316
CCDC No.	1008607

2.4   Biological studies

2.4.1   Materials and devices

2.4.1.1   Equipments and devices

Various equipments and devices used throughout this study are listed in **Table 2.2.**

Table 2.2 List of equipments/devices employed for the cellular and non-cellular biological assays

Equipment/ device	Manufacturer
Bacterial incubator	Memmert
Cell culture incubator	CO_2-Auto-Zero (Heraeus)
Gel electrophoresis system	Mini PROTEAN system (Bio-Rad)
Semi-dry Transfer system	Biometra
X-ray processor	Optimax (Classic X-ray)
Light microscopy	Axiovert 35 (Zeiss)
UV spectrophotometer	UV 1000 (Shimadzu)
Plate reader	Infinite® 200 PRO (Tecan)
Centrifuges	5810R (Eppendorf)
Electrochemical work station	CHI 604D (CH Instruments)
Laminar airflow	Maxisafe 2020 (Thermo Fisher Scientific)
Cell counter	Cedex XS (Innovatis)
Shaker	Titramax 1000 (Heidolph)

2.4.1.2 (Bio)Chemicals and antibodies

All chemicals and biochemicals were obtained from Carl Roth (Karlsruhe, Germany), Gibco® Life Technologies (Darmstadt, Germany), Invitrogen (Karlsruhe, Germany), Merck (Darmstadt, Germany), Roche Diagnostics (Manheim, Germany), Thermo Fisher Scientific (Dreieich, Germany), Promega (Manheim, Germany), Bio-Rad (Munich, Germany) or Sigma-Aldrich Chemie (Steinheim, Germany). The antibodies required for the Western Blot analysis and DARTS experiment were purchased from Cell Signalling Technology (New England Biolabs, Frankfurt, Germany).

2.4.1.3 Assay Kits / Reagents

The respective assay kitsused for the cellular assays are listed in Table 2.3. These kits were purchased from commercial sources.

Table 2.3 List of commercially available biochemical kits/ reagents for cell-based *in-vitro* assays, with their relevant commercial source

Assay/ Reagent	Manufacturer
Caspase-Glo® 3/7 Assay	Promega (Manheim, Germany)
Cell Titre Glo® ATP assay	Promega (Manheim, Germany)
Cell-Death detection ELISA	Roche Diagnostics (Manheim, Germany)
Flexi Rabbit Reticulocyte Lysate system (Nuclease treated)	Promega (Manheim, Germany)
BCA Protein Assay kit	Pierce (Thermo Fisher Scientific, Dreieich, Germany)

2.4.2 Cell Culture studies

Several cell-based assays were carried out *in-vitro* to determine the biological activity of three distinct categories of organoselenium compounds,

namely organomonoselenides (**1-9**), diselenides (**10-15**) and chalcophenes (**ARS-01 to ARS-06**). A standard MTT assay was carried out initially in order to assess and compare the anti-proliferative activities of these compounds against several tumour cell lines [144].

On the basis of this comparative analysis, the most active compounds (**10**, **11** and **12**) were further analysed for their molecular mode of action against a human cervix carcinoma (KB-3-1) cell line. For this, an ELISA and caspase 3/7 assay were employed to determine the ability of **10**, **11** or **12** to induce apoptosis in KB-3-1 cells.

For a considerably active compound **12**, cell-free and *in-cell* translation assays were also carried out in order to investigate the modulatory effects exerted by the compound (**12**) on the translational machinery of KB-3-1 cells. In due consideration of a widely discussed relationship between intra-cellular translation and several oncogenic cellular pathways, a Western Blot analysis was also carried out to determine the ability of **12** in altering the expression and activity of several oncogenic proteins, upon treatment with KB-3-1 cells. Furthermore, in attempts to investigate potential cellular targets of **12** in KB-3-1 cells, a relatively new target identification approach called DARTS was also employed [95]. In a similar context, yet for representative examples (**16** and **17**) of another distinct group of chalcogen-containing naphthoquinones, a TrxR-inhibition assay was carried out to assess a possible role of this mammalian cellular enzyme (TrxR) as part of a further elucidation of the biochemical mode of action of **16** or **17** against tumour cells [151]. In the end, in addition to their anti-cancer effects, **10**-**12** were also subjected to a preliminary anti-microbial assay in order to obtain hints about a possibility of their cytotoxicity, if any, against microbial strains as well [146].

2.4.2.1 Cell type and media

The mammalian cell cultures and their corresponding media that were used for the cytotoxicity assay and related *in-vitro* assays are listed in **Table 2.4**.

Cell line	Origin	Medium	Manufacturer	Supplements
L-929	Transformed mouse fibroblast	MEM	Gibco	10% FBS (Lonza)
KB-3-1	Human cervix carcinoma	DMEM	Lonza	10% FBS (Gibco)
MCF-7	Breast carcinoma	DMEM	Gibco	1X Non essential amino acids (Gibco) 1.5% insulin (Gibco) 10% FBS (Lonza)
PC-3	Prostate carcinoma	F-12K	Gibco	10% FBS (Lonza)

Table 2.4 List of mammalian cell lines and their respective growth media used for *in-vitro* cell-based assays.

2.4.2.2 Cell culture

Studies with mammalian cell cultures were performed under sterile conditions. The respective media (listed in **Table 2.4**) required were warmed to 37°C prior to use. Cells were cultured in cell culture flasks in an incubator at 37°C and 10% CO_2. The volume of media required for cells varies as per the size of culture flasks like 10 mL for 25 $cm^2$and 30 ml for 75 cm^2 flasks. Adherent cells like L-929 and KB-3-1 were harvested and passaged upon 80-90 % confluency. The latter involved the scraping or trypsinisation of thecell layer followed by suspension of the cells by repeatedpipetting up and down with a sterile disposable plastic pipette. Upon attaining confluency, all cell lines were passaged by trypsinisation. To trypsinise the cells, the culture media was removed followed by rinsing of the cell surface with EBSS, followed by addition of 1 mL of trypsin (0.1 %). Then, the flasks were incubated at 37 °C for 3 min. The trypsinisation was stopped by removing the trypsin and replaced with a fresh culture medium. Subsequently, an aliquot of the freshly prepared cell-suspension was transferred to a new cell culture flask and diluted with a fresh medium.

2.4.3   Cell-based assays

2.4.3.1   3-(4,5-Dimethylthiazol-2-yl)-2,5-diphenyltetrazolium bromide (MTT) assay

The anti-proliferative activity of the compounds screened against mammalian cell lines was measured using the standard MTT assay with minor modifications [144]. This assay was carried out in the laboratory of Dr. Florenz Sasse (Helmholtz Centre for Infection Research, Braunschweig, Germany).In each well of a 96-well micro-titre plates 60.0 µl of serial dilutions of the compounds were added to 120.0 µl of suspended cells (around 5×10^4 cells ml^{-1}). The final concentrations which were assessed ranged approximately within 37 µgml^{-1}- 0.2 ng ml^{-1}. After five days of incubation with the compound, the metabolic activity of the cells in each well was determined using the MTT dye. 20.0 µl of MTT solution (at an approximate concentration of 5 mg ml^{-1} in PBS) was added in each well to a final concentration of 0.5 mg ml^{-1} and incubated for 2 h. In principle, MTT is reduced by dehydrogenases of viable cells to form purple-coloured formazan crystals. The precipitate was washed with 100.0 µl of PBS followed by dissolution of the formazan crystals in 100.0 µl isopropanol (containing approximately 0.4 % HCl). Absorbance of the resulting solutions was measured spectrophotometrically at a wavelength of 595 nm using a plate reader.

3-(4,5-dimethylthiazol-2-yl)-2,5-diphenyltetrazolium bromide

(2E,4Z)-(4,5-dimethylthiazol-2-yl)-3,5-diphenylformazan
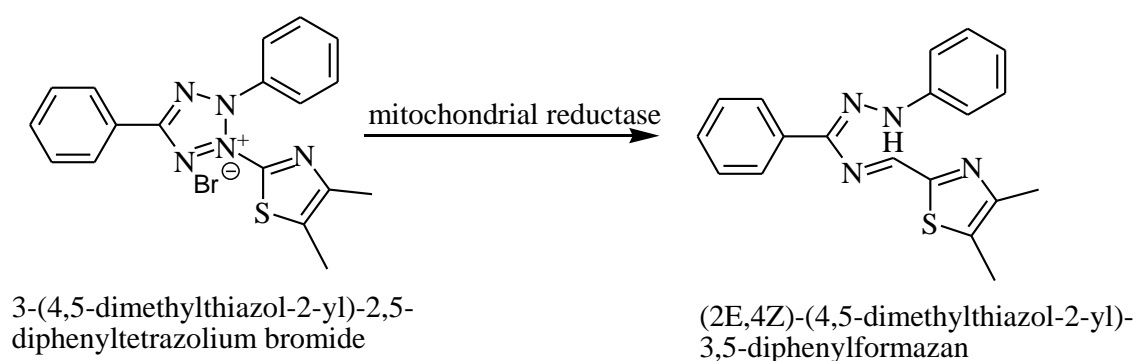
Figure 2.6 Reduction of MTT into insoluble formazan crystals by viable cells.

2.4.3.2 Cell-Titre Glo ATP assay

The ATP levels of a cell are widely recognised as a parameter of its viability [17]. The cytotoxic effects of compound screened against KB-3-1 cancer cells were also measured using the Cell Titre-Glo® assay [147] at Helmholtz Centre for Infection Research, Braunschweig.As per the describedprocedure, around 1×10^4 cells per well were seeded in a 96-well micro titre plate, grown overnight and then treated with serial dilutions of the compounds. The final volume in each well was maintained at 100.0 µl. Cells treated with methanol served as negative control. After either 24 or 48 h of incubation, the compound-treated cells were mixed with 100.0 µl of Cell Titre-Glo reagent and incubated in the dark at 37 °C for 30 min. The plates were then left in the dark or wrapped in aluminium foil to normalise to room temperature.
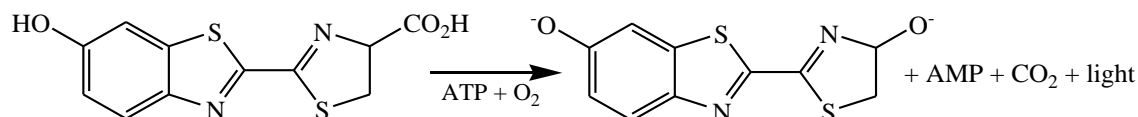
Figure 2.7 Scheme of generation of luminescence as part of the intra-cellular ATP analysis assay. Figure has been adopted from [147].

The plates were shaken on a shaker for one minute and centrifuged briefly. The luminescence which correlates to the ATP levels in the cell was measured spectrophotometrically using a plate reader.

2.4.3.3 Apoptosis assay- Cell Death detection ELISA assay

The apoptosis assay was carried out in the laboratory of Dr. Florenz Sasse (Helmholtz Centre for Infection Research, Braunschweig, Germany) in cooperation with Ms. Bettina Hinkelmann. Based on the quantitative sandwich enzyme immunoassay principle, the detection of cell death using an ELISA was performed to quantify the pro-apoptotic activity of the screened compounds. This particular method relies on the detection of histone-associated DNA fragments (mono- and oligonucleosomes) generated by apoptotic cells [145]. In accordance with the procedure, equivalent number of KB-3-1 cells were plated in 96-well culture plates (around 6×10^3 per well) in serum-supplemented DMEM medium and allowed to

adhere overnight. At the time of sample collection, confluent cells were washed with PBS and treated overnight with serial dilutions of the screened compounds.Cells were dissociated gently using EDTA (0.1 M in PBS) and pelleted along with floating cells (mostly apoptotic cells) collected from the conditioned media. The cell pellets were used to prepare the cytosolic fractions that contained the smaller fragments of DNA.
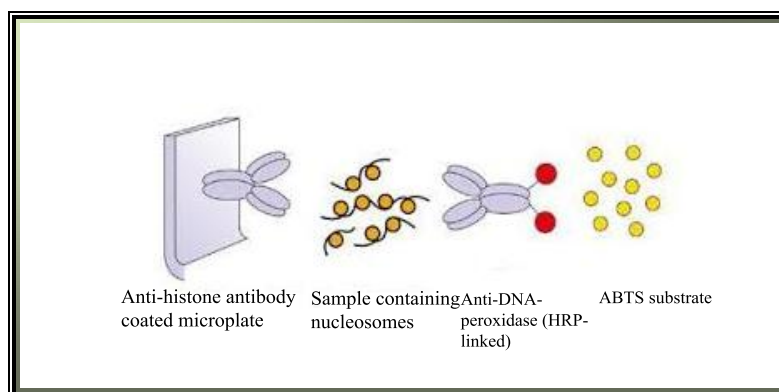
Figure 2.8 Mechanism of analysis of apoptosis analysis by the ELISA technique. Figure has been adopted from [145].

Equal volumes of these cytosolic fractions were incubated in anti-histone antibody-coated wells (96-well plates) and histones (from the DNA fragments) were allowed to bind to its corresponding antibody. The peroxidase-labelled mouse monoclonal DNA antibodies were used to localize and identify the bound fragmented DNA by photometric detection using ABTS as the substrate.

2.4.3.4 Caspase-3/7 activation assay

Since caspase 3 and caspase 7 are essential for executing apoptotic cell death, a caspase 3/7 Glo-assay kit was utilised to measure their presence in KB-3-1 cells [57, 148]. This assay was carried out in the labs of Helmholtz Centre for Infection Research, Braunschweig, Germany.

The Caspase-3/7 Assay employs a pro-luminescent substrate with an optimized bifunctional cell lysisactivity buffer for caspase-3/7 (DEVDase) activity assays. As per the manufacturer´s instructions, approximately 2×10^4 cells per well were plated in 96-well micro-titre plates and allowed to adhere overnight in a humidified environment at 37 °C and 5 % CO_2. Apoptosis was induced by treating the cells with the selected

compounds in a dose-dependent manner for 12 h and 24 h respectively. Cells treated with DMSO alone were considered as negative control. After treatment, the freshly prepared caspase glo-reagent was added to the each well such that the final volume was around 200 µl per well (resulting in cell lysis).
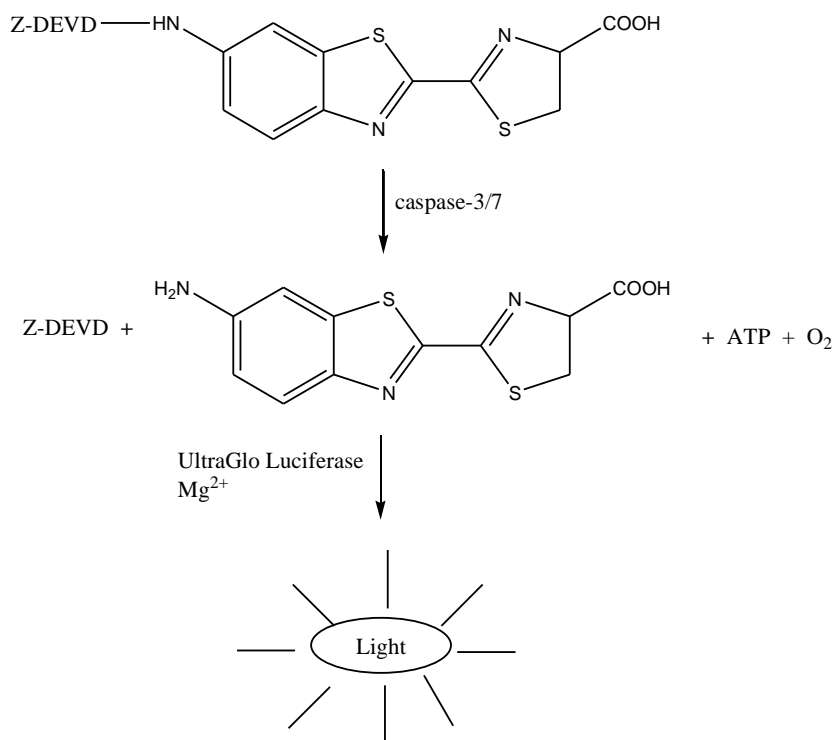
Figure 2.9 Basis of assessing caspase 3/7 stimulation using Cell-titre Glo assay.

The plates were adjusted to room temperature for 30 min before recording luminescence using a plate reader. The amount of luminescence quantified was proportional to the level of caspase 3/7 activation in KB-3-1 cells.

2.4.3.5   Translation assays

Based on the significant activity of compound **12** against several tumour cell lines in general and PC-3 cells in particular (in the MTT assay), an *in-vitro* and *in-cell* translation assay was carried out in order to determine the translation-modulatory efficiency of compound **12** in mammalian cells. For this purpose, rabbit reticulocyte lysates and KB-3-1 cells were selected as experimental systems for this purpose. The former cell-free system is commonly employed as a translation-enriched system to "rank" chemical libraries in order of their translation-inhibiting or translation-promoting

ability. For carrying out an *in-cell* translation assay, a KB-3-1 cell line was used in order to assess a possible link between the translation-modulatory effects of **12** with its apoptosis-inducing ability in KB-3-1 cells.

Both the cell-free and *in-cell* translation assays are based on the quantification of alterations in the generation of bioluminiscence in the compound-treated translation systems where the bioluminiscent levels are in direct proportion to the translational activity. This bioluminiscence, in a translation system, can be generated upon the expression of a luciferase enzyme (firefly luciferase, as in this study) which catalyses the oxidation of luciferin (present in the translation system) by a multi-step process to produce light which can be subsequently measured. In the *in-cell* translation system, this firefly luciferase enzyme has been introduced via a reporter gene pRL-SV40 (which encodes the luciferase enzyme).Therefore, a comparison of the extent to which the luciferase enzyme is expressed in the compound-free and compound-containing translation system can be used to determine a compound's effect on the translational activity of the system.
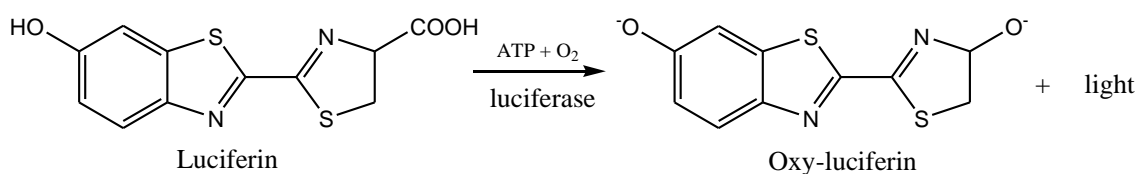
Figure 2.10 Luciferase-catalysed generation of bioluminiscence as a basis of measurement of the translational activity in cell-free and *in-cell* translation systems.

2.4.3.5.1 *In-vitro* **translation assay**

The *in-vitro* translation inhibition assay was carried out at Helmholtz Centre for Infection Research, Braunschweig, Germany. This assay was performed using the Flexi Rabbit Reticulocyte Lysate system, as per the manufacturer's instructions [154]. In this cell-free system, the rabbit reticulocytes which are prepared from New Zealand white rabbits containthe cellular components which are necessary for protein synthesis (tuna, ribosome's, amino acids, initiation, elongation and termination factors) thus serving as a translation-enriched system. Briefly, about 500 ng of firefly luciferase mRNA was combined with 17.5 µl of rabbit reticulocyte lysate, 0.3 µl each of 1 mM of

Met- and Leu- amino acid mixtures, 0.7 µl of 2.5 M KCl, 10 U RNasin, 3.3 µl of nuclease free water and 1.0 µl of a methanolic solution of compound (to yield an approximate compoundconcentration ranging within 0.1 - 10 µg ml^{-1}). An equivalent volume of methanol was added in place of the compound to serve as negative control. The reaction mixtures were incubated at 30 °C for 90 min, followed by measurement of the luminescence in a plate reader by mixing 2.0 µl of the mixture with 10 µl of the firefly luciferase substrate in a 96-well microtitre plate.

2.4.3.5.2 *In-cell* translation inhibition assay

Confluent KB-3-1 cells were trypsinised and quantified using a cell counter. These cells were resuspended to obtain a final concentration of around 1×10^5 cells ml^{-1}. 100.0 µl of this cell suspension was plated in each well of a 96-well plate and allowed to adhere overnight. The following day, the medium in each well was exchanged with around 100 µl of fresh medium and the cells were incubated at 37 °C for 1 h. In the meantime, approximately 48 µg of pRL-SV40was mixed with 480.0 µl of DMEM and incubated for 5 min. To this mixture, PEI (96.0 µl, 1 µg ml^{-1}) was added, mixed gently and incubated at room temperature for 15 min. At the end of the incubation period, the 96-well plate (containing KB-3-1 cells) was removed from the incubator and 85.0 µl of the media was aspirated from each well. Then, 6.5 µl of a mixture ofpRL-SV40 and PEI (kindly provided by Dr. Yazh Muthukumar) was added to each well and incubated for 30 min at37 °C. Finally, around 100 µl of fresh medium was added and incubated for another 48 h to achieve maximal transfection.

The *in-cell* translation assay was carried out in accordance with a procedure as described previously [188]. Briefly, the medium from the 96-well plate containing the transfected KB-3-1 cells was replaced by a fresh medium followed by treatment with serial dilutions of the compound under investigation (0.1-100 µg ml^{-1}). The plate containing treated cells was incubated for 3 h. Cells were then lysed with 1x lysis buffer. Finally, in a 96-well microtitre plate, 5.0 µl of the cell lysate was mixed with 10 µl of the assay buffer and the luminescence was measured using a plate reader. In principle, the intensity of luminiscence corresponds to the level of protein translational activity in the cells.

2.4.3.6 Immunodetection of modulations in intracellular signalling pathways

2.4.3.6.1 Preparation of buffers

a)   SDS running buffer (10x)

A 10x SDS running buffer was prepared by dissolving 288.1 g of glycine, 60.4 g tris baseand 20.5 g SDS in approximately 1.8 l of double distilled water. This buffer was subsequently diluted by 10 fold in double distilled water to obtain the working form of the buffer.

b)   TBS buffer (10x)

This was prepared by dissolving 160.6 g NaCl, 4.3 g KCl and 12.2 g Tris basein nearly 2.0 l of double-distilled water. The working TBS solution was prepared by diluting the 10x TBS buffer to 1x with double distilled water. Afterwards, TBS(T) buffer was prepared by adding 1.0 ml of Tween-20 (surfactant) to 1 l of 1x TBS buffer.

c)   Blotting buffer

The blotting buffer was prepared by mixing equivalent volumes of aqueous solutions of approximately 25 mM of Tris-HCl and 192 mM glycine.

2.4.3.7 Western Blot analysis

2.4.3.7.1 SDS-PAGE

SDS PAGE was performed by using a 4-20 % tris-HCl gradient gel (Bio-Rad, Munich, Germany). Treated cells were lysed using MPER cell lysis buffer (Thermo Fisher Scientific, Dreieich, Germany) and supplemented with 100 x Halt protease/phosphatase inhibitor(Pierce, Thermo Fisher Scientific, Dreieich, Germany) before keeping the lysate in an eppendorf under ice-cold conditions for 15 min. This was followed by centrifugation of the lysate at 1×10^4 rpm for 10 min. The protein

content in the upper layer of the lysate was subsequently quantified using the BCA Protein Assay kit.

Approximately 80 µg of protein from the KB-3-1 cell lysate was subsequently mixed with 5.0 µl of 4x SDS loading dye (Carl Roth, Karlsruhe, Germany) and incubated at 96 °C for 10 min. The protein samples were then loaded into wells of an SDS gel which was placed in an electrophoresis tank containing freshly prepared SDS buffer. A protein marker was also loaded into one well to determine the extent of electrophoresis. Electrophoresis was carried out at 150 V for around 1.5 h *i.e.* until the loading dye reached the bottom-end of the gel.

2.4.3.7.2 Protein-transfer

Proteins from the SDS PAGE gel were transferred onto a nitrocellulose membrane by a semi-dry Western Blot method. Briefly, a nitrocellulose membrane and six Whatman filter papers (6 x 9 cm) were soaked in 1x blotting buffer (containing nearly 20 % methanol) under mild shaking conditions. After 30 min of shaking, the nitrocellulose membrane, sandwiched between double-layered Whatman filter papers, was placed onto the transfer apparatus. The transfer was allowed to proceed at 15 V and 0.5 mA for 30 min.

2.4.3.7.3 Blocking and incubation with antibodies

After completion of protein transfer, the nitrocellulose membrane was incubated for 2 h with 5 % non-fat milk prepared in TBS(T) buffer, at room temperature, to block unspecific binding sites. The membrane was then washed shortly once with TBS (T). After preparation of the prescribed dilutions of each antibody as per the manufacturer´s instructions, the antibody solutions were added to the membrane, followed by incubation at room temperature for 2 h or overnight at 4°C. The primary antibody solution was removed and the membrane was washed three times with TBS (T). The blot was then incubated with 10 ml of TBS (T) containing roughly 1 % BSA and 0.5 µl of secondary antibody conjugated to HRP. The membrane was washed with TBS (T) again and prepared for chemi-luminiscent detection.

2.4.3.7.4 Detection

Supersignal West Pico® or Supersignal West Femto® chemiluminescence detection kit (Thermo Fisher Scientific, Bonn, Germany) was used for the detection of the intensity of the protein bands. For this purpose, the nitrocellulose membrane was incubated with a mix of Enhancer and Stable Peroxide Buffer, in equal volumes, for approximately 5 min. The membrane was afterwards transferred onto an X-ray cassette. In a dark room, an X-ray film was placed onto the cassette and exposed for 1 - 5 min. Finally, the film was developed using an X-ray film processor (Optimax, Protec, Germany).

2.4.3.8 Drug-affinity responsive target stability (DARTS)approach

For the identification of probable interactions of compounds with cellular proteins, the DARTS experiment was carried out in KB-3-1 cells according to the method of Lomenick *et al.* with minor modifications as specified below [95].

2.4.3.8.1 Preparation of cell lysate

KB-3-1 cells were cultured to 70-80% confluency in a $75cm^2$ cell culture flask. The cells were trypsinised and centrifuged. The cell pellet was washed once with PBS and centrifuged again. The pellet was resuspended in 800.0 µl of M-PER lysis buffer (Thermo Fisher Scientific, Dreieich, Germany). Afterwards, the cell lysates were subjected to cell lysis on ice for 15 min. After that, the tubes were centrifuged, the supernatant of lysate was collected and the protein content was quantified using BCA Protein assay kit. Aliquots of the cell lysate containing around 100 µg of protein content were treated with 1.0 µl of serial dilutions of the compound (0.333 mM - 0.03 µM) in methanol and kept on a shaker at 700 rpm under ice-cold conditions. Then, each aliquot was digested with 0.1 % pronase at 37°C. The digestion was stopped after 30 min by addition of 5 µl of 4x loading dye (Carl Roth, Karlsruhe, Germany) followed by incubation of the protein lysate at 95 °C.

2.4.3.8.2 Detection

The protein samples were separated on SDS-PAGE using 4-20 % Tris-HCl gels (Bio-Rad, Munich, Germany) and were subjected to Western Blot analysis, adopting the previously described procedure as mentioned in **Section 2.4.3.7**.

2.4.3.9 Ligand binding affinity assay

The ligand binding affinity assay was carried out in co-operation with DiscoverX (California, USA). This assay serves as a platform which employs a novel and proprietary active site-directed competition binding assay to quantitatively measure interactions between the compounds under investigation and specific cellular proteins, as ERK2 in this particular study. This robust and reliable assay technology does not requireATP and thereby determines the correct thermodynamic interaction affinity of a given compound (as **12** in this study) with a recombinant ERK2 protein as opposed to the IC_{50} values which are measured by more traditional methods and are often imprecise as they may depend on the ATP concentrations.

For the ERK2-binding assay, a full-length recombinant ERK2 kinase (accession number NP_620407.1) was used. A six-point serial dilution of the compound under investigation (compound **12**, as in this study) was prepared in DMSO at 100 x final analysis concentration and subsequently diluted to 1x in the assay (final DMSO concentration of 1%). Binding constants (*Kd*s) were calculated with a standard dose-response curve using the Hill equation:

$$\text{Response} = \text{Background} + \frac{\text{Signal - Background}}{1 + (Kd^{\text{Hill Slope}} / \text{Dose}^{\text{Hill Slope}})}$$

In accordance with the established protocol, the Hill Slope was set to -1 and the background was minimised to 0.The binding interactions for each concentration of the compound under investigation was analysed in terms of the percentage, relative to the control (DMSO) and calculated according to the following equation:

$$\left[\frac{\text{test compound signal - positive control signal}}{\text{negative control signal - positive control signal}} \right] \text{ x } 100$$

Where test compound = compound **12** (in this study); negative control = DMSO (100 % control); positive control = control compound (0 % control).

2.4.3.10   Anti-microbial studies

2.4.3.10.1   Microbial strains and their growth media used for anti microbial analysis

The microbial strains used for a primary analysis of the anti-microbial activity of the most active organoselenium compounds (**10**-**12**) in this study are provided in **Table 2.6**.

Table 2.6 Strains used for anti-microbial analysis

Microorganism	Abbreviations	Source
Escherichia coli	*E. Coli*	Ciba-Geigy, Basel
Micrococcus phlei	*M. phlei*	HZI Collection
Micrococcus luteus	*M. luteus*	HZI Collection
Candida albicans	*C. albicans*	DSM 1386
Paeonia anomala (Pichia)	*P. anomala*	DSM 70263
Saccharomyces cerevisiae	*S. cerevisiae*	Euroscarf
Botrytis cinerea	*B. cinerea*	DSM 877

For inoculation of bacteria and fungi, EBS and MYC media were used, respectively. All nutrients for the media were purchased from Sigma-Aldrich (Industriestrasse, Germany) and Carl Roth (Karlsruhe, Germany).

For the agar media (agar diffusion assay), 15 gl^{-1}of Muellor-Hinton agar (Sigma-Aldrich GmbH, Industriestrasse, Germany) was added. The medium was prepared in double-distilled water and autoclaved immediately. The autoclaved media were then stored at 4°C before further use.

Table 2.7 Composition of media for inoculation of microbial strains

Medium	Composition
EBS medium (pH 7.0)	Casein Peptone (5 g l^{-1}), Protease peptone (5 g l^{1}) , Meat extract (1 g l^{-1}), Yeast extract (1 g l^{-1}), HEPES (10 g l^{-1})
MYC medium (pH 7.0)	(10 g l^{-1} glucose, 10 g l^{-1} phytone peptone and 50 mM HEPES)

2.4.3.10.2 Selection criteria of microbial strains used as a part of this study

Amongst the fungal strains, *Saccharomycescerevisiae*, *Botrytis cinerea, Candida albicans and Paeonia anomala* (also called *Pichia)* were selected for anti-microbial screening of the relevant compounds. For several centuries, *S. cerevisiae* has been used in the production of food and alcoholic beverages. Although this form of yeast is not acutely pathogenic to healthy individuals, it has been reported to yield its virulence in immune compromised patients by secretion of pro-inflammatory cytokines [171]. On the other hand, *B. cinerea* causes critical pre-and post-harvest diseases in agronomically important crops, in addition to a disease called winegrower´s lungs that induce an allergic reaction to the lungs, resulting in breathing problems. Although commonly found within the digestive tracts of a healthy human body, *C. albicans* is known to exert its pathogenic effects through a disease called "Candidacies" that infects the mouth, throat and various other parts of the body. *Pichia*has also been recognized as a pathogenic fungal strain since it is notorious for causing morbidity and morbidity in neonatal and immune compromised infants [172].

Amongst the bacterial strains, extensive research is being carried out against the pathogenic gram-negative bacterium *Escherichia Coli*. This pathogen has been reported in numerous instances to cause urinary tract infections, in addition to occasional fatality from severe anaemia or kidney failure. Usually found to inhabit the

skin microflora and serve as a commensal microorganism, *Micrococcus luteus* has also been reported to induce several infections in the form of intracranial abscesses, pneumonia and meningitis. *Mycobacterium phlei,* on the other hand, is a not-so-easily diagnosable bacteria that has been associated with inflammation of the foot. *M. phlei* has recently been reported for the first time to be also involved in cardiac-device related infections [173]. Therefore, in consideration of the pathogenic characteristics of these strains, we endeavoured to identify possible inhibitory potential of selected compounds against these strains in an agar-diffusion assay. This assay was carried out in the laboratory of Dr. Florenz Sasse at Helmholtz Centre Braunschweig.The antibiotics oxytetracyclin (OTC) and nystatins were included in these assays as positive controls.

2.4.3.10.3   Handling of microorganisms

All microbiological studies were carried out under sterile conditions. The bacteria and fungi were not maintained as a continuous culture. Whenever required, the cells were revived from frozen samples (kept at -20 °C). Fungi were stored at 4°C as spore-suspension cultures. To revive each microbe, its frozen culture was placed in a fresh medium and inoculated overnight at 30 °C. The next day, the optical density (OD) of the microbial suspension was determined at a wavelength of 600 nm (bacteria) or 548 nm (fungi) using a spectrophotometer.

2.4.3.10.4   Agar diffusion assay

A disk-diffusion susceptibility analysis was carried outaccording to the method of Wang *et al*. with minor modifications to determine the sensitivity or resistance of pathogenic microbial strains towards the compounds under investigation [146]. For performing the inoculation of bacteria and fungi, EBS and MYC media were used. The medium (with Mueller-Hinton agar) was heated in a microwave-oven until the agar had melted, followed by adjustment of the temperature to 50 °C in a water bath. Afterwards, the selected bacterial or fungal strains were added to the agar-containing medium at a final OD of 0.01 and 0.10 for the bacteria and fungi, respectively. Under a laminar flow hood, 15 ml of the inoculated medium (with agar) was then poured into 90 mm sterile Petri dishes (TPP, Trasadingen, Switzerland) and allowed to solidify. Then, a filter-

paper disk (Schleicher & Schuell GmbH, Dassel, Germany) of 6 mm diameter was impregnated with a relevant compound under investigation (20 µl of a 1.0 mg ml^{-1} stock solution) and air-dried under the laminar air flow hood. Afterwards, the filter-paper disk was placed on the inoculated plate by using flame-sterilized forceps. The Petri dishes were subsequently incubated at 30 °C in an incubator for 1-2 d, depending on the speed of growth (usually 1 d for bacteria and 2 d for fungi). The diameter of the resulting inhibition zones around the disk served as an indicator of the anti-microbial potential of the compounds screened.

2.4.3.11 Thioredoxin Reductase (TrxR) enzyme-inhibition assay

In order to investigate into additional cellular targets of chalcogen-containing naphthoquinones (**16** and **17**) in an attempt to further elucidate their biochemical mode of action against tumorigenic cells, a TrxR enzyme inhibition assay was carried out. The TrxR enzyme is well-documented to behave as a natural cellular antioxidant and has been frequently reported as a prime target of several chemotherapeutic drugs that induce ROS-mediated death in tumour cells. In due consideration of this fact and a previous report by Jacob *et al.* highlighting the induction of ROS-mediated apoptosis in tumour cells by organochalcogen compounds like **16** and **17**, the TrxR enzyme inhibition assay was carried out using a modified micro-plate reader based assay to assess possible modulatory effects of **16** and **17** on mammalian TrxR enzyme [151]. Briefly, a rat-recombinant Thioredoxin Reductase-1 was acquired from IMCO Corporation Ltd., AB (Sweden). 0.04 U ml^{-1} concentrations of the mammalian enzyme were prepared in double-distilled water. As per the procedure, to every 25.0 µl aliquot of the enzyme solution, 25.0 µl of potassium phosphate buffer (PBS, pH7.0) containing the sample compound in serial dilutions, or DMSO (vehicle control) was added. The resulting solutions (maintaining a final DMSO concentration of 0.5 % v/v) were incubated with moderate shaking at 37°C in a 96-well micro-titre plate for 75 min. 225.0 µl of a reaction mixture, prior to adding in each well, was prepared by mixing PBS (500.0 µl, pH 7.0), EDTA solution (80.0 µl, 100.0 mM, pH 7.5), BSA solution (0.05% w/v, 20.0 µl), NADPH solution (100.0 µl, 20.1 mM) and double distilled water (300.0 µl).This was followed by the initiation of the reaction by the addition of 25.0 µl of a 20.0 mM concentrated ethanolic solution of 5,5'-dithio-bis(2-nitrobenzoic acid) (DTNB). After

proper mixing, the formation of 2-nitro-5-thiobenzoic acid (5-TNB) was monitored spectrophotometrically using a microplate reader at a wavelength of 405 nm at 10 s intervals for 6 min. The increase of 5-TNB concentration over time followed a linear trend and the enzymatic activity was calculated from the increase in absorbance per second. For each test compound, non-interference with the assay components was confirmed by a negative control experiment using an enzyme-free solution. The IC_{50} value was calculated as the concentration of the compounds decreasing the enzymatic activity of the untreated control by 50 % and was given as the mean of values obtained from three individual experiments ($\pm$ SD).

2.5   Non-cellular assays

2.5.1   Characterization of redox properties employing the electrochemical method of cyclic voltammetry

Cyclic voltammetry has been used to define the general redox properties of biologically active selenium-containing compounds. It is a particularly useful method to estimate the oxidation and reduction potential of such selenium-containing molecules and to investigate reversible and irreversible aspects of electron transfer. The electrochemical method uses a reference electrode, a working electrode and a counter electrode that in combination are referred to as a three-electrode setup. An electrolyte is added to the test solution to ensure sufficient conductivity.

In this particular case, the electrochemical experiments were carried out using a CHI 604D electrochemical work station (CH Instruments, USA) linked to a glassy carbon electrode. This electrode served as the working electrode with a standard Ag/AgCl (SSE) reference and a platinum wire counter electrode. The reference electrode was calibrated against the $[Fe (CN)_6]^{4-}/Fe (CN)_6]^{3-}$ redox pair. The experiments were performed in acetonitrile containing 0.1 M TBAPas the supporting electrolyte at a scan rate of 100.0 mV s^{-1}. All experiments were performed at room temperature.

2.5.2   Anti-oxidant assays

2.5.2.1   Diphenyl-(2,4,6-trinitrophenyl)iminoazanium (DPPH) Assay

In order to determine the general antioxidant behaviour and the radical-scavenging potential of the selected organoselenium compound in particular, a standard DPPH radical scavenging assay was carried out according to previously established protocols, with minor modifications [149]. In this assay, a non-physiological but a stable free radical called DPPH is employed. Due to a strong absorption exhibited by DPPH at a wavelength of 517 nm, this radical displays an intense violet colour in solution which becomes colourless or pale yellow upon neutralization by electron-donating molecules. This property enables a visual or spectrophotometric analysis of the alteration in the levels of DPPH before and after a treatment with a compound under investigation.

a)   Preparation of DPPH reagent

A 300 µM stock (approximate) of a methanolic solution of DPPH reagent (Sigma-Aldrich, Steinheim, Germany) was prepared freshly at the time of experiment by dissolving 1.2 mg of DPPH in 10.1 ml of absolute methanol. The solution was kept in the dark at all times to avoid any photochemical degradation.

b)   Assay protocol

In each well of a 96-well microtitre plate, a methanolic solution of DPPH reagent (~300 µM, 200.0 µl) was treated with 40.0 µl of serial dilutions of the organoselenium compounds, ascorbic acid (positive control) and methanol (negative control) in a concentration range (125-1000 µg ml^{-1}). The final mixture (containing DPPH and the sample/ methanol) was allowed to react at room temperature in the dark

Figure 2.11 Structure of DPPH radical

for 30 min. A blank assay was run initially only with the DPPH reagent to confirm its

stability under experimental conditions. After the incubation, the decrease in absorbance was measured spectrophotometrically at a wavelength of 517 nm using a plate reader. In principle, a decrease in absorbance is directly proportional to the extent of quenching (or scavenging) of DPPH radicals. The methanol treated wells were considered as negative control whereas the wells containing untreated DPPH radicals were considered as blank control. The radical-scavenging effect of the compounds was calculated as per the following formula-

% DPPH scavenging ability = [Abs $_{(blank)}$ − Abs$_{(compound\ at\ 1mM)}$/Abs$_{(blank)}$] x 100

2.5.2.2   Ferric reducing ability of plasma (FRAP) assay

This assay was carried out in accordance with previously established procedures with minor modifications [150]. To perform this assay, a FRAP reagent mix was prepared using freshly produced constituent reagents.

a)   Preparation of FRAP assay reagents

An approximately 300 mM of acetate buffer (pH 3.6) was prepared by dissolving 3.1 g of sodium acetate (trihydrate) in 16 ml of glacial acetic acid and distilled water was added to obtain a final volume of 1.0 l. The buffer was stored at $4\,^{\circ}C$, prior to use. 10.6 mM stock solution of 2,4,6-tripyridyl-*s*-triazine (TPTZ) was prepared freshly by dissolving 0.1 g of TPTZ in HCl (30.0 ml, ~40
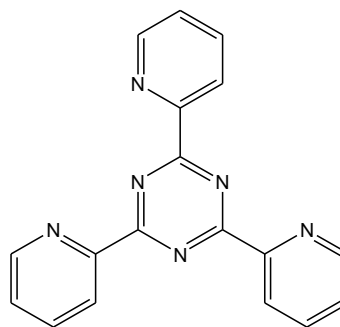
Figure 2.12 Structure of 2,4,6-tripyridyl-s-triazine (TPTZ)

mM). The 40 mM HCl solution required for this purpose was prepared by diluting 3.6 ml of concentrated HCl (36% w/v) with double-distilled water to obtain a final volume of 1.0l. Furthermore, 20.6 mM stock solution of ferric chloride was also prepared by dissolving 0.1 g of $FeCl_3\cdot6H_2O$ in 20 ml of double-distilled water. The final FRAP reagent, required for this assay, was prepared by mixing TPTZ solution

(2.5 ml, 10.6 mM) and $FeCl_3$ solution (2.5 ml, 20.6 mM) with acetate buffer (25 ml, ~300.0 mM, pH 3.6). The final FRAP reagent mixture was prepared afresh at the time of experiment.

b) Assay protocol

The assay was performed in a 96-well microtitre plate. For the determination of the antioxidant potential, a blank reading with only FRAP reagent (300.0 µl) was taken initially at a wavelength of 594 nm. Subsequently, in each well of the microtitre plate, the freshly prepared FRAP reagent (300.0 µl) was mixed with serial dilutions of a benchmark standard (ascorbic acid) or the methanolic solutions of the compounds under investigation (63-1000 µg ml^{-1}, 40.0 µl). In order to run a negative control assay, an equivalent volume of methanol (negative control) was also treated simultaneously with the FRAP reagent. The first absorbance reading (at 594 nm) was taken immediately after addition of FRAP reagent to samples (at time t = 0 min). The mixture was then allowed to incubate at 37°C for 10 min before absorbance values were measured. The absorbance values obtained from methanol-treated FRAP reagent were considered as negative control. Values from the negative control were subtracted from values corresponding to compound-treated wells in order to obtain the reducing effect of the compounds on the FRAP reagent. Calibration of the experiment was carried out by plotting standard curves that were obtained from treatment of FRAP reagent with serial dilutions of an aqueous solution of $FeSO_4 \cdot 7H_2O$. The antioxidant potential of a screened molecule was calculated as it's FRAP value with reference to the absorbance values given by the $FeSO_4$ solution. This value was expressed in µmol equiv of $Fe^{2+}l^{-1}$. In principle, a higher FRAP value indicates a greater anti-oxidant potential of the screened samples. Henceforth, the mean and standard deviations of FRAP values from individual experiments were calculated to obtain a measure of the reducing activity of the compounds under investigation.

2.6 Statistical analysis

Student's t-test has been used to analyze the difference between the means of the treated groups and the control group. Differences with a p value < 0.05 have been considered statistically significant and have been symbolically expressed as * for $p < 0.05$ and as # for $p < 0.001$. The data has been presented as the mean of valuesobtained from individual experiments ± Standard Deviation (SD). SD has been expressed as error bars.

Chapter 3

Results

3.1 Chemical synthesis

During the past several years, numerous articles have delved into investigating the promising effects of organoselenium compoundsin combating cancer, in addition to a plethora of several other oxidative stress-related disorders [105, 136]. Such potentially chemotherapeutic compounds and a cascade of active metabolites associated with them have also been well documented to play a significant role in exploiting the acute susceptibility of cancercells towards intra-cellular redox alterations.

3.1.1 Synthesis of heteroaryl group-conjugated monoselenides

In accordance with the popular saying, "Two is always greater than one", several reports in the literature havehighlighted a higher chemotherapeutic efficacy of organodiselenides in comparison to monoselenides [153]. Although this observation has been supported strongly by the facile generation of active selenium metabolites in the former due to a facile cleavage of a selenium-selenium bond in comparison to selenium-carbon bond in the latter, certain measures have been undertaken to enhance the anti-cancer efficacy of several monoselenides. In principle, this could be achieved partially by enhancing the intra-cellular penetration efficacy of monoselenides. Since lipophilicity has often been observed to serve as a key to enhance cellular uptake and cytotoxicity against tumour cells, successful attempts have been made to generate a section of aryl monoselenides with hydrophobic alkyl groups of varying chain-lengths.

The primary protocol that was employed for the synthesis of alkyl-substituted selenopyridines involved the reductive hydrolysis of 2,2'-dipyridyl diselenide with hydrazine hydrate or sodium borohydride to furnish a reactive 2-pyridyl selenolate species *in-situ* [141]. This was followed by a facile nucleophilicsubstitution of the

reactive selenolate anion with haloalkanesto yield a range of alkyl-substituted selenopyridines as yellow oily liquids.
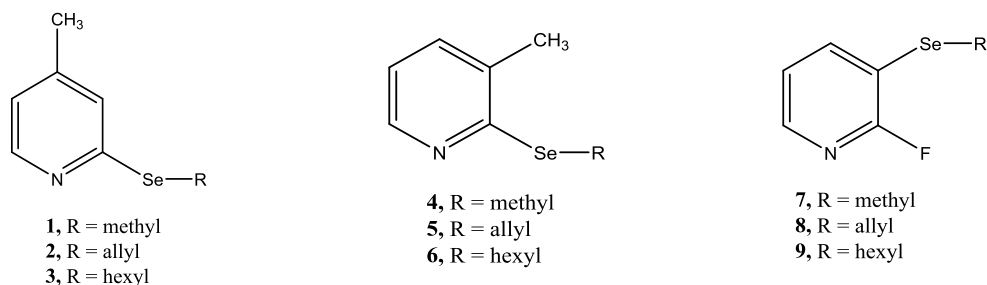
Figure 3.1 Representation of alkyl-functionalized monoselenopyridines

Similar to organodiselenides, the alkyl-substituted monoselenides were also obtained in moderate yields with a significant degree of stability at 4°C even after two months. In addition, these monoselenides along with the heteroaryl diselenides (**Section 3.1.1**) were observed to be resist photolytic degradation under visible light.

3.1.2 Synthesis of heteroarene-conjugated diselenides

Amongst the various categories of organoselenium compounds, (di)aryl diselenides have been reported in literature to exhibit an ability to disrupt the redox-statusof tumour cells and hence trigger or stimulateseveral redox-related signaling pathways [152]. Theredox-altering feature of such compounds has beenrelated to the presence of a physiologically labile and redox-active dichalcogenide bridge that serves as a precursor to a series of bio-active primary and secondary metabolites. With regard to the synthesis of organodiselenides, a plethora of phenyl-substituted diselenides have been synthesized and analysed previously by several research groups. In contrast, the chemical synthesis of several heteroarene-substituted diselenides was successfully carried out in this study in order to broaden the existing information of the biological efficacy of diaryl diselenides. A popular methodology that was adopted for the formation of pyridine or pyrimidine-substituted diselenides (**13-15**) involved a halogen-selenium exchange reaction between halogen-functionalized heterocycles and sodium diselenide (Na_2Se_2) or sodium hydrogen selenide (NaHSe). The latter species were initially prepared *in-situ* by the alkali-mediated reduction of elemental selenium in DMF

or ethanol [140-142]. This was followed by the critical step involving a halogen-selenium exchange reaction which proceeded smoothly via a nucleophilic substitution of the halogen (attached to the aromatic ring) with the nucleophilic selenium (as in NaHSe/Na$_2$Se$_2$) followed by aerial oxidation to furnish a range of heteroaryl diselenides as solids. Dipyridyl diselenide (**15**) that has served as a precursor for the synthesis of the alkyl-functionalized monoselenides (**1-9**) was alsoprepared by this methodology [141].

On the other hand, pyridine carbaldehydes were employed as precursors for the synthesis of heteroarene-conjugated methylenyl diselenides (**10**-**12**). The key step in this synthetic scheme involved the reduction of pyridine carbaldehydes by sodium hydrogen selenide. The latter was prepared *in-situ* upon the reduction of elemental selenium by sodium borohydride.
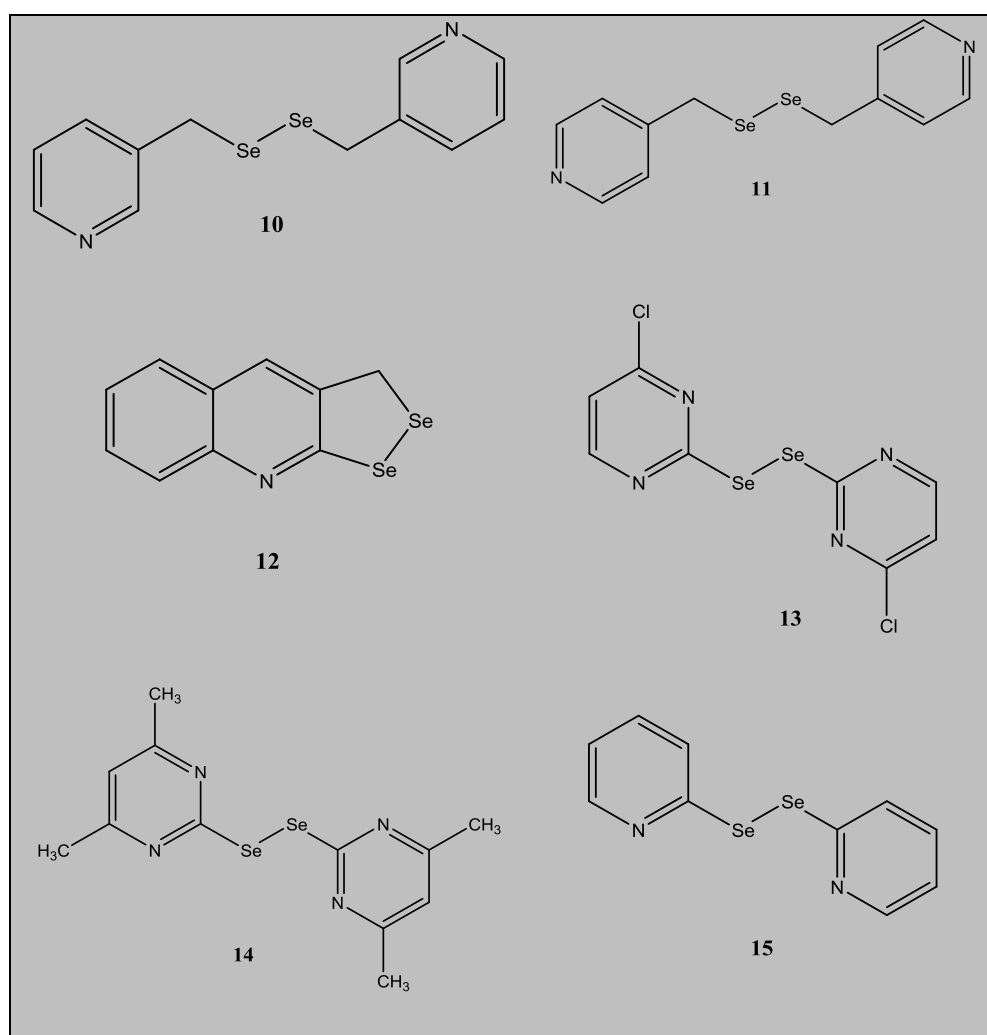
Figure 3.2 Representation of heteroarene-conjugated diselenides

This reaction was carried out under the catalytic action of piperidine hydrogen chloride. The corresponding selenoaldehyde thus formed was subsequently oxidized to yield the desired products (**10** and **11**) in quantitative yields. A similar synthetic methodology was also utilised for preparing **12** from a quinoline-functionalized carbaldehyde. The compound **12** was characterised by its unique diselenide bond that constitutes a part of a closed ring system. In addition, the electronic environment of the two selenium moieties that constitute the diselenide bridge in **12** was apparently asymmetric which could also probably provide an interesting reactivity. Accordingly, it was hypothesized that due to a probable ring strain, this diselenide bridge could react rather readily and hence, causes a significant biological activity, in part due to an apparently facile cleavage under physiological conditions.

All the heteroaryl diselenides were synthesized under tolerable experimental conditions. The yields were moderately high in all cases with a high level of purity. In addition, most of these compounds were also observed to be significantly stable after isolation and purification. Only in case of **11**, a certain degree of degradation was observed upon standing at room temperature for more than a week. This was apparently due to the exclusion of selenium as a black powder from **11**. However, no such exclusion of selenium was observed upon storage of **11** at 4°C upto three weeks. Interestingly, therelated compound **10** was observed to be fairly stable even when kept at room temperature for a month.

3.1.3   Synthesis of chalcogen-containing naphthoquinones

In addition to the heteroarene-functionalized diselenides and monoselenides, two selenium and tellurium-containing naphthoquinones (**16** and **17** respectively) were also re-synthesized with an aim to further elucidate their mode of chemotherapeutic action against tumorigenic cell lines. The synthetic protocol leading to these compounds was a straight-forward scheme which involved the facile nucleophilic substitution of phenyl selenolate/tellurolate, prepared *in-situ*, with halogen-functionalized naphthoquinones to yield black-coloured solids [143].
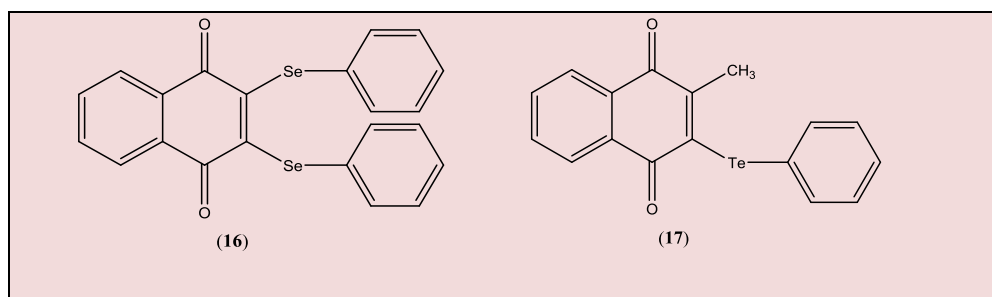
Figure 3.3 Representation of chalcogen-containing naphthoquinones

These compounds were isolated in favourable yields with a high level of purity. In addition, these compounds were stable at room temperature for at least two months. Similar to the behaviour of monoselenides and diselenides, both these compounds were also observed to resist photochemical decomposition under visible light.

Overall, in this current study, organoselenium compounds have been employedas the prime focus of attention in comparison to their sulfur and tellurium containing analogues. This has been apparently due to their relatively higher biological activity over organo-sulfur compounds, on one hand and a relatively stable chemical profile in comparison to organotellurides, on the other.

3.2   Physico-chemical characterization of synthesized compounds

3.2.1 ^{1}H and ^{13}C NMR analysis

The ^{1}H NMR spectrum of pyridine-substituted selenoalkanes (**1-9**) consisted of peaks of the aromatic protons (corresponding to the pyridine ring) in the downfield region of 6.7 - 8.2 ppm as doublets or singlets depending upon the position of the methyl group which is attached directly to the pyridine ring. The ethylene group (from the hexyls side-chain) which is attached directly to the selenium moiety was consistently observed as a triplet peak at 3.0 ppm, followed by the relatively upfield shifts of remaining methylene peaks of the alkyl groups as multiplets between 1.2 - 1.8 ppm. In contrast, in case of the allylic side chain, the methylene group which is directly bonded to the selenium atom appeared relatively downfield as a doublet at 3.7 ppm due

to splitting by the adjacent allylic protons. The ^{1}H NMR spectra thereby displayed a change in the resonance of the hydrogen atoms of the ethylenegroup (attached directly to selenium) depending upon a variation in the nature of the conjugated alkyl side-chain. The terminal methyl group of the functionalized alkyl side-chain appeared up-field (**3**, **6** or **9**) as a triplet at 0.8 ppm. In contrast, the methyl group attached directly to the pyridine ring appeared in a relatively downfield region at 2.2 ppm. The terminal allylic protons appeared in close separation from each other within the range of 4.9 - 5.3 ppm. Although both these protons are attached to the same carbon, a difference in their conformational arrangement could apparently lead to a difference in their splitting patterns. In addition, the non-terminal allylic protons resonate at a more downfield shift compared to their terminal counterparts at 6.0 ppm. This could most probably be due to their splitting by multiple adjacent protons, in addition to their closer proximity to a more electronegative selenium atom. In line with the alkyl-functionalized monoselenopyridines, the aromatic protons of the (di)aryl diselenides (**10**-**15**) also resided in the downfield region within 6.8 -8.4 ppm. On the contrary, the protons of the methylene group which are attached directly to the selenium moiety (Se-CH_2) resonated at 3.7 ppm (in case of **10** or **11**) and at 4.6 ppm (in case of **12**). The relatively downfield shift in case of **12** could apparently be due to a relatively higher electronegative effect of the quinoline ring in comparison to the pyridine ring (**10** or **11**) [142].

^{1}H NMR characterization of (**16**) and (**17**) displayed the resonating region of the aromatic protons of the naphthoquinone ring system between 7.8 - 8.0 ppm. Further, in case of **16** or **17**, the downfield peaks lying within 7.2 **-** 7.8 ppm corresponded to the aromatic protons of the benzene ring(s) which are attached directly to the selenium or tellurium moiety, respectively. In case of compound **17**, the non-aromatic protons corresponding to a methyl group which is attached directly to the naphthoquinone ring appeared at an upfield shift of 1.9 ppm. With respect to their ^{13}C NMR analysis, compounds **1**-**9** shared a common set of peaks corresponding to the carbon atoms of the pyridyl ring (120.0-160.0 ppm). The carbonatom of the methylenegroup which is attached directly to selenium appeared upfield at 30 ppm. On the other hand, the carbon peaks corresponding to the remaining methylene groups of the hexyl alkyl chain appeared in the region between 20 - 30 ppm.

Table 3.1 ^{1}H and ^{13}CNMR spectra data of compounds, synthesized as part of this study

Compound	^{1}H NMR (δ, *ppm*)	^{13}C NMR (δ*ppm*)
Monoselenides		
1*	8.2 (d, 1H), 7.0 (s, 1H), 6.7 (d, 1H), 2.3 (s, 3H), 0.9 (s, 3H)	155.5, 149.3,146.8, 130,121, 20.6, 7.7
2*	8.4(dd, 1H), 7.1 (dd, 1H), 7.2 (dd, 1H), 6.0 (m, 1H), 5.2 (dd, 1H), 5.1 (m, 1H), 3.8 (d, 2H), 2.1 (s, 3H),	154.7, 146.3, 139.5, 137.1, 135.8, 121.4, 115.8, 28.7, 20.6
3	8.3(dd, 1H), 7.3 (dd, 1H), 7.0 (dd, 1H), 6.1 (m, 1H), 5.3 (dd, 1H), 5.0 (m, 1H), 3.9 (d, 2H), 2.2 (s, 3H),	155.4, 147.0, 136.1, 135.1, 133.3, 119.9, 116.7, 27.6, 19.6
4*	8.2 (d, 1H), 7.1 (d, 1H),6.8 (dd, 1H), 2.3 (s, 3H), 0.7 (s, 3H)	155.6, 146.7, 135.4, 132.8, 118.8, 19.8, 4.9
5	8.2 (d, 1H), 7.2 (s, 1H), 6.7 (d, 1H), 3.1 (t, 2H), 2.2 (s, 3H), 1.6- 1.7 (m, 2H), 1.2-1.4 (m, 6H), 0.8 (t, 3H)	155.5, 149.5, 146.6, 125.9, 121.3, 96.2 31.4, 30.3, 29.7, 25.7, 22.6, 20.7, 14.1
6	8.2 (d, 1H), 7.2 (d, 1H), 6.7 (d, 1H), 3.2 (t, 2H), 2.2 (s, 3H), 1.6- 1.7 (m, 2H), 1.2-1.4 (m, 6H), 0.8 (t, 3H)	156.2, 146.9, 135.7, 133.2, 119.5, 96.2,31.5, 30.2, 29.8, 25.4, 22.6, 19.7, 14.1
7*	7.8-7.9(d,1H),7.6-7.7(t, 1H), 6.9-7.1(m, 1H), 0.8 (s, 3H)	158.3, 149.8, 140.9, 121.8,114.5,7.06
8*	7.9 (dd, 1H), 7.7 (dd, 1H), 6.9 (dd, 1H), 5.9 (m, 1H), 4.9 (m, 1H), 4.7(m, 1H), 3.5 (d, 2H)	160.5, 145.5, 143.2, 121.6, 113.3, 31.9, 26.3, 22.9, 13.6
9	8.1(m, 1H), 7.8 (m, 1H), 7.1(m, 1H), 2.9-3.0 (m, 2H), 1.3-1.7 (m, 4H), 1.2-1.3 (m, 4H), 0.9 (t, 3H)	162.6,161.2,145.4, 143.4, 121.9, 113.4, 31.2, 29.8, 29.4, 26.7, 22.5, 14.0
Organodiselenides		
10	8.5(d, 2H), 7.1(d, 2H), 3.8 (s, 2H)	150.0, 147.8, 124.0, 30.6
11	8.5 (d, 1H), 8.4(d,1H),7.5(m, 1H), 7.2(m, 1H), 3.7(s, 2H)	149.8, 148.4, 136.2, 134.6, 123.3, 28.8
12*	7.9-7.8 (d,1H), 7.7-7.6(m, 2H), 7.5-7.4 (m, 1H), 7.3 (s, 1H), 4.6(s, 2H)	165.4, 135.3, 131.7, 130.0, 129.7, 127.9,127.4, 126.6, 124.9, 31.4
13*	8.3-8.2 (d, 1H), 7.6-7.5 (d, 1H)	167.9, 161, 158.8, 118.7
14	6.6 (s, 1H), 2.3 (s, 6H) [140]	168.9, 167.3, 116.9, 23.9 [140]
15*	7.8-7.7 (d, 2H), 7.5-7.4 (m, 2H), 7.1-7.0 (m, 2H), 8.4-8.3 (d, 2H)	154.2, 137.5, 121.0, 123.0, 149.5
Chalcogen-containing naphthoquinones		
16*	7.9 (dd, 2H), 7.8 (dd, 2H), 7.5 - 7.4 (m, 4H), 7.3 - 7.2 (m, 6H)	178.3, 151.8, 134.0, 132.4, 132.2, 131.1, 129.4, 127.6, 126.8
17 *	8.0.- 7.9 (m, 1H), 7.9 (dd, 1H), 7.8 (dd, 2H), 7.8 - 7.7(m, 1H), 7.4 - 7.3 (m, 1H), 7.3 - 7.2 (m, 2H), 1.9 (s, 3H)	183.7, 180.7, 153.1, 141.4, 138.5, 134.2, 133.7, 131.6, 131.2, 129.5, 128.2, 126.6, 126.5, 115.0, 20.5

* NMR spectra data is in accordance with the published literature values [140-143**]**

In contrast, the allylic carbon atoms appeared at a relatively much higher chemical shift in the region between 120-135 ppm. The carbon atom of the terminal methyl group of the hexyl side chain and the methyl group attached directly to the pyridine ring appeared rather upfield at around 14 ppm and 22 ppm, respectively. In case of the (di)aryl diselenides, similar trends in shifts were found for the aromatic carbon atoms corresponding to the heteroaryl moiety (**10**-**12**). With respect to their ^{13}C spectra analysis, **10** and **11** shared a similar set of peaks corresponding to the aromatic carbon atoms between 120 - 150 ppm. In case of **12,** the peaks corresponding to the aromatic carbon atoms of quinoline ring also appeared downfield within a similar region (120-160 ppm).

The carbon signal corresponding to the methylene groups, which are attached directly to selenium, appeared upfield at around 30 ppm (for **10**, **11** and **12**). With respect to their ^{13}C spectra analysis, **16** and **17** shared a similar set of carbon peaks due to the presence of a common naphthoquinone and benzene ring system (115 - 185 ppm). The peak corresponding to the carbon of the methyl group (in case of **17**) could be observed at 20.5 ppm [143].

3.2.2 ^{77}Se NMR and elemental analysis

In the current studies, due to a primary biological focus on the most potent compounds **10, 11** and **12**, ^{77}Se NMR and elemental analysis of these relevant compounds were further carried out to ensure their high synthetic purity, which is essential to obtain a clear and comprehensive understanding of their biological efficacy.

Table 3.2 ^{77}Se NMR and elemental analysis of compounds **10, 11** and **12**

Compound	[77]Se (δ, *ppm*)	Analytical Data % found (Theoretical%)		
		C	H	N
10	283.0	40.98 (42.12)	3.40 (3.54)	7.81 (8.19)
11	274.8	40.16 (42.12)	3.41 (3.54)	7.89 (8.19)
12*	409.8, 369.9	39.76 (40.16)	2.24 (2.36)	4.50 (4.68)

* Data is in accordance with the published literature values [142]

3.2.3   Mass spectrometric analysis

On the basis of the results from a primary cytotoxicity screen, the mass spectrometric analysis of the three most potent compounds (**10**- **12**) was also carried out to reconfirm their synthetic purity prior to their further biological evaluation. In case of compound **10** and **11,** distinct mass peaks corresponding the mass of the complete molecules were observed at 345 (m/z). In addition, characterisitc peaks corresponding to a pyridyl group attached to a selenium atom were also observed at 173 (m/z). This peak has been observed due to the apparent cleavage of the *CH$_2$-Se* bond upon injection in a high intensity electron beam.In case of **10** and **11**, another peak in addition to its original mass peak was also observed at 253 (m/z). This peak could correspond to the formation of a diselenide species attached to a single pyridinyl ring [Aryl-CH$_2$-Se-Se]$^+$. In case of **12**, only the mass peak corresponding to the complete molecule was observed. The mass spectrometric data of representative compounds **10**, **11** and **12** has been listed in **Table 3.3**.

Table 3.3 Mass spectral analysis of **10**, **11** and **12.**

Compound	*m/z*[molecular ion, relative intensity]
10	345([C$_{12}$H$_{12}$N$_2$Se$_2$]$^+$,54%), 253([C$_6$H$_6$NSe$_2$]$^+$,39%), 173([C$_6$H$_6$NSe]$^+$, 87%)
11	345([C$_{12}$H$_{12}$N$_2$Se$_2$]$^+$, 63%),253([C$_6$H$_6$NSe$_2$]$^+$,35%),173([C$_6$H$_6$NSe]$^+$, 96%)
12*	301([C$_{10}$H$_7$NSe$_2$]$^+$,40%), 302 ([C$_{10}$H$_7$NSe$_2$+1]$^+$,20%).

* Data is in accordance with the published literature values[142]

3.2.4   X-ray structure elucidation of compound, 11

Orange coloured crystals of diffraction quality were grown by the slow evaporation of compound **11** after being dissolved in a solvent mixture of dichloromethane and hexane (1: 4). To have a better understanding of the structural

details, the molecular structure of **11** was unambiguously established by single crystal X-ray diffraction analysis. The single crystals were chosen from a crop of crystals mounted on glass fibres.The corresponding structural data was collected on Bruker Smart Apex and Bruker Smart diffractometer using graphite monochromated Mo $K_\alpha$radiation {(0.71069 Å) and (0.71073 Å)} for the cell determination and intensity data collection. The crystal structure was solved by direct methods (SHELX-97) and (SHELX-2013) and refined by the full matrix least squares method.

A perspective view and the atomic-numbering scheme of 1,2-*bis*{(pyridin-4-yl)methyl}diselane (**11**) is shown in **Figure 3.4.**
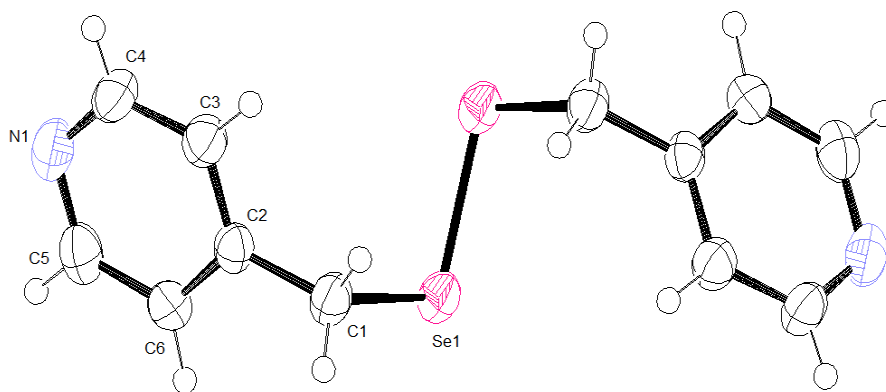
Figure 3.4 Perspective view of 1, 2-*bis*{(pyridin-4-yl)methyl}diselane (**11**) showing the atomic-numbering scheme

The crystallographic data reveals that compound **11** crystallizes into monoclinic, P2 (1)/c space group with the following cell parameters.

Cell parameters

a = 13.569(3)	b = 7.8407(15)	c = 11.984(2)
α = 90.00	β = 109.101(4)	γ = 90.00

The selected bond distances and bond angles are presented in **Table 3.4**. Relevant information regarding the data collection and refinement parameters (**Table 2.2, Chapter 2)** supports the structural framework of compound **11**.

Table 3.4: Selected bond distances [A°], bond angles [°] and torsional angles [°] of 1,2-*bis*{(pyridin-4-yl)methyl}diselane (**11**)

Se(1)-Se(2)	2.305(3)	Se(1)-C(1)	1.94(4)
N(1)-C(4)	1.30(6)	N(1)-C(5)	1.18(5)
C(3)-C(4)	1.32(7)	C(5)-C(6)	1.40(6)
C(1)-C(2)	1.27(5)	C(7)-C(8)	1.36(5)
C(1)-Se(1)-Se(2)	100.8(11)	C(7)-Se(2)-Se(1)	100.6(12)
C(2)-C(1)-Se(1)	114(2)	Se(2)-C(7)-C(8)	114(3)
C(1)-Se(1)-Se(2)-C(7)	179.1(10)	Se(1)-Se(2)-C(7)-C(8)	-72(3)
Se(2)-Se(1)-C(1)-C(2)	-76(4)	C(3)-C(2)-C(1)-Se(1)	101(4)

The Se-Se bond length has been found to be 2.305 Å which relates well with the corresponding distances reported for other diselenides, ranging from 2.29 to 2.39 Å(Pauling scale). The C–Se bond distances of 1.997 Å [C(7)−Se(1)] and 1.995 Å [C(6)−Se(2)] in the structure are in agreement with the literature values.The expanded short contacts view of **11** reveals intermolecular N···H, Se···Se and Se···H interactions.

3.3 Cytotoxicity studies

3.3.1 Primary cytotoxicity of organo-selenium compounds against mammalian cell lines

Due to the presence of a redox-active and physiologically labile diselenide moiety, organodiselenides have been frequently proposed to furnish, intracellularly, a greater level of biologically-active metabolites like selenols with relative "ease", in comparison to monoselenides. This, in turn, has been observed in the significantly

higher level of anti-tumour efficacy of the former, in both *in-vitro* and *in-vivo* experiments, relative to their monoselenide counterparts [153].

In the past, several reports have highlighted the biological efficacy of a plethora of phenyl-substituted diselenides against tumorigenic cell lines. However, there is lack of information regarding the biological efficacy of heteroaryl-substituted diselenides. In due consideration of the natural occurrence of *N*-containing heterocyclic moieties like pyridine or pyrimidine rings in biologically active substances, the present studies were aimed at investigating the anti-tumour efficacy of such hetero-aryl conjugated diselenides (**10**-**15**), thereby shifting the attention from the routine synthesis and biological analysis of diphenyl diselenide and its derivatives. On the other hand, in view of the concept that an enhancement in the ability of monoselenides to enter cells via an enhanced lipophilicity could possibly lead to an enhancement in their cytotoxicity against tumour cells and possibly bridge the difference between the anti-tumour efficacy of organodiselenides and monoselenides. Attempts were made to introduce a characteristic amphiphilicity into these rather poorly active monoselenidesvia functionalization with hydrophobic alkyl chains of varying carbon lengths. This led to the synthesis of a number of alkyl-functionalized monoselenides (**1**-**9)**. The design and synthesis of some of the monoselenides and diselenides were carried in the research group of Prof. K.K. Bhasin (Department of Chemistry, Panjab University, Chandigarh, India).

Further, in order to carry out a comparative analysis of the anti-tumour efficacy of organoselenium compounds on a relatively broader scale, several chalcophenes provided by Dr. Pavel Arsenyan (Latvian Institute of Organic Synthesis, Aizkraukles 21, Riga LV-1006, Latvia) were also included in the primary screen. This facilitated in establishing a comparison between the anti-cancer activities of three distinct different groups of organo-selenium compounds, namely monoselenides, diselenides and selenophenes. Here again, it must be mentioned that organoselenium compounds have been selected for study over organosulfur compounds due to their relatively higher anti-tumour efficacy [153]. In addition, organoselenium compounds have been reported to have a safer pharmacological profile in comparison to organotellurium compounds.

In view of the above arguments, representative examples of the synthesized organodiselenides and alkyl-functionalized monoselenides were screened for their anti-proliferative ability against a spectrum of tumorigenic cell lines. Amongst the tumour cell lines, KB-3-1, PC-3 and MCF-7 cell lines were selected, since these tumour cell lines are fairly robust and therefore, can clearly distinguish between of the chemotherapeutic potential of toxic and non-toxic molecules. Due to the inclusion of an MCF-7, a breast cancer cell line, **ARS-01**, an FDA-approved organo-chalcogen drug used in the treatment of breast carcinoma has been included as a benchmark compound in the primary screening. In addition, a transformed mouse fibroblast cell line (L-929) was alsoselected in order to observe a selectivity of any of the screened compounds towards tumorigenic cells.

The primary screening of the diverse range of organselenium compounds against the selected mammalian cell lines were carried out by means of a standard MTT assay, as described in **Section 2.4.3** [144]. This assay was carried out in the laboratory of Dr. Florenz Sasse (Helmholtz Centre for Infection Research, Braunschweig, Germany). Briefly, this assay is based on the principle of conversion of a commercially available MTT dye into insoluble formazan crystals by the activity of dehydrogenase enzyme in viable cells. In accordance with this principle, viability of treated cells was calculated with respect to the corresponding solvent-treated cells. The IC_{50} values that represent the concentration of the compound needed to elicit half of the maximum biological response are depicted in **Table 3.5** for the screened compounds.

3.3.1.1 *In-vitro* chemotherapeutic effects of heteroarene-substituted monoselenides and diselenides

According to the results presented in **Table 3.6**, the best inhibitory activities against the selected tumourigenic cell lines were displayed by the aryl (di)selenides. Amongst the representative examples of the synthesized (di)aryl diselenides viz.,**10, 11** and **12** displayed the maximum anti-proliferative potential against the selected mammalian cell lines. On the other hand, compounds **13, 14** and **15** also displayed a moderate anti-cancer activity which was still higher as compared to the one of the alkyl-substituted monoselenopyridines (**1-9**).

Table 3.5 IC$_{50}$ values (µM) of organoseleniumcompounds against mammalian cell lines[a] obtained from a standard MTT assay. Values have been expressed as mean IC$_{50} \pm$ SD.*$p < 0.05$; [#]$p < 0.001$ compared with solvent-treated cells. n = 3.

Compound	L-929	KB-3-1	PC-3	MCF-7
1	>37	35.5± 1.5	34.3 ± 1.5	>37
2	>37	>37	31.8 ± 1.9	>37
3	>37	31.1± 1.5	>37	>37
4	>37	34.8± 1.6	31.6 ± 1.6	>37
5	>37	>37	34.5 ± 1.8	>37
6	>37	>37	>37	>37
7	30.3 ± 1.4	31.1 ± 1.6	>37	>37
8	>37	>37	31.4 ± 1.1	>37
9	>37	>37	30.1 ± 1.3	>37
10	0.4 ± 0.1[#]	0.4 ± 0.2[#]	0.6 ± 0.3[#]	0.8 ± 0.3[#]
11	0.7 ± 0.4[#]	0.4 ± 0.1[#]	0.9 ± 0.3[#]	n.d.
12	0.6 ± 0.3[#]	0.8 ± 0.4[#]	0.02 ± 0.3[#]	n.d.
13	10.5 ± 1.1*	17.5 ± 1.8*	18.6 ± 1.7*	16.8 ± 1.1*
14	15.1 ± 1.6*	18.5 ± 1.3*	16.1 ± 1.3*	18.6 ± 1.9*
15	6.4 ± 1.3[#]	16.3 ± 1.4*	18.8 ± 1.6*	17.5 ± 1.4*
ARS-01 (positive control)	9.1 ± 1.1[#]	5.3 ± 0.7[#]	5.8 ± 0.6[#]	3.5 ± 0.8[#]

[a]L-929: transformed mouse fibroblasts; KB-3-1: humancervix carcinoma; PC-3: prostate carcinoma; MCF-7: breast carcinoma. n.d. - not determined

In accordance with the results obtained from the MTT assay, compound **12** displayed a significantly high activity against several tumorigenic cell lines. Based on the results obtained from the MTT assay, the inhibitory values of **12** against the selected mammalian cancer cell lines were found within the sub-micromolar range. Prostate cancer cells, in particular, displayed an acute sensitivity towards this compound (IC$_{50}$ = 0.02 ± 0.3 µM). Compound **12** also yielded a significant inhibitory activity against cultured KB-3-1 cells (IC$_{50}$ = 0.8 ± 0.4 µM). The dose-response curves of **12** against KB-3-1 cells have been

demonstrated in **Figure 3.5**. It also displayed a certain level of toxicity even against L-929 (IC_{50} of 0.6 ± 0.3 µM), thereby indicating an apparently low selectivity towards cancer cells and a risk of general toxicity against mammalian cells.
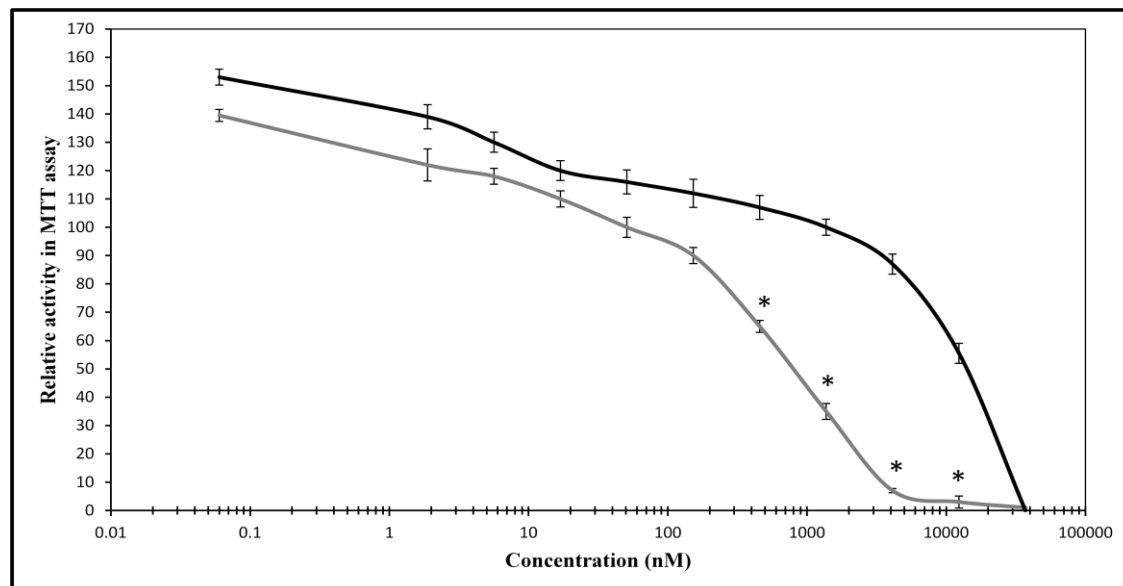
Figure 3.5 Dose-response curves of compound **12** (grey curve) and an "equivalent volume" of DMSO (black curve) against KB-3-1 cells, *in-vitro,* in an MTT assay following a 5 d incubation. $IC_{50} = 0.8 \pm 0.4$ µM for **12**. Activities have been plotted as the mean values $\pm$ SD. $*p < 0.001$ *versus* DMSO-treated cells. $n = 3$.

In line with the results obtained for **12** in the MTT assay, the IC_{50} values of the isomeric diselenides **10** and **11** against the selected mammalian cell lines were also observed within the sub-micromolar range. The anti-cancer activity of **11** was slightly less compared to **10**. Amongst the tumorigenic cell lines, both **10** and **11** exerted a similar inhibitory activity against human cervix carcinoma (KB-3-1) cells, *in-vitro*, with an IC_{50} of 0.4 ± 0.2 µM, and 0.4 ± 0.1 µM, respectively. Further, **10** yielded a relatively higher inhibitory activity against PC-3 cells (IC_{50} of 0.6 ± 0.3 µM) compared to **11** (IC_{50} of 0.9 ± 0.3 µM). However, on similar lines with **12**, both **10** and **11** apparently did not exhibit a selectivity towards tumorigenic cells. The dose-response curves of **10** and **11** against KB-3-1 cells have been demonstrated in **Figure 3.6.**
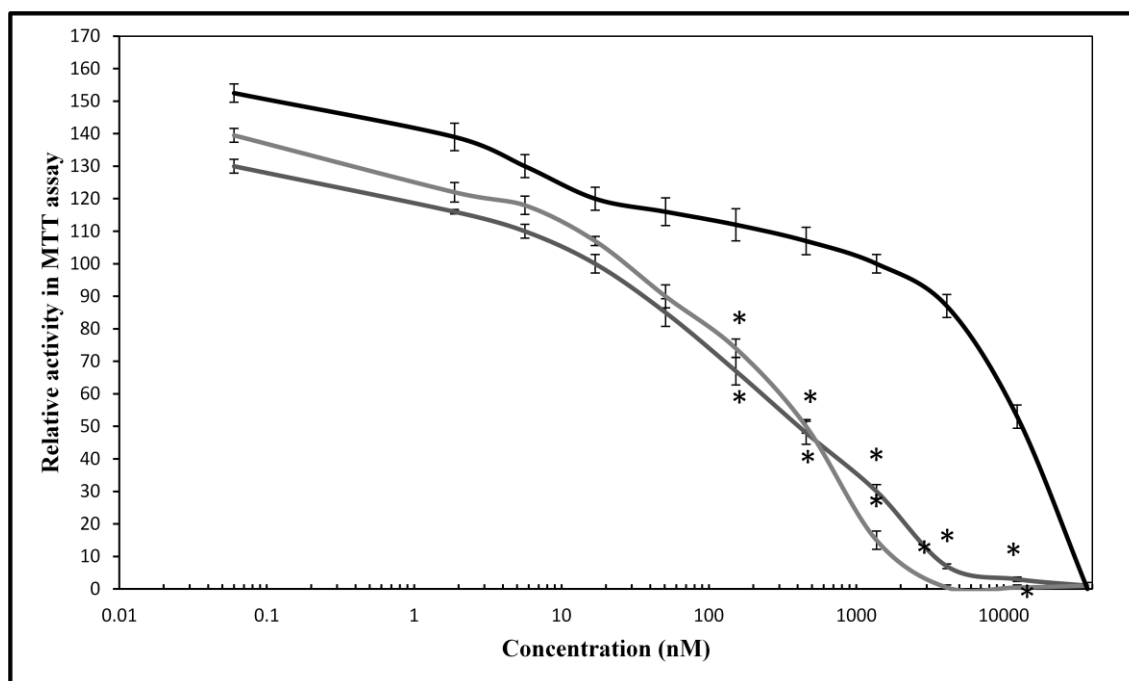
Figure 3.**6** Dose-response curves of **10** (light grey curve), **11** (dark grey curve) and an equivalent volume of DMSO (black curve) against KB-3-1 cells, *in- vitro*, in an MTT assay following a 5 d incubation. **10** and **11** exert a similar IC$_{50}$ of 0.4 ± 0.2 and 0.4 ± 0.1 μM, respectively. Relative activities have been plotted as the mean values obtained from individual experiments ± SD. *$p < 0.001$ compared to DMSO-treated cells. $n = 3$.

As poined out earlier, the significant intra-cellular efficacy of diselenides has been attributed to the facile generation of active selenols upon enzymatic cleavage of the diselenide bond (**Figure 3.7**). An interaction of the proteins (which are active in their oxidized form) with these strongly nucleophilic selenols has been reported to trigger the opening up of the disulfide bonds of such proteins, thereby resulting in the formation of an activated selenyl sulfide intermediate. The latter has been proposed to undergo subsequently a facile reaction with GSH to form glutathione-protein mixed sulfides which finally undergoes a further reduction to form an inactivated protein thiol. An inactivation of several oncogenic proteins that are redox-activated in their oxidized state, thereby, could contribute to the anti-proliferative potential of diselenides via redox-cycling. In contrast, due to the absence of physiologically labile diselenide bonds in monoselenides, the ease of formation of active metabolites like methyl selenol are apparently far less. As a consequence, the anti-tumour efficacy of monoselenides has been relatively weak, as observed in the present studies.
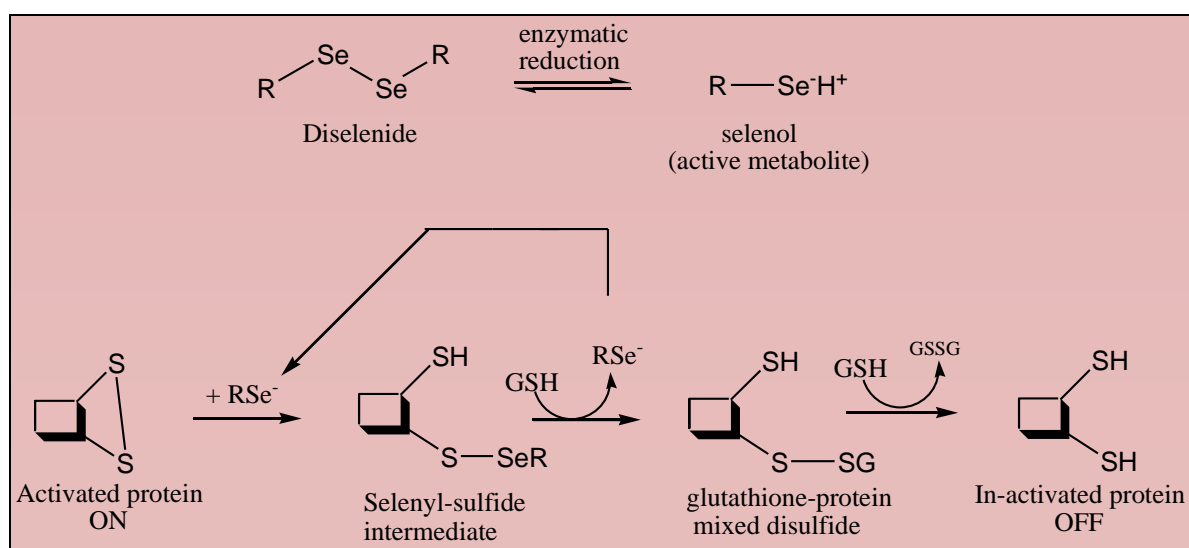
Figure 3.7 Mechanism of organodiselenide-catalysed inactivation of redox-regulated proteins [97].

The alkyl-functionalized monoselenides, in contrast, irrespective of variation in chain length, were apparently ineffective towards inhibiting the proliferation of the selected tumour cells. These monoselenides displayed an average IC_{50} of 30 μM against the selected tumour cell lines, which is far beyond a significant benchmark value assigned to potential chemotherapeutic molecules. The not-so promising results obtained with respect to these alkyl-functionalized mono selenides, apparently due to their poor activity and/or penetration ability into cells, were in concordance with results recorded previously in the literature for certain monoselenides [153]. A variation in the carbon chain-length of the conjugated alkyl side group appeared to induce a minimal alteration in activity, counting against the notion that modulation of lipophilicity may improve the biological activity significantly.

3.3.1.2 *In-vitro* **chemotherapeutic efficacy of selenophenes: First insights**

In addition to organo-monoselenides and diselenides of *N*-containing heterocyclic ring systems, a third chemotype belonging to a unique group called "selenophenes" were also subjected to a comparative cytotoxicity analysis using a standard MTT assay. These compounds basically involve a selenium (or sulfur in case of **ARS-01**) moiety that is integrated into a "stable" aromatic system (**Figure 3.8**).
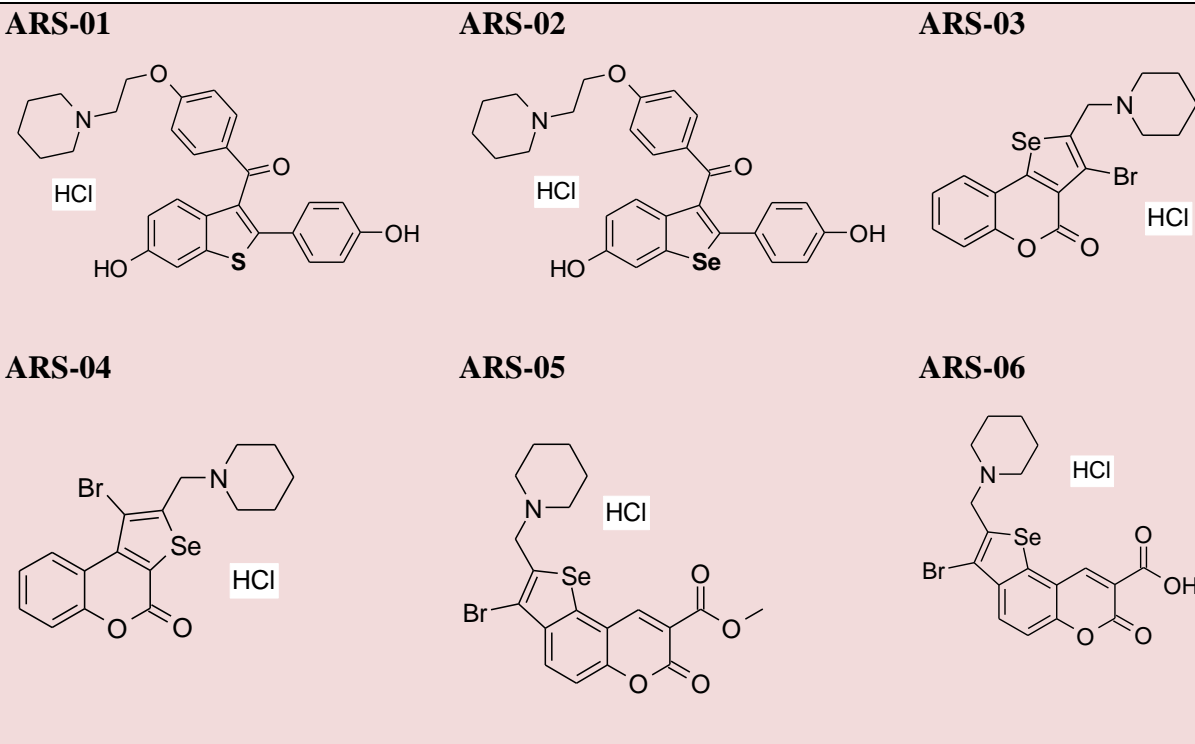
Figure 3.8 Chemical structures of **ARS-01** (raloxifene), **ARS-02** (the selenium analogue of raloxifene) and various other selenophenes.

These compounds (**ARS-02** to **ARS-06**) had been supplied by Dr. Pavel Arsenyan (Latvian Institute of Organic Synthesis, Aizkraukles 21, Riga LV-1006, Latvia) for a first-hand report on the biological efficacy of these newly synthesized molecules. In this case, raloxifene (**ARS-01**) which is an FDA approved anti-cancer drug and shares a close structural similarity with the selenophenes (**ARS-02**, in particular) was included as a reference compound to facilitate a comparative analysis of the chemotherapeutic efficacy of the screened compounds with the anti-cancer drug.

Based on the results obtained from an MTT analysis, raloxifene **(ARS-01)** and its selenium-substituted analogue **(ARS-02)** displayed the highest anti-proliferative potential against the selected cell lines. Whereas **ARS-01** demonstrated a maximum sensitivity against MCF-7 cells (IC$_{50}$ of 3.5 ± 0.8 μM), **ARS-02** yielded a weaker effect against the same cell line (IC$_{50}$ of 10.7 ± 1.4 μM).Compound **ARS-02,** however, displayed its maximal inhibitory active selenium moiety in **ARS-02** compared to a sulfur moiety in **ARS-01**, the latter apparently displayed a better inhibitory potential against the selected tumour cell lines.

Table 3.6 IC_{50} values of various selenophenes obtained against mammalian cell lines[a] obtained from a standard MTT assay. Inhibitory values have been calculated as mean IC_{50} values $\pm$ S.D. *$p < 0.05$; #$p < 0.001$ *versus* DMSO-treated cells. $n = 3$.

Compound	L-929	KB-3-1	PC-3	MCF-7
ARS-01 (positive control)	9.1 ± 1.1#	5.3 ± 0.7#	5.8 ± 0.6#	3.5 ± 0.8#
ARS-02	12.6 ± 0.9*	7.1 ± 1.1#	11.7 ± 0.8*	10.7 ± 1.4*
ARS-03	13.1 ± 1.5*	21.1 ± 1.8	18.6 ± 1.3	22.6 ± 1.6
ARS-04	19.5 ± 1.4	17.1 ± 1.8	22.4 ± 1.5	31.3 ± 1.8
ARS-05	11.5 ± 1.3*	10.6 ± 1.8*	21.1 ± 1.5	34.6 ± 1.4
ARS-06	11.8 ± 1.1*	10.8 ± 1.8*	16.4 ± 1.5	35.6 ± 1.6

[a]L-929: transformed mouse fibroblasts; KB-3-1: human cervix carcinoma; PC-3: prostate carcinoma; MCF-7: breast carcinoma.

The remaining four selenium-containing coumarin derivatives (**ARS-03** to **ARS-06**) displayed an average activity against the selected tumour cell lines in the higher micromolar range (IC_{50} = 10 - 35 µM). These four selenophenes, however, have displayed a relatively high activity towards KB-3-1 cells, in comparison to the other selected cell lines. Although the exact reason behind the higher susceptibility of KB-3-1 cells towards selenophenes remains unclear, it can be assumed that KB-3-1 cells, in comparison to the other tumour cells, are probably more sensitive to redox-active changes that could be mediated by these selenophenes.

Amongst **10**, **11** and **12** that exhibited the maximum anti-cancer activity in the MTT assay, **12** have a unique feature of belonging to the category of aliphatic and aromatic diselenides. This implies that one selenium atom in **12** is attached to a quinoline (aromatic) ring and the other selenium atom is attached to a methylene (aliphatic) group. This feature is due to the cyclic framework of this particular

heterocyclic diselenide. Interestingly, this heterocyclic diselenide (**12**) also exhibited a very strong inhibitory potential (IC$_{50}$ = 0.02 ± 0.3 µM) against the fairly stable prostate cancer (PC-3) cells. Although **10** and **11** have also exhibited potent inhibition of PC-3 cells in addition to other tumour cell lines, the promising anti-proliferative ability of **12** stands out in comparison to the other analysed molecules in this study. Therefore, in due consideration of its significantly low inhibitory value registered against PC-3 cells to its overall significant inhibitory effect against other tumour cells as well, **12** was eventually selected for a more-detailed biological study with attempts to comprehend its molecular and cellular mode of biochemical action against tumorigenic cells. Nevertheless, **10** and **11** were also studied in parallel due to an interest in these compounds and for an overall comparison. It must also be mentioned that these three compounds **10**, **11** and **12** which were synthesized by a similar synthetic methodology also share a common biologically active functionality in the form of a methylene group attached to a selenium atom.

In conclusion, as evident from the results, aryl diselenides (**10**-**15**) demonstrated a much higher chemotherapeutic efficacy *in-vitro* than the alkyl-substituted monoselenides (**1**-**9**) and the chalcophenenes (**ARS-01** - **ARS-06**). On the basis of their potent inhibitory values, compounds **10, 11** and **12** were further investigated for their biochemical mode of action against tumour cells. Results regarding the same have been discussed in the subsequent sections.

3.3.2 Comparative evaluation of compounds 10, 11 and 12 for their biological activity in KB-3-1 cells

As has been reported in the previous section, compound **12,** in addition to compounds **10** and **11**, exhibited a significant inhibitory activity against the selected tumorigenic cell lines *in-vitro* in the sub-micromolar range. In consideration of such findings, **10, 11** and **12** were selected for a more in-depth biological analysis.

3.3.2.1 ATP (Cell viability assay)

As observed in the MTT assay, **12** displayed a significant inhibitory activity against KB-3-1 cells. To further validate this observation, compound **12** was subjected to an ATP assay in order to investigate and quantify the decline in ATP levels in KB-3-1 cells upon treatment with **12**.

In addition to cellular dehydrogenase activity that has been quantified using the MTT assay, intracellular ATP levels are also widely recognised as a parameter of cell viability. In principle, when cells lose their membrane integrity, they also lose the ability to synthesize ATP and endogenous ATPases rapidly deplete any remaining ATP from the cytoplasm [147]. Therefore, to analyse the effects of the heterocyclic diselenide (**12**) upon ATP levels in KB-3-1 cells, a firefly luciferase-assisted ATP assay was employed using the Cell-titre Glo assay kit. This is one of the most commonly applied and commercially available methods for estimating cell viability in high content screening applications [147]. In accordance with the manufacturer´s instructions, this assay was carried out in the laboratory of Dr. Florenz Sasseusing KB-3-1 cells at two different time points (24 h and 48 h).

According to the results, **12** displayed a decrease in the ATP levels in KB-3-1 cells in a concentration and time-dependent manner**.** Whilst the intracellular ATP levels had not decreased significantly after the first 24 h of incubation ($IC_{50} = 4.5 \pm 0.7$ μM), **12** was observed to induce a significant decline in the ATP levels of KB-3-1 cells ($IC_{50} = 0.6 \pm 0.3$ μM) after 48 h (**Figure 3.9**). This value was close to the inhibitory value obtained previously for **12** against KB-3-1 cells using the MTT assay.

Similar to compound **12,** both **10** and **11** also caused a decline in the ATP levels of KB-3-1 cells in a concentration and time-dependent manner. As can be seen from **Figure 3.9**, the ATP levels of KB-3-1 cells did not decrease significantly after the first 24 h of incubation with either **10** or **11**. The IC_{50} values after 24 h of incubation were observed at 4.0 ± 0.7 μM and 9.5 ± 0.9 μM respectively. However, after 48 h of incubation, both **10** and **11** caused a significant decline in the ATP levels of KB-3-1 cells with a 50 % inhibitory value of 1.0 ± 0.4 μM and 2.5 ± 0.7 μM respectively.

a)

b)
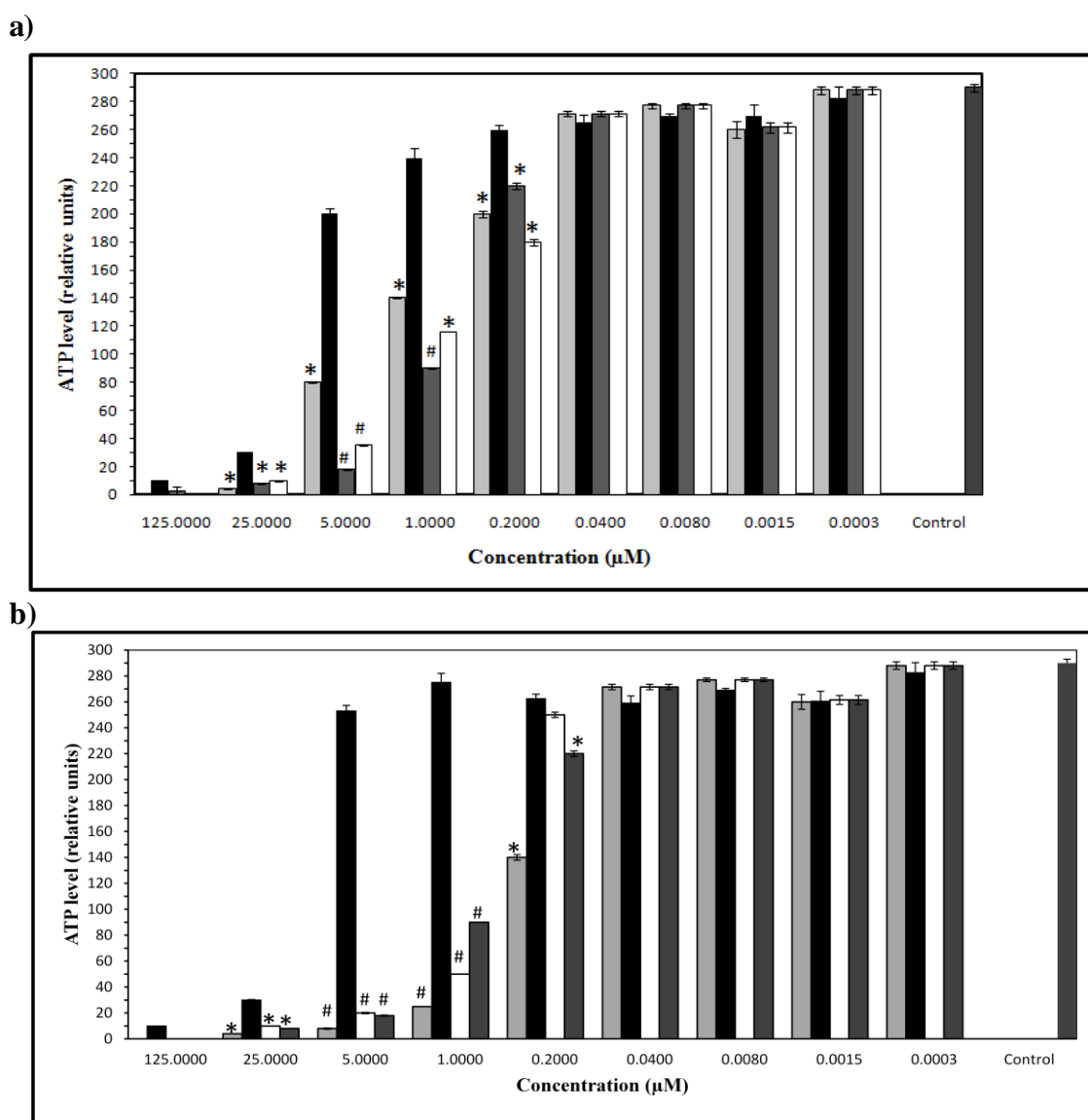
Figure 3.9 Concentration-dependent effect of **10** (white bars), **11** (dark grey bars), **12** (light grey bars) and equivalent volume of DMSO (black bars) on ATP levels in KB-3-1 cells treated for **(a)** 1 d and **(b)** 2 d. Untreated KB-3-1 cells correspond to the control. Luminescence, proportional to relatively intra-cellular ATP levels, was measured using a plate reader. Curves are plotted from mean values. Obtained from individual experiments $\pm$ S.D. *p <0.05; #p < 0.001 *versus* DMSO-treated cells. $n = 3$.

To conclude, compounds **10, 11** and **12** were observed to exert a significant decline in ATP levels of KB-3-1 cells after 48 h incubation. Although **10** and **12** were found to display a similar activity at either time intervals (1 d or 2 d), **11** appeared to be slightly less active especially after 1 d treatment with KB-3-1 cells. Although **10** and **11** are structural isomers, it could be possible that a poorer chemical stability of the latter in the biological medium could attribute to its relatively low activity.

3.3.2.2 Apoptosis assay: Cell-Death Detection ELISA Assay

The apoptosis assay studies were carried out at Helmholtz Centre for Infection Research, Braunschweig, Germany.

Based on the quantitative sandwich enzyme immuneassay principle, an ELISA assay for the detection of tumour cell death was performed to quantify the apoptotic index of compounds by detecting histone-associated DNA fragments (mono- and oligonucleosomes) generated by the apoptotic cells [145]. In accordance with the previous assays, KB-3-1 cell lineswere used to investigate the molecular mode of cell death. The enrichment of mono- and oligonucleosomes released into the cytoplasm of KB-3-1 cells by treatment with a compound was quantified in terms of "apoptotic index" of the compound. This index also serves as a direct parameter for comparing the apoptotic potential of different compounds. In principle, a higher apoptotic index signifies a greater extent of fragmentation of cellular DNA and therefore, higher levels of apoptosis.

According to the results obtained in this study, **12** was observed to induce apoptosis in KB-3-1 cells in a dose-dependent manner. The extent of apoptosis induced by **12** was observed to be maximal at a concentration of 30 µM.At this concentration, **12** demonstrated a maximum apoptotic index of 9.5 ± 0.6. As can be seen in **Figure 3.10**, therewas a sharp increase in the apoptotic potential of **12** within the concentration range of 10 µM to 30 µM. In contrast, equivalent volumes of DMSO (negative control) exhibited a negligible induction of apoptosis, in comparison to **12**.Similar to **12**, both **10** and**11** were also analysed for their potential to induce apoptosis in KB-3-1 cells. According to the results displayed in **Figure 3.10,** both isomeric diselenides potently induced apoptosis in KB-3-1 cells in a dose-dependent pattern. The apoptotic indices of **10** and **11**were observed to be considerably high, even at concentrations as low as 17 µM (apoptotic index of 8.5 ± 0.5 and 8.4 ± 0.3, respectively). At a lower concentration of 5.6 µM, compound **10** wasobserved to possess an apoptotic index of 7.1 ± 0.3, in contrast to a rather low apoptotic index of 3.9 ± 0.7 for **11**. Therefore, **10** demonstrated a higher efficacy in inducing apoptosis at lower concentrations as compared to its isomer **11**.

a)
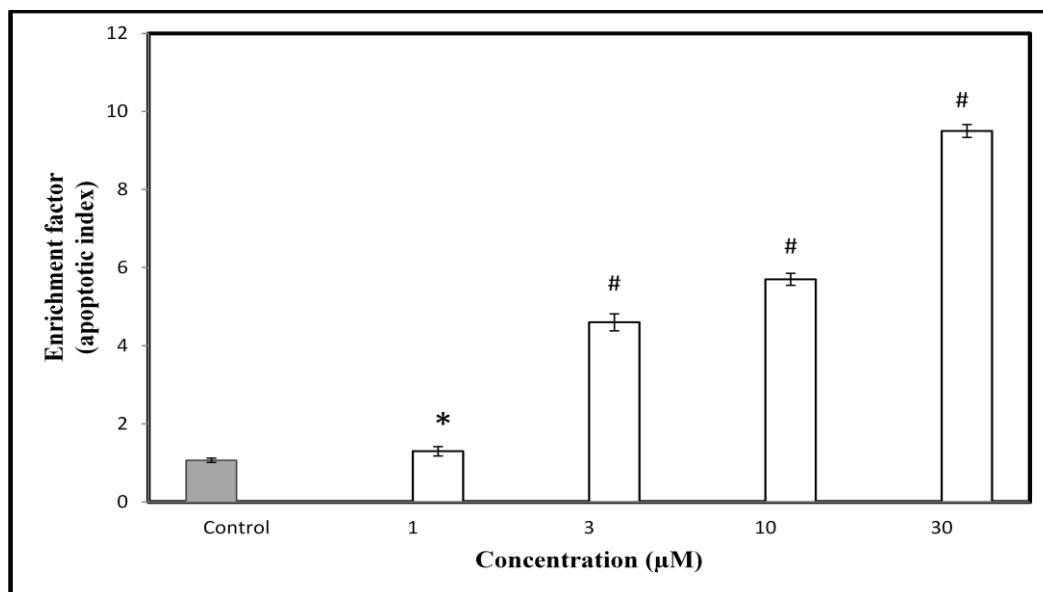
b)
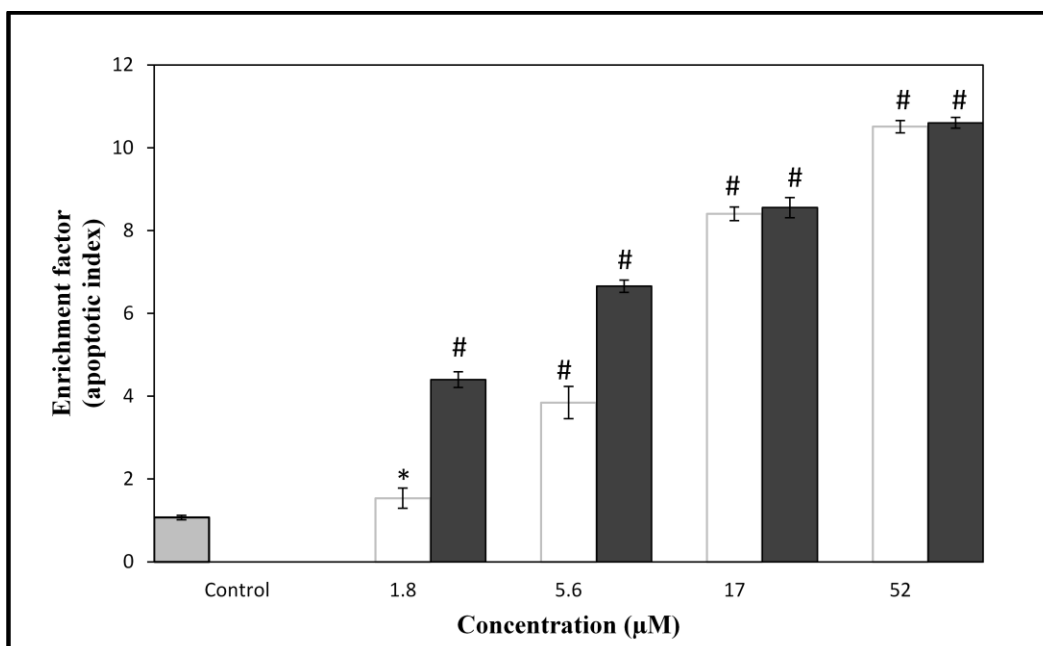
Figure 3.10 Induction of apoptosis by **(a)** compound **12** (white bars) and **(b)** compound **10** (dark grey bars) and **11** (white bars), after subtraction of effects caused by equivalent volumes of DMSO in KB-3-1 cells in a concentration-dependent manner. The apoptotic index (also called enrichment factor) represents the ratio of fragmented DNA in treated cells relative to untreated cells (control bar). Bars have been plotted from mean values ± S.D. *$p < 0.05$; #$p < 0.001$ *versus* untreated cells. $n = 3$.

To conclude, both **10** and **11** demonstrated a potent induction of apoptosis in KB-3-1 cells. Compound **10** apparently exhibited a relatively higher apoptotic potential compared to **11** or **12**, particularly at the lower concentrations used. Therefore, it is evident that **10**, **11** and **12** exert their anti-proliferative effects against KB-3-1 cells via an induction of apoptosis.

3.3.2.3 Caspase 3/7 activation assay

It has been reported that selenium-containing molecules mediate apoptosis in tumour cells. Depending upon the chemical nature of species, selenium-containing compounds induce apoptotic mode of cell death with or without the aid of caspases [57, 104]. In order to better comprehend the mechanism of apoptosis induced in compound-induced KB-3-1 cells, a caspase 3/7 assay was carried out to confirm the potential involvement of caspases 3 and 7 in mediating apoptotic cell death in KB-3-1

Figure 3.11 Degree of activation of caspases 3/7 in KB-3-1 cells upon treatment of KB-3-1 cells with different concentrations of **12,** after subtraction of effects caused by equivalent volume of DMSO. Caspase 3/7 activity levels, after an incubation of **12** with KB-3-1 cells for 12 h (dark grey bars) and 24 h (white bars), are in direct proportion to the recorded luminiscence values. Caspase activity corresponding to untreated cells (control) has been arbitrarily normalized to 10.0. Bars have been plotted from mean values ± S.D.*$p < 0.05$; #$p < 0.001$ *versus* untreated cells. $n = 3$.

cells and quantifying the extent of its activation upon compound treatment [148]. This assay was carried out at Helmholtz Centre for Infection Research, Braunschweig, using a commercially available Caspase3/7 Glo assay kit. Briefly, in accordance with the manufacturer´s instructions, KB-3-1 cells were incubated with serial dilutions of the compounds in 96-well micro-titre plates for 12 h and 24 h. After the treatment, the Caspase Glo-reagent (prepared freshly) was added to compound-treated KB-3-1 cells resulting in a luciferase reaction with the production of luminiscence. The amount of generated luminescence was quantified using a plate reader. In principle, the amount of luminiscence generated is proportional to the degree of activation of caspase 3/7 in KB-3-1cells.

Results from this assay pointed towards a concentration and time-dependent stimulation in caspase3/7 activity in KB-3-1 cells upon treatment with **12**. The stimulation of caspase3/7 was more pronounced after 24 h incubation relative to 12 h incubation. This was evident from an approximately 5-fold and 4-fold increase in the activation of caspase 3/7 in KB-3-1 cells upon incubation with 30 μM of **12** relative to incubation with 1 μM of **12** for 12 h and 24 h, respectively.

Similar to **12**, both **10** and **11** induced astimulation in the activation of caspase 3/7 in KB-3-1 cells in a concentration and time-dependent manner. Upon an increase in the concentration from 1.8 μM to 52 μM, both **10** and **11** induced an approximately 3-fold and 4-fold increase in the activation of caspase 3/7 after treatment with KB-3-1 cells for 12 h and 24 h, respectively. The ability of the isomers **10** and **11** to stimulate caspase 3/7 activity in KB-3-1 cells was similar with **10** being relatively more effective than **11**. Similar to **12**, stimulation of caspase 3/7 by **10** or **11** was more pronounced after 24 h incubation, relative to 12 h incubation.

To sum up, the results that were obtained from the cellular assays *in-vitro*, amongst the screened compounds **10**, **11** and **12** demonstrated the highest activity against tumour cells. This was evident from an appreciable decline in the dehydrogenase activity and ATP levels of cultured cervix carcinoma (KB-3-1) cellsupon treatment with **10**, **11** or **12** at concentrations in the sub-micromolar range.

a)
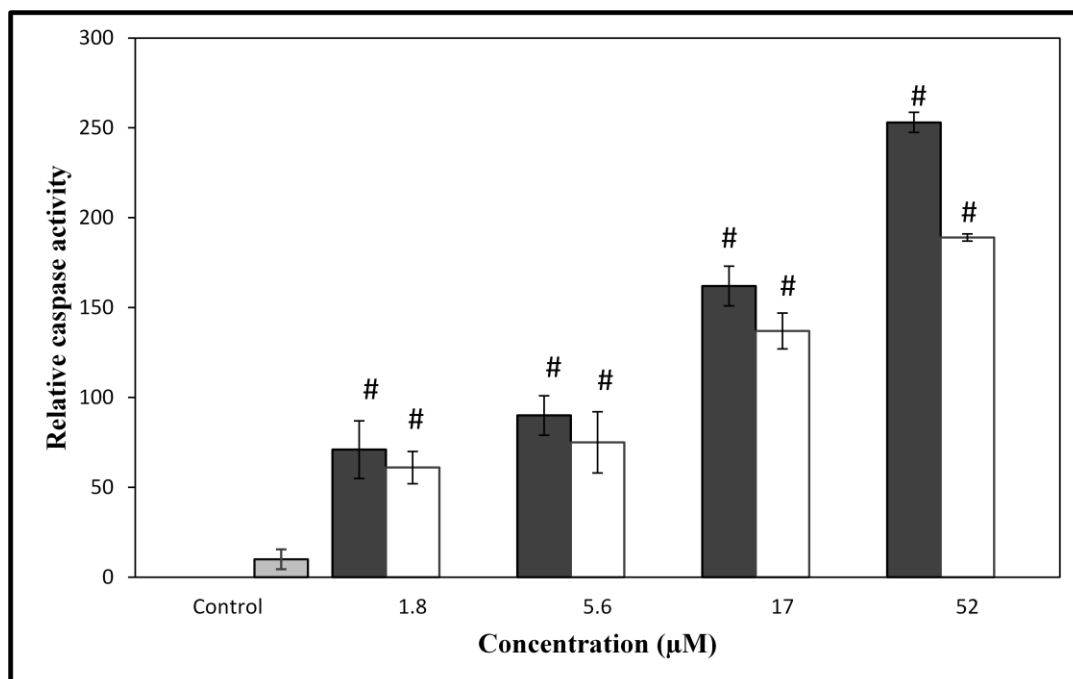
b)

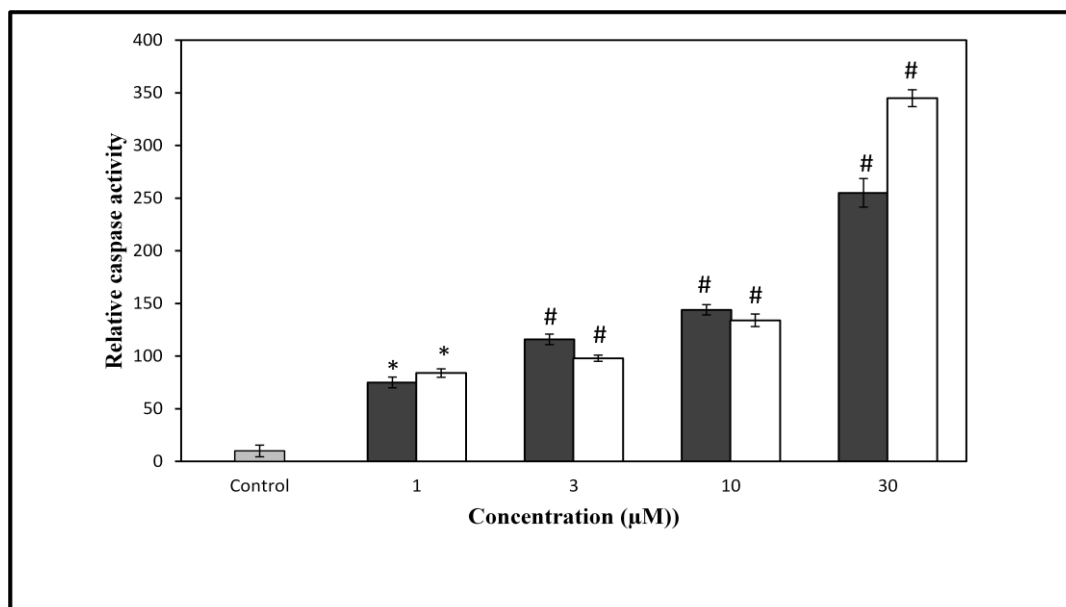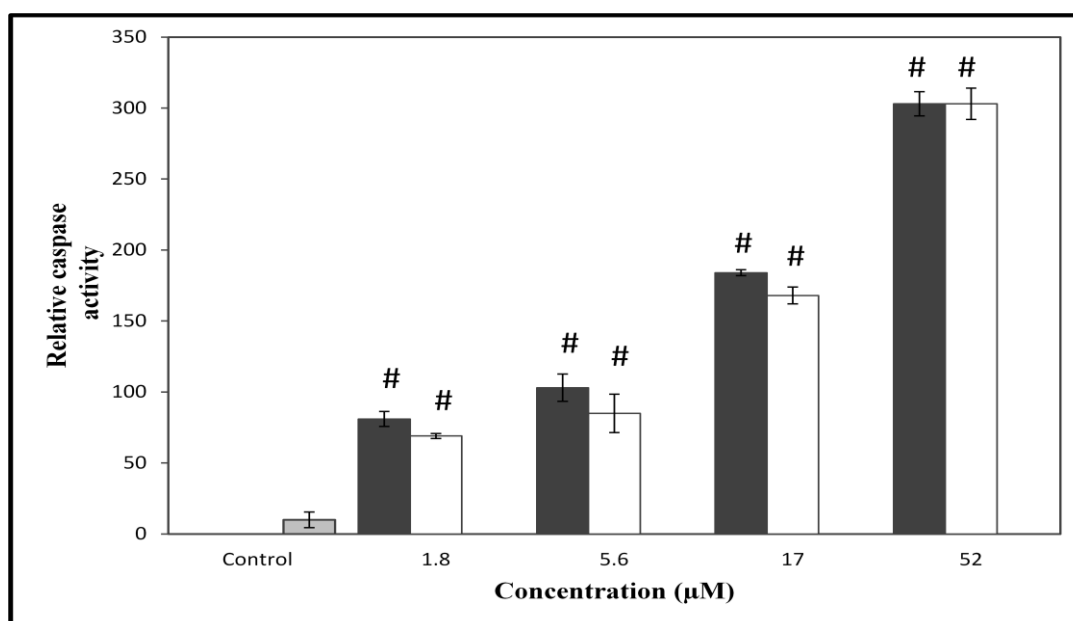**Figure 3.12** Degree of activation of caspases 3/7 in KB-3-1 cells upon its treatment with different concentrations of **10** (dark grey bars) and **11** (white bars)**,** after subtraction of effects caused by DMSO. Caspase 3/7 activity levels, after an incubation of **10** and **11** with KB-3-1 cells for **(a)** 12 h and **(b)** 24 h, are in direct proportion to recorded values. Caspase activity corresponding to untreated cells (control) has been arbitrarily normalized to 10.0.*$p < 0.05$; [#]$p < 0.001$ *versus* untreated cells. $n = 3$.

Further, in accordance with the results obtained from the ELISA assay and caspase 3/7 assay, these compounds (**10**-**12**) demonstrated a significant induction of apoptosis in KB-3-1 cells via stimulation of caspase 3/7 activity. Since **10** and **11** are isomers of each other, both these compounds share an identical chemical composition and subsequently a similar biological activity. Further, on a close introspection of their chemical structures, these three compounds (**10**, **11** and **12**) possess a rather labile and reactive functional moiety comprising of a selenium atom attached to a methylene group. Since such a functional moiety has also been observed in various biologically active organoselenium compounds like SEM or Sec, it could be hypothesized that this characteristic chemical functionality could attribute to somewhat similar, yet significantly high biological activities of these compounds.

3.3.2.4 Translation inhibition assays

Since the up-regulation of protein translation has emerged as a critical aspect for proliferation and survival of cancer cells, this study explored any possible suppressive effects of **12** towards the intra-cellular translational machinery of such cells. For this, two models of translation were selected: a rabbit reticulocyte system and a KB-3-1 cell model. These experiments were, therefore, designed to establish a potential correlation between the anti-proliferative effects of **12** against mammalian cells, on the one hand, and possible down-regulatory effects on the protein-translationalefficiency of mammalian cells on the other. A particular emphasis on KB-3-1 cells was made in one of these assays since this type of tumour cells were also used as part of the previous studies.

3.3.2.4.1 *In-vitro* protein translation inhibition assay

This assay, involving a rabbit reticulocyte system which is enriched with essential amino acid mixtures and several translation-enhancing components, is frequentlyemployed to screen small molecules and extracts on the basis of their translation-inhibiting or promoting efficacy [154]. The inhibitory activity of the screened compounds is measured by means of a luciferase activity output assay. In principle, an expression of the luciferase enzyme, which is encoded within reporter genes like Renilla (which has been used in this study), is measured in the cell-free rabbit

reticulocytes to quantify the translational activity of the reticulocyte system after treatment with the compounds of interest. A lower luciferase activity corresponds to a greater inhibition of translation of the respective system.

As is evident from the results depicted in **Figure 3.13**, compound **12** caused a decline in the translational activity of the reticulocyte system in a concentration-dependent manner. The maximum inhibitory activity of **12** which was observed at its highest concentration selected (10 µg ml^{-1} or 33.3 µM) was comparable to the inhibitory potency of the standard inhibitorof translation cycloheximide at its highest concentration selected (10 µg ml^{-1} or 35.5 µM).
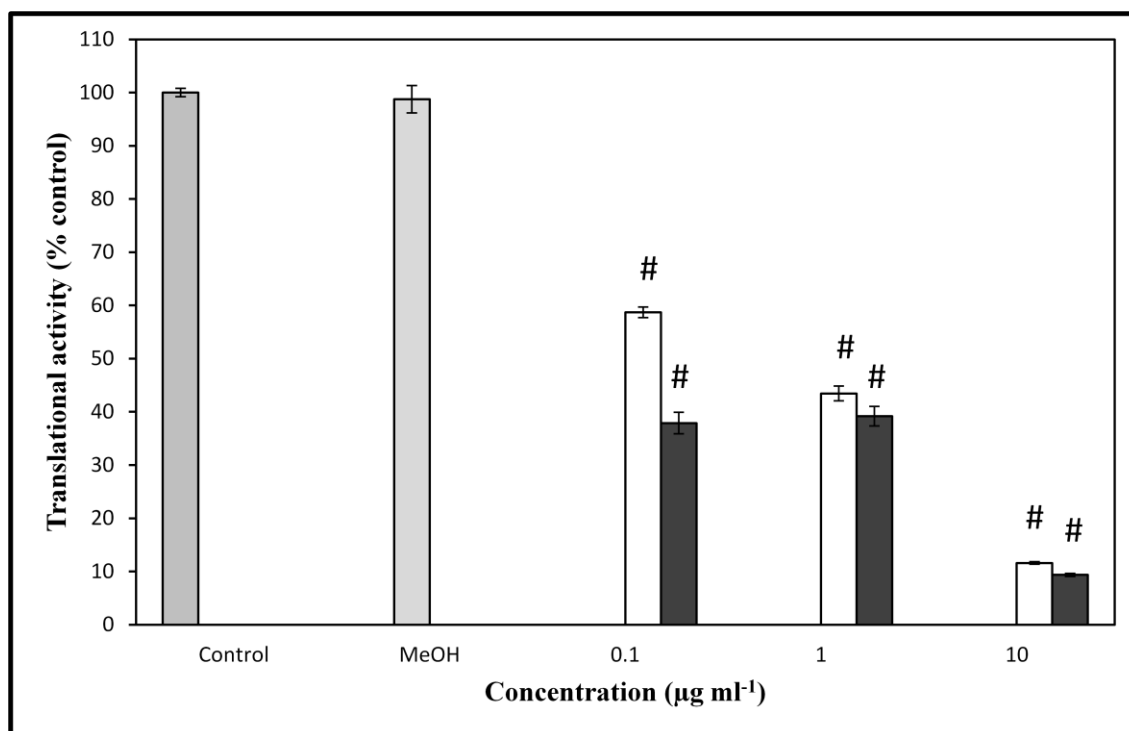
Figure 3.13 Inhibition of protein synthesis in an *in-vitro* rabbit reticulocyte system by **12** (white bars) and cycloheximide (dark grey bars), a standard translation inhibitor and used as a benchmark positive control. Recorded values, displayed as mean values ± SD, are in direct proportion to translation efficiency. Luminescence values corresponding to untreated cells (control) have been normalized to 100. *$p < 0.05$; #$p < 0.001$ *versus* untreated KB-3-1 cells. $n = 3$.

In addition, both **12** and cycloheximide caused a 43.6 ± 1.8 % and 61.3 ± 2.1 % inhibition of translational activity of the reticulocyte system at concentrations as low as 0.3 µM (0.1 µg ml^{-1}) and 0.4 µM (0.1 µg ml^{-1}), respectively. In contrast, methanol (as

negative solvent control) was found to exert negligible effects on the inhibition of the translational efficiency of the reticulocyte system.

3.3.2.4.2 *In-cell* translation inhibition assay

In line with the encouraging results obtained in the eukaryotic rabbit reticulocyte system, the translation-inhibitory potential of **12** was analysedfurther in KB-3-1 cells.
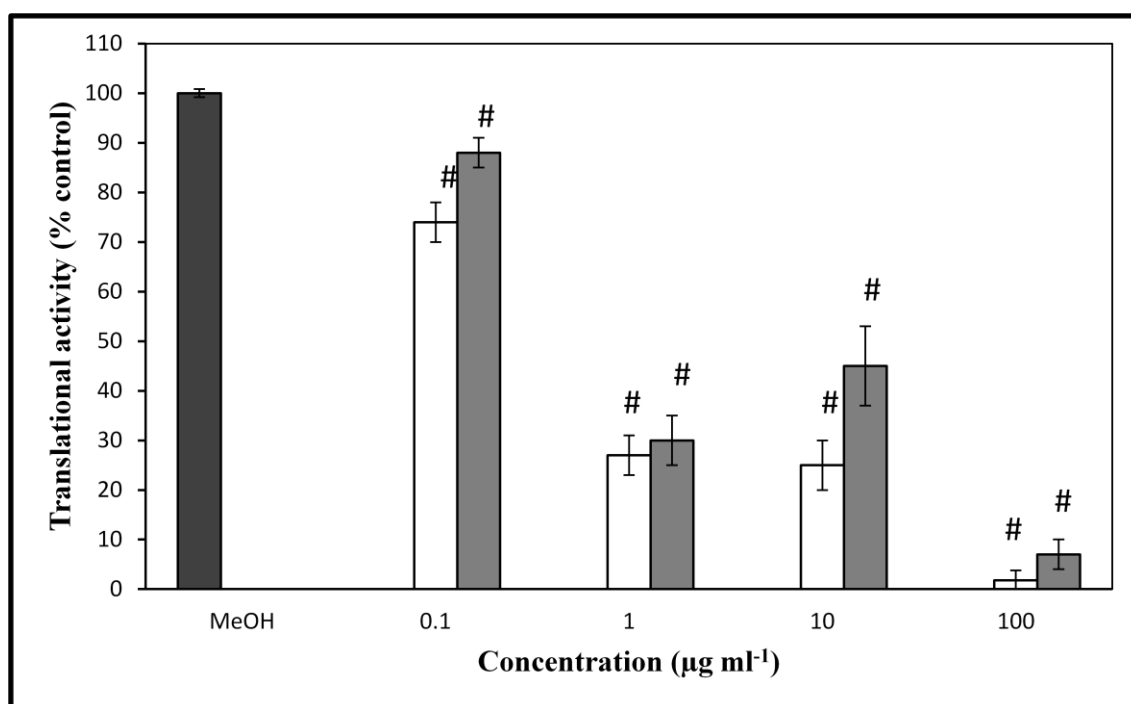
Figure 3.14 Inhibition of protein synthesis by **12** (white bars) and cycloheximide (light grey bars; positive control) in KB-3-1 cells after transfection with pRL-SV40 vector expressing Renilla luciferase. Recorded values, displayed as mean values ± SD, are in direct proportion to translation efficiency. Luminiscence of methanol-treated cells has been normalized to 100. The histograms are plotted as mean values. Error bars indicate ± S.D. *$p < 0.05$; [#]$p < 0.001$ *versus* methanol-treated cells. In remaining cases, $p > 0.05$, $n = 3$.

In accordance with the procedure described in **Section2.4.3.5.2**, prior to treatment of KB-3-1 cells with **12**,KB-3-1 cells were transfected with a suitable plasmid (in this case, pRL-SV40) by using polyethyleneimine (PEI) as the transfection agent (kindly provided by Dr. Yazh Muthukumar). This was followed by treatment of the

transfected KB-3-1 cells with different concentrations of **12**, cycloheximide (as positive control) and an equivalent volume of methanol (as negative solvent control). Following incubation for 4 h, the transfected KB-3-1 cells were lysed with 1x Passive Lysis Buffer and then mixed with a luciferase assay buffer. Based on the same principle as used in the *in-vitro* translation assay, the luminescence generated upon expression of the luciferase enzyme in KB-3-1 cells was quantified by using a plate reader. The intensity of the recorded luminiscence is directly proportional to the level of protein translational activity of the KB-3-1 cells.

As evident from the results displayed in **Figure 3.14**, both **12** and cycloheximide were observed to induce a similar dose-dependent decrease in the translational efficiency of transfected KB-3-1 cells. Apart from the maximum attenuating effects exerted by both compounds at 100 µg ml^{-1} (333.3 µM and 355.8 µM for **12** and cycloheximide, respectively), both **12** and cycloheximide drastically suppressed the translational efficiency of KB-3-1 cells by 71.7 $\pm$ 3.9 % and 68.4 $\pm$ 4.3 %, respectively even at a low concentration of 3.3 µM (1 µg ml^{-1}) and 3.5 µM (1 µg ml^{-1}), respectively. In contrast, methanol, under similar experimental conditions, did not display any inhibitory activity in the transfected KB-3-1 cells.

Therefore, the hypothesis that **12** inhibits protein translation in KB-3-1 cells may well explain its potent anti-proliferative potential against tumorigenic cells, in general, and against KB-3-1 cells in particular.

3.3.2.5 Identification of 12-mediated inhibition of oncogenic pathways in KB-3-1 cells by immunoblot analysis

During the past decade, several reports have demonstrated that specificintra-cellular pathways in tumorigenic cells also behave as agonists of protein translation [85, 28]. This implies that these specific pathways, when mutated or over-activated, stimulate higher levels of protein translation, as in the case of tumour cells. This, in turn, is reflected by an uncontrolled proliferation and enhanced survival of tumour cells. Amongst such signalling pathways, the ERK and mTOR-mediated signalling pathways

have been reported to individually or synergistically contribute to intra-cellular protein translation [86, 28].

In due consideration of the potent inhibitory potential of **12** on protein translationagainst KB-3-1 cells, in this study, attempts were made to explore modulatory effects of **12** on the mTOR and ERK-mediated signalling pathways. Such modulatory effects may well antagonize the protein translation of KB-3-1 cells.
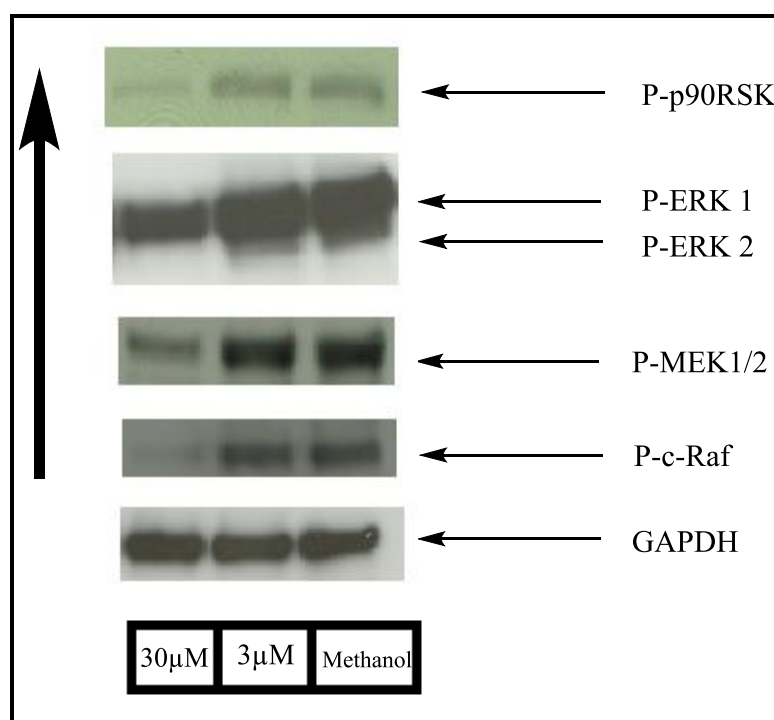
Figure 3.15 Western Blot analysis depicting changes in phosphorylation status of signalling proteins within the MAPK pathway induced in KB-3-1 cells, after treatment with 30 μM and 3 μM of compound **12**. Maximum dephosphorylation is visible at highest concentration of 30 μM. GAPDH serves as the loading control. Methanol-treated KB-3-1 cells are taken as a negative control.

Western blot analysis was carried out to determine alterations in the expression of critical proteins within the above mentioned pathways in **12**-treated KB-3-1 cells. Methanol-treated KB-3-1 cells served as a negative solvent control. As can be observed from **Figure 3.16** which displays the intensities of the protein bands following gel-electrophoresis of the compound/methanol-treated KB-3-1 cell lysates, there was a significant dephosphorylation and hence deactivation of oncogenic c-Raf in KB-3-1 cells upon treatment with **12** in a concentration-dependent manner.

a)

b)
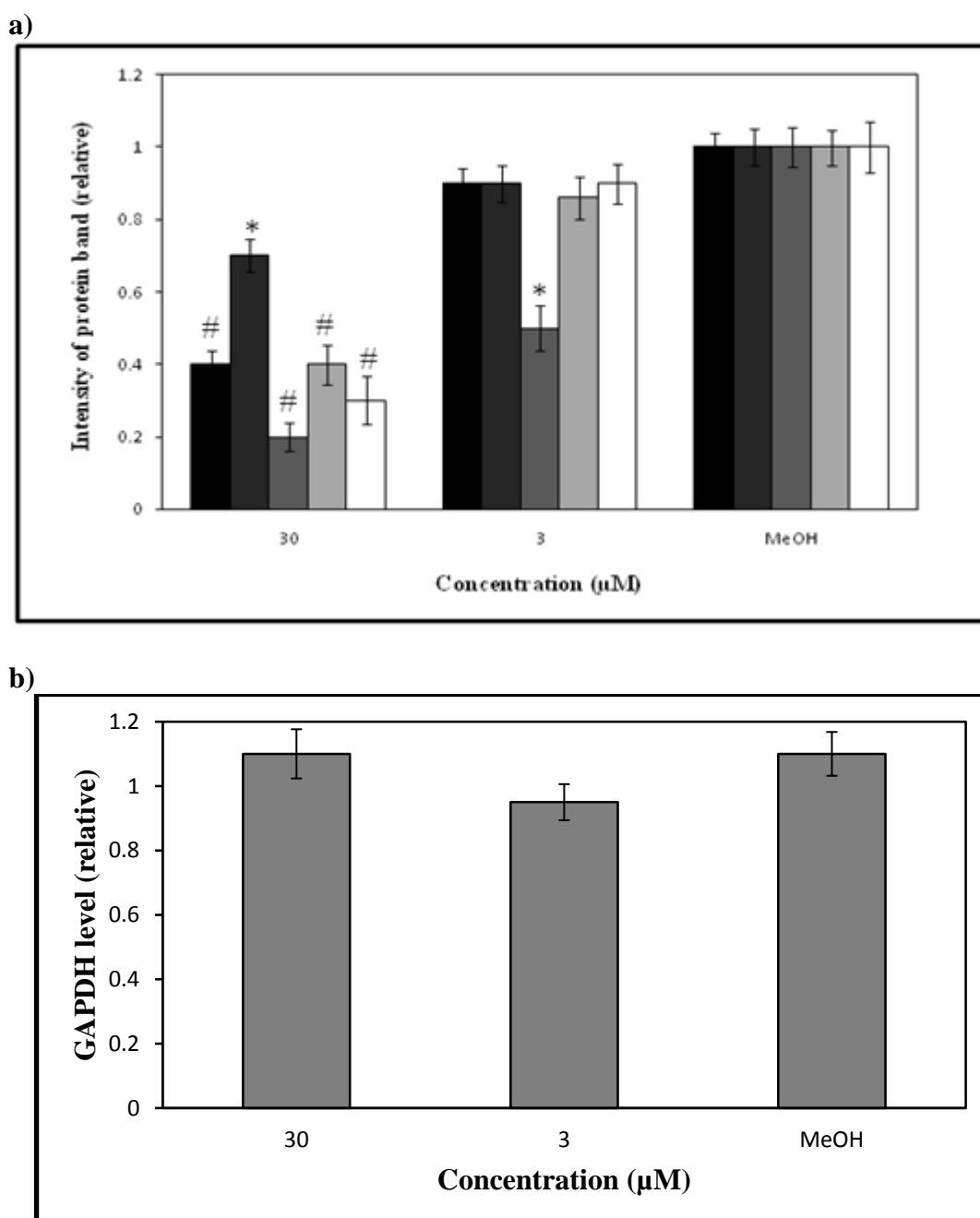
Figure 3.16 Quantitative evaluation of phosphorylation status of **a)** c-Raf (white bars), MEK 1/2 (light grey), ERK 1 (dark grey), ERK 2 (medium grey) and p90RSK (black) and **(b)** GAPDH protein (loading control) derived from Western-Blot analysis of **12**-treated KB-3-1 cell lysate. Band-intensities have been quantified using Gel-Quant.NET 1.8.2. Error bars indicate $\pm$ S.D. $*p < 0.05$; $^{\#}p < 0.001$ *versus* methanol-treated cells. $n = 3$.

This protein, which forms the head of the ERK-mediated MAPK cellular pathway and has been frequently reported to be over-activated via hyper-phosphorylation in tumour cells, was observed to be de-phosphorylated by approximately 70 % in KB-3-1 cells upon treatment with **12** at 30 µM relative to a

negligible dephosphorylation observed in case of methanol-treated cells [53].However, upon a 10-fold decrease in the concentration, the phosphorylation status of c-Raf was quite similar to that observed in case of methanol-treated KB-3-1 cells. Therefore, **12** was observed to modulate the phosphorylation status and hence activity of oncogenic c-Raf protein in KB-3-1 cells at a minimum concentration of 30 µM with an apparently negligible down-regulatory effect at 3 µM.

A similar down-regulatory effect was also observed in the phosphorylation status and activity of the downstream substrate of c-Raf, namely MEK1/2. As in the case of c-Raf, higher levels of the phosphorylation state of the MEK isoforms, namely MEK1 and MEK2, have been reported in cancer cells [48]. Since the MEK isoforms are widely recognised as a direct substrate of c-Raf, alterations in their phosphorylation status of the latter have been observed to exert a direct impact on the phosphorylation state and activity of MEK 1/2.As demonstrated in **Figure 3.15** and **Figure 3.16**, 30 µM of compound **12** induced a down-regulation in the expression of phosphorylated MEK1/2 by nearly 60 % of the phosphorylated levels of MEK 1/2 observed in case of methanol-treated KB-3-1 cells. However, there was no such observable decrease by **12** at a lower concentration of 3 µM when compared to the effects induced by an equivalent amount of methanol (negative solvent control).

As observed for c-Raf and MEK1/2, a similar trend was also observed in case of the proteins ERK1/2which act as downstream substrates of MEK1/2. As discussed in **Chapter 1**, the ERK1/2 proteins have been observed to be over-activated in tumour cells and also recognised to promote protein translation in tumorigenic cells [36]. As observed in **Figure 3.15**, the phosphorylation status and the activity of ERK1/2 proteins also experienced a down-regulation in KB-3-1 cells, upon treatment with **12** in a dose-dependent manner. In a slight contrast to its modulatory effects exerted against c-Raf and MEK1/2 particularly at a higher dosage, **12** appeared to effectively attenuate the phosphorylation status of ERK2 not only by approximately 80 % at a higher concentration of 30 µM but even at a lower concentration of just 3 µM by nearly 50 % of the phosphorylation status of ERK2 visible in case of methanol-treated cells (**Figure 3.15** and **Figure 3.16**). On the other hand, at a concentration of 3 µM the phosphorylation status of ERK1 was apparently not suppressed significantly. Interestingly, inspite of the fact that both ERK1 and ERK2

proteins exist intracellularly as isoforms and share a close structural and biochemical similarity, **12** was seen to dephosphorylate and hence deactivate ERK2 to a greater extent in comparison to ERK1 in KB-3-1 cells [178].

Further downstream, a direct substrate of ERK2, p90RSK, was also observed to be dephosphorylated by nearly 60% upon treatment of KB-3-1 cells with 30 μM of **12** compared to an inappreciable dephosphorylation observed in case of methanol-treated cells. A lower concentrations of **12** (3 μM)**,** however**,** displayed a negligible decline in the phosphorylation state and hence activity of p90RSK, when compared to the same in methanol-treated KB-3-1 cells. Like ERK1/2, p90RSK has also been widely considered as an oncogene due to its over-activation via hyper-phosphorylation in cancer cells. As discussed earlier, hyper-phosphorylated p90RSKwhich is commonly found in tumorigenic cells has not only been reported to inhibit apoptosis but also enhance protein translation [70].

In addition to the ERK-mediated MAPK signalling pathway, **12** was also observed to attenuate the activation of critical proteins within the mTOR-mediated pathway (**Figure 3.17**).
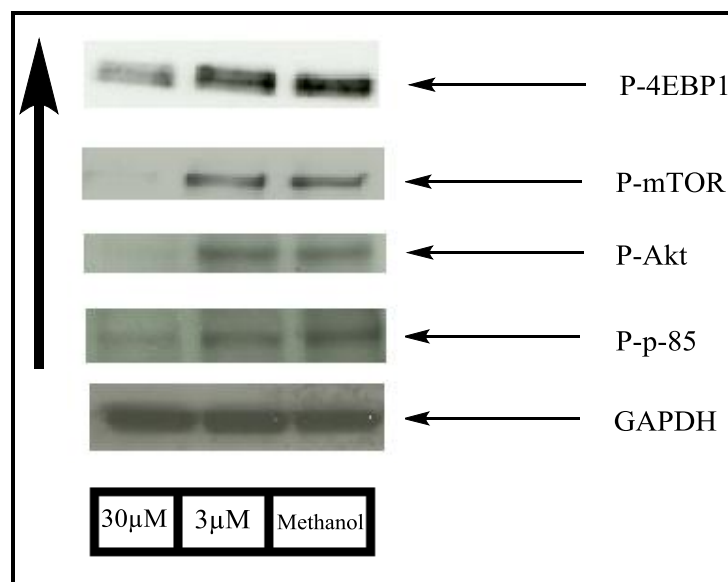
Figure 3.17 Western Blot analysis depicting changes in phosphorylation status of signalling proteins within the PI3K-mediated pathway induced in KB-3-1 cells upon treatment with different concentrations of **12**. Maximum dephosphorylation is visible at the highest concentration of 30 μM. GAPDH serves as the loading control. Methanol-treated KB-3-1 cells are taken as a negative control.

The catalytic sub-unit of PI3K protein, p85, that forms the head of this signalling pathway and has been frequently reported to be hyper-phosphorylated in tumour cells experienced a nearly 60% decline in its phosphorylated levels in KB-3-1 cells upon teatment with 30 μM of **12** in comparison to the phosphorylated levels observed in case of methanol-treated cells [74].

As discussed in **Chapter 1**, an over-activation of the downstream substrates of PI3K protein, namely Akt and mTOR proteins, via hyper-phosphorylation has also been commonly implicated in the genesis of cancer [30]. According to the results displayed in **Figure 3.17** and **Figure 3.18**, 30 μM of compound **12** exerted a marked decrease in the phosphorylation status of both Akt and mTOR proteins in KB-3-1 cells by around 70%of the protein levels detected in methanol-treated cells. A lower concentrations of compound **12** (3 μM), however**,** did not demonstrate any appreciable decline in the phosphorylation state and activity of either Akt or mTOR, when compared to the same in methanol-treated KB-3-1 cells.

Upon treatment of KB-3-1 cells with **12** at the highest concentration of 30 μM, the phosphorylation level of a downstream substrate of mTOR, 4E-BP1, decreased to nearly 40% in comparison to the level noticed in case of methanol-treated KB-3-1 cells. As described previously, hypo-phosphorylated (or dephosphorylated) 4E-BP1protein has been reported to behave as an intracellular translation antagonist by binding to eIF4 (translation-promoting protein). This leads to a reduced formation of translation-promoting complexes and a subsequent induction in tumour cell death *via* a decrease in the rate of intracellular synthesis of proteins [26].

a)
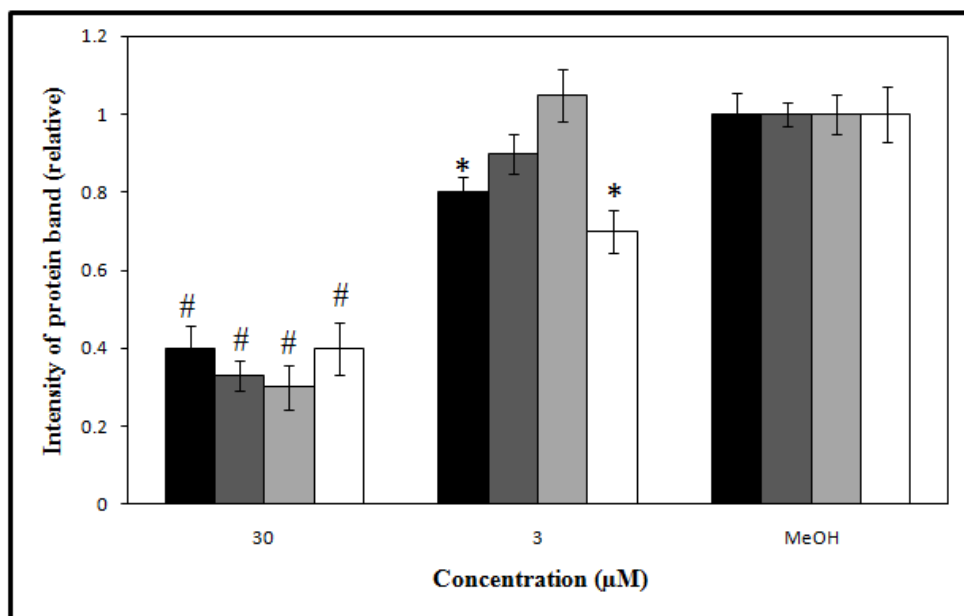
b)
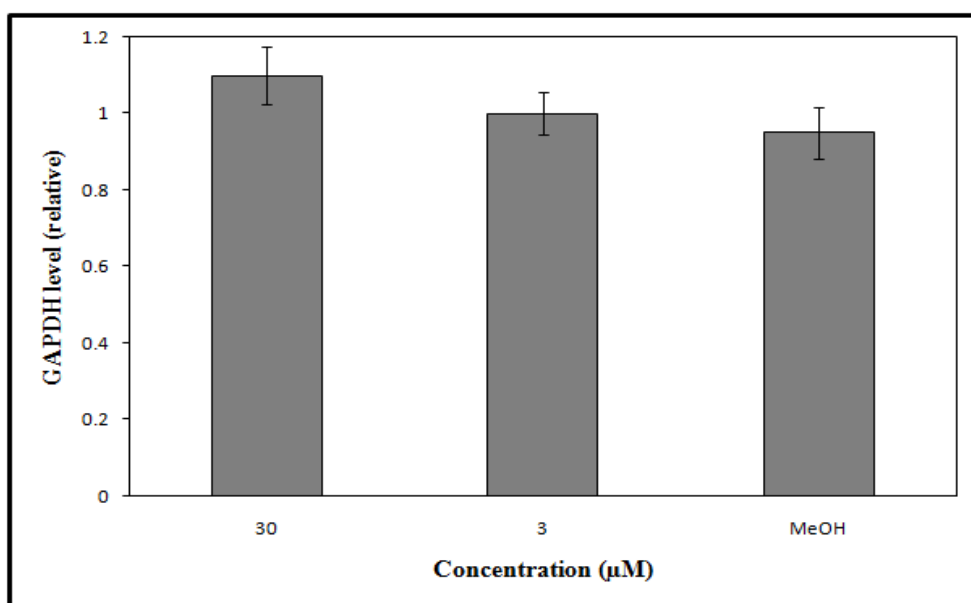
Figure 3.18 Quantitative evaluation of phosphorylation status of **a)** p-85 (white bars), Akt (light grey), mTOR (dark grey) and 4E-BP1 (black) and **(b)** GAPDH protein (loading control) derived from Western-Blot analysis of **12**-treated KB-3-1 cell lysate. Band-intensities have been quantified using Gel-Quant.NET 1.8.2. Error bars indicate ± S.D.*$p < 0.05$; #$p < 0.001$ *versus* methanol-treated cells. $n = 3$.

Therefore, the hypothesis that **12** inhibits the ERK-mediated and mTOR-mediated signalling pathway in KB-3-1 cells which also involves the suppression in phosphorylation and activity of anti-apoptotic proteins like p90RSK may well explain

the significant apoptosis-inducting potential of **12**, in addition to the confirmation of a direct cross-talk between these two oncogenic pathways and the translational system in KB-3-1 cells.

3.3.2.6 Drug Affinity Responsive Target Stability (DARTS)

In consideration of the significant anti-proliferative activity demonstrated by **12** via caspase-mediated apoptosis in KB-3-1 cells**,** a target-identification approach called DARTS was also carried out in search of potential cellular targets of **12** in KB-3-1 cells [95].
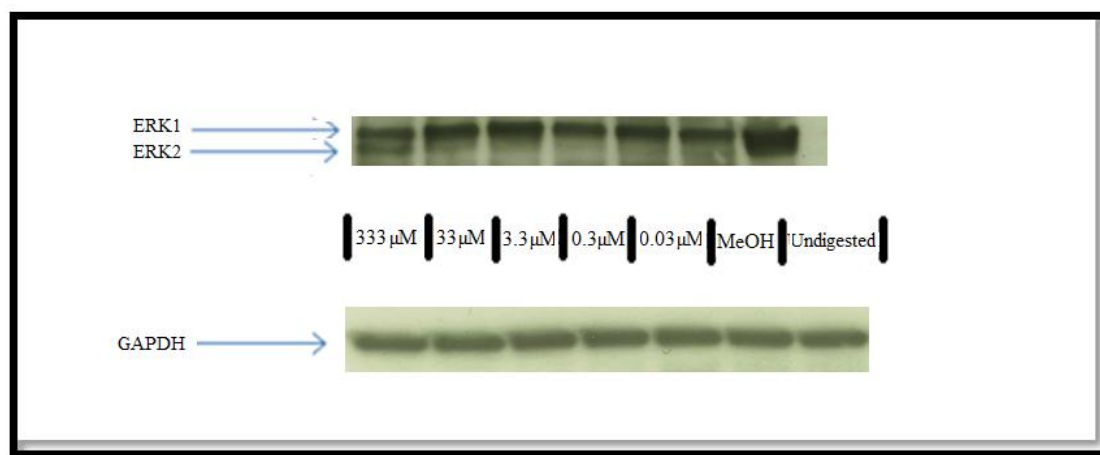
Figure 3.19 Protection of ERK2 in the KB-3-1 cell lysate after a dose-dependent incubation with **12** with the cell lysate. Susceptibility of ERK2 to proteolysis has decreased drastically after subsequent digestion of KB-3-1 cells with pronase, when treated with the highest dose of **12** (333.3 μM).

In line with its protocol, KB-3-1 cell lysates were prepared freshly and equivalent amounts of protein from different aliquots of the cell lysates were treated with varying concentrations of **12** and an equivalent volume of methanol (solvent negative control) under ice-cold conditions. After incubation for 2 h under ice-cold conditions, these proteins were digested with pronase enzyme (0.1 μg ml^{-1}) for 30 min. One aliquot of **12**-treated cell lysate was left undigested as a control. After an incubation of the proteins with pronase for 30 min, the digested proteins were loaded onto a polyacrylamide gel. Equivalent amounts of these proteins were separated by

electrophoresis followed by probing of the proteins for the presence of ERK2 by using the Western Blot technique.

a)

b)
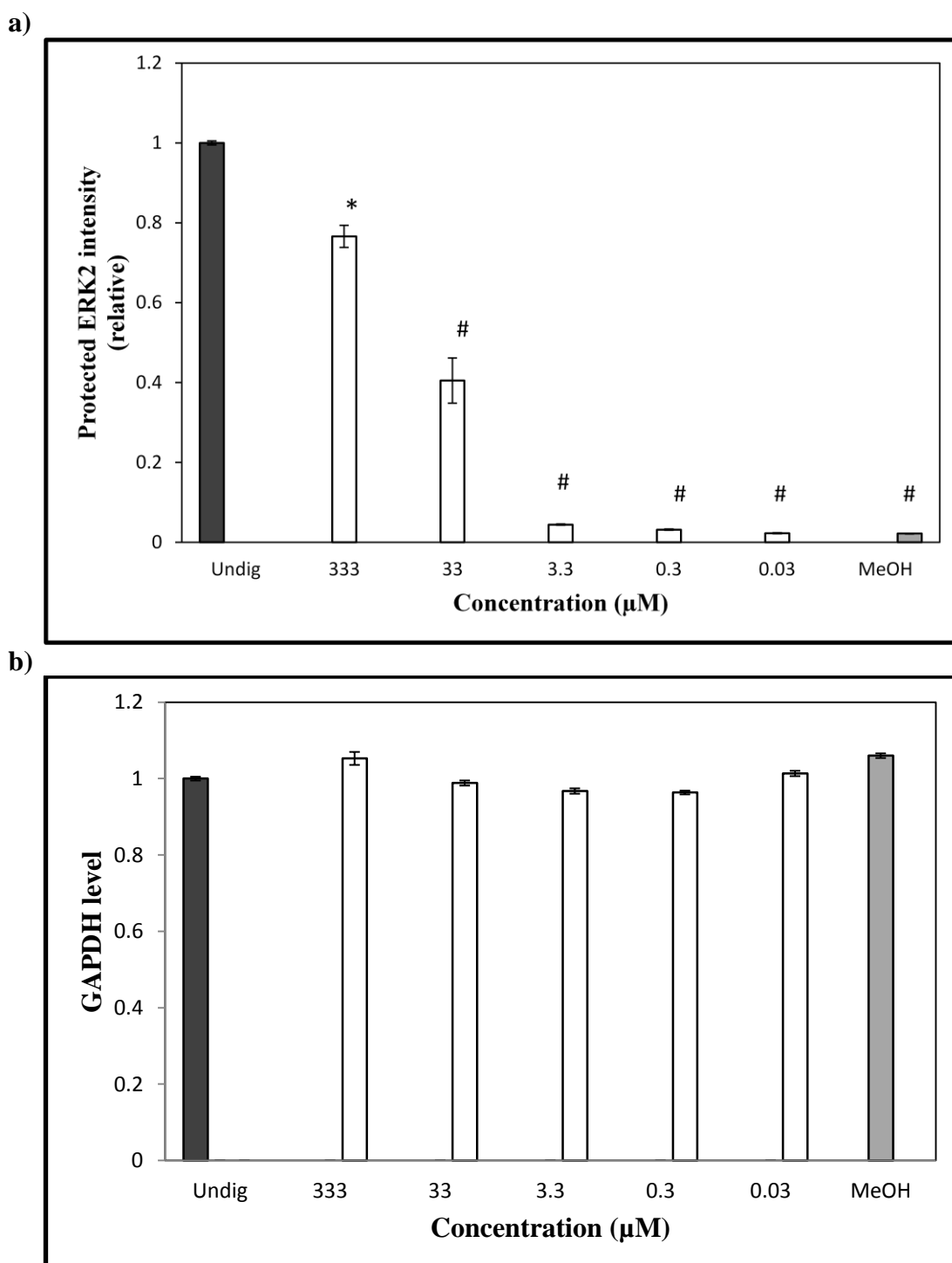
Figure 3.20 Quantitative evaluation of band intensities of **(a)** ERK2 protein and **(b)** GAPDH protein (loading control) derived from Western-Blot analysis of **12**-treated KB-3-1 cell lysate, using the DARTS approach. Band-intensities have been quantified using Gel-Quant.NET 1.8.2. Error bars indicate ± S.D. *$p < 0.05$; #$p < 0.001$ *versus* undigested cells. $n = 3$.

As has been seen in **Figure 3.19**, ERK2 appeared to be "protected" in the protein lysate of KB-3-1 cells treated with 333.3 µM of **12**. The intensity of protected ERK2 protein band was observed to be similar to that observed in case of undigested cell lysate, which served as control.

In addition, the intensity of protected ERK2 protein band increased in a concentration-dependent manner. In a sharp contrast, methanol (negative control) was unable to "protect" ERK2 from pronase-mediated digestion. As a result, in the methanol-treated KB-3-1 cells, there was no visible detection of protection of ERK2. Therefore, **12** seems to "protect" and therefore interact with ERK2, prior to enzymatic digestion by the protein-degrading pronase enzyme.

3.3.2.7 Binding affinity assay

Binding affinity assays represent a powerful screening tool and are ideally suited for the analysis of compounds in preclinical and clinical development. This assay isemployed to provide a robust kinome-wide affinity profile which may reveal unanticipated opportunities that could extend the therapeutic potential or potential off-target liabilities.

In order to provide further evidence to strengthen the ERK2-protecting findings perceived previously in the DARTS approach, this binding affinity assay was carried out to determine the binding ability of **12** towards ERK2. This assay was carried out in co-operation with DiscoverX (California, USA). In accordance with this assay, 6-point serial dilutions of **12** were prepared in 100 % DMSO at 100 x final analysis concentration and subsequently diluted to 1x in the assay (final DMSO concentration of 1%) were incubated with a full-length recombinant ERK2 kinase (accession number NP620407.1) followed by a quantification of any possible binding of QD with the protein. This was calculated in terms of binding constant (K_d) from a standard dose-response curve using the Hill equation. TheK_d value obtained for **12** from a dose-response curve was calculated to be approximately 3.7 µM. Interestingly, this value coincided with the concentration at which **12** displayed an inhibition of activated ERK2 in the cell lysate from KB-3-1 cells using the Western Blot analysis technique. DMSO,

on the other hand, displayed a negligible quenching of the ERK2 signal, under the same experimental condition.
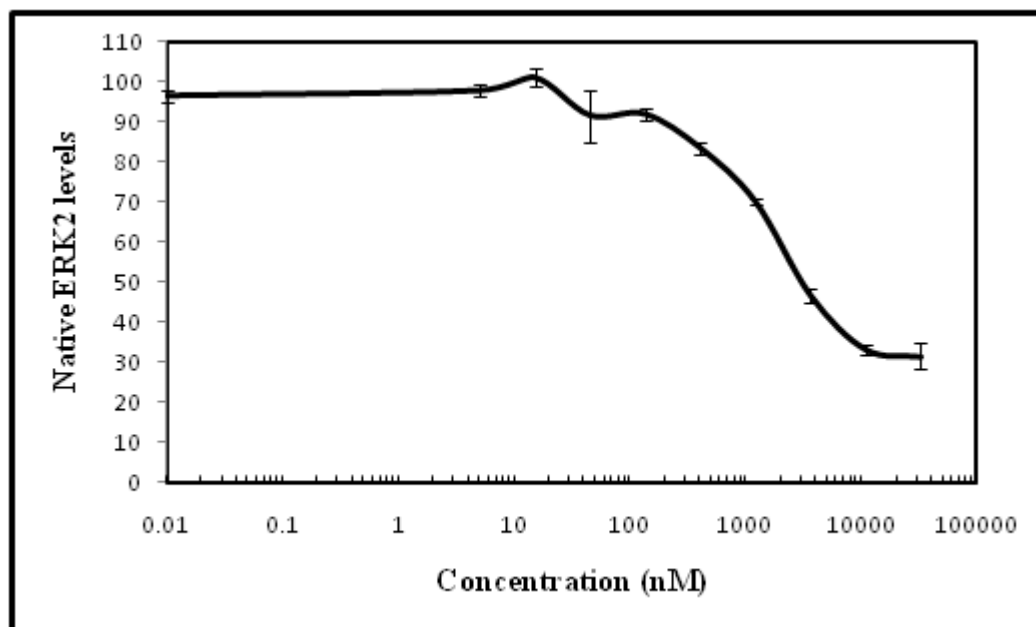
Figure 3.21 K_d binding affinity assay of ERK2 against **12.**The K_d, calculated from the dose-response curve, using the Hill equation, is ~3.7 µM. The K_d value generated in this study is proposed to be a true thermodynamic constant that reflects the binding affinity of **12** for native ERK2 protein. A dip in ERK2 levels (Y axis) indicates binding to **12.** DMSO (0.1 %; negative control) displayed negligible dip in ERK2 levels, under similar experimental conditions.Curves have been plotted from mean values ± SD.

3.3.2.8 Anti-microbial studies

In consideration of the close association between cancer and infection, apart from an investigation into the anti-cancer mode of action of the most potent compounds **10, 11** and**12** with a deeper analysis into the molecular and cellular mode of action of **12,** theanti-microbial effects of these three compounds were also investigated against a panel of selected pathogenic strains using an agar-diffusion assay [146]. The agar assay was carried out in the laboratory of Dr. Florenz Sasse. Briefly, this assay involves the treatment of the selected microbial strains in an agar solution with compounds of interest. Antibiotics, oxytetracycline (OTC) and nystatin were included as positive controls. In this assay, methanol served as a negative solvent control. After incubation of the selected microbial strains with the compounds, the diameter of zone of inhibition

of microbial growth was measured as an indicator of anti-microbial activity. In principle, a greater zone of inhibition depicts a stronger anti-microbial activity [146].

In this assay, **12** displayed a modest zone of inhibition against the fungal strains, *Saccharomyces cerevisiae*and *Botrytis cinerea* (approximately 20 mm and 24 mm, respectively). The inhibitory activity of **12** against the latter was comparable to that of Nystatin. The zone of inhibition of **12** against *Paeoniaanomala*and *Candidaalbicans,* however, was relatively modest (approximately 17 mm or 12 mm respectively). Furthermore, **12** displayed a low to moderate level of activity against the selected bacterial strains, *Micrococcus luteus*, *Mycobacterium phlei* and *Escherichia Coli*. OTC and nystatin, on the other hand, displayed significant inhibitory activity against the selected microbial strains.

Table 3.7 Antimicrobial activity of **10**, **11** and **12.** Methanol (used as negative control) exhibited a negligible growth inhibition zone**.** OTC and Nystatin served as positive controls. Values signify the diameter (in cm) of growth inhibition zone and is calculated as mean value ± SD. $n = 3$. n.d. - not determined.

Compd.	*C. albicans*	*M. Luteus*	*M. phlei*	*E.Coli*	*P. anomala*	*S. cerevisiae*	*B. cinerea*
10	1.7 ± 0.1	2.9 ± 0.1	1.5 ± 0.1	0.6 ± 0.2	3.0 ± 0.2	2.9 ± 0.1	3.1 ± 0.2
11	1.5 ± 0.2	2.5 ± 0.1	1.6 ± 0.2	1.1 ± 0.12	2.6 ± 0.1	2.5 ± 0.2	3.4 ± 0.2
12	1.2 ± 0.2	1.2 ± 0.2	0.9 ± 0.2	1.4 ± 0.1	1.7 ± 0.3	2.0 ± 0.2	2.4 ± 0.1
OTC	n.d.	3.51 ± 0.2	2.5 ± 0.1	2.6 ± 0.17	n.d.	n.d.	n.d.
Nystatin	3.2 ± 0.2	n.d.	n.d.	n.d.	2.1 ± 0.3	2.6 ± 0.1	2.8 ± 0.1

Similarly, **10** and **11** also exhibited moderate anti-microbial activity against the microbial strains under investigation. Both isomers displayed significant anti-microbial activity against *S. cerevisiae, B. cinerea and P. anomala* with inhibitory zones above 25 mm. In contrast, **10** and **11** appeared to be rather insensitive against *E. Coli* with an inhibitory zone diameter around 6 mm and 11 mm, respectively. Compound**10** and **11** yielded a rather moderate effect against *C. albicans* with an inhibitory zone of approximately 17 and 15 mm diameter, respectively. Both isomers also exerted a

moderate anti-bacterial effect against *M. luteus,* with a mean inhibition diameter exceeding 25 mm. Compound **10** and **11** yielded an average inhibition zone of around 15 mm against *M. phlei*, in contrast. Methanol, as a negative solvent control, yielded a rather insignificant inhibitory activity against the selected pathogenic strains.

3.3.2.8 Inhibition of mammalian thioredoxin reductase (TrxR) by selenium and tellurium-containing naphthoquinones

Earlier research focussing on analysing the biological mode of action of the chalcogen-containing naphthoquinones has revealed their inducing ability to induce oxidative-stress (OS) in tumorigenic cell lines [121]. This behaviour has been attributed either to a direct or indirect generation of ROS or a possible disruption of one or more of the intra-cellular antioxidant defense systems, thereby resulting in OS-related cellular insults. Amongst the several cellular antioxidant systems, the selenoprotein thioredoxin reductase (TrxR) is known to play a pivotal role in maintaining the redox homeostasis of cells *via* reduction of the cysteine-containing proteins and also of GSSG [124]. It is now well accepted that a modulation of this enzyme may serve as an important therapeutic tool for killing tumour cells by employing oxidative stress [130]. Amongst the many chemotherapeutic agents designed so far to target this enzyme, gold-containing compounds like auranofin and TPPG have proven to be highly potent TrxR-binding inhibitors [151].

In an attempt to further elucidate the underlying biochemical reasons responsible for induction or maintenance of OS by certain chalcogen-containing naphthoquinones, an investigation into the possible inhibitory effects of these compounds against TrxR was carried out in the laboratory of Prof. I. Ott (Department of Bioinorganic Medicinal Chemistry, Technical University, Braunschweig, Germany). The TrxR inhibition assay that has been employed in this study utilises the fact that TrxR has the catalytic ability to reduce the disulfide bonds of 5,5'-dithiobis(2-nitrobenzoic acid) with formation of 5-thionitrobenzoic acid (5-TNB) which can be detected spectrophotometrically. Therefore, a compound that can modulate the activity of TrxR and subsequently alter the formation of 5-TNB can be identified by this assay.

According to the results obtained in the TrxR-inhibition assay, **16** and **17** demonstrated an inhibition in the activity of TrxR with an IC_{50} of 0.6 ± 9.5 µM and 0.5 ± 1.7 µM, respectively. In the same experiment, DMSO (negative control) displayed only a negligible inhibitory effect on the activity of TrxR. It must be mentioned that upon following the same assay protocol and under similar experimental conditions as employed in this study, Ott *et al.* have earlier reported an IC_{50} of approximately 0.3 µM for a well- known "gold standard" of TrxR inhibitor, TEPG [151]. It can, therefore, be said that the inhibitory potentials of the chalcogen-containing naphthoquinones compared favorably with that of the potent TrxR inhibitor TEPG.
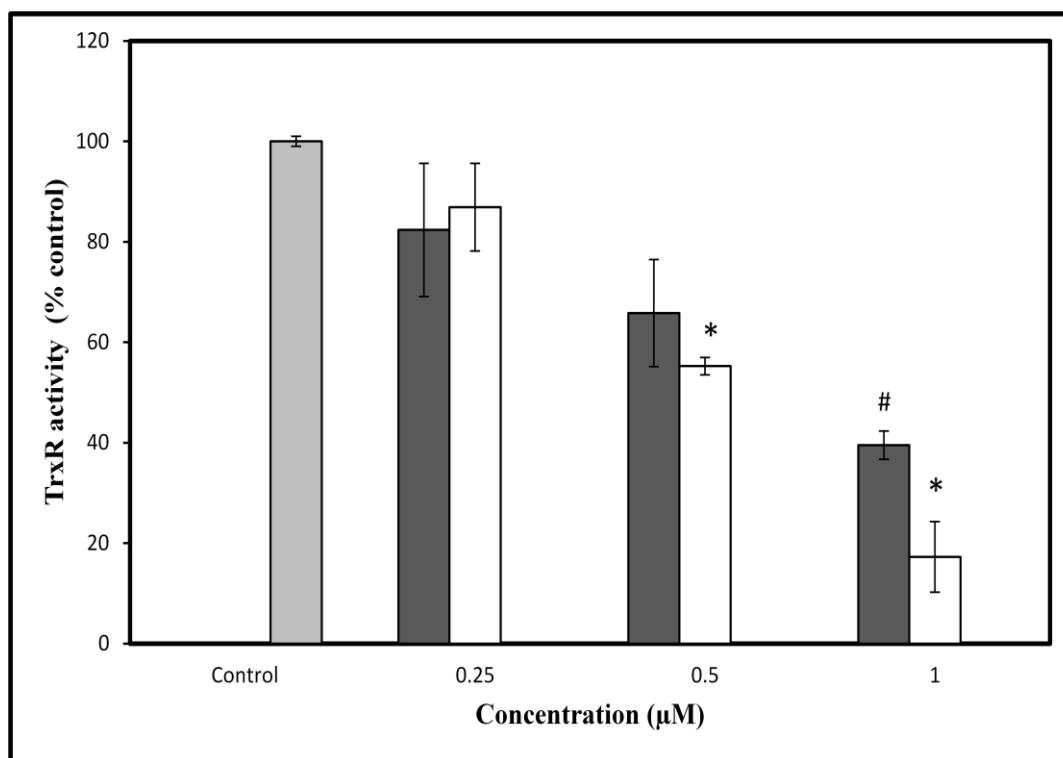
Figure 3.22 Inhibition of mammalian TrxR activity by chalcogen-containing naphthoquinones **16** (grey bars) and **17** (white bars). The catalytic reduction of DTNB, in the presence of TrxR, by NADPH is observed to decrease with increasing concentration of **16** or **17**. The TrxR activity corresponding to DMSO- treatment (control) has been normalised to 100. Curves have been plotted with the mean values $\pm$ SD. *$p < 0.05$; #$p < 0.001$ *versus* control. $n = 3$.

Interestingly, in addition to previously described cellular targets for such selenium and tellurium-containing compounds, TrxR-1 has been identified in this study as another potential cellular target of these compounds [143]. Indeed, an inhibition of

this particular cellular antioxidant defense, *in-vitro*,as seen in the case of **16** and **17**, may also in-part explain the accumulation of intra-cellular ROS and subsequent induction of ROS-mediated cellular apoptosis particularly in tumorigenic cell lines. Notably, such an increase in ROS levels would not require a ROS-generating action of the compounds. An enhanced selectivity of these chalcogen-containing TrxR inhibitors towards tumour cells as described earlier may, therefore, be attributed to the specific environment of tumour-cells that is characterised by raised levels of OS. In order to maintain these OS levels to an extent that is sufficient for the proliferation of cancer cells and without posing any risk of cellular suicide, tumour cells adopt certain biochemical pathways including the over-expression of the natural cellular antioxidant enzymes such as TrxR. This is quite evident from the abnormally increased levels of TrxR found in highly invasive and metastatic tumours [129, 135]. Furthermore, higher levels of TrxR in tumour cells in comparison to normal cells have been linked to an increased resistance of tumour cells towards ROS-inducing chemotherapeutic agents including doxorubicin, cis-platin, docetaxel and tamoxifen [124].

Under such conditions, compounds **16** and **17** may, therefore, possess a potential edge over commonly employed ROS-inducing chemotherapeutic agents due to their dual ability of inducing ROS and inhibiting the activity of ROS-removing cellular enzymes such as TrxR. Such an action would, therefore, not only push tumorigenic cells towards cellular suicide but would also lend such compounds a certain degree of selectivity towards cancer cells over normal cells.

3.4   Non-cellular studies

In order to corroborate the encouraging data obtained regarding the anti-cancer activity of compound **12** from the detailed mechanistic studies carried out using several cell-based redox assays, some relevant studies regarding the (redox) physico-chemical properties of such biologically active compounds were also carried out using electrochemistry on the one hand, and the DPPH and FRAP redox assays, on the other.

3.4.1   **Electrochemical studies**

The electrochemical analysis of any compound is generally carried out using a reference electrode, working electrode, and a counter electrode, which in combination, are sometimes referred to as a three-electrode setup.

Compound **12** contains a selenium-selenium bond as a part of a 5-membered ring, which can be reduced and oxidized electrochemically using a dropping mercury electrode. This electrode, however, often suffers from the disadvantage of an unwanted adsorption of selenium-containing molecules on the electrode surface, resulting in a strong interference with the mercury electrode. This may imply the formation of a complex between selenium and mercury, thereby resulting in a sharp "dip" in the cyclic voltammogram. In order to avoid such problems, a glassy carbon electrode was deployed, as part of these studies, to obtain the oxidation and reduction potentials of compound **12**.

The oxidation and reduction potentials corresponding to **12,** which are clearly visible as signals in the cyclic voltammogram can be seen in **Figure 3.23**. Compound **12** exhibited an oxidation and reduction signal in the biologically relevant range of -900 mV to 0 mV *vs.* Ag/AgCl (SSE) reference electrode, corresponding to approximately a one electron transfer process ($\Delta E_{p,1/2} = 3.53$ RT/nF = 90.6/n mV).In addition to the reduction peak of **12** at around -42mV, the appearance of a larger reduction peak at around 800mV could probably be due to the reduction of tetrabutyl ammonium (Bu_4N^+) ions which formed a part of the electrolyte. As can be seen in **Figure 3.23**, compound **12** displayed a redox couple at around 100mV in the defined potential range with quasi-reversible characteristics with a peak current ratio (I_{pa}/I_{pc}) around 1.

Further, **12** has exhibited an E° [($E_{pa} + E_{pc}$)/2] value of around -92 mV, which is much higher than the previously published E° value for heteroaryl diselenides like dipyridyl diselenide [155]. This indicated that **12** may apparently be a rather poorly reducing diselenide and probably a poor anti-oxidant.
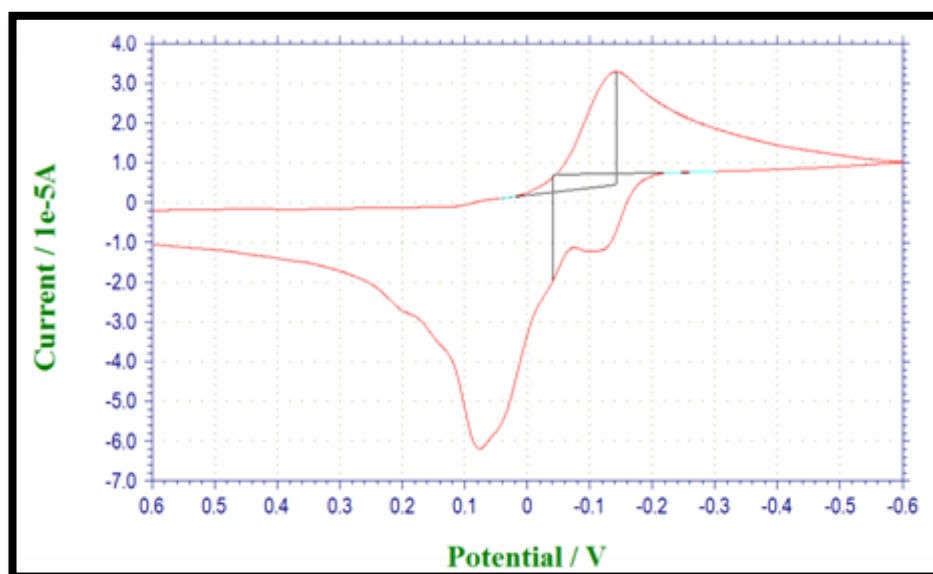
Figure 3.23 Cyclic voltammogram of **12** was recorded on a CHI 604D electrochemical analyzer (USA) at a scan rate of 100 mV s^{-1}using a glassy carbon electrode as a working electrode and Ag/AgCl (SSE) reference electrode in acetonitrilecontaining 0.1 M TBAP as the supporting electrolyte. The electrochemical potentials are provided *vs*. SSE and have been calibrated with the $[Fe(CN)_6]^{4-}/[Fe(CN)_6]^{3-}$ redox pair. $n = 3$.

Nevertheless, the electrochemical studies of **12** that were carried out on CHI 604D electrochemical analyzer (USA) confirm that **12** was able to undergo reversible oxidationand reduction reactions within the physiologically relevant potential range. Its redox activity, however, was not comparable to that depicted by several other heteroaryl organodiselenides reported previously in literature [155].

3.4.2   Anti-oxidant assays

As reported previously in the literature, organo-selenium compounds exhibit rather pronounced anti-oxidant properties that are usually attributed to their low oxidation potentials*i.e.,* ability to "donate" electrons rather easily (as observed previously) during electrochemical analysis. As described in **Chapter 2**, there are several analytical techniques, besides basic electrochemical methods, that have been established to determine the antioxidant and radical-quenching potential of such small molecules. Amongst them, for this study, aDPPH-radical scavenging assay was selected as a valuable and relatively quick analytical technique to assess the radical scavenging capability of biologically active compounds [149]. Although DPPH is not a

physiological free radical, this assay surely gives a positive and conclusive idea of the reducing activity of compounds.

3.4.2.1 DPPH radical scavenging assay

From the results obtained, at a concentration of 1 mg ml^{-1}(3.3 mM), compound **12** quenched 33.5 ± 1.6% of the original DPPH content (normalized to 100%). Though not very significant, rather moderate radical-scavenging ability of **12** may be due to the nitrogen atom contained within the quinoline ring. Diphenyl diselenide, on the other hand, appeared to quench only 5.3 ± 0.8% of the original DPPH at the same concentration (1 mg ml^{-1}, 3.2 mM).
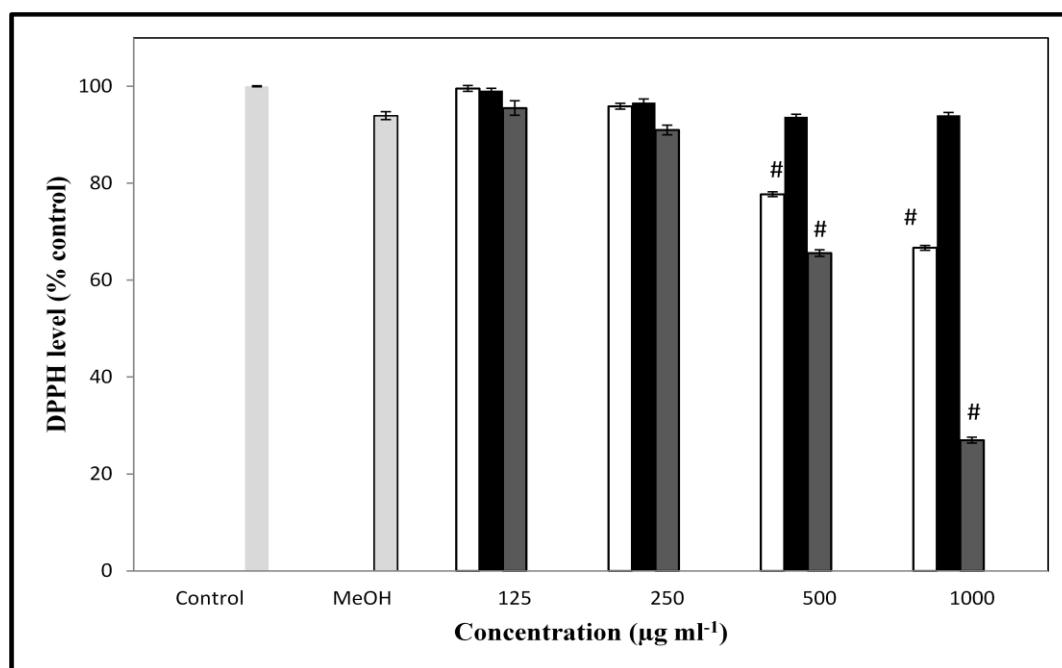
Figure 3.24a Concentration-dependent quenching of DPPH radicals by **12** (white bars), diphenyl diselenide (black bars) and ascorbic acid (grey bars; positive control). Equivalent amount of methanol depicted negligible DPPH quenching (methanol bar). DPPH content in untreated samples (control bar) has been normalized to 100 %. Bars have been plotted as mean values ± S.D. [#]$p < 0.001$ *versus* untreated sample. $n = 3$.

In line with diphenyl diselenide, the other two selected isomeric diselenides, **10** and **11,** also failed to elicit any noticeable DPPH radical scavenging behaviour, even at the highest selected concentration of 1 mg ml^{-1}. In sharp contrast, ascorbic acid which

isa widely known antioxidant and an important constituent of citrus fruits was able to sequester 72.0 ± 1.2 % of the total DPPH radicals at a concentration of 1 mg ml^{-1}(5.6 mM).
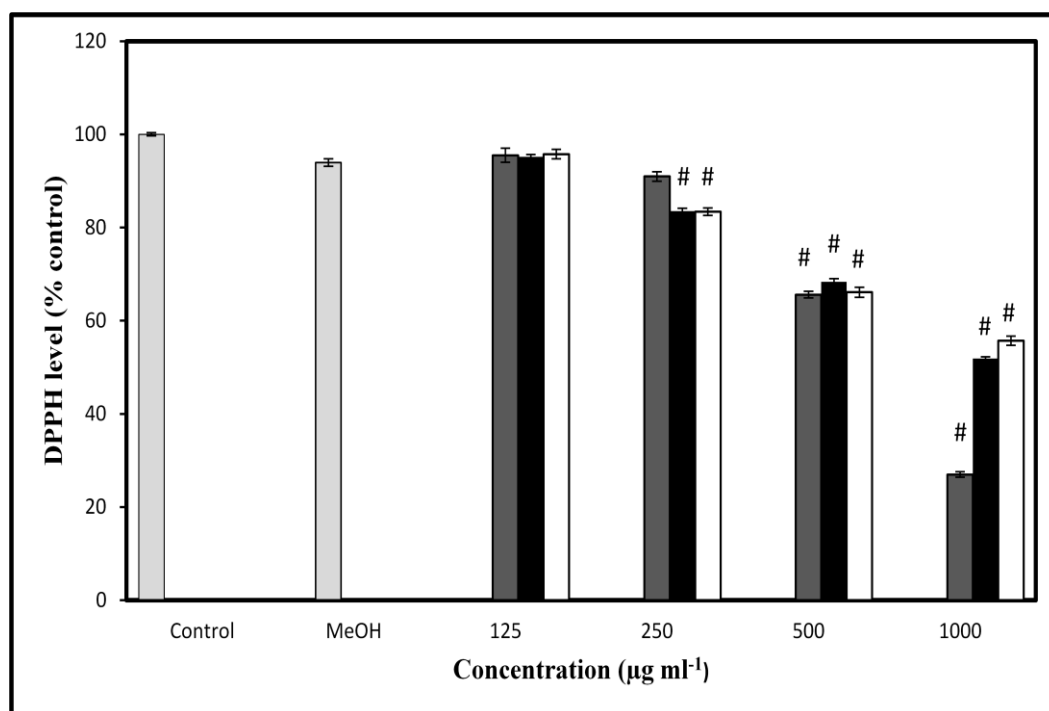
Figure 3.24b Concentration-dependent quenching of DPPH radicals by **ARS-01** (black bars), **ARS-02** (white bars) and ascorbic acid (grey bars; positive control). Equivalent amount of methanol depicted negligible DPPH quenching (dark grey bar). DPPH content in untreated samples (control bar) has been normalized to 100%. Bars have been plotted as mean values $\pm$ S.D. $^{\#}p < 0.001$ *versus* untreated sample. $n = 3$.

Amongst the selenophenesscreened, only **ARS-01** and **ARS-02** displayed a significant DPPH radical scavenging activity. At a concentration of 1 mg ml^{-1} (equivalent to 1.9 mM and 1.8 mM for **ARS-01** and **ARS-02**, respectively), these compounds exhibited a similar radical quenching activity of $49.5 \pm 0.7\%$ and $47.3 \pm 1.6\%$, respectively. In contrast, the remaining selenophenes displayed a negligible quenching of the DPPH radical in the concentration range studied. As mentioned earlier, diphenyl diselenide (used as a reference compound) also did not exhibit any significant radical-scavenging ability.To sum up, amongst the chalcophenes studied, only **ARS-01** and **ARS-02** have displayed an appreciable radical scavenging activity which was comparable to the radical-scavenging ability of a standard radical scavenger ascorbic

acid. In contrast, compounds **10**, **11** and **12** have not exhibited any appreciable radical-sequestering ability in the DPPH assay.

3.4.2.2 Ferric reducing ability of plasma FRAP assay

The FRAP assay is a quick and rapid analytical technique to determine the reducing ability of samples under investigations. In principle, upon an electron-transfer from given compounds, the straw-coloured Fe^{3+}-TPTZ complex is converted into a blue-coloured Fe^{2+}-TPTZ complex. The formation of the latter by the relevant compounds can be quantified spectrophotometrically in terms of an absorbance measurement (at a wavelength of 594 nm). A higher level of formation of the Fe^{2+}-TPTZ complex is a measure of the reducing activity of the compounds which is subsequently expressed in terms of a FRAP value. In principle, a compound with a higher FRAP value is an indicator of its higher anti-oxidant activity.

Using a standard spectrophotometric setup, this assay was carried out in a 96-well microtitre plate in accordance with an established protocol but with some minor modifications [150]. Methanol and ascorbic acid were included as negative and positive control respectively, under similar experimental conditions. Results from this assay indicated that the reduction of the Fe^{3+}- TPTZ complex by **12** was moderately enhanced an effect which depended on theconcentration of **12**.

In comparison to ascorbic acid (a benchmark compound) which exhibited a FRAP value of 2664 ± 51 μmol equiv of Fe^{2+} l^{-1} (equivalent to an absorbance = 3.1 ± 0.2) used at aconcentration of 250 μg ml^{-1}, the FRAP value of **12** was rather low at 221 ± 39 μmol equiv of Fe^{2+} l^{-1} (equivalent to an absorbance = 0.2 ± 0.1). Interestingly, at the same concentration, diphenyl diselenide displayed hardly any anti-oxidant ability as is evident from its rather low FRAP value below 200 μmol equiv of Fe^{2+} l^{-1} (equivalent to an absorbance = 0.1 ± 0.1).
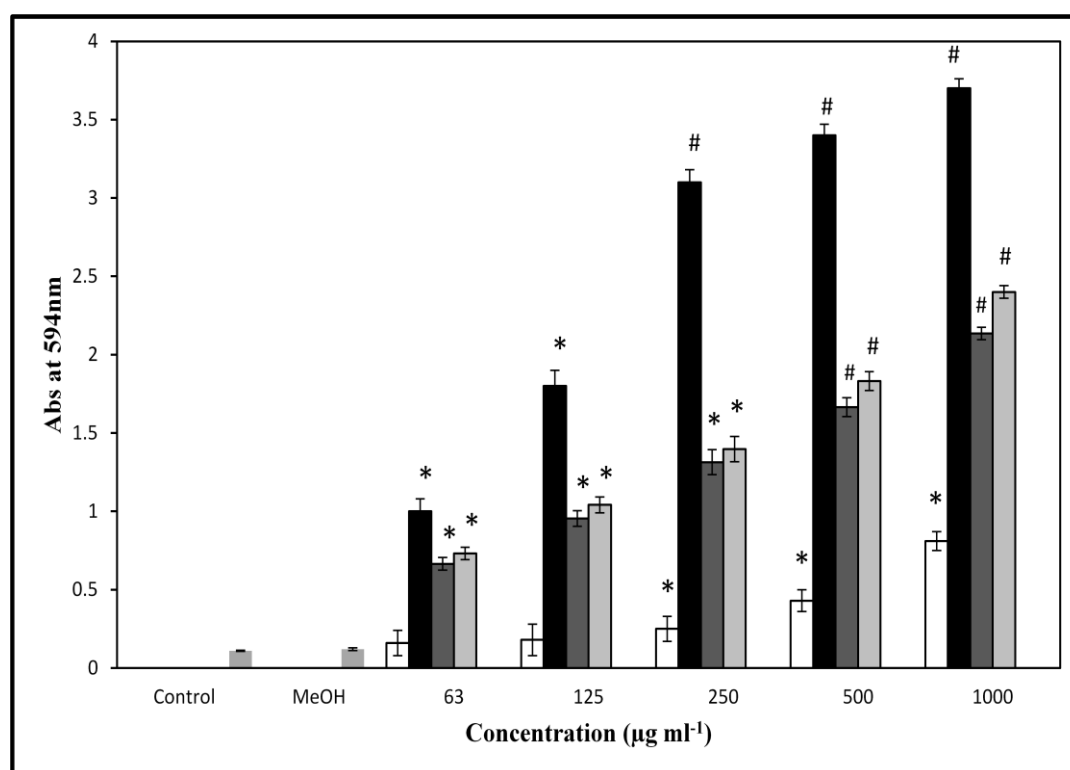
Figure 3.25 Concentration-dependent increase in the formation of Fe(TPTZ)$_2$ upon a 10 min incubation of FRAP reagent with the "most active" compounds- **ARS-01** (dark grey bars), **ARS-02** (light greybars), **12** (white bars) and ascorbic acid (black bars).The level of Fe(TPTZ)$_2$ in the FRAP reagent left untreated or treated with methanol represents the control bar or MeOH bar, respectively. The increase in absorbance at a wavelength of 594 nm corresponds to an increase in reduction of the Fe(TPTZ)$_3$ complex to Fe(TPTZ)$_2$ complex. Bars have been plotted as mean values ± S.D. *$p < 0.05$; #$p < 0.001$ *versus* untreated sample (control). $n = 3$.

Compound **10** and **11** also displayed a negligible reduction of Fe^{3+}-TPTZ complex even at the highest selected concentration of 250 μg ml^{-1}. Both **10** and **11**, therefore, behaved in a similar manner as diphenyl diselenide by yielding a FRAP value below 200 μmol equiv of Fe^{2+} l^{-1} (equivalent to an absorbance = 0.1 ± 0.1 and 0.1 ± 0.2, respectively) at a concentration of 250 μg ml^{-1}. The poor anti-oxidant effects of **10** and **11,** as observed in the FRAP assay also corresponded with their poor DPPH radical scavenging effects as reported in the previous section.

Interestingly and in sharp contrast to the anti-oxidant activity of **10**, **11** or **12**, the formation of Fe^{2+}-TPTZ complex was enhanced significantly by **ARS-01** and **ARS-02** in a concentration-dependent manner. At a concentration of 250 μg ml^{-1},

raloxifene (**ARS-01**) exhibited a FRAP value of 1200 ± 69 µmol equiv of Fe^{2+} l^{-1} (equivalent to an absorbance = 1.3 ± 0.2). A similar FRAP value of 1287 ± 43 µmol equiv of $Fe^{2+}l^{-1}$ (equivalent to an absorbance = 1.4 ± 0.1) was observed in case of the selenium-substituted analogue of raloxifene (**ARS-02**) at the same concentration (**Figure 3.24**). In contrast, the remaining selenophenes (**ARS-03** to **ARS-06**) were less active. Even at the highest selected concentration of 1mg ml^{-1}, these selenophenes (**ARS-03** to **ARS-06**) produced a FRAP value of less than 200 µmol equiv of $Fe^{2+}l^{-1}$ (equivalent to an absorbance = 0.1 ± 0.1). Since a phenolic group has been reported to serve as an efficient radical scavenger via an electron-transfer mediated by phenoxide anions, the significantly high FRAP values of **ARS-01**, **ARS-02** and ascorbic acid (a benchmark sample) could be reasonably attributed to the presence of the phenol group in their chemical structures [182, 183]. In contrast, this functional moiety is absent in the other selenophenes (**ARS-03** to**ARS-06**), that could possibly result in their poor radical-quenching activity.

Chapter 4

Discussion

The design and synthesis of organoselenium compounds continues to serve as a challenging, yet encouraging enterprise, not only in the area of pharmaceutical drug design but also to comprehend the biochemical aspects and diversity of this trace element in physiological and non-physiological systems. During the last two decades, remarkable synthetic progress has been seen in broadening the existing arsenal of compounds and the biochemical know-how of selenium, particularly regarding its potential uses against cancer and several other life-threatening diseases [109].

In view of the extensive yet mixed results regarding the biological efficacy of selenium, the first step in this study has been involved in the further investigation of the biological activity of some hitherto unexplored examples of organoselenium compounds. Since organic seleniumchemistry is popularly and widely recognized in the form of organodiselenides and monoselenides, a pool of representative examples of organoselenium compounds has been created of several known and unknown heteroaryl-conjugated monoselenides and diselenides. In addition, several lesser known and less widely studied selenophenes have also been included for a first-hand comparative analysis of their chemotherapeutic efficacy. More importantly, these efforts have been closely followed by studies regarding their biological activity and subsequent attempts to explore the underlying biochemical reasons behind any chemotherapeutic efficacy observed for some of the more potential candidates (especially compound **12**), based on its modulatory biochemical effects, both at the molecular and at the cellular level.

In order to perform a comparative analysis of the chemotherapeutic efficacy of organoselenium compounds as an initial step of this project, a diverse collection of alkyl-functionalized monoselenides (**1-9**) and heteroaryl diselenides (**10-15**) have been synthesized by adoption of previously established synthetic procedures [140-142]. In the past, certain monoselenides have been observed to demonstrate a relatively poor anti-cancer activity in comparison to the corresponding diselenides [153]. This dramatic

difference in biological activity can be attributed to the redox-active and relatively labile diselenide bond which is not observed in case of the monoselenides. The ease of cleavage of a selenium-selenium bond (as in an organodiselenide) relative to a carbon-selenium bond (as in a monoselenide), thereby resulting in a cascade of biologically active metabolites, is due to the lower bond disassociation energy of the former (331 kJ mol^{-1} *versus* 583 kJ mol^{-1}of the latter bond [156]. Considering this aspect, it has been assumed that an enhancement in the ability of monoselenides to enter cells via an enhanced lipophilicity could also possibly lead to an enhancement in their cytotoxicity against tumour cells. Therefore, in this study, in order to impart a characteristic amphiphilicity into these rather poorly active molecules, several heteroaryl-diselenides have been successfully subjected to functionalization with alkyl chains of different carbon-chain lengths. Such alkyl-functionalized monoselenides (**1**-**9**) have been, however, synthesized initially on a relatively small scale in order to obtain initial inputs of any increased potential against tumorigenic and microbial cells.

With regard to the organodiselenides, in order to shift from the conventional synthesis of phenyl-substituted (di)selenides, the synthesis of N-containing heteroaryl-conjugated analogues has been carried out (**10**-**15**). A combination of *N*-containing heterocyclic ring system with the redox-active dichalcogenide bridge has been undertaken with the awareness of the presence of such ring systems as valuable pharmacophores found frequently in synthetic and naturally-occurring biologically active small molecules. Therefore, substitution of the commonly employed benzene ring with *N*-containing heterocyclic ring has been carried out in an attempt to synergize the biological efficacy of these heterocyclic pharmacophores with those of the diselenide moiety. This work has been designed and carried out in the research group of Prof. Dr. K.K. Bhasin (Department of Chemistry, Panjab University, Chandigarh, India). Re-synthesis of chalcogen-containing naphthoquinones (**16** and **17**) has been carried out, primarily as a part of an on-going investigation in elucidating the biochemical reasons behind its ROS-induced chemotherapeutic effects against tumorigenic cells.

In addition to these diselenides and monoselenides, selenophenes (**ARS-01** to **ARS-06**) have also been included in the panel of heteroaryl-conjugated organo-(di)selenides. These compounds contain the redox-active chalcogen moiety as a part of the aromatic ring rather than being attached to the ring. Such a design may, in theory,

provide an enhanced stability and reactivity. The latter effect, however, has not been apparently observed during the biological analysis. These compounds have been synthesized and kindly provided by the research team of our collaborator, Dr. Pavel Arsenyan (Latvian Institute of Organic Synthesis, Aizkraukles 21, Riga LV-1006, Latvia).

All the newly synthesized and re-synthesized compounds have been characterised by NMR spectral analysis. In accordance with the spectroscopic data, these compounds have been judged to possess purity greater than 95 %. In addition, elemental analysis and^{77}Se NMR of these compounds (**10**, **11** and **12**), that had been selected from a primary screening, have also been carried out to re-confirm their synthetic purity, prior to a more comprehensive biological investigation [142]. In addition, the crystal structure of compound **11** has also been solved successfully.

As part of the main objective of this study, a comparative analysis of the chemotherapeutic and anti-microbial potential of mono and di-selenium-containing compounds, together with a study of the biological activity of certain selenophenes has been carried out.

Upon a preliminary screening of the inhibitory potential of a set of alkyl-functionalized selenoarenes, in parallel to their diselenide counterparts and selenophenes against tumorigenic cell lines, the alkyl-functionalized monoselenides have not appeared to exhibit any promising inhibitory effects against proliferation of the tumour cell lines selected. All the compounds (**1-9**) have displayed an average inhibitory value (IC$_{50}$) exceeding 30 μM. These IC$_{50}$ values have not been significantly high; hence these compounds are not particularly useful in the context of cancer research. In contrast, **ARS-01,** which served as apositive control, has displayed a much higher anti-proliferative potential against the mammalian cell lines. This indicated that simple introduction of a mere lipophilic character into such molecules was not successful. Furthermore, since alkyl groups usually do not possess any cytotoxicity of their own, the overall chemotherapeutic efficacy of these monoselenides has apparently remained unaltered. Since a hexyl- group has been the longest alkyl chain employed in this strategy, a future investigation into the effects of even longer alkyl chain lengths (like a decyl- or even a dodecyl- chain) would be interesting. In this case, however, the

overall chemical and physiological stability of such molecules would also need to be assessed before further biological analysis could be carried out.

On the other hand, representative examples of various diselenides and some of the selenophenes, inspite of their relatively lower degree of lipophilicity, have appeared to possess a far better biological activity against the tumorigenic cells selected. Amongst these diselenides *viz.***10**, **11** and **12** have demonstrated a considerable anti-proliferative ability against the tumour cell lines. The cyclic diselenide**12** has been observed to display a promising anti-proliferative ability against several tumour cell lines like KB-3-1 ($IC_{50} = 0.8 \pm 0.4$ µM) cells using the MTT assay. Compound **12** has also exhibited a similar activity ($IC_{50} = 0.6 \pm 0.3$ µM) by decreasing the ATP levels of KB-3-1 cells after a 48 h treatment. Compound **12**, however, has also exerted a certain level of toxicity against L-929 (IC_{50} of 0.6 ± 0.3 µM) cells, thereby pointing towards a promising, yet relatively low specificity towards cancer cells. Inspite of a certain degree of non-selectivity, its acute sensitivity towards PC-3 cells (IC_{50} of 0.02 ± 0.3 µM), in particular, had encouraged us to pursue further investigations to explore the possible biochemical reasons leading to its significant anti-tumour activity.

Apart from **12**, isomeric diselenides, **10** and **11**, have also displayed a promising anti-proliferative activity against tumour cells like KB-3-1 ($IC_{50} = 0.4 \pm 0.2$ µM and 0.4 ± 0.1 µM, respectively) in the MTT assay. This has been further evident by a significant decline in the ATP levels of KB-3-1 cells after a 48 h treatment with either **10** or **11** (IC_{50} of 1.0 ± 0.4 µM and 2.5 ± 0.7µM, respectively. However, the anti-proliferative potential of **10** has been significantly higher compared to **11** towards PC-3 cells ($IC_{50} = 0.6 \pm 0.3$ µM and 0.9 ± 0.3 µM, respectively). The relatively higher anti-proliferative activity of **10** in some cases could be possible due to its higher cellular uptake, as a consequence of an attenuated steric hindrance, in comparison to **11**. Similar to compound **12**, both **10** and **11** have displayed a poor selectivity towards tumorigenic cells by exerting cytotoxicity against L929 ($IC_{50} = 0.4 \pm 0.1$ µM and 0.7 ± 0.4 µM respectively).

The experimental findings from the MTT cytotoxicity analysis of the chalcophenes have suggested that their inhibitory (IC_{50}) values against tumour cell lines reside, on an average, within the sub-millimolar range. Amongst the cell lines selected, the chalcophenes have displayed a relatively higher activity against cervix carcinoma

(KB-3-1) cells. Raloxifene (**ARS-01**), an FDA approved drug for treating metastatic breast cancer and used in this study as a positive control, has exhibited the highest activity amongst all chalcophenes studied. **ARS-02** has also demonstrated considerable cytotoxicity against tumour cell lines with a maximum inhibitory effect against KB-3-1 and MCF-7 cells (IC_{50} = 7.1 ± 1.1 µM, and 10.7 ± 1.4 µM respectively). Interestingly, in spite of their close chemical similarity, **ARS-01** has been relatively more active against KB-3-1 and MCF-7 cells (IC_{50} = 5.3 ± 0.7 µM and 3.5 ± 0.8 µM, respectively) compared to **ARS-01**.In many previously published articles, the cytotoxicity of organoselenium compounds has been demonstrated to be superior to one of their sulfur-containing analogues [159].

Due to the relatively higher anti-cancer activity of **ARS-01** in comparison to that of **ARS-02**, it appears that the selenium moiety in these selenophenes may not necessarily play a predominant role in the anti-tumour effects of these compounds. In contrast, **ARS-03** - **ARS-06** have exhibited a rather average anti-proliferative potential against the cancer cell lines. These compounds, however, have displayed the maximum activity towards KB-3-1 cells with a mean IC_{50} exceeding 10 µM. These selenopheneshave also appeared to be hardly active against MCF-7 cells with an average IC_{50} exceeding 20 µM. Upon critical observation of the structural differences between **ARS-01** or **ARS-02**, on the one hand, and the remaining selenophenes (**ARS-03** - **ARS-06**), on the other, it is quite probable that the relative biological inactivity of the latter could be attributed partially to the absence of phenolic hydroxyl groups in their chemical structure. These phenolic groups endow an appreciable level of redox activity on their own and are widely recognised to attenuate tumour proliferation by interfering with tumour-associated oxidative stress [160, 161]. This argument could be verified further by the observation of an enhanced radical scavenging effect by **ARS-01** and **ARS-02,** in comparison to a rather poor effect exhibited by the other selenophenes (**ARS-03** to **ARS-06)** in the DPPH and FRAPS redox assays. This matterhas been discussed in the section dealing with non-cellular based assays.

To sum up, the redox-active diselenides (**10**, **11** and **12**), on one hand, and selenophenes **ARS-01** and **ARS-02**, on the other hand, have exhibited the highest activity against tumour cell lines. The significant activities of the latter can be attributed to the raloxifene motif in **ARS-01** that bears an "almost identical" resemblance to the

chemical structure of **ARS-02**. On the basis of a "ranking" in anti-cancer activity, **10, 11** and **12** have been subsequently selected for further analysis of their mode of action against such tumorigenic cells. The activity of these compounds against cancer cells, in general, and KB-3-1 cells, in particular, has been discussed in greater detail in the subsequent cell-based assays.

In the past couple of decades, basic anti-cancer research has generated remarkable advances in our comprehension of the etiology of cancer biology. These investigations have also led to the unraveling of new biochemical mechanisms which may be useful to combat this life-threatening disease. Among the most prominent of these advances is the realization that the apoptotic pathway, comprising of several pro- and anti-apoptotic enzymes and signalling pathways, has a profound effect on the malignant phenotype. Earlier, during the 1970s, pathologists noticed that radiation and chemotherapy can induce cell death with morphological features of apoptosis. It was not until the late 1990s, however, that it was established that anticancer agents prevent carcinogenesis by induction of apoptosis, in addition to the notion that disruption of the apoptotic cellular path contributes to the reduced chemo sensitivity of malignant cells [165].

During apoptosis, cellular DNA degradation occurs few hours prior to breakdown of the plasma membrane. Therefore, DNA degradation into mono and oligonucleosomes is an important indicator of the stage of apoptotic cell death. Induction of apoptosis is considered as an important cellular event that has been taken into account for the therapeutic effects of organoselenium compounds against cancer [16]. To confirm that the treatment of KB-3-1 cells with the most active organodiselenides (**10**-**12**) leads to apoptotic cell death, a possible degradation of nuclear DNA of KB-3-1 cells into nucleosomal fragments has been assessed in this study by employing the cell-death detection ELISA assay. The results have indicated that chemotherapeutic diselenides **10, 11** and **12** exert their chemotherapeutic effects against KB-3-1 cells *in-vitro* by a concentration-dependent induction of apoptosis, which is characterized by the fragmentation of the nuclear DNA that serves as a hallmark of apoptosis [112]. Therefore, apoptosis has served as a prominent molecular mode of action of these diselenides.

Caspases form a family of endoproteases that provides a critical link in the cell -regulatory networks which control apoptosis-mediated cell death. Stimulation of the general activity of the executioner caspases-3 and 7 is prevented by their production as inactive procaspase dimers. The latter must be cleaved first by the initiator caspases. Upon activation, these pro-apoptotic caspases trigger a cascade of signalling events that lead to controlled degradation of cellular components, via apoptosis [57]. This is evident from previous reports that highlight the role of activated caspase 3/7 in promoting cleavage and subsequent activation of a pro-apoptotic factor BAD that serves as a more potent inducer of cytochrome *c* release and apoptosis [61]. The importance of caspase-3 in the etiology of cancer has been reflected in reports concerned with its mutation in the MCF-7 breast cancer cell line [167]. Caspase-7 is another effector that is also important, with respect to caspase-3 in executing apoptosis, especially in the cells with deficient or under-expressed caspase-3.

In order to better comprehend the mechanism of compound-induced apoptosis in KB-3-1 cells, it was considered interesting to investigate whether this type of apoptosis is caspase-mediated or not. There have been numerous reports in the past regarding the mixed role of caspases in apoptotic cell death induced by various selenium-containing compounds [134]. Depending upon the cell type, several prominent selenium-containing compounds like sodium selenite, ebselen and methyl selenol have been reported to induce cell death with or without the activation of caspases [104,106]. In this assay, compound **10, 11** and **12** have been observed to induce significant levels of apoptosis in KB-3-1 cells *in-vitro* via stimulation of activity of pro-apoptotic caspase 3/7in a concentration and time-dependent manner.Therefore, it can be hypothesized that the significant activity of the organodiselenides (**10**-**12**) observed previously in the MTT and ATP assays, particularly against KB-3-1 cells, could be attributed to their ability to induce caspase-mediated apoptosis in such type of cancer cells.

In addition to apoptosis, protein translation represents another complex set of biochemical reactions involving the interaction of a large number of factors that catalyze the assembly of ribosomes, mRNA templates and amino-acylated tRNAs. As the role of a non-regulated, out-of-control protein synthesis in tumorigenesis becomes even better understood, the therapeutic potential of drugs targetingprotein synthesis becomes even more evident [20]. In this regard, there has also been increasing evidence

to support the theory thatapoptosis leads to modifications in the phosphorylation status of several translation factors like eIF4E binding proteins (4E-BPs) in mammalian cells [19].A caspase-dependent cleavage of such translation initiation factors has been well-documented to increase the rate of protein degradation, thereby playing a major role in the inhibition of protein translation in apoptotic cells. This concept has led us to investigate whether the broad anti-proliferative activity exerted by the selenium-incorporated heterocyclic compounds (like **12**), via caspase-mediated apoptosis in KB-3-1 cells *in-vitro*also impacted on intra-cellular protein synthesis.

In this regard, there have been several reports highlighting the inhibition of protein translation by several organoselenium compounds such as methyl selenocysteine (MSC) and methyl seleninic acid MSA, both of which are potential precursors of the active metabolite, methyl selenol [117]. In the past, a number of clinical trials, including the SELECT and NPCT trials of organic selenium, have also indicated that translational control could potentially constitute an important theme for future drug development. Many previous studies, involving the translation-modulatory potential of active selenium metabolites like methyl selenol and naturally occurring compounds like methyl selenocysteine have given a fresh thrust to the application of organic selenium compounds for therapeutic intervention, particularly against prostate cancer [176].

As a result of the significant anti-cancer activity of **12** *in-vitro,* in particular against prostate carcinoma cells (IC$_{50}$ = 0.02 ± 0.3 µM), this organoselenium compound has been studied in more detail in an attempt to elucidate its molecular mode of action, especially in the context of protein synthesis. For this purpose, two experimental models of translation, a rabbit reticulocyte system and a KB-3-1 cell model have been selected. An *in-vitro* rabbit reticulocyte lysate system has been utilized as a cell-free translation system to measure the inhibitory potential of **12** in the context of protein translation. Prepared from New Zealand white rabbits, the rabbit reticulocyte system has been used widely as a standard procedure to "rank" chemical compounds in order of their translation inhibitory potential [174]. The *in-vitro* translation inhibition assay has been performed in the labortory of Dr. Florenz Sasse. As can be concluded from the results provided in **Section 3.3.2.4.1**, compound **12** has potently inhibited protein translation in the rabbit reticulocytesystem *in-vitro* with an approximately 43% inhibition at 0.3 µM. Cycloheximide has also been appreciably active with a roughly 61% inhibition at a

similar concentration of 0.4 μM. Methanol, in contrast, has not exhibited any down-regulatory effects on the translational efficiency of the rabbit reticulocytes. Such an inhibition may imply that **12** may either act directly on the translational machinery or alternatively may share methyl selenol as a common metabolite, with previously studied organoselenium compounds such as SeMC. Under physiological conditions, the cleavage of the methylenated selenium in **12** could indeed result in the formation of methyl selenol. Therefore, it is quite possible that the methylenated selenide moiety could serve as the active pharmacophore, responsible for the anti-tumour and translation-inhibiting efficacy of **12**.

Based on the potential translation inhibiting potential demonstrated by **12** on the eukaryotic system, the modulatory effects of **12** towards the translation efficiency of KB-3-1 cells have also been investigated. Similar to their translation inhibiting activity in the rabbit reticulocytes, both **12** and cycloheximide (benchmark compound) have been found to potently attenuate the translation activity of KB-3-1 cells. Although this effect has been observed to be maximumat the highest selected concentrations, both **12** and cycloheximide have also been observed to considerably inhibit translation in KB-3-1 cells by roughly 71% and 68% even at lower concentrations of approximately 3.3 μM and 3.5 μM, respectively. These results have clearly indicated that the anti-proliferative potential of **12** against KB-3-1 cells can be attributed to the disruption of its intra-cellular translational machinery. Hence, compounds like **12** that deprive tumour cells from the proteins necessary as an indispensable "fuel" for their proliferation and survival could, in the future, form a part of an effective anti-tumour strategy [177].

Several reports in the literature have attributed the anti-cancer effects of active selenium metabolites such as methyl selenol to their inhibitory effects against several oncogenic biochemical pathways [110, 111]. Amongst them, the ERK-mediated and mTOR-mediated cellular pathways, when over-activated, have been observed to either individually or synergistically contribute to tumour cell proliferation and survival by promoting intra-cellular protein translation, on one hand, and /or suppressing apoptosis, on the other [36, 120]. In order to find a similar link between the translation-inhibiting and apoptosis-inducing ability of **12** with a probable modulation of such intracellular signalling pathways in KB-3-1 cells, Western Blot analysis of **12**-treated KB-3-1 cells has been carried out at Helmholtz Centre.

Results from the Western Blot analysis have revealed that **12** demonstrates a significant down-regulatory effect on the activity of the Raf-mediated signalling cascade (also called MAPK signalling cascade), in KB-3-1 cells. This has been evident from a concentration-dependent decrease in the phosphorylation status of core proteins constituting this pathway, such as c-Raf and its downstream substrates MEK1/2, ERK1/2 and p90RSK in **12**-treated KB-3-1 cells. These proteins when activated via phosphorylation have been reported to trigger a chain of cellular events by regulating the activity of several transcription and translation factors, thereby contributing to cellular proliferation and survival [70]. A mutation or over-activation of any of these MAPK proteins, as observed by their hyper-phosphorylation, has been implicated in a majority of cancer cells [36, 152].

As discussed in **Chapter 1**, in light of the recent success in the clinical development of several inhibitors of protein kinases, components of the Raf-mediated signalling cascade have been a "hot" subject of research and drug discovery efforts. Of these, ERK1 and ERK2 have attracted considerable research interest because of their over-activation and critical involvement in the regulation of protein translation and cellular apoptosis in tumour cells [120]. Furthermore, latest studies on this intensetopic have reported that ERK2, in addition to its downstream substrate p90RSK, apparently plays a lead actor in promoting cellular proliferation whereas ERK1 plays a lesser and a rather mixed role towards sustaining cellular survival [79, 80].Therefore, as has been observed in this study, a pronounced deactivation of ERK1/2 in KB-3-1 cells by **12** with a drastically more pronounced effect on ERK2 may, therefore, contribute partially to this compound´s potential anti-proliferative and translation-inhibitory ability.

In addition to the ERK-mediated MAPK pathway, compound **12** has also exerted its down-regulatory effects on the activation of the PI3K-Akt-mTOR signalling pathway. As discussed in **Chapter 1** and elsewhere, mTOR-mediated signalling is frequently over-activated in tumorigenic cell lines. The core nodes constituting this signalling pathway, namely PI3K, Akt and mTOR, thereby serve as potential cancer promoters due to genetic mutations, in tumorigenic cells [115]. In addition, a close association of this signalling cascade with translation factors like 4E-BP1 characterizes it as an important protein-translation agonist [33]. As per immunoblot analysis, **12** has been observed to significantly reduce the phosphorylation and, therefore, the activation

of these critical proteins in the PI3K-mediated signalling cascade, when employed at a concentration of 30 µM. Compound **12** has also induced a moderate dephosphorylation of eukaryotic translation factor binding protein 4E-BP1 that acts as a downstream substrate of mTOR protein within the PI3K signalling cascade. This may contribute to the disruption of the eIF4F complex that is responsible for the stimulation of mTOR-mediated cellular translation in KB-3-1 cells.

As displayed in **Figure 4.1**, the results from the Western Blot analysis, therefore, point towards a synergistic effect of **12** on the ERK-mediated and mTOR-mediated signalling pathways.
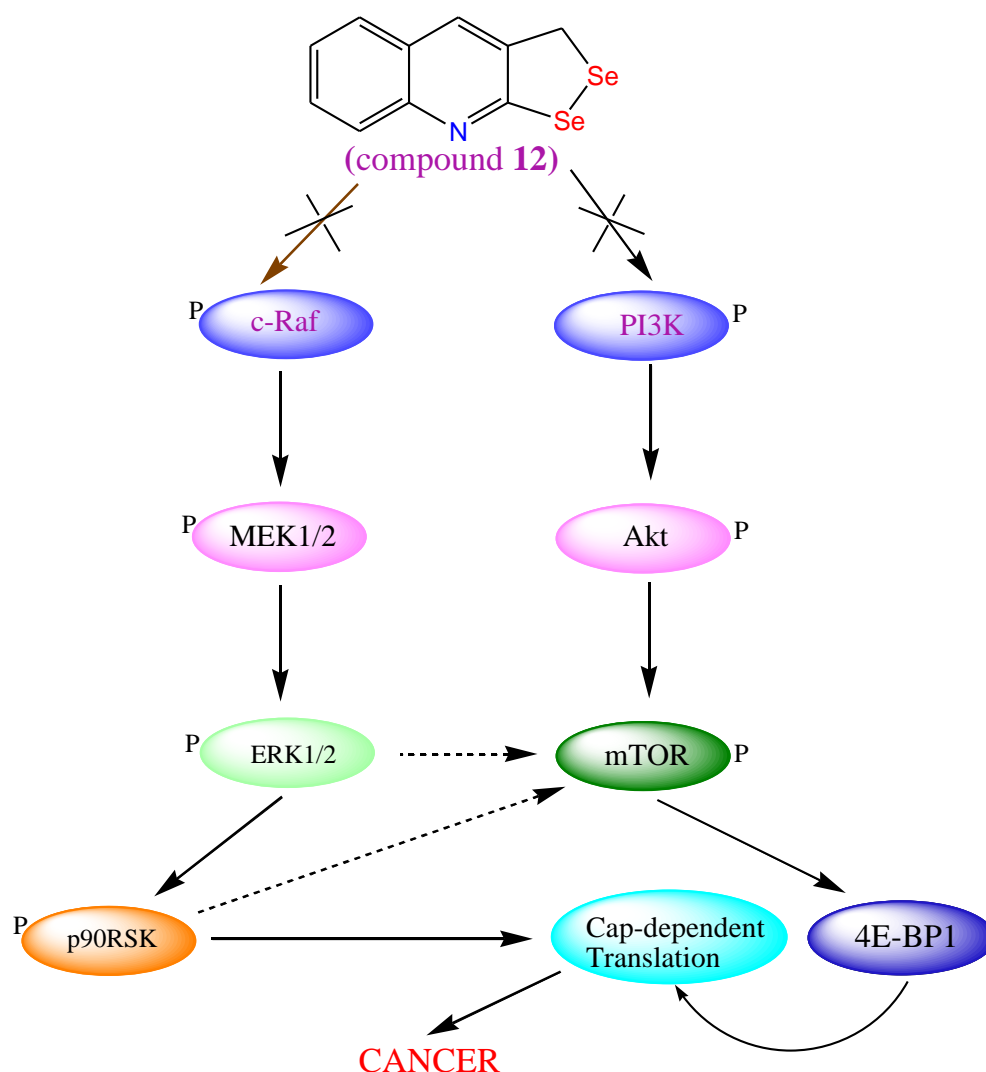
Figure 4.1 Inhibition of protein translation in association with a synergistic inhibition of ERK-mediated and mTOR-mediated cellular signalling by **12** in KB-3-1 cells.

Since these signalling pathways share an interesting cross-talk with the translational machinery of the mammalian cells, these findings further corroborate the notion of a distinct inhibition of protein translation and an anti-carcinogenic action of **12**. We can, therefore, postulate that the anti-proliferative activity of **12** against KB-3-1 cells is a consequence of attenuated levels of protein translation in KB-3-1 cells, which in turn is, at least partially, the result of the simultaneous down-regulation of the aberrantly activated ERK and mTOR-mediated signalling cascades.
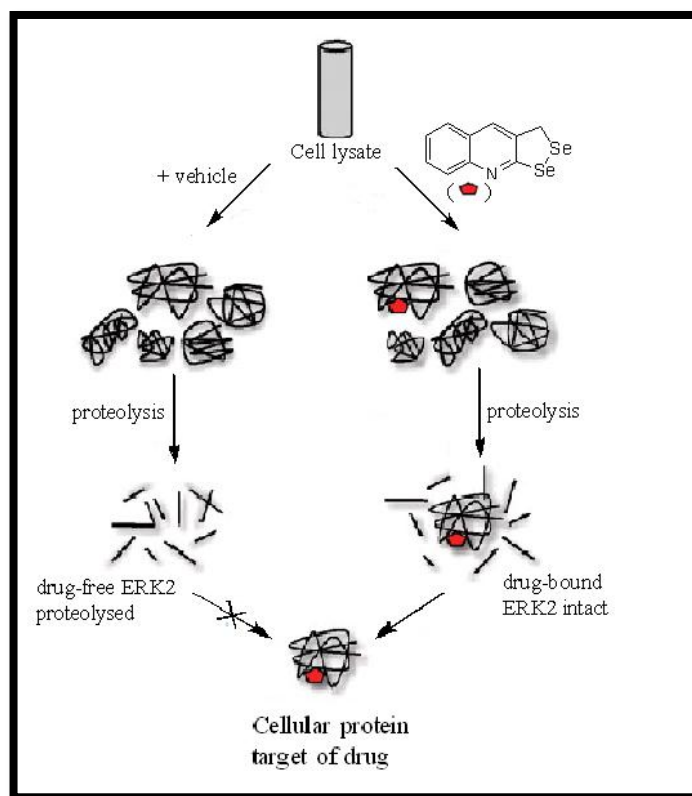
Figure 4.2 Protection of ERK2 by **12** in KB-3-1 cells**,** as demonstrated by the DARTS approach.

To obtain a better insight into the cellular protein(s) which may be targeted by **12**, a well-established drug-responsive target stability (DARTS) approach has been used in this study [95]. During the past few years, this relatively new methodology has been often employed as a relatively simple and widely applicable target identification approach for assessing drug-binding cellular targets. Based on the principle that a protein significantly peters out upon proteolysis when it is drug-free, yet it is resistant to protease digestion when it is drug-bound. The DARTS approach has been exploited for the identification of possible intra-cellular target(s) of **12**. As demonstrated in **Figure 4.2**, the results from the DARTS

experiment have revealed that **12** "protects" ERK2 protein from enzymatic degradation in a dose-dependent manner.This finding is in partial agreement with the down-regulatory effects of **12** on ERK2. To the best of my knowledge, this is for the first time that a selective protection of non-phosphorylated ERK2 (and not ERK1) by an organodiselenide has been found using a target-identification approach.

As mentioned in **Chapter 1**, there are several reports that distinguish between the biochemical roles of the closely related ERK isoforms [178]. Although both of these isoforms share around 85% homology, ERK2 has been reported to exert a more prominent effect on cellular viability when compared to ERK1. Many arguments have been put forward to explain the distinct roles of ERK1 and ERK2 in maintaining cellular vitality and survival and several knock-down experiments have suggested that ERK2 retains the upper-hand in maintaining cell viability, when compared to ERK1 [179]. In consideration of these arguments, a selectivity of **12** towards ERK2 resulting in the latter's dephosphorylation may partially explain the marked decrease in tumour cell survival upon incubation with **12**. The reasons underlying the specific preference of **12** for ERK2, relative to ERK1 are more difficult to fathom. They may include a structural preference of **12** for a particular binding motif within ERK2 which may be difficult in case of ERK1. An alternative argument may consider the selectivity of potential metabolites of **12** most likely involving methyl selenol.

Future experiments need to investigate the exact structural and/or biochemical reasons behind this bias of **12** towards ERK2. It is believed that this observation could serve as a valuable hint for drug development involving the anti-carcinogenic effects of organodiselenides.Somewhat surprisingly, however, no potential interaction of **12** with the core proteins within the PI3K-Akt-mTOR signalling cascade have been observed during the course of current investigations, using this particular DARTS approach

In order to substantiate the findings obtained previously from the DARTS experiment, a ligand-binding assay has been carried out, in co-operation with DiscoverX (USA) in order to assess the extent of thermodynamic interactions of **12** with a full-length ERK2 kinase.This assay has served as a platform for measuring quantitatively measure interactions between **12** and ERK2. In accordance with the results obtained, the *Kd* (binding affinity) value, obtained from a dose-dependent incubation of **12** with recombinant ERK2 protein has been calculated to be around 3.7

µM. Interestingly, at a similar concentration, the cyclic diselenide (**12**) had also been observed to display an inhibition in activation of ERK2 in the KB-3-1 cell lysate, using the Western Blot analysis technique. The K_d obtained, therefore, has indicated a moderate interaction of ERK2 with **12**. Nonetheless, this study does not provide any information regarding the chemical nature of the binding interactions between ERK2 and **12**.

In a follow-up of this study, therefore, future experiments need to be designed in order to investigate the probable binding domains in the ERK2 protein that could serve as potential interaction sites for **12**. Such studies may surely provide a more detailed in-sight into the chemical and biochemical factors that underlie the selective affinity to **12** towards ERK2**.**

In a related context, it is well documented that tumour cells harbor higher levels of OS relative to normal and healthy cells [14]. This OS has been proposed to be utilised by cancer cells as a "driving force" for their proliferation *via* the activation of several genetic factors and signalling pathways [15]. On the contrary, "too much" intracellular accumulation of OS may also push tumour cells towards cellular suicide. This situation can be conveniently considered to a situation of giving a dose of poison ("*extra*" ROS induced by an external stimulus) to a critically-sick patient (tumour cells, in this case). This additional dose of ROS may be effectively induced by the inhibition of ROS-scavenging cellular antioxidants like TrxR (in this case). The potent inhibition of mammalian TrxR by two selenium and tellurium-containing naphthoquinones (**16** or **17**) in the sub-micromolar range, as observed in this study, has partially explained the ROS-inducing ability of such compounds against cancer cells. The latter effect had been previously reported by Jacob *et al.* [143]. Unlike several other anti-cancer organoselenium compounds like ebselen and methyl seleninate that have been reported to exert their redox-regulatory effects by serving as a substrate of mammalian TrxR, the chalcogen-containing naphthoquinones such as **16** and **17** have proved themselves as potential inhibitors of mammalian TrxR in the TrxR inhibition assay that has been carried out in the research group of Prof. Ingo Ott (Department of Bioinorganic Medicinal Chemistry, Technical University, Braunschweig) [151]. Future studies are needed to provide an explanation for the comparably high inhibitory potential of the tellurium-containing naphthoquinone in comparison to its selenium-containing

counterpart. In addition, it would also be interesting to carry out detailed structure-activity relationship (SAR) studies of these redox-active molecules in order to identify the distinct pharmacophore(s) or reactive sites in these molecules which are ultimately responsible for inhibiting TrxR.

In addition to a detailed investigation into the anti-cancer activities of **10**, **11** and **12** against mammalian cell lines, an anti-microbial assay of these chemotherapeutic compounds has been also carried out with a basic motive to explore possible wider spectra of their potential targets in the microbial domain. In accordance with the results, the anti-microbial activities of **10**, **11** and **12** against the selected microbial strains have been observed to be rather modest. Additional experiments with many other pathogenic strains, however, are needed to have a broader scenario of the anti-microbial spectrum of such chemotherapeutic compounds, in addition to identifying precise biochemical reasons behind the higher activity of these compounds towards some fungal strains in comparison to bacterial strains, as has been observed in this study. Therefore, such organodiselenides may, therefore, exhibit some cytotoxic effects against mammalian cell lines, but are apparently not potential candidates for the future development of innovative redox-modulatory anti-microbial agents.

The relationship between the electrochemical behaviour of compounds and their redox-regulated biological activity is very interesting. Based on this concept, an investigation into the relationship between the significant biological activity of **12** and its electrochemical characteristics has been carried out in co-operation with Dr. Joseph (Noorul Islam University, Tamil Nadu, India). According to the electrochemical results observed in this study, a high reduction potential of compound **12** may well indicate it to be rather oxidising which may attribute to its apoptosis-inducing activity in tumour cells. In contrast, the selenophenes (**ARS-01** to **ARS-06**) have not been observed to be redox-active as far as the chalcogen moiety is concerned, which is surprising and disappointing. This may, however, be due to the "extra stability" of the chalcogen moiety within the aromatic framework of the selenophenes. However, the redox activity of the most active selenophenes **ARS-01** and **ARS-02** may have resulted from their phenolic groups which also ultimately explains their significant anti-oxidant effects, as observed in the DPPH and FRAP redox assays. The redox activities of **ARS-01** and **ARS-02** are probably not due to a redox modulation (in the presence of sulfur or

selenium) but due to their binding to specific cellular targets (like estrogen receptors as in the case of **ARS-01**) which may have no relation with the chalcogen moiety or indeed redox modulation [189]. The results obtained from the DPPH assay point towards a relatively low radical-scavenging activity of **12** at 1 mg ml^{-1} (33.5 ± 1.6 %) in comparison to a more significant effect displayed by ascorbic acid at 1 mg ml^{-1} (72.0 ± 1.2%). A similar result has also been obtained in the FRAP assay where a relatively low FRAP value (of 221 ± 39 µmol equiv of Fe^{2+} l^{-1} has been measured for **12**, in comparison to that of ascorbic acid (2664 ± 51 µmol equiv of Fe^{2+} l^{-1}). Though not promising, the average radical-scavenging effect of **12** could probably be due to the presence of the electron-donating nitrogen atom of the quinoline ring. However, this argument has not been found to be valid in case of **10** and **11**, which despite the presence of a nitrogen-containing pyridine ring have neither exhibited any observable decline in DPPH levels nor a significant reduction of the Fe(TPTZ)$_3$ complex. Such a contrast in the reducing ability of **12** on the one hand, and **10** or **11** on the other is even more surprising despite the similar basicities (pK_a ~5) of pyridine (in case of **10** or **11**) and quinoline ring systems (in case of **12**) [181].
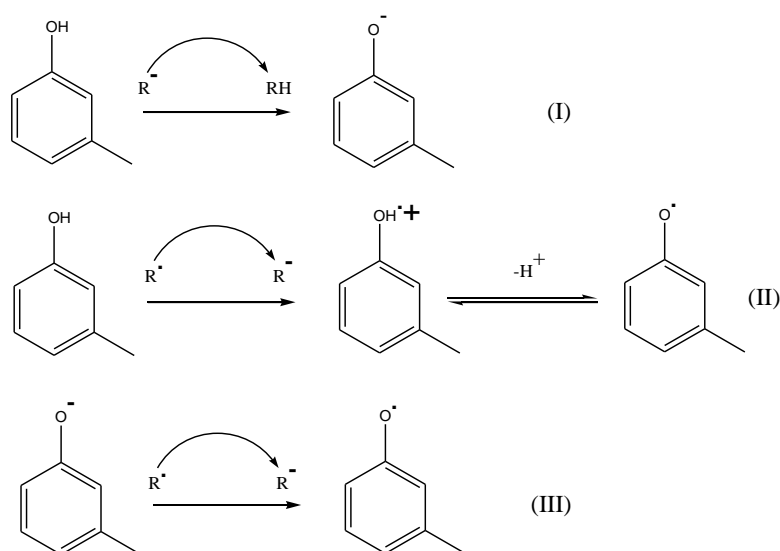
Figure 4.3 Proposed mechanism of radical-scavenging activity of phenolic groups by -
  (a) One-step hydrogen transfer (reaction I) or
  (b) Electron transfer (reaction II or III)

The anti-oxidant activities of coumarins has been demonstrated to be due to their hydroxyl groups that serve directly as free radical scavengers via facile generation. As displayed in **Figure 4.3**, this radical-scavenging effect has been proposed to proceed either by an electron transfer (ET) from phenolate anions or by a hydrogen atom transfer from the phenolic hydroxyl group [182].

Owing to a lower redox potential, however, the phenolate anion furnished by a phenolic group-bearing compound has been reported to harbor a higher radical-scavenging ability compared to its parent phenolic form [183].

In regard to the above arguments that explain the possible mechanism of anti-oxidative effects of phenols, it can be hypothesized that the potential radical-scavenging ability of **ARS-01** and **ARS-02** could be convincingly attributed to the presence of free phenolic hydroxyl groups in these molecules, that probably serve as the critical functionality to explain the significant DPPH radical scavenging effects for these compounds in addition to their significantly high FRAP values. In contrast, the inconsequential anti-oxidant effects of the other selenophenes (**ARS-03** to **ARS-06**) could be due to the absence of phenolic hydroxyl groups and an apparently non-active role of the chalcogen moiety in their chemical structure.

In consideration of the above arguments, the presence of phenolic groups in **ARS-01** and **ARS-02** could serve as a logical hypothesis for their potential anti-oxidant and radical-scavenging ability. In contrast, the potentially low anti-oxidant ability of the selenium-containing coumarins (**ARS-03** to **ARS-06**) could be attributed to the absence of phenolic hydroxyl groups and an apparently non-relevant role of the chalcogen moiety in such molecules.

Conclusion and Outlook

Remarkable progress has been made during the past few decades in expanding the existing knowledge of the biological action of organoselenium compounds in its diverse chemical and biochemical forms. Inspite of the chemical sensitivity and susceptibility of selenium, significant synthetic progress has been achieved in expanding the chemical library of organoselenium compounds, with a particular emphasis towards the chemical synthesis and derivatisation of naturally occurring and biologically active organoselenium compounds [184]. This, in turn, has provided biologists and biochemists with ample sources of organoselenium compounds for evaluating their unique biochemical mode of action of such molecules, particularly against cancer cells.

In spite of the diverse nature of organoselenium compounds that have been analysed so far for chemotherapeutic efficacy, most of these compounds have apparently discharged their therapeutic effects through a common cascade of biologically active metabolites such as methyl selenol and hydrogen selenide. These compounds have been frequently reported to exert their anti-cancer effects by monitoring the redox-regulated transcriptional and translational pathways within the intracellular environment of various tumours [185]. The extent of effectiveness of these organoselenium compounds against cancer, however, has been observed to vary considerably with dosage and nature of the administered source of selenium. In this study, the anti-cancer activity of the main compound of study (**12**) has been observed to bear a close resemblance with that of the previously reported anti-cancer effects of methyl selenol in terms of its apoptosis-inducing activity, on the one hand, and its inhibitory effects against the translational and oncogenic ERK-mediated MAPK pathway, on the other [108]. On this note, an apparent selectivity of **12** towards ERK2, as observed in the DARTS experiment, points towards a possible affinity of naturally occurring organic selenium sources like SEM or SeMC towards ERK2.

Since tumour cells are observed to thrive under high levels of oxidative stress, an attenuation of the latter by potential antioxidants has been proposed to serve as an effective strategy to counter cancer [186]. In spite of the widely discussed and frequently observed cross-talk between the anti-oxidant and anti-cancer effects of small

molecules, such a relationship has apparently not been observed in this study in case of compounds **10**, **11** or **12**. In contrast, the chalcophenes **ARS-01** and **ARS-02** that have been observed to display relatively weaker anti-cancer effects than the organodiselenides (**10**, **11** or **12**) have demonstrated rather significant anti-oxidant properties than the latter. This may raise questions regarding the extent of contribution of the direct and indirect antioxidant activities of polyphenols (like **ARS-01** or **ARS-02**) towards suppressing proliferation of cancer cells. In this regard, however, till date there is apparently no concrete and consistent link between the anti-oxidant and chemotherapeutic effects of small molecules.

On the contrary, an induction of an extra pinch of oxidative stress in tumour cells has been an alternative and an apparently more effective strategy in the treatment of cancer. Thriving at a precarious level of oxidative stress, the fate of tumour cells has been observed to be highly susceptible to modulation in the activities of cellular anti-oxidant enzymes like TrxR. This concept has been extensively exploited by a range of molecules like auranofin which have been reported to induce ROS-mediated apoptosis in tumour cells via inhibition of TrxR [187]. A similar mode of action has also been observed, during the current study, in case of chalcogen-containing naphthoquinones (**16** and **17**). In due consideration of the fact that only a few chalcogen-containing compounds have so far been identified as TrxR-inhibitors, with a majority of them serving rather as TrxR substrates, such chalcogen-containing naphthoquinones may serve as a potential lead in the design of futuristic TrxR-inhibiting chemotherapeutics.

In the current situation, the exact biochemical anti-cancer effects of organoselenium compounds are still clouded by contradictory results and opinions. Inspite of selenium's promising chemotherapeutic effects observed in several *in-vitro* and *in-vivo* experiments, there is still a wide scope for a deeper comprehension of the precise biochemistry that organoselenium compounds share and ultimately may impact on cancer, its formation, progression and eradication.

To sum up this study, from a diverse range of organoselenium compounds belonging to distinct categories of monoselenides (**1**-**9**), diselenides (**10**-**15**) and chalcophenes (**ARS-01** to**ARS-06**), the diselenides have exhibited the highest anti-cancer activity *in-vitro*. However, such an appreciable activity of the diselenides can be more reasonably attributed to their cytotoxicity against mammalian cells rather than to

their selectivity against tumour cells. Such anti-cancer effects of the most active diselenides (**10**-**12**) have been observed to be an outcome of caspase 3/7 - mediated apoptosis which has been induced by these diselenides in cervix carcinoma (KB-3-1) cells. Furthermore, compound **12** hasnot only inhibited the translational machinery but also targeted the translation-associated Raf/MEK/ERK and PI3K/Akt/mTOR pathways of KB-3-1 cells. On this note, a DARTS approach has also indicated a selective interaction of **12** with ERK2. Inspite of their considerable anti-cancer activities, these diselenides (**10**-**12**) have displayed poor anti-oxidant effects. In contrast, only the selenophenes (**ARS-01** and **ARS-02**) have demonstrated a significant anti-oxidant effect in the DPPH and FRAP redox assays primarily due to the action of the phenolic hydoxyl groups and apparently not due to the chalcogen moiety.

In another context, compounds **16** and **17** which belong to a distinct group of chalcogen-containing naphthoquinones have been studied to act as active inhibitors of mammalian TrxR. This behaviour could form an additional biochemical reason to further explain their previously reported ROS-mediated induction of apoptosis in tumour cells.

In view of the appreciable chemotherapeutic potential demonstrated by organoselenium compounds in a range of *in-vitro* and *in-vivo* experiments carried out over the last decade, it can be safely proposed that such compounds should not be ignored in the design and synthesis of drugs against cancer. Moreover, compared to a rather narrow focus on the efficacy of organoselenium compounds against primary tumours, more attention should be diverted towards the identification and a probable exploitation of the therapeutic effects of these compounds in tackling cancer progression and metastasis.

References

1. C. Thiry, A. Ruttens, L.D. Temmerman, Yves-Jacques Schneider and L. Pussemier, Current knowledge in species-related bioavailability of selenium in food, *Food Chem* **2012**, 130(4), 767-784.

2. Y. Yamashita, M. Yamashita and H. Iida, Selenium content in seafood in Japan, *Nutrients* **2013**, 5, 388-395.

3. M. Bajaj, S. Schmidt and J. Winter, Formation of Se (0) nanoparticles by Duganella sp. and Agrobacterium sp. isolated from Se-laden soil of North-East Punjab, India, *Microb Cell Fact* **2012**, 11, 64.

4. L. Johansson, G. Gafvelin and E.S. Arnér, Selenocysteine in proteins-properties and biotechnological use, *Biochim Biophys Acta (BBA)* **2005**, 1726(1), 1-13.

5. M. Yamashita, Y. Yamashita, T. Suzuki, Y. Kani, N. Mizusawa, S. Imamura, K. Takemoto, T. Hara, M.A. Hossain, T. Yabu and K. Touhata, Selenoneine, a novel selenium-containing compound, mediates detoxification mechanisms against methylmercuryaccumulation and toxicity in zebrafish embryo, *Mar Biotechnol* **2013**,15(5), 559-570.

6. Y.Yamashita, T. Yabu and M. Yamashita, Discovery of the strong antioxidant selenoneine in tuna and selenium redox metabolism, *World J Biol Chem* **2010**, 1(5), 144–150.

7. P. Rakesh, H.B. Singh, J.P. Jasinski and J.A. Golen, Synthesis, structure and reactivity of [*o*-(2,6-diisopropylphenyliminomethinyl)phenyl]selenenyl seleno-cyanate (RSeSeCN) and related derivatives, *Dalton Trans* **2014**, 43(25), 9431-9437.

8. C. Méplan and J. Hesketh, Selenium and cancer: A story that should not be forgotten-insights from genomics, *Advances in Nutrition and Cancer*, Springer Berlin Heidelberg **2014**, 159,145-166.

9. K.W. Jasperson, T.M. Tuohy, D.W. Neklason and R.W. Burt, Hereditary and familial colon cancer, *Gastroenterology* **2010**, 138(6), 2044-2058.

10. I.Stepanov, J. Jensen, L. Biener, R.L. Bliss, S.S. Hecht and D.K. Hatsukami, Increased pouch sizes and resulting changes in the amounts of nicotine and tobacco-specific N-nitrosamines in single pouches of Camel Snus and Marlboro Snus, *Nicotine Tob Res* **2012**, 14(10), 1241-1245.

11. C. Oliai and L.X. Yang, Radioprotectants to reduce the risk of radiation-induced carcinogenesis, *Int J Radiat Biol* **2014**, 90(3), 203-213.

12. S. Marur, G. D'Souza, W.H. Westra and A.A. Forastiere, HPV-associated head and neck cancer: a virus-related cancer epidemic, *Lancet Oncol* **2010**, 11(8), 781-789.

13. G. Dennert, M. Zwahlen, M. Brinkman, M. Vinceti, M. P. Zeegers and M. Horneber, Selenium for preventing cancer, *Cochrane Database Syst Rev* **2011**, 5.

14. N. Özören and W.S. El-Deiry, Cell surface death receptor signalling in normal and cancer cells, *Sem Can Biol,* Academic Press **2003**, 13(2), 135-147.

15. D. Hanahan and R.A. Weinberg, Hallmarks of cancer: the next generation, *Cell* **2011,** 144(5), 646-674.

16. C. Sanmartín, D. Plano, A.K. Sharma and J.A. Palop, Selenium compounds, apoptosis and other types of cell death: an overview for cancer therapy, *Int J Mol Sci* **2012**, 13(8), 9649-9672.

17. F. Buttgereit and M.D. Brand, A hierarchy of ATP-consuming processes in mammalian cells, *Biochem J* **1995**, 312, 163-167.

18. S.P. Blagden and A.E. Willis, The biological and therapeutic relevance of mRNA translation in cancer, *Nat Rev Clin Oncol* **2011**, 8(5), 280-291.

19. M. Bushell, M. Stoneley, P. Sarnow and A.E. Willis, Translation inhibition during the induction of apoptosis: RNA or protein degradation? *Biochem Soc Trans* **2004**, 32(4), 606-10.

20. N. Sonenberg and A.G. Hinnebusch, Regulation of translation initiation in eukaryotes: mechanisms and biological targets, *Cell* **2009**, 136(4), 731-745.

21. R.J. Jackson, C.U. Hellen and T.V. Pestova, The mechanism of eukaryotic translation initiation and principles of its regulation, *Nat Rev Mol Cell Biol* **2010**, 11(2), 113-127.

22. J.R. Graff, B.W. Konicek, J.H. Carter and E.G. Marcusson, Targeting the eukaryotic translation initiation factor 4E for cancer therapy, *Canc Res* **2008**, 68(3), 631-634.

23. D. Ruggero, L. Montanaro, L. Ma, W. Xu, P. Londei, C. Cordon-Cardo and P.P. Pandolfi, The translation factor eIF-4E promotes tumor formation and cooperates with c-Myc in lymphomagenesis, *Nat Med* **2004**, 10(5), 484-486.

24. I. Topisirovic and K.L.B. Borden, Homeodomain proteins and eukaryotic translation initiation factor 4E (eIF4E): an unexpected relationship, *Histol Histopathol* **2005**, 20, 1275-1284.

25. L. Furic, L. Rong, O. Larsson, I.H. Koumakpayi, K. Yoshida, A. Brueschke, E. Petroulakis, N. Robichaud, M. Pollak, L.A. Gaboury, P.P. Pandolfi, F. Saad and N. Sohnenberg, eIF4E phosphorylation promotes tumorigenesis and is associated with prostate cancer progression, *Proc Natl Acad Sci USA* **2010**, 107(32), 14134-14139.

26. T.P. Herbert, A.R. Tee and C.G. Proud, The extracellular signal-regulated Kinase pathway regulates the phosphorylation of 4E-BP1 at multiple sites, *J Biol Chem* **2002**, 277, 11591-11596.

27. A.C. Gingras, B. Raught and N. Sonenberg, mTOR signaling to translation, *Curr Top Microbiol Immunol* **2004**, 279,169-197.

28. D. Shahbazian, P.P. Roux, V.Mieulet, M.S. Cohen, B. Raught, J. Taunton, J. W. Hershey, J. Blenis, M. Pende and N. Sonenberg, The mTOR/PI3K and MAPK pathways converge on eIF4B to control its phosphorylation and activity, *EMBO J* **2006**, 25(12), 2781-2791.

29. E. Tchevkina and A. Komelkov, Protein phosphorylation as a key mechanism of mTORC1/2 signaling pathways, *Protein Phosphorylation in Human Health*, **2012**, Ch. 1, *3*-50, C. Huang (Ed.), InTech, Crotia.

30. R.R.Yuan, A. Kay, W.J. Berg and D. Lebwohl, Targeting tumorigenesis: development and use of mTOR inhibitors in cancer therapy, *J Hematol Oncol* **2009**, 2(1), 45.

31. A. Younes and D.A. Berry, From drug discovery to biomarker-driven clinical trials in lymphoma, *Nat Rev Clin Oncol* **2012**, 9(11), 643-653.

32. A.S. Strimpakos, E.M. Karapanagiotou, M.W. Saif and K.N. Syrigos, The role of mTOR in the management of solid tumours: an overview, *Canc Treat Rev* **2009**, 35(2), 148–159.

33. A.C. Hsieh, M. Costa, O. Zollo, C. Davis, M.E. Feldman, J.R.Testa, O. Meyuhas, K.M. Shokat and D. Ruggero, Genetic dissection of the oncogenic mTOR pathway reveals druggable addiction to translational control via 4EBP-eIF4E, *Canc Cell* **2010**, 17(3), 249-261.

34. H. Zhou, Y. Luo, and S. Huang, Updates of mTOR inhibitors, *Anticanc Agents Med Chem* **2010**, 10(7), 571-581.

35. T. Ueda, R. W. Fukunaga, H. Fukuyama, S. Nagata and R. Fukunaga, Mnk2 and Mnk1 are essential for constitutive and inducible phosphorylation of eukaryotic initiation factor 4E but not for cell growth or development, *Mol Cell Biol* **2004**, 24(15), 6539-6549.

36.   M.M. Monick, L.S. Powers, T.J. Gross, D.M. Flaherty, C.W. Barrett and G.W. Hunninghake, Active ERK contributes to protein translation by preventing JNK-dependent inhibition of protein phosphatase, *J Immunol* **2006**, 177(3), 1636-1645.

37.   P.Cohen, Protein kinases- the major drug targets of the twenty-first century? *Nat Rev Drug Discov* **2002**, 1(4), 309–315.

38.   R. Seger and E.G. Krebs, The MAPK signalling cascade*, FASEB J* **1995**, 9(9), 726-735.

39.   M. Cargnello and P.P. Roux, Activation and function of the MAPKs and their substrates, the MAPK-activated protein kinases, *Microbiol Mol Biol Rev* **2011**, 75(1), 50-83.

40.   L.I.U. Jing and L. Anning, Role of JNK activation in apoptosis: a double-edged sword, *Cell Res* **2005**, 15(1), 36-42.

41.   M. Hüser, J. Luckett, A. Chiloeches, K. Mercer, M. Iwobi, S. Giblett, X.M. Sun, J. Brown, R. Marais and C. Pritchard, MEK kinase activity is not necessary for Raf-1 function, *EMBO J* **2001**, 20(8), 1940-1951.

42.   J. Zhu, V. Balan, A. Bronisz, K. Balan, H. Sun, D.T. Leicht, Z. Luo, J. Qin, J. Avruch and G. Tzivion, Identification of Raf-1 S471 as a novel phosphorylation site critical for Raf-1 and B-Raf kinase activities and for MEK binding, *Mol Biol Cell* **2005**, 16(10), 4733–4744.

43.   B. Wefers, C. Hitz, S.M. Hölter, D. Trümbach, J. Hansen, P. Weber and B. Pütz, MAPK signalling determines anxiety in the juvenile mouse brain but depression-like behavior in adults, *PloS one* **2012**, 7(4), e35035.

44.   X.Wang and G.P. Studzinski, Phosphorylation of raf-1 by kinase suppressor of ras is inhibited by "MEK-specific" inhibitors PD 098059 and U0126 in differentiating HL60 cells, *Exp Cell Res* **2001**, 268(2), 294-300.

45.   K.C. Corbit, N. Trakul, E.M. Eves, B. Diaz, M. Marshall and M.R. Rosner, Activation of Raf-1 signalling by protein kinase C through a mechanism involving raf kinase inhibitory protein, *J Biol Chem* **2003**, 278, 13061-13068.

46.   J. Downward, Targeting RAS signalling pathways in cancer therapy, *Nat Rev Cancer* **2003**, 3(1), 11-22.

47.   C.P. Webb, A.L. Van, M.H. Wigler and G.F. Woude, Signalling pathways in Ras-mediated tumorigenicity and metastasis, *Proc Natl Acad Sci USA* **1998**, 95, 8773-8778.

48. L. Voisin, C. Julien, S. Duhamel, K. Gopalbhai, I. Claveau, M.K. Saba-El-Leil, I.G. Rodrigue-Gervais, L. Gaboury, D. Lamarre, M. Basik and S. Meloche, Activation of MEK1 or MEK2 isoform is sufficient to fully transform intestinal epithelial cells and induce the formation of metastatic tumours, *BMC Cancer* **2008**,8, 337.

49. J.E. Dixon, Selective activation of MEK1 but not MEK2 by A-Raf from epidermal growth factor-stimulated hela cells, *J Biol Chem* **1996**, 271, 3265-3271.

50. E. Skarpen, L.I. Flinder, C.M. Rosseland,S. Ørstavik, L. Wierød, M.P. Oksvold,B.S. Skålhegg and H.S. Huitfeldt, MEK1 and MEK2 regulate distinct functions by sorting ERK2 to different intracellular compartments, *FASEB J* **2008***, 22(2), 466–476.

51. F. Catalanotti, G. Reyes, V. Jesenberger, G. Galabova-Kovacs, R.S. de Matos, O. Carugo, M. Baccarini, A Mek1-Mek2 heterodimer determines the strength and duration of the Erk signal, *Nat Struct Mol Biol* **2009**, 16(3), 294-303.

52. A. Bessard, C. Fre´min, F. Ezan, A. Fautrel, L. Gailhouste and G. Baffet, RNAi-mediated ERK2 knockdown inhibits growth of tumour cells *in- vitro* and *in-vivo*, *Oncogene* **2008**, 27(40), 5315–5325.

53. E.A. Collisson, A. De, H. Suzuki, S.S. Gambhir and M.S. Kolodney, Treatment of metastatic melanoma with an orally available inhibitor of the Ras-Raf-MAPK cascade, *Canc Res* **2003**, 63(18), 5669–5673.

54. D. Sinha, S. Bannergee, J.H. Schwartz, W. Lieberthal and J.S. Levine, Inhibition of ligand-independent ERK1/2 activity in kidney proximal tubular cells deprived of soluble survival factors upregulates Akt and prevents apoptosis, *J Biol Chem* **2003**, 279, 10962-10972.

55. D. Tang, D. Wu, A. Hirao, J.M. Lahti, L. Liu, B. Mazza, V.J. Kidd, T.W. Mak andA.J. Ingram, ERK activation mediates cell cycle arrest and apoptosis after DNA damage independently of p53, *J Biol Chem* **2002**, 277 (15), 12710-12717.

56. J. Hayakawa, M. Ohmichi, H. Kurachi, Y. Kanda, K. Hisamoto,Y. Nishio, K. Adachi, K. Tasaka, T. Kanzakiand Y. Murata, Inhibition of BAD phosphorylation either at serine 112 via extracellular signal-regulated protein kinase cascade or at serine 136 via Akt cascade sensitizes human ovarian cancer cells to cisplatin, *Canc Res* **2000**, 60, 5988-5994.

57. C. Jiang, Z. Wang, H. Gantherand J. Lu, Caspases as key executors of methyl selenium-induced apoptosis (anoikis) of DU-145 prostate cancer cells, *Canc Res* **2001**, 61(7), 3062-3070.

58. W.X. Zong and C.B. Thompson, Necrotic death as a cell fate, *Genes Dev* **2006**, 20(1), 1-15.

59. E. Berra, M. T. Diaz-Meco and J. Moscat, The activation of p38 and apoptosis by the inhibition of erk is antagonized by the phosphoinositide 3-kinase/Akt pathway, *J Biol Chem* **1998**, 273, 10792-10797.

60. T. Shonai, M. Adachi, K. Sakata, M. Takekawa, T. Endo, K. Imai and M. Hareyama, MEK/ERK pathway protects ionizing radiation-induced loss of mitochondrial membrane potential and cell death in lymphocytic leukemia cells, *Cell Death Differ* **2002**, 9, 963 – 971.

61. F. Condorelli, P. Salomoni, S. Cotteret, V. Cesi, S.M. Srinivasula, E.S. Alnemri and B. Calabretta, Caspase cleavage enhances the apoptosis-inducing effects of BAD, *Mol Cell Biol* **2001**, 21(9), 3025–3036.

62. X.Fang, S.Yu, A. Eder, M. Mao, R.C. Bast, D. Boyd, and G.B. Mills, Regulation of BAD phosphorylation at serine 112 by the Ras-mitogen-activated protein kinase pathway, *Oncogene* **1999,** 18(48), 6635–6640.

63. S.J. Leuenroth, P.S. Grutkoski, A. Ayala and H. H. Simms, The loss of Mcl-1 expression in human polymorphonuclear leukocytes promotes apoptosis, *J Leuk Bio* **2000**, 68(1), 158-166.

64. Q. Ding, L. Huo, J.Y. Yang, W. Xia, Y. Wei, Y. Liao, C.J. Chang, Y. Yang, C.C. Lai, D.F. Lee, C.J. Yen, Y.J. Chen, J.M. Hsu, H.P. Kuo, C.Y. Lin, F.J. Tsai, L.Y. Li, C.H. Tsai and M.C. Hung, Down-regulation of myeloid cell leukemia-1 through inhibiting Erk/Pin 1 pathway by sorafenib facilitates chemosensitization in breast cancer, *Canc Res* **2008**, 68(15), 6109-6117.

65. A.S. Gillings, K. Balmanno, C.M. Wiggins, M. Johnson and S.J. Cook, Apoptosis and autophagy: BIM as a mediator of tumour cell death in response to oncogene-targeted therapeutics, *FEBS J* **2009**, 276(21), 6050-6062.

66. F. Luciano, A. Jacquel, P. Colosetti, M. Herrant, S. Cagnol,G. Pages and P. Auberge, Phosphorylation of Bim-EL by Erk1/2 on serine 69 promotes its degradation via the proteasome pathway and regulates its proapoptotic function, *Oncogene* **2003**, 22, 6785–6793.

67. A. Paterson, C.I. Mockridge, J.E. Adams,S. Krysov, K.N. Potter, A.S. Duncombe, S.J. Cook, F.K. Stevenson and G. Packham, Mechanisms and clinical significance of BIM phosphorylation in chronic lymphocytic leukemia, *Blood* **2012**, 119(7), 1726-1736.

68. M. Walton, A.M. Woodgate, A. Muravlev, R. Xu,M.J. During and M. Dragunow, CREB phosphorylation promotes nerve cell survival, *J Neurochem* **1999**, 73(5), 1836-1842.

69. B.E. Lonze, A. Riccio, S. Cohen and D.D. Ginty, Apoptosis, axonal growth defects and degeneration of peripheral neurons in mice lacking CREB, *Neuron* **2002**, 34, 371–385.

70. M. Böhm, G. Moellmann, E. Cheng, M. Alvarez-Franco, S. Wagner,P. Sassone-Corsi and R. Halaban, Identification of p90RSK as the probable CREB-Ser133 kinase in human melanocytes, *Cell Growth Differ* **1995**, 6(3), 291-302.

71. J.S. Arthur and P. Cohen, MSK1 is required for CREB phosphorylation in response to mitogens in mouseembryonic stem cells, *FEBS Lett* **2000**, 482, 44–48.

72. M. Deak, A.D. Clifton, L.M. Lucocq and D.R. Alessi, Mitogen- and stress-activated protein kinase-1 (MSK1) is directly activated by MAPK and SAPK2/p38, and may mediate activation of CREB, *EMBO J* **1998**, 17, 4426–4441.

73. T. Mantamadiotis, T. Lemberger, S.C. Bleckmann, H. Kern, O. Kretz, A.M. Villalba, F.Tronche, C. Kellendonk, D. Gau, J. Kapfhammer, C. Otto, W. Schmid and G. Schütz, Disruption of CREB function in brain leads to neurodegeneration, *Nat Genet* **2002**, 31(1), 47-54.

74. M. Krasilnikov, V.N Ivanov, J. Dong and Z. Rona, ERK and PI3K negatively regulate STAT-transcriptional activities in human melanoma cells: implications towards sensitization to apoptosis, *Oncogene* **2003,** 22, 4092-4101.

75. S. Nandi, L.S. Reinert , A. Hachem, K. Mazan-Mamczarz, P. Hagner, H. He and R.B. Gartenhaus, Phosphorylation of MCT-1 by p44/42 MAPK is required for its stabilization in response to DNA damage, *Oncogene* **2007**, 26, 2283-2289.

76. N. Plesnila, C. Zhu, C. Culmsee, M. Gröger, M.A. Moskowitz and K. Blomgren, Nuclear translocation of apoptosis-inducing factor after focal cerebral ischemia, *J Cereb Blood Flow Metab* **2004**, 24(4), 458-466.

77. S.A. Susin, H.K. Lorenzo, N. Zamzami, I. Marzo, B.E. Snow, G.M. Brothers, J. Mangion, E. Jacotot, P. Costantini, M. Loeffler, N. Larochette, D.R. Goodlett, R. Aebersold, D.P. Siderovski, J.M. Penninger and G. Kroemer, Molecular characterization of mitochondrial apoptosis-inducing factor, *Nature* **1999**, 397, 441-446.

78. S. Ghavami, M. Hashemi, S.R. Ande, B. Yeganeh, W. Xiao, M. Eshraghi, C.J. Bus, K. Kadkhoda, E. Wiechec, A.J. Halayko and M. Los, Apoptosis and cancer: mutations within caspase genes, *J Med Genet* **2009**, 46(8), 497-510.

79. M.K. Saba-El-Leil, F.D. Vella, B. Vernay, L. Voisin, L. Chen, N. Labrecque, S.L. Ang and S. Meloche, An essential function of the mitogen-activated protein kinase Erk2 in mouse trophoblast development, *EMBO Rep* **2003**, 4(10), 964- 968.

80. Y. Satoh, S. Endo, T. Nakata, Y. Kobayashi, K. Yamada, T. Ikeda, A. Takeuchi, T. Hiramoto,Y. Watanabe and T. Kazama, ERK2 Contributes to the Control of Social Behaviors in Mice, *J Neurosci* **2011**, 31(33), 11953–11967.

81. A.M. Aronov, Q. Tang, G. Martinez-Botella, G.W. Bemis, J. Cao, G. Chen, N.P. Ewing, P.J. Ford, U. A. Germann, J. Green, M.R. Hale, M. Jacobs, J. W. Janetka, F. Maltais,W. Markland, M.N. Namchuk, S. Nanthakumar, S. Poondru, J. Straub,E. ter Haar and X. Xie, Structure-guided design of potent and selective pyrimidylpyrrole inhibitors of extracellular signal-regulated kinase (ERK) using conformational control, *J Med Chem* **2009**, 52, 6362–6368.

82. I.G. Wool, Extraribosomal functions of ribosomal proteins, *Trends Biochem Sci* **1996**, 21(5), 164-165.

83. K. Inoki, Y. Li, T. Zhu, J. Wu and K.L. Guan, TSC2 is phosphorylated and inhibited by Akt and suppresses mTOR signalling, *Nat Cell Biol* **2002**, 4(9), 648-57.

84. J. Avruch, K. Hara, Y. Lin, M. Liu, X. Long, S. Ortiz-Vega and K. Yonezawa, Insulin and amino-acid regulation of mTOR signalling and kinase activity through the Rheb GTPase, *Oncogene* **2006**, 25(48), 6361-6372.

85. R. Anjum and J. Blenis, The RSK family of kinases: emerging roles in cellular signalling, *Nat Rev Mol Cell Biol* **2008**, 9(10), 747-758.

86. X. Wang, M. Janmaat, A. Beugnet, F. Paulin and C. Proud, Evidence that the dephosphorylation of Ser535 in the e-subunit of eukaryotic initiation factor (eIF) 2B is insufficient for the activation of eIF2B by insulin, *Biochem J* **2002**, 367, 475-481.

87. O. Meyuhas, Physiological roles of ribosomal protein S6: one of its kind, *Int Rev Cell Mol Biol* **2008**, 268, 1-37.

88. L. Ma, Z. Chen, H. Erdjument-Bromage, P. Tempst and P.P. Pandolfi, Phosphorylation and functional inactivation of TSC2 by Erk: implications for tuberous sclerosis and cancer pathogenesis, *Cell* **2005**, 121(2), 179-193.

89. K. Aoki, M. Yamada, K. Kunida, S.Yasuda and M. Matsuda, Processive phosphorylation of ERK MAP kinase in mammalian cells, *Proc Natl Acad Sci USA* **2011**, 108(31), 12675-12680.

90. R.A. Reisfeld, The tumor microenvironment: a target for combination therapy of breast cancer, *Crit Rev Oncog* **2013**, 18(1-2), 115-33.

91. M. Bantscheff and G. Drewes, Chemoproteomic approaches to drug target identification and drug profiling, *Bioorg Med Chem* **2012**, 20(6), 1973-1978.

92. L. S. Lerman, A biochemically specific method for enzyme isolation, *Proc Natl Acad Sci USA* **1953**, 39(4), 232–236.

93. J.C. Meunier, R. Sealock, R. Olsen and J.P. Chanqeux, Purification and properties of the cholinergic receptor protein from electrophorus electricus electric tissue, *Eur J Biochem* **1974**, 45, 371–394.

94. U. Rix and G. Superti-Furga, Target profiling of small molecules by chemical proteomics, *Nat Chem Biol* **2009**, 5(9), 616–624.

95. B. Lomenick, R. Hao, N. Jonai, R.M. Chin, M. Aghajan, S. Warburton,J. W, R.P.Wu, F. Gomez, J.A. Loo, J.A. Wohlschlegel, T.M. Vondriska, J. Pelletier, H.R. Herschman, J. Clardy, C.F. Clarke and J. Huang, Target identification using drug affinity responsive target stability (DARTS), *Proc Natl Acad Sci USA* **2009**, 106, 21984–21989.

96. M.F. Robinson, C.P. Jenkinson, G. Luzhen, C.D. Thomson and P.D. Whanger, Urinary excretion of selenium (Se) and trimethyl-selenonium (TMSe) by NZ women during long term supplementation with selenate or selenomethionine (Semet), *Sel Biol Med* **1989**, 250-253.

97. H.E. Ganther, Selenium metabolism, selenoproteins and mechanisms of cancer prevention: complexities with thioredoxin reductase, *Carcinogenesis*, **1999**, 20(9), 1657-1666.

98. C. Ip and H.E. Ganther, Combination of blocking agents and suppressing agents in cancer prevention, *Carcinogenesis* **1991**, 12(2), 365-367.

99. G.F. Combs, Status of selenium in prostate cancer prevention, *Br J Canc* **2004**, 91(2), 195-199.

100. G. N. Schrauzer, Anticarcinogenic effects of selenium, *Cell Mol Life Sci* **2000**, 57, 1864–1873.

101. E. Seitomer, B. Balar, D. He, P.R. Copeland and T.G. Kinzy, Analysis of saccharomyces cerevisiae null allele strains identifies a larger role for DNA damage versus oxidative stress pathways in growth inhibition by selenium, *Mol Nutr Food Res* **2008**, 52(11), 1305 – 1315.

102. M.S. Stewart, J.E. Spallholz, K.H. Neldner and B.C. Pence, Selenium compounds have disparate abilities to impose oxidative stress and induce apoptosis, *Free Rad Biol Med* **1999**, 26(1-2), 42–48.

103. C. Jiang, Z. Wang, H. Ganther, J. Lü, Distinct effects of methylseleninic acid versus selenite on apoptosis, cell cycle, and protein kinase pathways in DU145 human prostate cancer cells, *Mol Canc Ther* **2002**, 1(12), 1059-66.

104. C. Jiang, K.H. Kim, Z. Wang and J. Lü, Methyl selenium-induced vascular endothelial apoptosis is executed by caspases and principally mediated by p38 MAPK pathway, *Nutr Canc* **2004**, 49(2), 174-83.

105. J. Brozmanova, D. Manikova, V. Vlcˇkova and M. Chovanec, Selenium: a double-edged sword for defense and offence in cancer, *Arch Toxicol* **2010**, 84, 919–938.

106. F. Xing, S. Li, X. Ge, C. Wang, H. Zeng, D. Li, and L. Dong, The inhibitory effect of a novel organoselenium compound BBSKE on the tongue cancer Tca8113 in-vitro and in-vivo, *Oral Oncol* **2008**, 44, 963–969.

107. E. Spallholz, L.M. Boylan and M.M. Rhaman, Environmental hypothesis: is poor dietary selenium intake an underlying factor for arsenicosis and cancer in Bangladesh and West Bengal, India? *Sci Total Environ* **2004**, 323(1-3), 21-32.

108. H. Zeng, M. Wu and J.H. Botnen, Methylselenol, a selenium metabolite, induces cell cycle arrest in G1 phase and apoptosis via the extracellular-regulated kinase 1/2 pathway and other cancer signalling genes, *J Nutr* **2009**, 139(9), 1613–1618.

109. J. Lü and C. Jiang, Selenium and cancer chemoprevention: hypotheses integrating the actions of selenoproteins and selenium metabolites in epithelial and non-epithelial target cells, *Antioxid Redox Signal* **2005**, 7(11-12), 1715–1727.

110. Z. Wang, C. Jiang and J. Lu, Induction of caspase-mediated apoptosis and cell-cycle G1 arrest by selenium metabolite methylselenol,*Mol Carcinog* **2002**, 34, 113–20.

111. T. Kim, U. Jung, D.Y. Cho and A.S. Chung, Se-Methylselenocysteine induces apoptosis through caspase activation in HL-60 cells, *Carcinogenesis* **2001**, 22(4), 559–565.

112. A. Saraste and K. Pulkki, Morphologic and biochemical hallmarks of apoptosis, *Cardiovasc Res* **2000**, 45(3), 528-537.

113. K. Zu and C. Ip, Synergy between selenium and vitamin E in apoptosis induction is associated with activation of distinctive initiator caspases in human prostatecancer cells, *Canc Res* **2003,** 63(20), 6988-95.

114. Z. Liu, P. Hou, M. Ji, H. Guan, K. Studeman, K. Jensen, V. Vasko, A.K. El-Naggar, M. Xing, Highly prevalent genetic alterations in receptor tyrosine kinases and phosphatidylinositol 3-kinase/akt and mitogen-activated protein kinase pathways in anaplastic and follicular thyroid cancers, *J Clin Endocrinol Metab* **2008**, 93(8), 3106-16.

115. E.Ibanez, A. Agliano,C. Prior, P. Nguewa, M. Redrado, I. Gonzalez-Zubeldia, D. Plano, J.A. Palop, C. Sanmartin and A. Calvo,The quinoline imidoselenocarbamate EI201 blocks the AKT/mTOR pathway and targets cancer stem cells leading to a strong antitumor activity, *Curr Med Chem* **2012**, 19(18), 3031–3043.

116. Z. Wang, C. Jiang, H. Ganther and J. Lu, Antimitogenic and Proapoptotic Activities of Methylseleninic Acid in Vascular Endothelial Cells and Associated Effects on PI3K-AKT, ERK, JNK and p38 MAPK Signalling, *Canc Res* **2001**, 61, 7171–7178.

117. E. Unni, D. Koul, Wai-Kwan A. Yung and R. Sinha, Se-methylselenocysteine inhibits phosphatidylinositol 3-kinase activity of mouse mammary epithelial tumor cells in vitro, *Breast Canc Res* **2005**, 7(5), R699-R707.

118. D.L. Hatfield, M.H. Yoo, B.A. Carlson and V.N. Gladyshev, Selenoproteins that function in cancer prevention and promotion, *Biochim Biophys Acta* **2009**, 1790, 1541–1545.

119. G.H. Lyonsa, G.J. Judsonb, I. Ortiz-Monasterioc, Y. Gencd, J.C.R. Stangoulisa and R.D. Graham, Selenium in Australia: Selenium status and biofortification of wheat for better health, *J Trace Elem Med Biol* **2005**, 19(1), 75-82.

120. A. Verma, M.J. Atten, B.M. Attar and O. Holian, Selenomethionine stimulates MAPK (ERK) phosphorylation, protein oxidation, and DNA synthesis in gastric cancer cells, *Canc* **2004**, 49(2), 184-90.

121. J. Folkman, Tumor angiogenesis: therapeutic implications, *Engl J Med* **1971**, 285 (21), 1182–1186.

122. N.S. Chandel, D.S. McClintock, C.E. Feliciano, T.M. Wood, J.A. Melendez, A.M. Rodriguez and P.T. Schumacker, Reactive oxygen species generated at mitochondrial complex III stabilize hypoxia-inducible factor-1α during hypoxia: a mechanism of O_2 sensing, *J Biol Chem* **2000**, 275, 25130–25138.

123. A.R. Farina, A. Tacconelli, L. Cappabianca, M.P. Masciulli,A. Holmgren,G. J. Beckett, A. Gulino and A. R. Mackay, Thioredoxin alters the matrix metalloproteinase/tissue inhibitors of metalloproteinase balance and stimulates human SK-N-SH neuroblastoma cell invasion, *J Biochem* **2001**, *268*, 405–413.

124. H.J. Kim, H.Z. Chae, Y.J. Kim, Y.H. Kim, T.S. Hwang, E.M. Park, Y.M. Park, Preferential elevation of Prx I and Trx expression in lung cancer cells following hypoxia and in human lung cancer tissues, *Cell Biol Toxicol* **2003**, 19(5), 285–298.

125. Y.Taniguchi, Y. Taniguchi-Ueda, K. Mori and J Yodoi, A novel promoter sequence is involved in the oxidative stress-induced expression of the adult T-cell leukemia-derived factor (ADF)/human thioredoxin (Trx) gene, *Nucl Acids Res* **1996**, 24(14), 2746–2752.

126. G. Spyrou, E. Enmark, A. Miranda-Vizuete and Jan-Åke Gustafsson, Cloning and Expression of a Novel Mammalian Thioredoxin, *J Biol Chem* **1997**, 272, 2936–2941.

127. A. Miranda-Vizuete, J. Ljung, A.E. Damdimopoulos, Jan-Åke Gustafsson, R. Oko,M. Pelto-Huikkoand G. Spyrou, Characterization of sptrx, a novel member of the thioredoxin family specifically expressed in human spermatozoa, *J Biol Chem* **2001**, 276, 31567–31574.

128. L.M. Butler, X. Zhou, W.S. Xu, H.I. Scher, R.A. Rifkind, P.A. Marks and V.M. Richon, The histone deacetylase inhibitor SAHA arrests cancer cell growth, up-regulates thioredoxin-binding protein-2 and down-regulates thioredoxin, *Proc Natl Acad Sci USA* **2002**, 99(18), 11700-11705.

129. K.F. Tonissen and G.D. Trapani, Thioredoxin system inhibitors as mediators of apoptosis for cancer therapy, *Mol Nutr Food Res* **2009**, 53(1), 87–103.

130. J. Fang and A. Holmgren, Inhibition of thioredoxin and thioredoxin reductase by 4-hydroxy-2-nonenal in-vitro and in-vivo, *J Am Chem Soc* **2006**, 128(6), 1879-1885.

131. Y. Du, Y. Wu, X. Cao,W. Cui, H. Zhang, Tian W, M. Ji,A. Holmgren, and L. Zhong, Inhibition of mammalian thioredoxin reductase by black tea and its constituents: implications for anticancer actions, *Biochimie* **2009**, 91(3), 434-444.

132. R.L. Poerschke and P.J. Moos, Thioredoxin reductase 1 knockdown enhances selenazolidinecytotoxicity in human lung cancer cells via mitochondrial dysfunction, *Biochem Pharmacol* **2011**, 81(2), 211–221.

133. M. Honeggar, R. Beck and P.J. Moos, Thioredoxin reductase 1 ablation sensitizes colon cancer cells to methylseleninate-mediated cytotoxicity, *Toxicol Appl Pharmacol* **2009**, 241, 348–355.

134. U. Gundimeda, J.E. Schiffman, D. Chhabra, J. Wong, A. Wu and R. Gopalakrishna, Relevance to selenium-induced apoptosis in prostate cancer cells, *J Biol Chem* **2008**, 283, 34519–34531.

135. M. Selenius, A.K. Rundlöf, E. Olm, A.P. Fernandes and M. Björnstedt, Selenium and the selenoprotein thioredoxin reductase in the prevention, treatment and diagnostics of cancer, *Redox Signal* **2010**, 12(7), 867–880.

136. L. Wang, Z. Yang, J. Fu, H. Yin , K. Xiong, Q. Tan, H. Jina, J. Li, T. Wang, W. Tang, J. Yin, G. Cai, M. Liu, S. Kehr, K. Becker and H. Zeng, Ethaselen: a potent mammalian thioredoxin reductase 1 inhibitor and novelorganoselenium anticancer agent, *Free Radic Biol Med* **2012**, 52, 898–908.

137. X. Liu, K.E. Pietsch and S.J. Sturla, Susceptibility of the antioxidant selenoenyzmes thioredoxinreductase and glutathione peroxidase to alkylation-mediated inhibition by anticancer acylfulvenes, *Res Toxicol* **2011**, 24, 726–736.

138. F. Huang, J. Huang, Q. Lv, Y. Yang, G. Wu and C. Xu, Selenite induces apoptosis in colorectal cancer cells through interaction with thioredoxin reductase, *BMB Reports* **2013**, Dec.1.

139. X. Guan, Z. Liu, H. Liu, H. Yu, L.E. Wang, E.M. Sturgis, G. Li and Q. Wei, Inhibition of bacterial thioredoxin reductase: an antibiotic mechanism targeting bacteria lacking glutathione, *FASEB J* **2013**, 27(4), 1394-1403.

140. K.K. Bhasin, E. Arora, A.S. Grover, Jyoti, H. Singh, S.K. Mehta, A.K.K. Bhasin and C. Jacob, Synthesis and characterisation of new 2-pyrimidyl chalcogen (S, Se, Te) compounds: X-ray crystal structure of *bis*(4,6-dimethyl-2-pyrimidyl)diselenide and 4,6-dimethyl-2-(Phenylselanyl)pyrimidine, *J Organomet Chem* **2013**,732(15), 137-141.

141. K.K. Bhasin, V.K. Jain, H. Kumar, S. Sharma, S.K. Mehta and J. Singh, Preparation and characterization of methyl substituted 2,2′-dipyridyl diselenides, 2,2′-dipyridyl ditellurides and their derivatives, *Syn Comm* **2003**, 33(6), 977-988.

142. K.K. Bhasin, E. Arora, C.H. Kwak and S.K. Mehta, Synthesis and characterization of novel quinoline selenium compounds: X-ray structure of 6-methoxy-3H-[1,2]diselenolo[3,4-b]quinoline, *J Organomet Chem* **2010**, 695, 1065–1068.

143. M. Doering, L.A. Ba, N. Lilienthal, C. Nicco, C. Scherer, M. Abbas, A.A.P. Zada, R. Coriat, T. Burkholz, L. Wessjohann, M. Diederich, F. Batteux, M. Herling and C. Jacob, Synthesis and selective anticancer activity of organochalcogen based redox catalysts, *J Med Chem* **2010**, 53(19), 6954-6963.

144. T. Mosmann, Rapid colorimetric assay for cellular growth and survival-application to proliferation and cyto-toxicity assays, *J Immun Methods* **1983**, 65(1-2), 55-63.

145. D. Eisel, G. Fertig, B. Fischer,S. Manzow, K. Schmelig (Eds.) Apoptosis and Cell Proliferation,2nd edition (**1998**), Boehringer Mannheim GmbH, Biochemica.

146. J. Wang, Y.P. Chen, K. Yao, P.A. Wilbon, W. Zhang, L. Ren, J. Zhou, M. Nagarkatti, C. Wang, F. Chu, X. He,A.W. Decho and C. Tang, Robust antimicrobial compounds and polymers derived from natural resin acids, *Chem Comm* **2012***,* 48(6), 916-918.

147. T. Riss, R. Moravec and A. Niles, Selecting cell-based assays for drug discovery screening,*Cell Notes* **2005**, 13, 16–21.

148. J.H. Zhang, T.D. Chung and K.R. Oldenburg, A simple statistical parameter for use in evaluation and validation of high throughput screening assays, *J Biomol Screen* **1999**, 4, 67–73.

149. W. Brand-Williams, M.E. Cuvelier and C.L.W.T. Berset, Use of a free radical methodto evaluate antioxidant activity, *LWT-Food Sc Tech* **1995***,* 28(1), 25-30.

150. B. Ou, D. Huang, M. Hampsch-Woodill, J.A. Flanagan and E.K. Deemer, Analysis of antioxidant activities of common vegetables employing oxygen radicalabsorbance capacity (ORAC) and ferric reducing antioxidant power (FRAP) assays: A comparative study, *J Agric Food Chem* **2002**, 50(11), 3122–3128.

151. I. Ott, X. Qian, Y. Xu, D.H.W. Vlecken, I.J. Marques, D. Kubutat, J. Will, W.S. Sheldrick, P. Jesse, A. Prokop and C.P. Bagowski, A gold(I) phosphine complex containing a naphthalimide ligand functions as a TrxR inhibiting antiproliferative agent and angiogenesis inhibitor, *J Med Chem* **2009**, 52(3), 763–770.

152. T. Posser, M.T. de Paula, J.L. Franco, R.B. Leal and J.B. da Rocha, Diphenyl diselenide induces apoptotic cell death and modulates ERK1/2 phosphorylation in human neuroblastoma SH-SY5Y cells,*Arch Toxicol* **2011**, 85(6), 645-651.

153. K. Schwarz, L.A. Porter and A. Fredga, Biological potency of organic selenium compounds IV. Straight-chain dialkylmono- and diselenides, *Bioinorg Chem* **1974**, 3(2), 145-52.

154. N.Dai, J. Christiansen, F.C. Nielsen and J. Avruch, mTOR complex 2 phosphorylates IMP1 co-translationally to promote IGF2 production and the proliferation of mouse embryonic fibroblasts, *Genes Dev* **2013**, 27(3), 301-312.

155. C.A. Collins, F.H. Fry, A.L. Holme, A. Yiakouvaki, A. Al-Qenaei, C. Pourzand and C. Jacob, Towards multifunctional antioxidants: synthesis, electrochemistry, *in-vitro* and cell culture evaluation of compounds with ligand/catalytic properties, *Org Biomol Chem* **2005**, 3, 1541–1546.

156. J.A. Kerr, Bond dissociation energies by kinetic methods, *Chem Rev* **1966***,* 66(5), 465-500.

157. G.B. Bubols, R.D. Vianna, A. Medina-Remon, G. von Poser, R.M. Lamuela-Raventos, V.L. Eifler-Lima and S.C. Garcia, The antioxidant activity of coumarins and flavonoids, *Mini Rev Med Chem* **2013**, 13(3), 318-334.

158. A. Giacosaa, R. Baralec, L. Bavarescod, P. Gatenbyl, V. Gerbie, J. Janssensn, B. Johnstonm, K. Kaso, C.L. Vecchiaf, P. Mainguetn, P. Morazzonih, E. Negrif, C. Pelucchif, M. Pezzottii and M. Rondanell, Cancer prevention in Europe: the Mediterranean diet as a protective choice, *Eur J Canc Prev* **2013,** 22(1), 90–95.

159. C. Ip and H.E. Ganther, Comparison of selenium and sulfur analogs in cancer prevention, *Carcinogenesis* **1992**, 13(7), 1167-70.

160. S. Wang, K.A. Meckling, M.F. Marcone, Y. Kakuda and R.Tsao, Can phytochemical antioxidant rich foods act as anti-cancer agents? *Food Res Int* **2011**, 44(9), 2545-2554.

161. W.D. Ollis, The neoflavanoids, a new class of natural products, *Cell Mol Life Sci* **1966**, 22(12), 777-783.

162. G.N. Schrauzer, Nutritional selenium supplements: product types, quality, and safety, *J Am Colleg Nutr* **2001***,* 20(1), 1-4.

163. Y. Zhou, F. Tozzi, J. Chen, F. Fan, L. Xia, J. Wang,G. Gao, A. Zhang, X. Xia, H. Brasher, W. Widger, L.M. Ellis and Z. Weihua, Intracellular ATP levels are a pivotal determinant of chemoresistance in colon cancer cells, *Canc Res* **2012**, 72, 304-314.

164. R.D. Petty, L.A. Sutherland, E.M. Hunter and I.A. Cree, Comparison of MTT and ATP-based assays for the measurement of viable cell number, J *Biolumin Chemilumin* **1995**, 10(1), 29-34.

165. S.W. Lowe and A.W. Lin, Apoptosis in cancer, *Carcinogenesis* **2000**, 21 (3), 485-495.

166. Y. Gavrieli, Y. Sherman, and S.A. Ben-Sasson, Identification of programmed cell death in-situ via specific labeling of nuclear DNA fragmentation, *J Cell Biol* **1992**, 119(3), 493-501.

167. E.D. Crawford and J.A. Wells, Caspase substrates and cellular re-modeling, *Ann Rev Biochem* **2011***,* 80, 1055-1087.

168. J. Parsonnet, Bacterial Infection as a cause of cancer,*Environ Health Perspect* **1995**, 103(8), 263-268.

169. T.A. Phong and T.J. Webster, Selenium nanoparticles inhibit Staphylococcus aureus growth, *Int J Nanomed* **2011**, 6, 1553–1558.

170. J. Yang, K. Huang, S. Qin, X. Wu, Z. Zhao and F. Chen, Antibacterial action of selenium-enriched probiotics against pathogenic Escherichia coli. *Dig Dis Sci* **2009**, 54(2), 246-254.

171. R.T. Wheeler, M. Kupiec, P. Magnel, C. Abeijon and G.R. Fink, A Saccharomyces cerevisiae mutant with increased virulence, *Proc Natl Acad Sci USA* **2003**, 100(5), 2766-2770.

172. P.K.Mukherjee, J. Chandra, M. Retuerto, M. Sikaroodi, R.E. Brown, R. Jurevic, R.A. Salata, M.M. Lederman, P.M. Gillevet and M.A. Ghannoum, Oral Mycobiome Analysis of HIV-Infected Patients: Identification of Pichia as an Antagonist of Opportunistic Fungi, *PLoS pathogens* **2014**,10(3), e1003996.

173. S. Karnam, V.M. Alla, J. Kwon, T. Harbert, A. Sharma, K. Airey, and A. Mooss, Mycobacterium phlei, a previously unreported cause of pacemaker infection: Thinking outside the box in cardiac device infections, *Cardiol J* **2011***, 18(6), 687-690.

174. R.D. Synder and M.L. Edwards, Effects of polyamine analogs on the extent and fidelity of *in-vitro* polypeptide synthesis, *Biochem Biophys Res Commun* **1991**, 176, 1383-1392.

175. T. Schneider-Poetsch, J. Ju,D.E. Eyler, Y. Dang, S. Bhat, W.C. Merrick, R. Green, B. Shen and J.O. Liu, Inhibition of eukaryotic translation elongation by cycloheximide and lactimidomycin, *Nat Chem Biol* **2010**, 6(3), 209-217.

176. M.C.Ledesma, B. Jung-Hynes, T.L. Schmit, R. Kumar, H. Mukhtar and N. Ahmad, Selenium and Vitamin E for Prostate Cancer: Post-SELECT (Selenium and Vitamin E Cancer Prevention Trial) Status, *Mol Med* **2011**, 17(1-2), 134–143.

177. C.M. Chresta, B.R. Davies, I.Hickson, T. Harding, S. Cosulich, S.E. Critchlow, J.P. Vincent, R. Ellston, D. Jones, P. Sini,D. James, Z. Howard, P. Dudley, G. Hughes, L. Smith, S. Maguire, M. Hummersone, K. Malagu, K. Menear, R. Jenkins, M. Jacobsen, G.C.M. Smith, S. Guichard and M. Pass, *AZD8055* is a potent, selective, and orally bioavailable ATP-competitive mammalian target of rapamycin kinase inhibitor with *in-vitro* and *in-vivo* antitumor activity, *Cancer Res* **2010**, 70 (1), 288-298.

178. R.J. Roskoski, ERK1/2 MAP kinases: Structure, function, and regulation, *Pharmacol Res* **2012**, 66(2), 105–143.

179. C. Vantaggiato, I. Formentini, A. Bondanza, C. Bonini, L. Naldini, and R. Brambilla, ERK1 and ERK2 mitogen-activated protein kinases affect Ras-dependent cell signalling differentially, *J Biol* **2006***, 5(5), 14.

180. A. Eftekhari, Electrocatalysis and amperometric detection of hydrogen peroxide at an aluminum microelectrode modified with cobalt hexacyanoferrate film, *Microchim Acta* **2003**, 141 (1-2), 15–21.

181. R.S. Hosmane and J.F. Liebman, Paradoxes and paradigms: why is quinoline less basic than pyridine or isoquinoline? A classical organic chemical perspective, *Struct Chem* **2009**, 20 (4), 693–697.

182. R.M. Han, J.P. Zhang and L.H. Skibsted, Reaction dynamics of flavonoids and carotenoids as antioxidants, *Molecules* **2012**, 17(2), 2140-2160.

183. S.V. Jovanovic, S. Steeden, M. Tosic, B. Marjanovic and M.G. Simicg, Flavonoids as Antioxidants, *J Am Chem Soc* **1994**, 116 (11), 4846-4851.

184. M. Iwaoka, R. Ooka, T. Nakazato, S. Yoshida and S. Oishi, Synthesis of selenocysteine and selenomethionine derivatives from sulfur-containing amino acids, *Chem Biodivers* **2008**, 5(3), 359-374.

185. J.E. Spallholz, V.P. Palace and T.W. Reid, Methioninase and selenomethionine but not Se-methylselenocysteine generate methylselenol and superoxide in an in vitro chemiluminescent assay: implications for the nutritional carcinostatic activity of selenoamino acids, *Biochem Pharmacol* **2004**, 67(3), 547-554.

186. M.L. Hu, Dietary polyphenols as antioxidants and anticancer agents: more questions than answers**, *Chang Gung Med J* **2011**, 34(5), 449-460.

187. J.J. Liu, Q. Liu, H.L. Wei, J. Yi, H.S. Zhao and L.P.Gao, Inhibition of thioredoxin reductase by auranofin induces apoptosis in adriamycin-resistant human K562 chronic myeloid leukemia cells, *Pharmazie* **2011,** 66(6), 440-444.

188. V.V. Zeenko, C. Wang, M. Majumder, A.A. Komar, M.D. Snider, W.C. Merrick, R.J. Kaufman and M. Hatzoglou, An efficient *in-vitro* translation system from mammalian cells lacking the translational inhibition caused by eIF2 phosphorylation, *RNA* **2008**, 14(3), 593–602.

189. F. Abendroth, A. Bujotzek, M. Shan, R. Haag, M. Weber and O. Seitz, DNA-Controlled Bivalent Presentation of Ligands for the Estrogen Receptor, *Angew Chem Int Ed* **2011**, 50(37), 8592-8596.
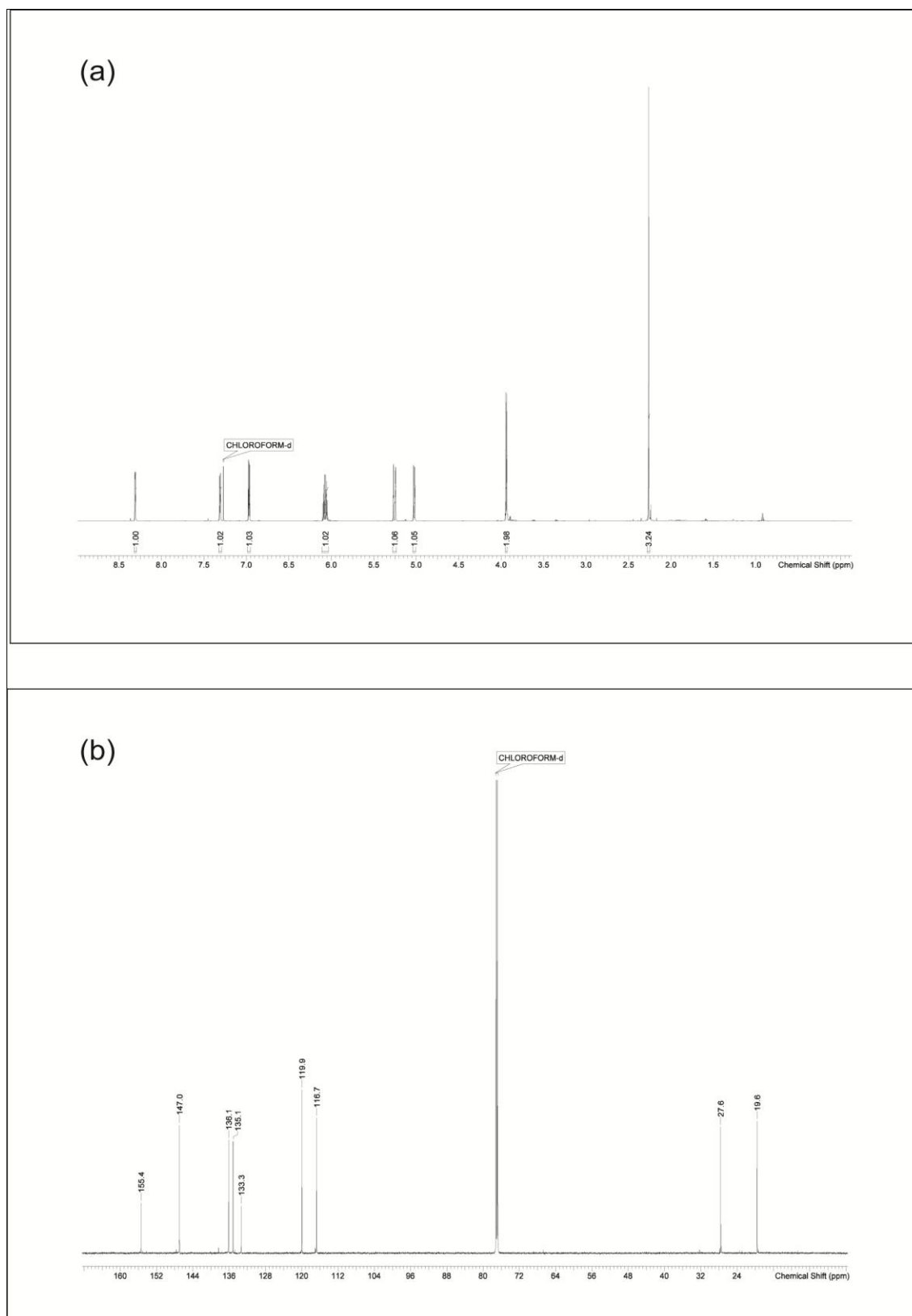
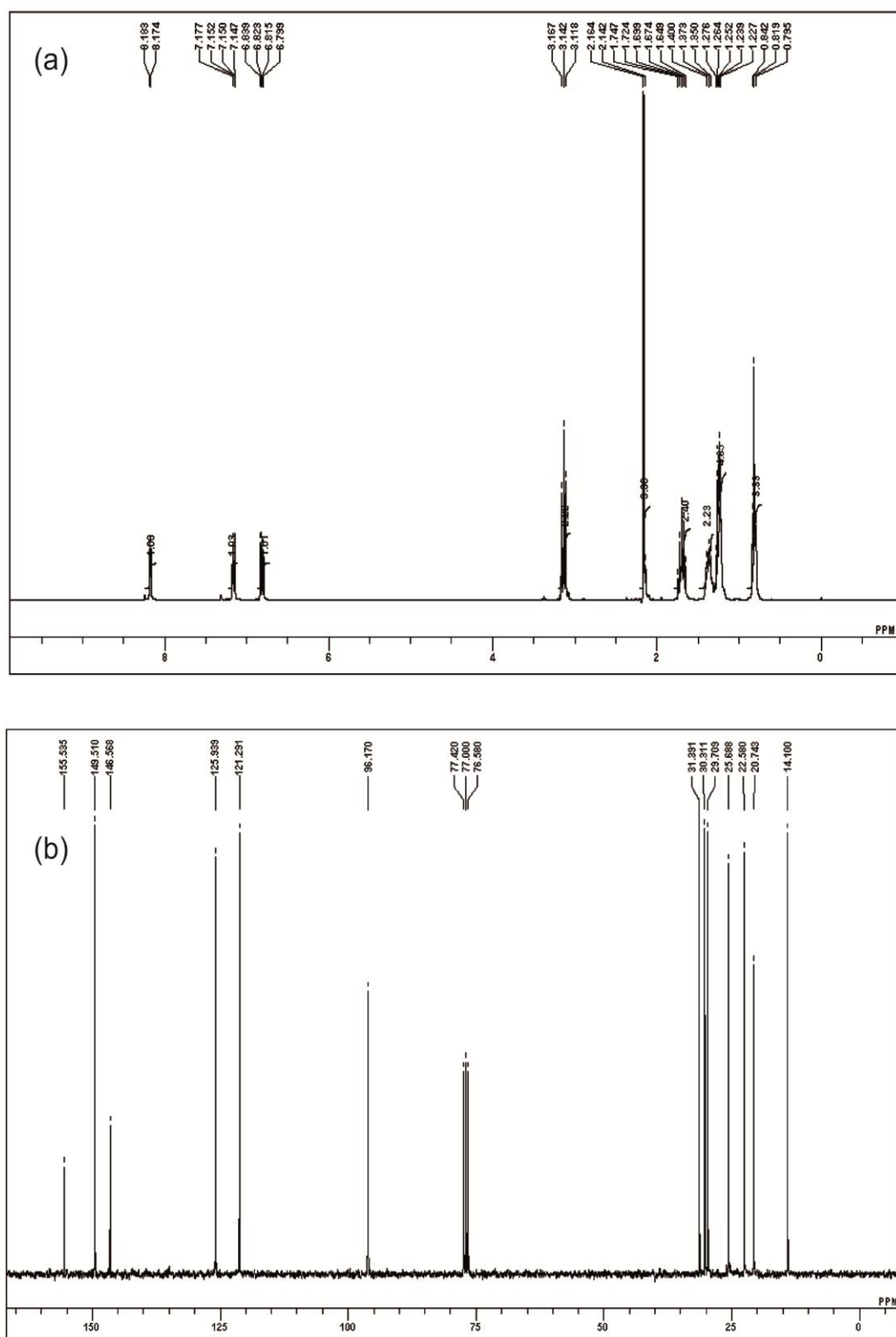**Figure 1.** ^{1}H (a) and ^{13}C (b) NMR of 2-(hexylselanyl)-4-methylpyridine, **3**

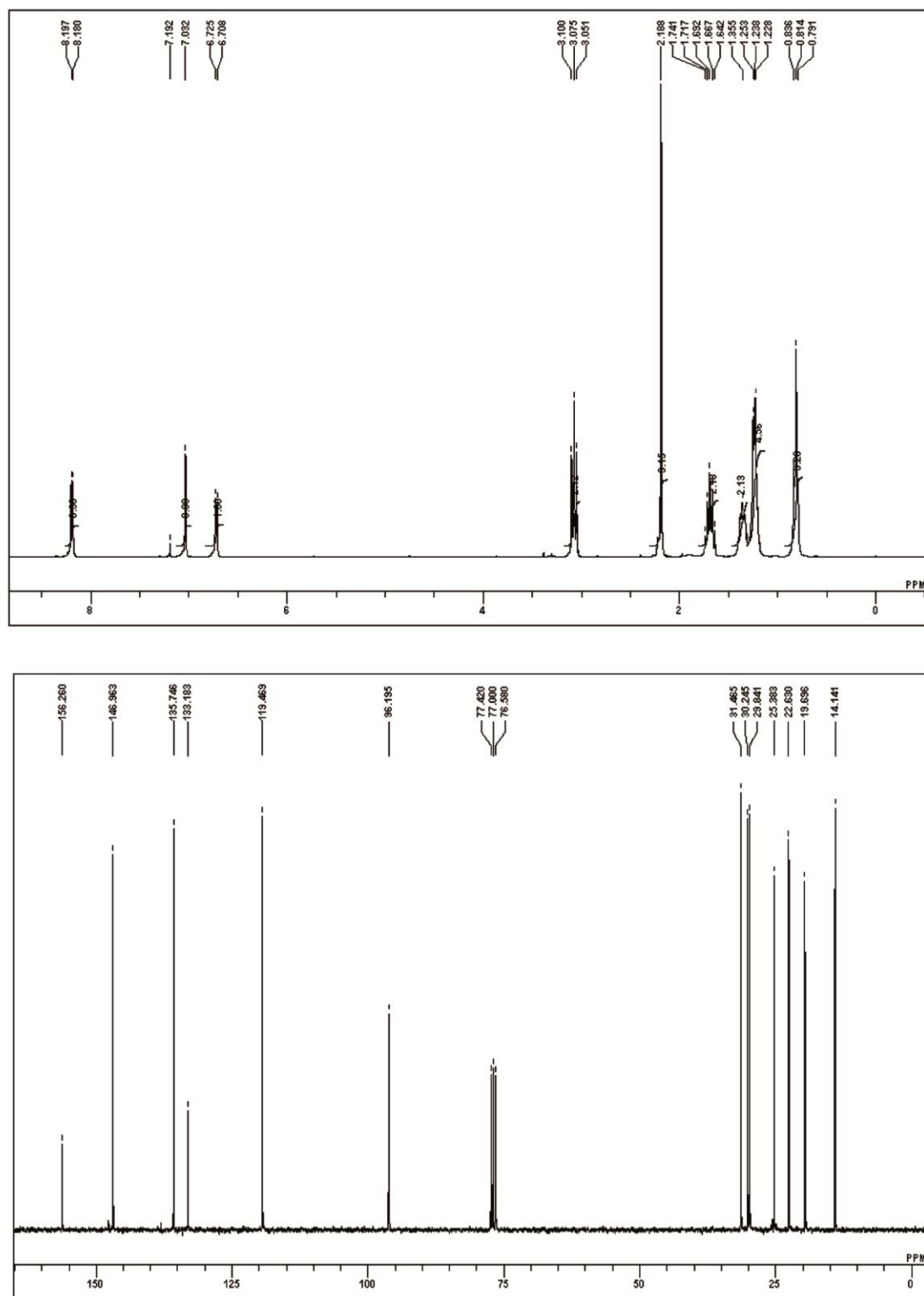**Figure 2.** ¹H (a) and ¹³C (b) NMR of 2-(allylselanyl)-3-methylpyridine, **5**

Figure 3. ^{1}H (a) and ^{13}C (b) NMR of 2-(hexylselanyl)-3-methylpyridine, **6**
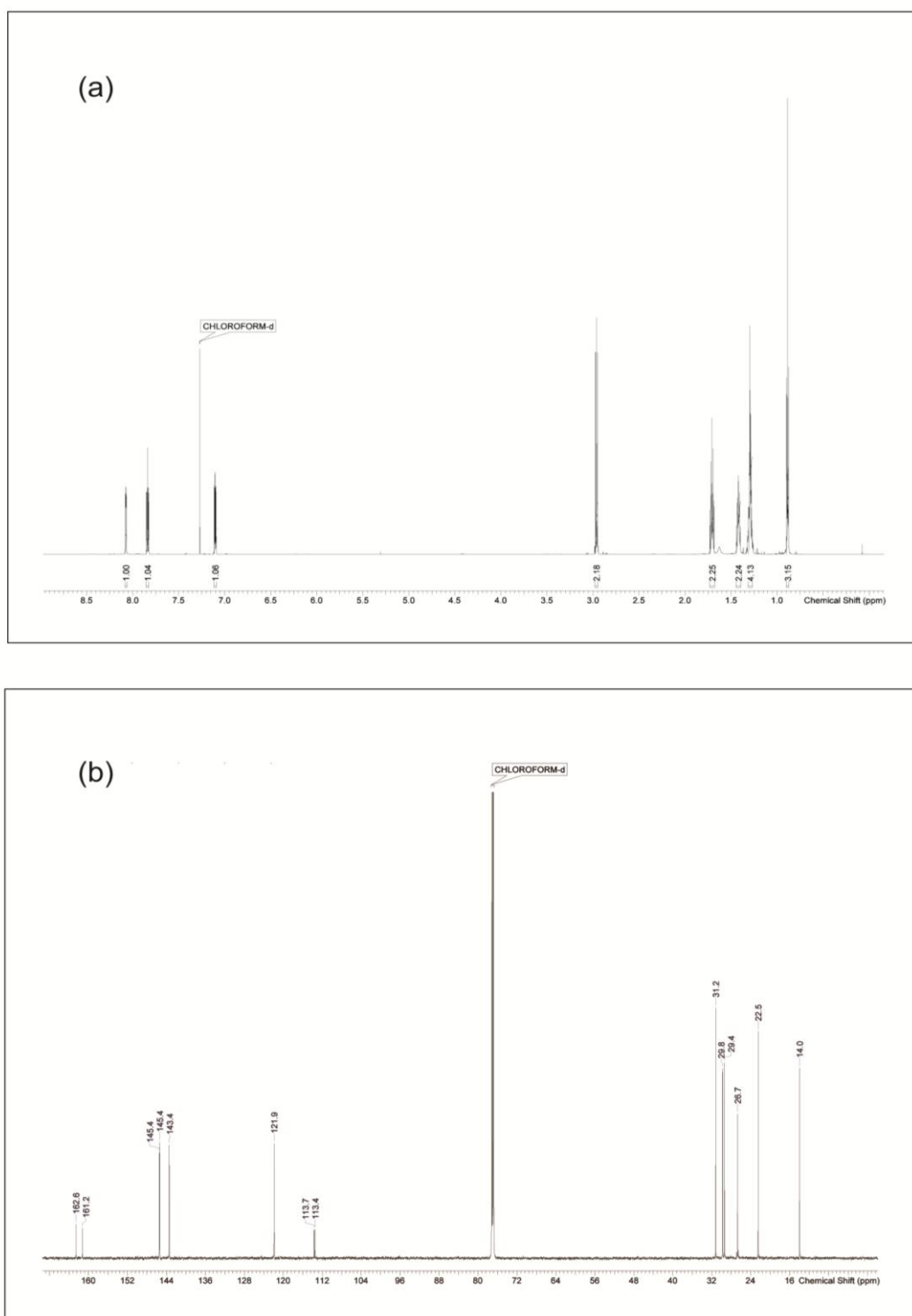
Figure 4. ¹H (a) and ¹³C (b) NMR of 2-fluoro-3-(hexylselanyl) pyridine, **9**
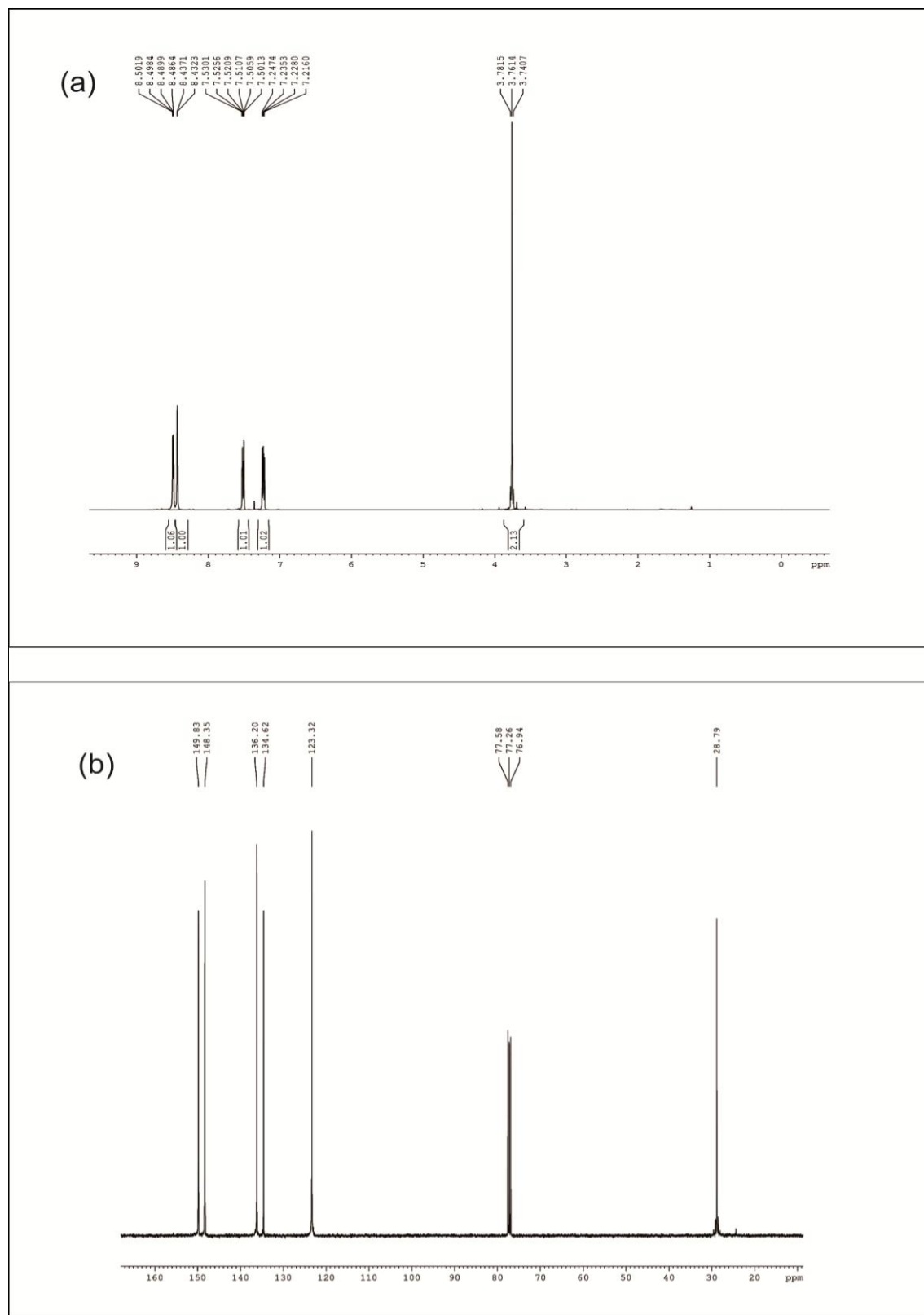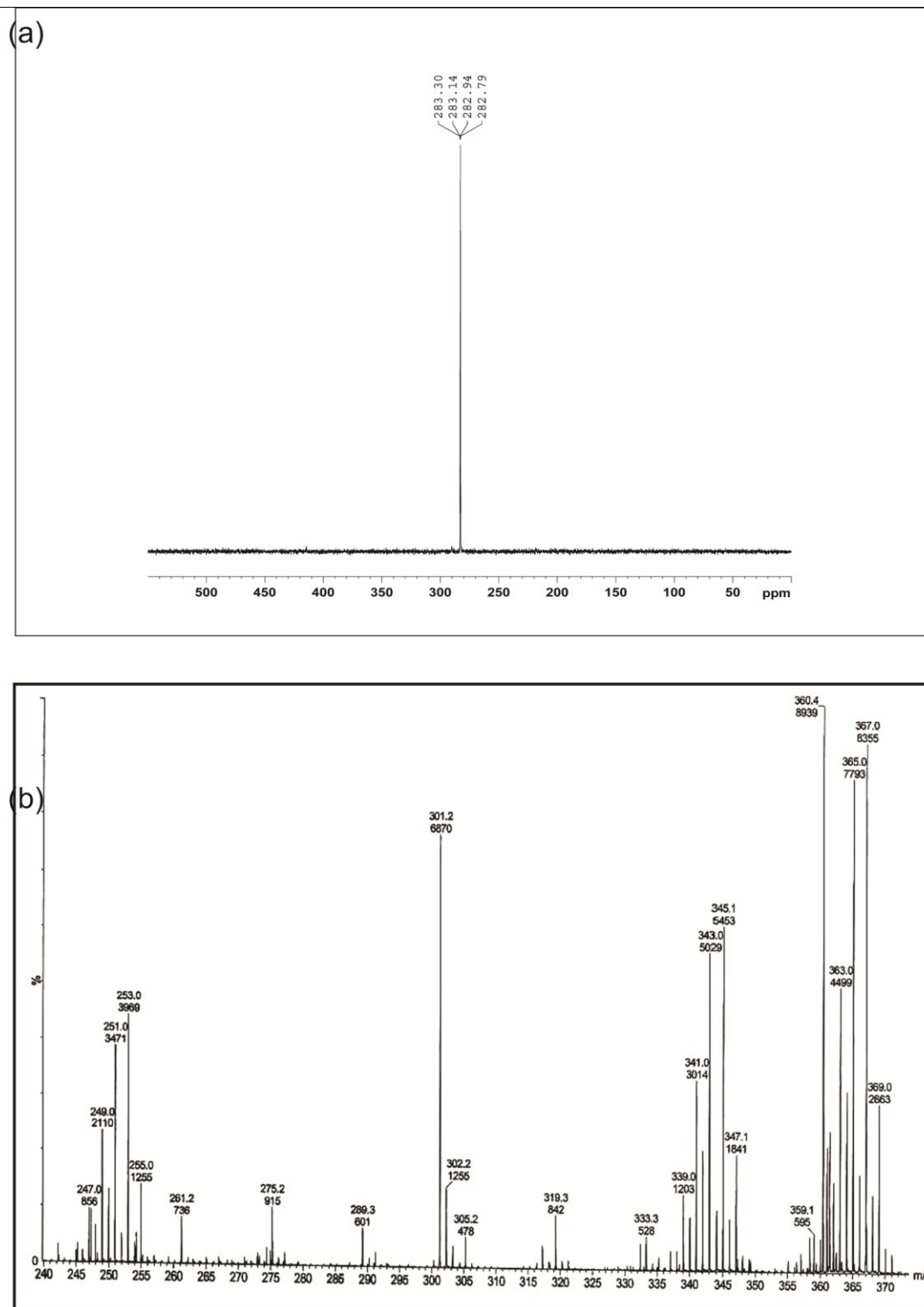
Figure 5. ^{1}H (a) and ^{13}C NMR of 1,2-bis{(pyridine-3-yl}methyl)diselane, **10**
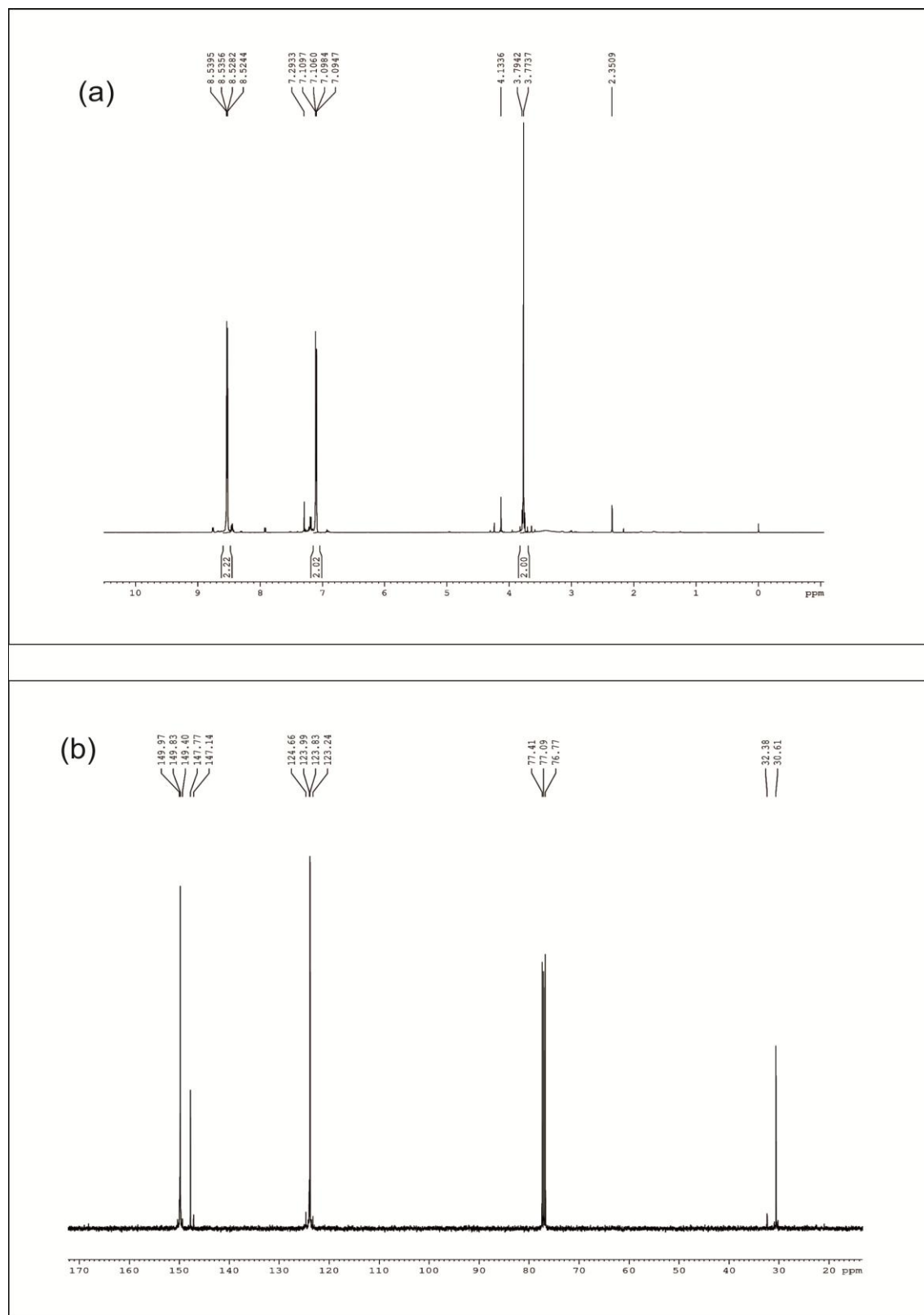
(a)

283.30
283.14
282.94
282.79

500 450 400 350 300 250 200 150 100 50 ppm

(b)

360.4
8939

367.0
8355

365.0
7793

301.2
6870

345.1
5453

343.0
5029

363.0
4499

253.0
3969

251.0
3471

341.0
3014

369.0
2663

249.0
2110

347.1
1841

255.0
1255

302.2
1255

339.0
1203

247.0
856

261.2
736

275.2
915

289.3
601

319.3
842

359.1
595

305.2
478

333.3
528

240 245 250 255 260 265 270 275 280 285 290 295 300 305 310 315 320 325 330 335 340 345 350 355 360 365 370 m/z

Figure 6. ^{77}Se NMR (a) and mass spectrum (b) of 1,2-*bis*{(pyridin-3-yl)methyl}diselane, **10**

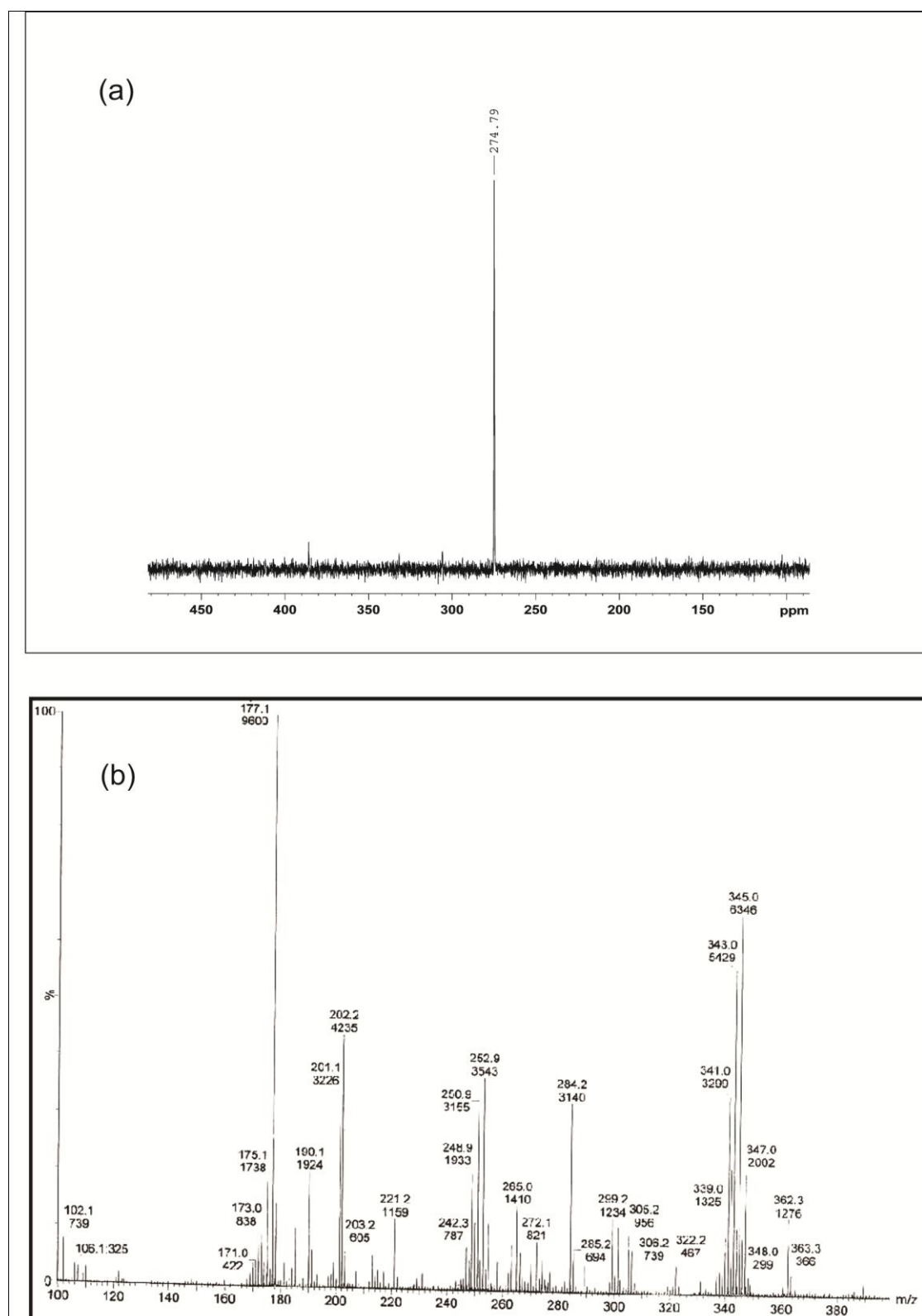**Figure 7**. ^{1}H (a) and ^{13}C NMR of 1,2-bis{(pyridine-4-yl}methyl)diselane, **11**

(a)

274.79

450   400   350   300   250   200   150   ppm

(b)

100 —

177.1
9600

%

345.0
6346

343.0
5429

202.2
4235

201.1
3226

252.9
3543

341.0
3200

250.9
3155

284.2
3140

175.1
1738

190.1
1924

248.9
1933

347.0
2002

265.0
1410

221.2
1159

299.2
1234

305.2
956

339.0
1325

362.3
1276

102.1
739

173.0
838

272.1
821

203.2
605

242.3
787

285.2
694

306.2
739

322.2
467

105.1:325

171.0
422

348.0
299

363.3
366

0 —

100   120   140   160   180   200   220   240   260   280   300   320   340   360   380   m/z

Figure 8. ^{77}Se NMR (a) and mass spectrum (b) of 1,2-*bis*{(pyridin-4-yl)methyl}diselane, **11**
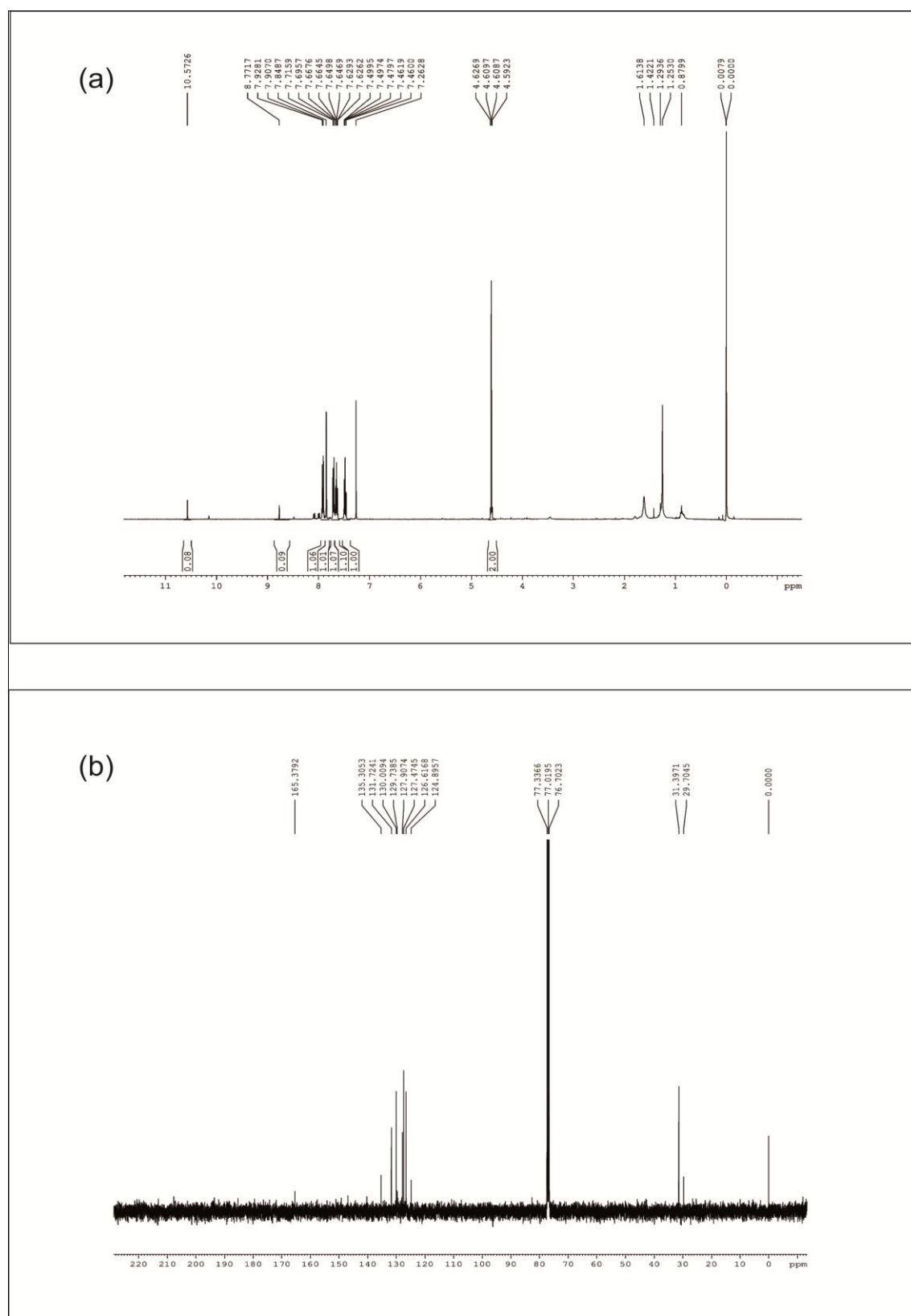
Figure 9. ^{1}H (a) and ^{13}C NMR (b) of 3H-[1,2]diselenolo[3,4-b]quinoline, **12**

(a)

409.882
369.919

PPM

600   500   400   300   200   100   0   -100

(b)

%

301.2
522

301.1
458

296.3
411

302.3
172

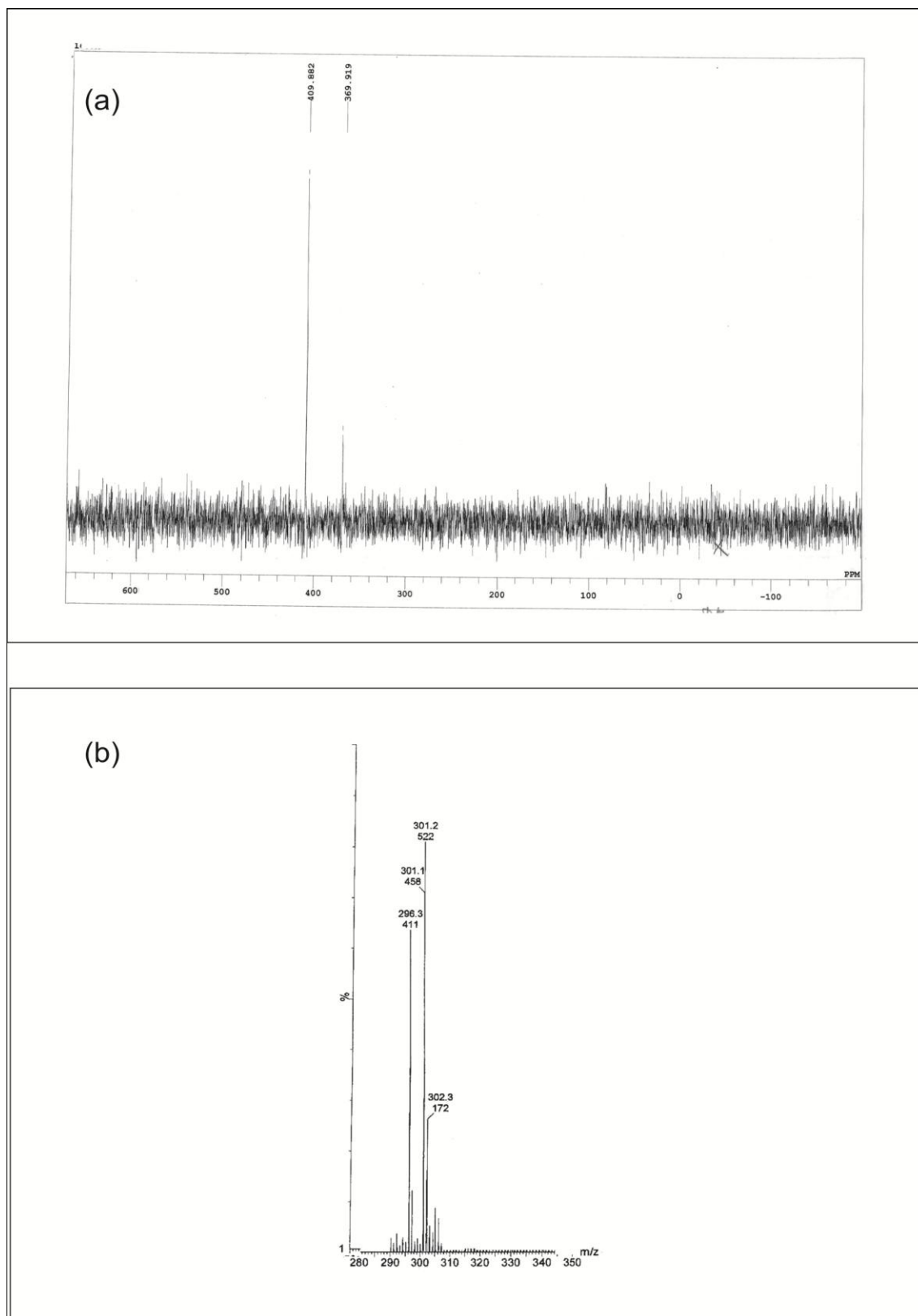m/z
280 290 300 310 320 330 340 350

Figure 10. ^{77}Se NMR (a) and mass spectrum (b) of 3H-[1,2]diselenolo[3,4-b]quinoline, **12**

Aman K.K.Bhasin, M. Sc. (Hons. School)

akkb8785@gmail.com

Born (July 10, 1987) and raised at Chandigarh (India)

Academic

- **Ph.D**. Dissertation "Synthesis and elucidation of biochemical mode of action of organoselenium compounds against cancer" with Prof. Claus Jacob, University of Saarland, Germany (July 2011- to date).

- **M.Sc. (Hons. Sch.)** Department of Chemistry & Centre of Advanced Studies in Chemistry, Panjab University, Chandigarh, India (2008-2010), in first division with distinction.

- **B.Sc. (Hons. Sch.)** Department of Chemistry & Centre of Advanced Studies in Chemistry, Panjab University, Chandigarh, India (2004-2008), in first division with distinction.

Experience

- **DAAD Siemens Fellow** School of Pharmacy, Saarland State University, Saarbruecken, Germany with Prof. Dr. Claus Jacob (July 2011-June 2014).

- **Research Fellow** Institute of Microbial Technology (IMTEC), Chandigarh (India) with Senior Principle Scientist, Dr. C.R. Suri (Dec. 2010-May 2011).

- **Student Internship** Institute of Chemistry, Technical University, Berlin (Germany) with Prof. Michael Gradzielski (May 2009- July 2009).

List of publications

1. K.K. Bhasin, E. Arora, A.S. Grover, Jyoti, H. Singh, S.K. Mehta, **A.K.K. Bhasin** and C. Jacob, Synthesis and characterization of new 2-pyrimidyl chalcogen (S, Se, Te) compounds: X-ray crystal structure of *bis*(4,6-dimethyl-2 pyrimidyl)diselenide and 4,6-dimethyl-2-(phenylselanyl)pyrimidine, *J Organomet Chem* **2013**, 732(15), 137-141.

2. E. Arora, K.K. Bhasin, S.K. Mehta, **A.K.K. Bhasin**, C. Jacob, V. Félix and S. Neogi, Synthesis of new organochalcogen (Se or Te) based multifunctional pyrimidine derivatives: X-ray structure determination of 2,4-bis(arylchalcogenyl) pyrimidine and 2-chloro-4,6-bis(arylchalcogenyl)pyrimidine compounds, *Polyhedron* **2014**, 81, 316-322.

3. K. K. Bhasin, S. Doomra, **A.K.K. Bhasin**, V. Trehan and C. Thone, Design and Synthesis of Pyridylselenoethers , Invited Paper on Electronic symposium on selenium chemistry (dedicated to Prof. M. Tiecco on his retirement on the site *http://eses1.chimfarm.unipg.it* (**2011**).

4. R.C. Boro, J. Kaushal, Y. Nangia, N. Wangoo, **A.K.K. Bhasin** and C. R. Suri, Gold nanoparticles catalyzed chemiluminescence immunoassay for detection of herbicide 2,4-dichlorophenoxyacetic acid, *Analyst* **2011**, 136, 2125-2130.

5. N. Wangoo, G. Shekhawat, J.S. Wu, **A.K.K. Bhasin**, C.R. Suri, K.K. Bhasin and V. Dravid, Green synthesis and characterization of size tunable silica-capped gold core– shell nanoparticles, *J Nanopart Res,* **2012**, 14(8), 1011.

6. P. Sharma, M. Kakkar, A. Ganguli, **A.K.K. Bhasin** and C.R. Suri, Plasmon enhanced fluoro-immunoassay using egg yolk antibodies for ultra-sensitive detection of herbicide diuron, *Analyst*, **2013**, 138, 4312-4320.

Papers presented in Conferences

1. **A.K.K. Bhasin**, F. Sasse, K.K. Bhasin, E. Arora, S.K.Mehta, T. Burkholz and C. Jacob, Synthesis, structural elucidation and anti-carcinogenic potential of a new selenium-incorporated tricyclic quinoline, Oral presentation at 3rd International Conference on Research Frontiers in Chalcogen Cycle Science & Technology held in Delft, Netherlands, **2013**.

2. **A.K.K.Bhasin**, Soft Template Synthesis of Super Paramagnetic Fe_3O_4 nano particles: Decomposing phenol by the hidden talent of ferromagnetic nanoparticles, Oral presentation at Chandigarh Science Congress, Panjab University, Chandigarh, Feb.26-28, **2009.**